Selective toluene disproportionation over ZSM-5 zeolite

A thesis submitted to the University of Manchester for the degree of

Doctor of Philosophy

in the Faculty of Science and Engineering

2018

Mohammed Z. Albahar

School of Chemical Engineering and Analytical Science

Table of Contents

Word count: 42,679

List of tables

List of Figures

List of Abbreviations

XRD	X-ray diffraction
SEM	Scanning electron microscopy
EDAX/EDX	Energy dispersive X-ray analysis
TGA	Thermogravimetric analysis
FTIR	Fourier transform infrared spectroscopy
MAS-NMR	Solid-state magic angle nuclear magnetic resonance spectroscopy
BET	Brunauer- Emmett-Teller
GC	Gas chromatography
ICP-OES	Inductively coupled plasma optical emission spectrometry
FID	Flame ionisation detector
SBU	Secondary building unit
IZA	International zeolite association
TOS	Time on stream
WHSV	Weight hourly space velocity
FCC	Fluid catalytic cracking
B/L	Brønsted/Lewis
Py	Pyridine
TEOS	Tetraethyl orthosilicate
APTES	Aminopropyl triethoxysilane
TMB	Trimethylbenzene
HC	Hydrocarbon
EFAL	Extraframework aluminium

University of Manchester
Student: Mohammed Z. Albahar
Degree: PhD
Thesis Title: Selective toluene disproportionation over ZSM-5
Date: 15/01/2018

Abstract

This research aimed at improving p-xylene selectivity in toluene disproportionation over ZSM-5 zeolite by exploring the effect of crystal size and various post synthetic modification methods. A comprehensive study of the effect of different modifications on the physicochemical properties of ZSM-5 was investigated using X-ray diffraction (XRD), pyridine adsorption, Fourier transform infra-red (FTIR), ^{29}Si magic-angle spinning nuclear magnetic resonance (MAS NMR), BET surface area by N_2 adsorption, inductively coupled plasma (ICP) and scanning electron microscopy (SEM). The catalytic performance of each catalyst was studied in a fixed bed reactor at a temperature 475 °C, WHSV 3-83 h^{-1} and two different pressures (1 and 10 bar).

ZSM-5 zeolites with different crystal sizes (5, 50 and 100 µm) were synthesized in house and compared with the commercially obtained ZSM-5 having a crystal size of 0.5 µm. The increase in crystal size improved p-xylene selectivity which was attributed to the diffusion constraints imposed by the longer diffusion path lengths of large crystals. The highest p-xylene selectivity (58 %) was achieved over ZSM-5 with the largest crystal size 100 µm at the highest WHSV 83 h^{-1}. However, it was accompanied by a low conversion (2 wt. %). ZSM-5 with crystal size of 5 µm delivered the best results in terms of the combination of para-selectivity (40 %) and toluene conversion (15 wt. %).

The p-xylene produced in the channels of ZSM-5 can quickly isomerise to o-xylene and m-xylene on the external unselective acid sites. Different post modification methods were applied in this study in attempt to suppress the fast isomerization reaction by deactivating the external acid sites. This was achieved to some extent by depositing an inert silica layer using different silica agents, amounts and number of modification cycles and as a result p-xylene selectivity was significantly improved (84 %), especially over large crystals 5 µm. The decrease in Brønsted acidity (FTIR) suggested the success of the silylation method. Furthermore, impregnation of lanthanum and phosphorus on ZSM-5 improved p-xylene selectivity (40 %). FTIR measurements showed a drastic drop in the number of Brønsted and Lewis acid sites after loading phosphorus which led to a large reduction in toluene conversion. Lanthanum impregnation had less effect on conversion and increased selectivity with decreased Brønsted sites and pore volume reduction showed by N_2 adsorption suggesting some pore narrowing.

There are several approaches that can be considered in future to further improve p-xylene selectivity. Improving the synthesis of large crystals to balance acidity and crystal size can lead to the enhancement of p-xylene selectivity. Also, performing toluene disproportionation on optimised pre-coked ZSM-5 large crystals at high pressure can help to maintain the conversion while increasing p-xylene selectivity. Another approach would be to apply silylation modification to extruded large crystals ZSM-5.

DECLARATION

No portion of the work referred to in this thesis has been submitted in support of an application for another degree or qualification of this or any other university or other institute of learning.

Copyright Statements

I. The author of this thesis (including any appendices and/or schedules to this thesis) owns certain copyright or related rights in it (the "Copyright") and s/he has given The University of Manchester certain rights to use such Copyright, including for administrative purposes.

II. Copies of this thesis, either in full or in extracts and whether in hard or electronic copy, may be made only in accordance with the Copyright, Designs and Patents Act 1988 (as amended) and regulations issued under it or, where appropriate, in accordance with licensing agreements which the University has from time to time. This page must form part of any such copies made.

III. The ownership of certain Copyright, patents, designs, trademarks and other intellectual property (the "Intellectual Property") and any reproductions of copyright works in the thesis, for example graphs and tables ("Reproductions"), which may be described in this thesis, may not be owned by the author and may be owned by third parties. Such Intellectual Property and Reproductions cannot and must not be made available for use without the prior written permission of the owner(s) of the relevant Intellectual Property and/or Reproductions.

IV. Further information on the conditions under which disclosure, publication and commercialisation of this thesis, the Copyright and any Intellectual Property and/or Reproductions described in it may take place is available in the University IP Policy (see http://documents.manchester.ac.uk/DocuInfo.aspx?DocID=2442 0), in any relevant Thesis restriction declarations deposited in the University Library, The University Library's regulations (see http://www.library.manchester.ac.uk/about/regulations/) and in The University's policy on Presentation of Theses

Acknowledgements

I would like to thank my supervisor Dr. Arthur A. Garforth for his invaluable guidance, constant encouragement, inspiration and assistance during my PhD.

I would also like to acknowledge and thank all academic staff for their great help and support throughout my time in the university especially (Mr. Loris Doyle, Dr. Barbara Gore, Mr. Patrick Hill, John Waters, Mrs. shahla khan and Miss Gemma Chapman). Also would like to thank Dr. Vladimir for devoting his time to help with the FTIR analysis in Keele University. Finally, I would like to thank my friends (Faisal Almulla, Mohammed Aldossary, Isaac Campbell, Chaozhou Li and Abeer Arjah) for their continuous support.

Special thanks go to Saudi Aramco for sponsoring me to pursue my PhD and for their support both academically and socially which was invaluable and eased my study. Also I thank the Research and Development Centre and ACS, London office for their continuous support.

Finally and most importantly, special thanks to my parents (Zuhair and Zahra), my wife (Eman) for their great support and encouragement. I would like to dedicate this work to them and my beloved son (Wesam).

Chapter 1 Introduction

1.1 Background

Xylenes are very important materials in the petrochemical industry. They are C_8 aromatics consisting of mixtures of three isomers: p-xylene, m-xylene and o-xylene (Figure 1-1) of which the para isomer is in greatest demand.

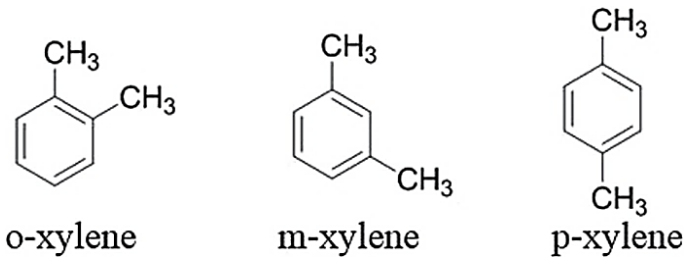

Figure 1-1: Xylene isomers

Para-xylene is mainly used as a raw material in the production of terephthalic acid, dimethyl terephthalate and purified terephthalic acid. These compounds are used to make polyesters such as polyethylene terephthalate (PET) which are widely used for making carbonated drinks and water containers [1,2].

1.2 Market demand of p-xylene

The demand on p-xylene has been increasing in recent years with an annual growth rate of 6-8%. Figure 1-2 shows that the consumption of p-xylene will outgrow the supply in the next few years (2018-2020) [3]. One of the main reasons for the growth in C_8 demand is their high consumption in Asia, which is around 70 % of the world production capacity [4]. The decline in cotton fibre global production is another factor that has resulted in increasing the demand on p-xylene as cotton fibre is used in the production of polyester fibres [5].

The p-xylene supply should be increased in the next few years to meet the increasing demand. However, most of the plants are operating at full capacity. The p-xylene production could be maximized by converting less valuable refinery products, such as toluene.

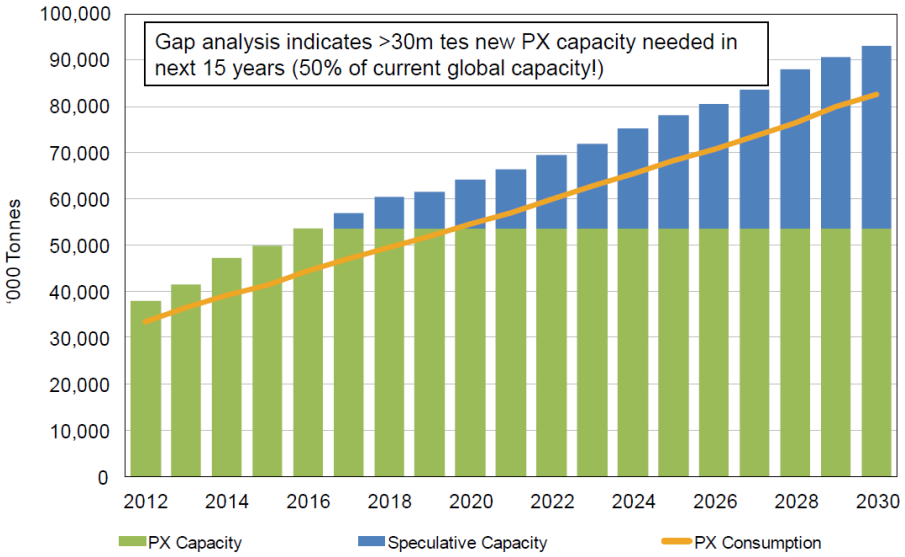

Figure 1-2: Worldwide p-xylene capacity and consumption [3]

1.3 Production technologies of p-xylene

In industry, the main source of xylene to the petrochemical world is the catalytic reforming process yielding 70 % of the world production. Then, approximately 17 % is produced by transalkylation followed by a further 7 % from toluene disproportionation and 4 % from pyrolysis gasoline [4].

1.3.1 Catalytic reforming as a source of BTX

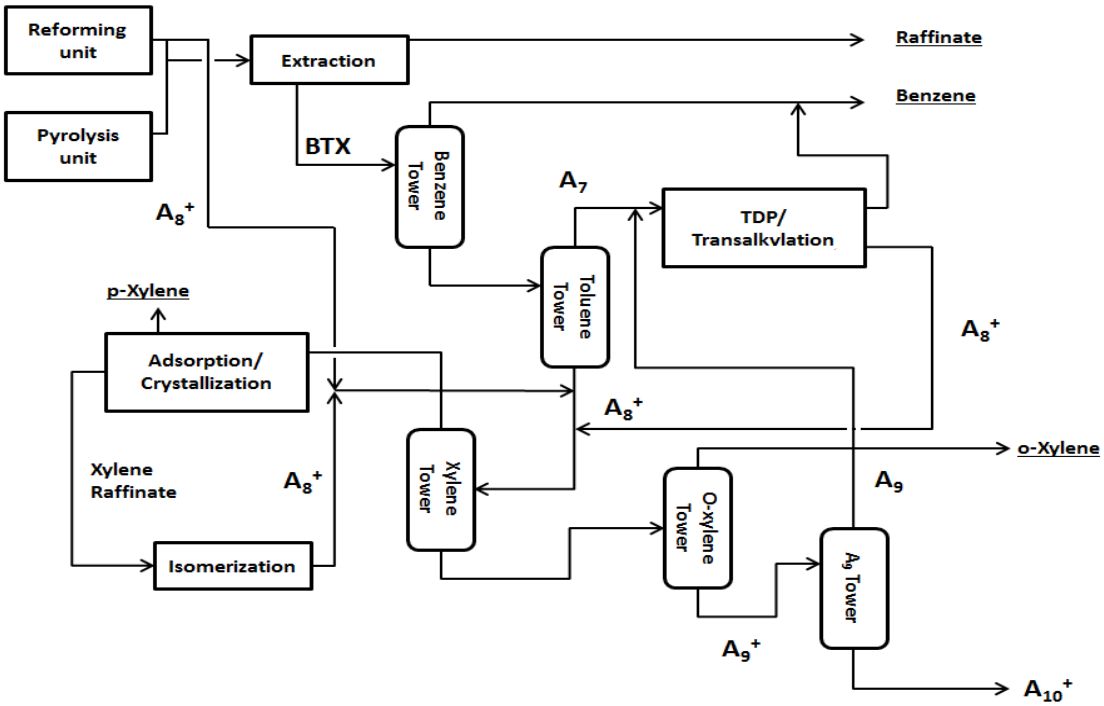

Figure 1-3: Typical scheme for aromatics production [1]

Catalytic reforming of naphtha contains two separate sections which are reforming and pyrolysis. BTX aromatics are attained from both processes and separated from the non-aromatics by extraction. The yields of these products are governed by thermodynamics resulting in a gap between the supply and the world demand. The world production capacity ratio for B:T:X obtained from different processes is 32:36:32 (Figure 1-4) whereas the demand in the petrochemical industry is 55:11:34 [6]. This mismatch could be addressed by converting the less valuable toluene which is produced in surplus.

Finally, p-xylene is separated from other isomers by more energy intensive processes such as adsorption or crystallization processes. Therefore, the production cost rises. It is noticeable that the demand for p-xylene isomer is very high compared to the supply. To increase the production volume of p-xylene, the less desirable o-xylene and m-xylene can be isomerized to p-xylene by isomerization process or to utilize the surplus toluene through toluene disproportionation or transalkylation processes to maximize the xylene yield [7].

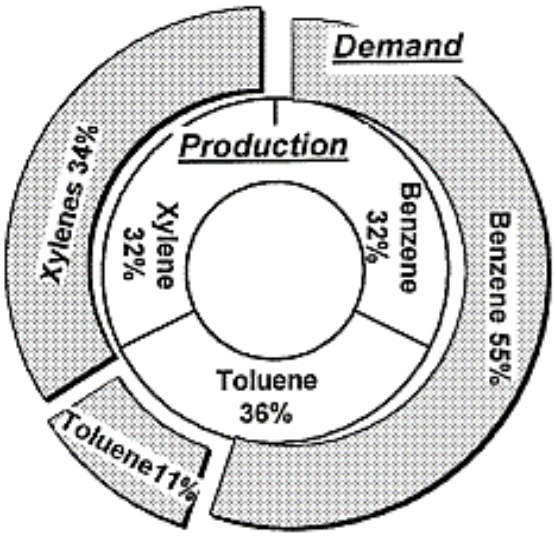

Figure 1-4: BTX worldwide supply and demand [1]

Furthermore, p-xylene is produced in a mixture with less valuable xylene isomers and ethylbenzene. The product stream from the catalytic reformer usually consists of 20 % of p-xylene, o-xylene and ethylbenzene as well as 40 % of m-xylene. Usually p-xylene and some o-xylene are separated through crystallization or adsorption processes. Table 1-1

shows the xylene isomers distribution obtained from the catalytic reforming of naphtha and pygas cut against worldwide demand [8].

Table 1-1: C_8 aromatics distribution from naphtha and pygas compared to worldwide demand [8]

Products	Ethylbenzene	p-xylene	m-xylene	o-xylene
Naphtha reformate C_8 cut	18 %	21 %	41 %	20 %
Pygas C_8 cut	52 %	12 %	25 %	11 %
Worldwide demand	1 %	86 %	3 %	10 %

1.3.2 Transalkylation process

Transalkylation process utilizes a mixture of toluene and C_9 aromatics where methyl group transfer produces benzene and xylene. It offers the use of lower value aromatics from catalytic reforming to maximize the production of the more demanded C_8 aromatics. Therefore, the transalkylation is a favoured process by refineries that produce large amount of C_9 aromatics. Commercial transalkylation such as Tatoray by UOP and TransPlus by ExxonMobil supply about 17 % of p-xylene worldwide production [9]. It was reported that increasing the C_9 aromatics amount in the feed mixture showed a significant enhancement in the total xylene yield at the expense of benzene. Accordingly, the transalkylation process is more suitable than toluene disproportionation for increasing the yield of total xylene in the product stream whereas, toluene disproportionation process increases the p-xylene in the xylene mixture [10].

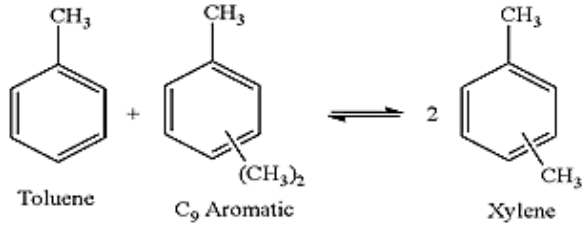

Figure 1-5: Transalkylation of toluene and trimethylbenzene reaction [6]

1.3.3 Toluene disproportionation

Toluene disproportionation is one of the available industrial processes to produce benzene and xylene (Figure 1-6) over an acid catalyst [11,12].

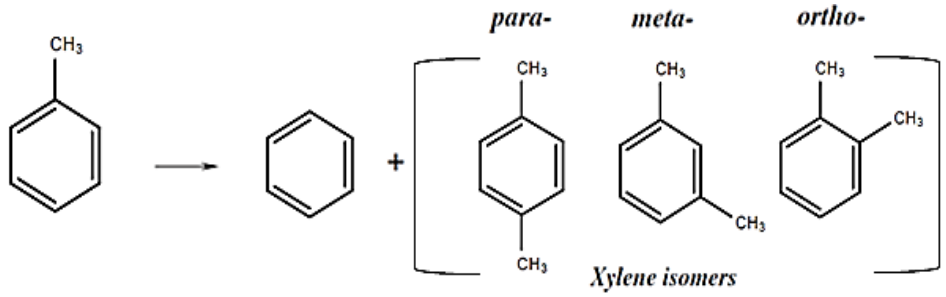

Figure 1-6: Toluene disproportionation over zeolites

One of the advantages of toluene disproportionation is that either zero or a very small amount of ethylbenzene is produced alongside benzene and xylene. The absence of ethylbenzene lowers the cost of xylene isomers recovery and separation [13].

1.4 Research objectives

The purpose of this thesis was to study various modification techniques of ZSM-5 zeolite to enhance p-xylene selectivity in toluene disproportionation using different feed flowrates and reaction pressure. Increasing the diffusion path and deactivating the external acid sites were investigated as possible ways to improve p-xylene selectivity by utilising different synthesis procedures and post modification methods.

Synthesized ZSM-5 zeolites with different crystal sizes (5, 50 and 100) µm were tested for toluene disproportionation to explore the effect of crystal size (diffusion path) on p-xylene selectivity and toluene conversion. Literature suggests that increasing the crystal size improved p-xylene selectivity as longer diffusion paths provide greater diffusion constraints for bulkier molecules and because of the high diffusivity of p-xylene the concentration of m-xylene and o-xylene increases in the channels promoting their isomerisation to p-xylene to diffuse faster resulting in the enhancement of p-xylene selectivity [14]. Isomerisation reaction of the xylenes produced on the external acid sites is fast compared to disproportionation suggesting that although p-xylene is the primary product in the pores of ZSM-5, it will isomerise to o-xylene and m-xylene once it leaves the pores resulting in the thermodynamic equilibrium of (p: m: o = 24: 53: 23) [1].

In this study, deactivation of the external acid sites using different silylation agents, amounts and number of modification cycles was explored to deposit inert silica layer on the surface to suppress the isomerisation reaction. Different loadings of phosphorus were

used in attempt to poison the acid sites on the surface or reduce its strength. Also, lanthanum was impregnated on ZSM-5 in attempt to deactivate the external acid sites alongside narrowing the pore mouth.

Another objective of this thesis was to study the chemical and physical effects imposed on the catalysts by the different modification methods through the application of various characterisation techniques. They include X-ray diffraction (XRD), scanning electron microscopy (SEM), pyridine FTIR, nuclear magnetic residence (NMR) and nitrogen adsorption. These techniques provide fundamental understanding of changes in crystallinity, morphology, acidity, surface area and pore volume and how p-xylene selectivity is affected.

1.5 References

1. Tsai T. Disproportionation and transalkylation of alkylbenzenes over zeolite catalysts. Applied Catalysis A General. 1999;181(2):355–398.

2. Vermeiren W, Gilson JP. Impact of zeolites on the refining and petrochemical industry. Topics in Catalysis. 2009; 52:1131–1161.

3. Jenkins S. Paraxylene – Is the Tail Wagging the Dog. [Presentation] IOC Petrochemical conclave. New Delhi, India; 2013. Available from: http://www.petrochemconclave.com/presentation/2013/Mr.SJenkins.pdf

4. Al-Khattaf S, Ali S, Aitani A, Žilková N, Kubička D, Čejka J. Recent advances in reactions of alkylbenzenes over novel zeolites: The effects of zeolite structure and morphology. Catalysis Review Science and Engineering. 2014; 56:333–402.

5. Polyester fiber market demand to drive global paraxylene growth [Internet]. Icis.com. 2012 [cited 2017 Sep 1]. Available from: https://www.icis.com/resources/news/2012/03/05/9537632/polyester-fiber-market-demand-to-drive-global-paraxylene-growth/

6. Waziri S, Aitani A, Al-Khattaf S. Transformation of toluene and 1,2,4-trimethylbenzene over ZSM-5 and mordenite catalysts: A comprehensive kinetic model with reversibility. Industrial and Engineering Chemistry Research.

2010;49(14):6376–6387.

7. Gentry J, Kumar S, Lee H. Innovations in paraxylene technology. In: 1st Russian petrochemicals technology conference; GTC Technology Corporation: Moscow, 2002.

8. Ashraf M. Analysis and optimization of p-Xylene production process. MSc Thesis. American University of Sharjah; 2013.

9. Perego C, Pollesel P. Advances in aromatics processing using zeolite catalysts. In: Ernst S, editor. Advances in nanoporous materials. 2010. p. 97–149.

10. Wang I, Tsai T, Huang S. Disproportionation of toluene and of trimethylbenzene and their transalkylation over zeolite beta. Industrial and Engineering Chemistry Research. 1990;29(10):2005–2012.

11. Uguina M, Sotelo J, Serrano D. Kinetics of toluene disproportionation over unmodified and modified ZSM-5 zeolites. Industrial and Engineering Chemistry Research. 1993;32(1):49–55.

12. Ali M, Ali S, Al-Nawad K. Disproportionation of toluene: enhanced para-xylene selectivity over modified HZSM-5. Current Catalysis. 2013;2(2):96–110.

13. Kareem A, Chand S, Mishra I. Disproportionation of toluene to produce benzene and p- Xylene - A review. Journal of Scientific and Industrial Research (India). 2001;60(4):319–327.

14. Chen N. Reactions of mixtures of toluene and methanol over ZSM-5. Journal of Catalysis. 1988;114(1):17–22.

Chapter 2 Zeolite structure and catalysis

2.1 Introduction

Zeolites are three dimensional, microporous, crystalline solids with well-defined structures containing aluminium, silicon, and oxygen in their regular framework. Also, cations and water molecules are located in the pores. The history of zeolites began when the first natural zeolite (Stilbite) was discovered by the Swedish mineralogist Cronstedt in 1756. He classified zeolites as new class of hydrated aluminosilicates including alkali and alkaline earth elements. The word zeolite is originated from two Greek words (Zeo) and (lithos) which means to (boil) and (stone) since when heated in a blowpipe they form a frothy mass [1,2]. The microporous properties of natural zeolites and their advantages, such as water adsorption, were gradually identified during the 19^{th} century. More than 40 types of natural zeolite have been discovered and some of them are widely used in the fields of drying and liquid and gas separation, softening of hard water and sewage treatment [3]. The high industrial demand on natural zeolites required the use of synthesized zeolites. The first hydrothermal synthesis of zeolites copying the geothermal formation of natural zeolites was introduced in the 1940s. In 1948, Barrer reported the first definitive synthesis of zeolites including the synthetic correspondent for the zeolite mineral mordenite [4]. Between 1949 and 1954 Milton and Breck discovered several commercially significant zeolites, which are zeolites A, X and Y [1]. In 1962, Mobil Oil introduced the use of zeolite X (FAU) as a refinery cracking catalyst. since then, the use of zeolites as catalysts became a key factor in the refining industry which significantly increased the production efficiency [5]. After this point, the use of zeolites was not limited to the petroleum and petrochemical industry and was introduced to the laundry detergents markets by 1974. In 1978, their selective ion exchange properties were used to clean up water contaminated by radiation in the united states [2].

The period from 1954 to 1980 is considered to be the “golden age” in zeolites development. During this time, zeolites with low, medium and high Si/Al ratios were discovered [3]. Zeolite Y was synthesized by Breck to increase the thermal stability and acidity of zeolites which played a very important role in the catalysis of hydrocarbon conversion processes [6]. In 1972, the most important member of the pentasil zeolite family, ZSM-5, was synthesized by Argauer and Landelt [7]. Later the high Silica Zeolite beta (BEA) was synthesized by Wadlinger and Kerr [8].

2.2 Zeolite structure

Zeolites consist of TO_4 tetrahedra units where T is silica or alumina with oxygen atoms connecting the neighbouring tetrahedral. Zeolites structure contains pores and cavities that are occupied by cations and water molecules. These two molecules move freely inside the cavities allowing ion exchange to take place [9]. In general zeolites can be described by the following formula [10]:

$$M_{x/n}\,[(AlO_2^-)_x\,(SiO_2)_y]\,zH_2O \qquad \text{Eq. 2-1}$$

Where M is a cation to balance the negative charge of the framework and n is the valence for the cation while x, y and z are the total number of aluminate, silicate and water molecules in the unit cell [10].

Many of the zeolite properties could be explained and clarified once the framework type is known. In addition to describing the topology of the framework tetrahedral atoms, the type of zeolite framework defines the pore opening size and shape, the dimensionality of the channel systems and the volume, and organization of the cages [1].

Zeolites are composed of primary and secondary building units as seen in Figure 2-1. The primary building block of a zeolite is tetrahedron of silicon or aluminium ion surrounded by four oxygen anions. These tetrahedra are arranged in a way where each one of the four oxygen anions is shared with another silicon or aluminium tetrahedron. Each silica tetrahedron is electrically neutral as every silicon ion has +4 charge balanced with four tetrahedral oxygen anions. On the other hand, aluminium has +3 charge but bonding to four oxygen anions will lead to a tetrahedron with a charge of -1, so each aluminium tetrahedron needs to be neutralized by a cation with a charge of +1, such as Na^+ [1,10].

The silica and alumina tetrahedra connect to form more complicated secondary units which form the building blocks of a zeolite crystal structure (secondary building unit, SBU). SBUs can be in different simple polyhedral forms such as hexagonal prisms, cubes or octahedra. All known zeolite structures can be described by nine different SBUs. SBUs can be made up of 4, 6 and 8-membered single rings, 4-4, 6-6 and 8-8-member double rings, and 4-4-1 branched rings as seen in Figure 2-1. The final zeolite structure consists of grouped SBUs. For example, FAU zeolites are made of sodalite framework which is built of 4-member ring and 6-member ring building units (Figure 2-1) [11].

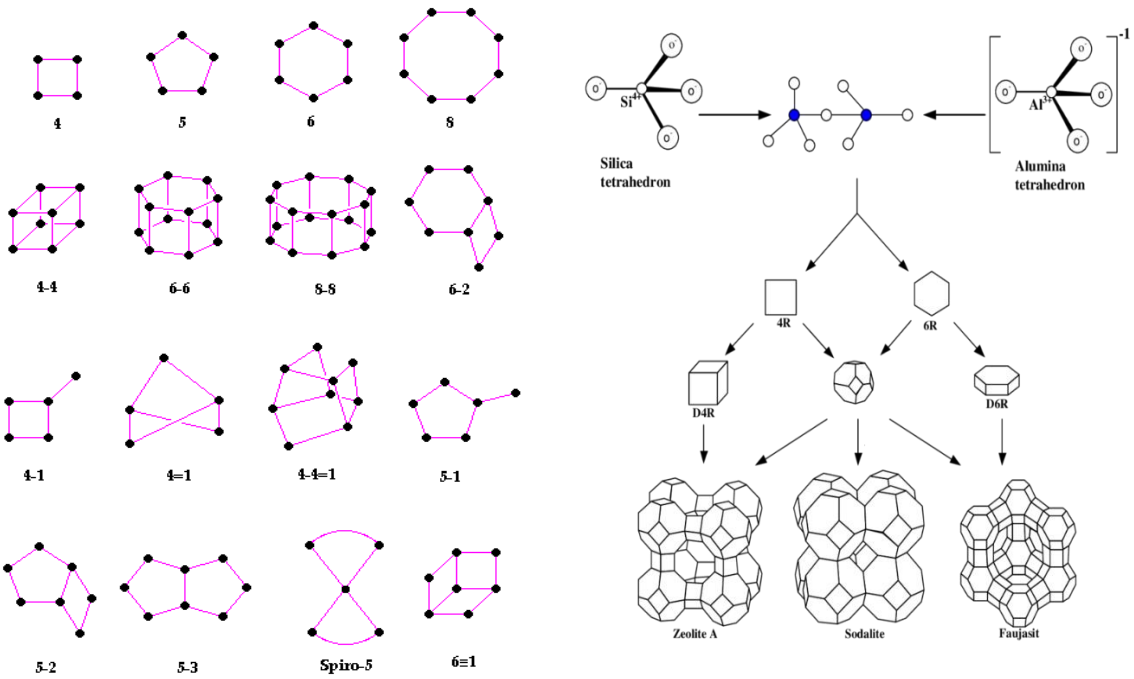

Figure 2-1: (a) SBU (b) assemblage of building units to form zeolite structure [12]

Zeolite structures consists of either internal pore system made of interconnected cages or uniform channels that can consist of one dimensional channel or intersected channel systems. Zeolites with different structures are used for different applications and reactions. They range in pore size from 0.3 nm to 0.8 nm making them molecular sieves for molecules with different sizes. As a result of this characteristic zeolites exhibit an important catalytic function called shape selectivity where steric restrictions are imposed on the formation of bulky transition states. Zeolites in literature are categorized based on their pore size into five categories. They are small pore zeolites with 8 ring pores, medium pores with 10 rings, large pores with 12 membered rings, zeolites with dual pore systems (e.g. mordenite with 12- and 8 – membered rings channels), and mesoporous systems. Figure 2-2 shows pore sizes of zeolites using oxygen packing models [13].

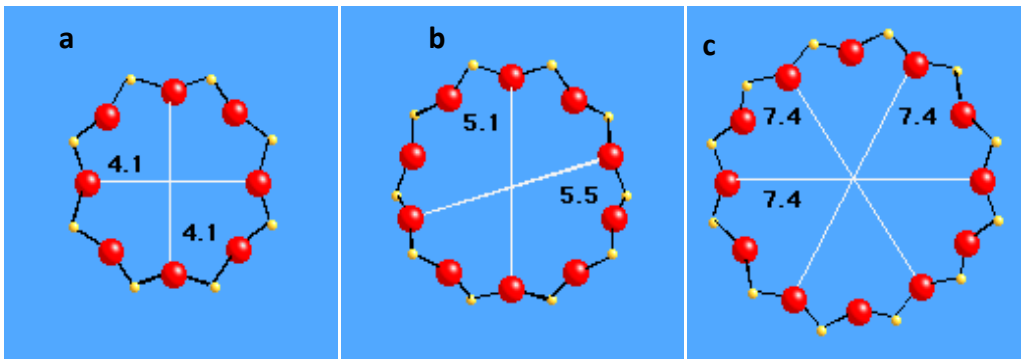

Figure 2-2: Typical pore structure of zeolites (a) small (b) medium (c) large pore size [12].

The international zeolite association (IZA) suggested the use of three letters as an identification code for a zeolite framework type. For example, LTA framework has 3-dimentional channel structure with 8-ring opening, while MFI has a 10-ring opening channel structure, e.g. ZSM-5, and FAU has 12-ring opening channel structure [14].

2.2.1 Medium pore zeolites

Medium pore zeolites exhibit high shape selectivity compared to other zeolites due to their pores openings consisting of 10 membered rings. Also, they have high resistance to coking as their structure does not have any cages and prevents reactions with bulky intermediates. The shape selectivity of medium pore zeolites is measured by the constraint index where values are obtained from n-hexane and 3-methylpentane cracking. Medium pore zeolites usually exhibit constraint index values between 3-12 whilst zeolites with large pores have indices between 1-3 or even less than 1. For instance, ZSM-5 showed a value of 8.3 while the value for zeolite Y and mordenite obtained was 0.5 [15].

2.2.1.1 Zeolite used in this study – ZSM-5

ZSM-5 (Zeolite Socony Mobil -5) is a shape selective catalyst that belongs to the pentasil family synthesised by Mobil. ZSM-5 framework is made of connected pentasil units linked together forming pentasil chains (Figure 2-3). These chains connect via an oxygen bridge forming 3- dimensional MFI structure with 10 ring pores. Moreover, ZSM-5 zeolite structure consists of two intersecting channels with similar pore opening sizes. These two channels are perpendicular to each other and they are straight channels (0.53-0.56 nm) and sinusoidal channels (0.51-0.55 nm). The content of aluminium in ZSM-5 can vary over a wide and hence has a wide range of Si/Al ratios range from around 10 to infinity. The configuration of ZSM-5 has not been reported in any other type of zeolites [16].

ZSM-5 possesses unique shape selectivity because of its 10-membered ring channel system making it a favourite candidate over other zeolites for the cracking of long chain, low-octane number normal paraffins and some olefins in the gasoline fraction [17]. The absence of cages combined with a small entrance in ZSM-5 gives it special coke resistance properties. ZSM-5 is one of the widely utilized catalysts in industry, especially in

petroleum and petrochemical industries such as in isomerization of xylenes, alkylation of toluene with methanol and toluene disproportionation. ZSM-5 zeolite is highly favourable for selective toluene disproportionation reaction to produce p-xylene as a result of the shape selectivity imposed by the pore size (0.51-0.56) nm which is close to the kinetic diameter of para-xylene (0.58 nm) compared to the other xylene isomers (ortho- and meta-) which possess larger kinetic diameters (0.68 nm) hindering their formation and slowing their diffusion through the channels [17].

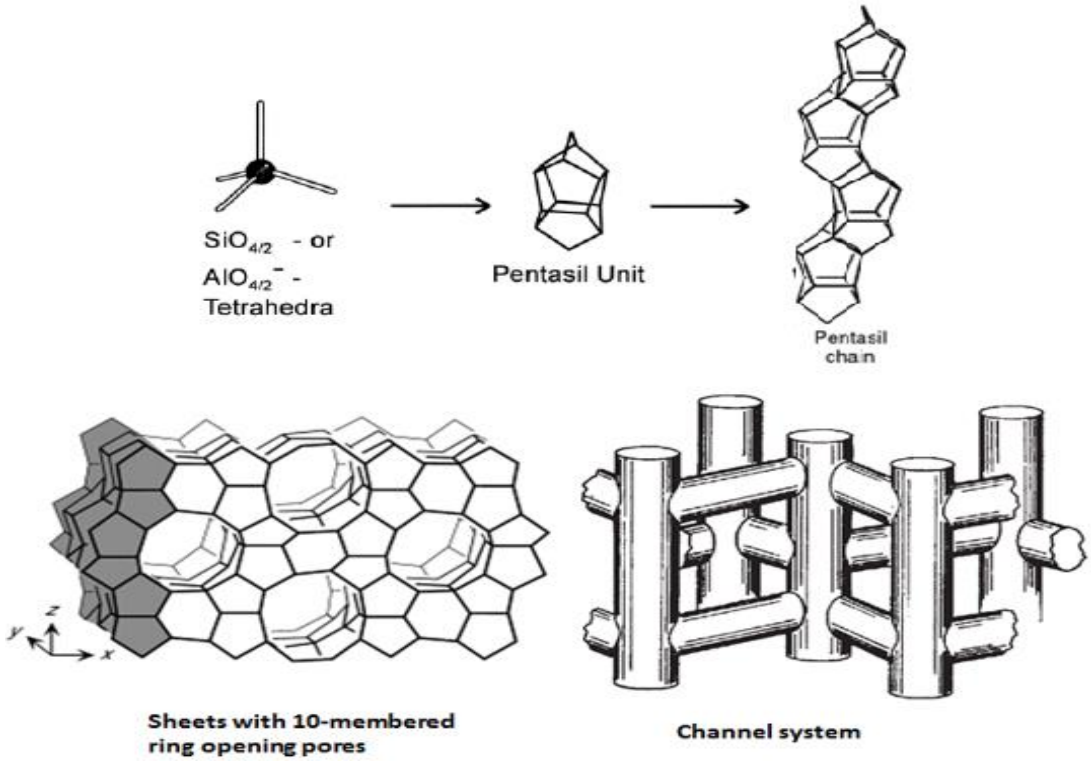

Figure 2-3: ZSM-5 zeolite structure [18]

2.3 Zeolite properties

Zeolites play a key role in catalysis because of their unique properties. Some of these properties are shape selectivity, ion exchange and acidity.

2.3.1 Shape selectivity

The variation of zeolites with different range of pore size between 0.3-0.8 nm makes each zeolite type selective to different molecules. Depending on the size of the molecule, the pore openings and channels will control the diffusion of the reactants, products and transition states. Thus, zeolites are called molecular sieves [19]. There are

three shape selectivity mechanisms imposed by zeolites on molecules as shown in Figure 2-4 and they are:

Reactant selectivity: it occurs when zeolite catalyst excludes some molecules due to their molecular sizes and structures from the channels by acting as a molecular sieve while allowing other less bulky molecules to enter [19].

Product selectivity: product shape selectivity can be looked at as the inverse of the reactant shape selectivity. This happens if the product molecules formed inside the pores are too bulky to diffuse out. They either block the pores leading to the deactivation of the catalyst or they could be converted to less bulky product [19].

Transition state shape selectivity: it occurs when some reactions are prevented from happening because of the corresponding transitions state would require more space than what is available in the channels. However, reactants and products which can diffuse through the pores and reactions that require smaller transition state proceed normally [19].

In the case of zeolites with two intersecting channels with varied sizes molecular, traffic control concept was proposed. In zeolites with this type of framework, smaller channels can be accessed by small molecules formed in catalytic reactions while larger channels are accessible by the large and the small molecules. This concept was first used by Derouane and Gabelica to account for the absence of counter-diffusion effects in the conversion of methanol to hydrocarbons in ZSM-5. They suggested that the smaller molecules such as methanol enter the sinusoidal channels while the heavier hydrocarbon products leave the zeolite through the straight channels as they are a bit larger than the sinusoidal channels [20,21].

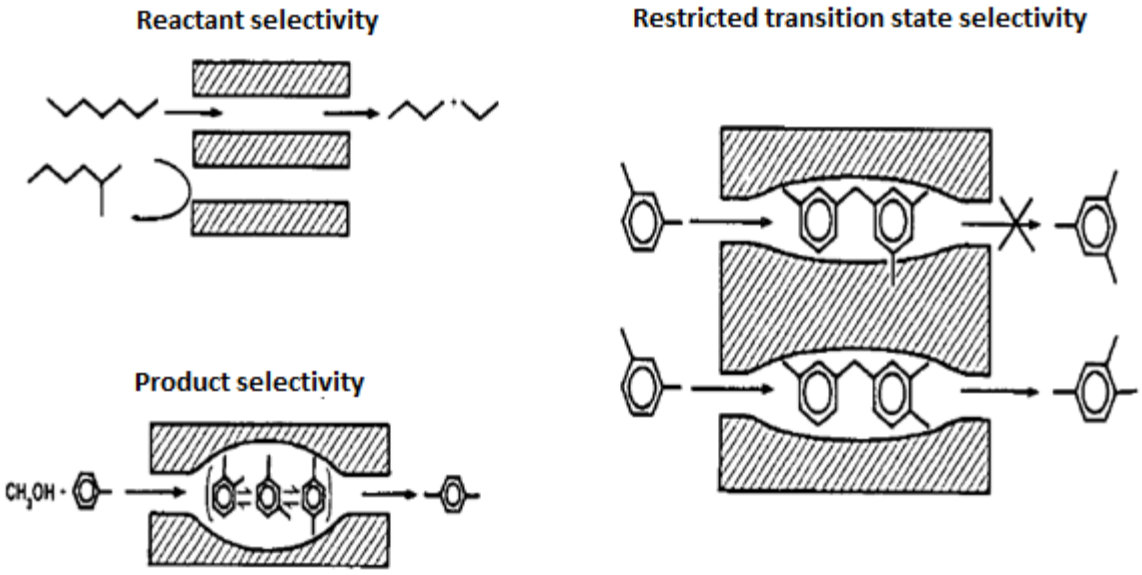

Figure 2-4: Shape selectivity in zeolites [22]

2.3.2 Ion exchange

A zeolite framework is made of SiO_4^{-4} and AlO_4^{-5} tetrahedra sharing oxygen ions leading to the general framework formula $(AlO_2)_x(SiO_2)_{(n-x)}$, where n is the number of tetrahedra per unit cell. Because aluminium is trivalent each (AlO_4) will have a negative charge which is balanced by the positive charge of a cation such as Na^+ during the synthesis process. Zeolites have different ion exchange capacity depending on the chemical composition (Si/Al). Ion exchange usually takes place in aqueous systems. After mixing the zeolite powder in the aqueous solution, ions of the zeolite interact with the solution allowing for the exchange of ions between the solid phase and the solution to occur. Cations are either hydrated or anhydrous [23]. Quaternary ammonium ions are anhydrous and have specific size and the ion exchange will only take place if they are able to enter the pores. Alkali ions are surrounded by a hydration shell. The large hydrated cations will be able to enter the pores after stripping off some water molecules by increasing the temperature while ion exchange with smaller hydrated cations will take place easily. The rate of ion exchange is determined by the concentration of ions having the right size to penetrate the pores of the zeolite. At room temperature, the solution may contain few hydrated ions with a size larger than the pore dimensions which will make the ion exchange rate very slow. However, the ion exchange rate will increase by rising the temperature as water will be stripped from the ions [20].

2.3.3 Acidity

In general, the acidity of zeolites is 1000 times higher than that of amorphous silica-alumina and is related to the content of alumina in the framework [24]. Zeolites have been used in industry as acid catalysts in hydrocracking, isomerization, alkylation and catalytic reforming due to their acidic properties. To describe the acidity of a zeolite properly it is important to understand the nature of the acid sites (Brønsted acid sites and Lewis acid sites) and their strength. The strength of acid sites is reliant on their distribution and location in the framework [25,26].

The generation of active sites is a very important step for the zeolite to be used as a catalyst. This is performed by ion exchanging the zeolite with ammonium hydroxide followed by calcination. The catalytic activity of zeolites is related to the number of Brønsted acid sites in the framework. However, the role of Lewis acid sites cannot be neglected and is still under investigation in the literature [27]. Almutairi et al [28] studied the effect of extraframework aluminium (EFAL) by adding aluminium species to zeolite Y through impregnation method and ion exchange with Al $(NO_3)_3$ and they were compared with commercial USY zeolites. The modification resulted only in small amount of stabilized cationic EFAL species at the exchangeable sites of the zeolite. Testing the modified catalysts for propane cracking, it was found that the higher the ration of cationic EFAL species and Brønsted acid the higher the rate of propane cracking. Brønsted acid sites are proton donors while Lewis sites accept electrons. The Brønsted acid sites are recognized by the bridging hydroxyl groups formed from the oxygen in the framework and the proton (H^+) (Figure 2-5). On the other hand, Lewis acid sites are formed by heating the zeolite to an elevated temperature where protons are lost as water molecules. It was reported that the amount of aluminium in the structure is proportional to the available number of acid sites [27]. The strength of the Brønsted acid sites depends on the number of aluminium atoms that are incorporated in the tetrahedral sites of the framework. Evidence is provided in the literature that the strongest Brønsted acid sites occur in isolated AlO_4 tetrahedra and the strength decreases with increasing adjacent Al atoms. This is why dealumination is used to increase the catalytic activity of zeolites in some cases to create super acid sites [29].

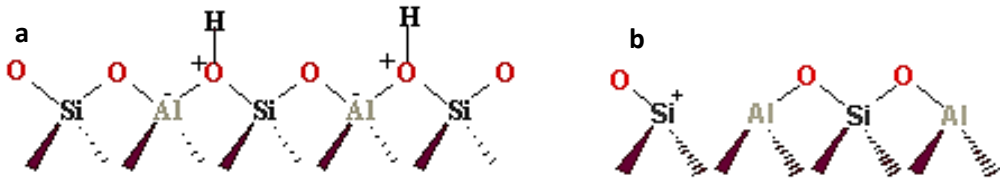

Figure 2-5:(a) Brønsted and (b) Lewis acid sites [30]

2.4 Applications of zeolites

Zeolites are mainly used as adsorbents, catalysts and ion exchange agents. Zeolites are extensively used as catalysts in the petroleum refining, petrochemical productions, coal and fine chemical industries. Also, they are used in the detergent industry and treatment of liquid waste as ion exchange agents.

Zeolite largest economic impact comes from the use in the fluid catalytic cracking (FCC) processes. FCC catalyst account for more than 95% of the zeolite catalyst consumption. The two most important zeolites used in the FCC are Zeolite Y and ZSM-5. Moreover, ZSM-5 is used as octane number booster. Different other zeolites also used to boost the octane number such as mordenite and zeolite beta [20,23].

Recently, technology of hydrocarbon production from methanol was commercialised to produce gasoline, aromatics and olefins [31,32]. Zeolite based materials are the core of this technology. Zeolites are also used in the treatment of car exhaust gases such as NO_x removal [33]. Furthermore, zeolites are being explored for their use in biomass catalysis [31].

Table 2-1: Example of different zeolites used in catalytic processes [34]

Catalyst	Catalytic processes
Zeolite Y	Catalytic cracking, alkylation, hydrocracking
Mordenite	Hydrocracking, hydroisomerization of light alkanes
ZSM-5	Alkylation of aromatics, disproportionation of toluene, isomerization, methanol to olefins reaction, dewaxing
Beta	Transalkylation, benzene alkylation, hydrocracking
ZSM-22	Hydroisomerization of alkenes
MCM-22	Benzene alkylation
SAPO-34	Methanol to olefin

2.5 Hydrothermal synthesis of zeolites

Synthesis of zeolites with micro- and meso- porosity is a subject of high interest as diffusion limitations and "molecules traffic" control can enhance the performance of the catalytic and separation processes. In 1948, the first synthesis of mordenite zeolite was confirmed by Barrer followed by the synthesis of zeolite A, at low temperatures, by Milton and Beck [35]. In the 1960s, Barrer and Denny replaced the use of inorganic bases with organic templates in the synthesis of zeolites. Later, ZSM-5 zeolite was synthesized using an organic template, such as tetrapropylammonium hydrxide (TPAOH), in the synthesis mixture [3]. In the last decade, different new synthetic approaches have been developed to synthesise zeolites with specific properties and structures based on the use of pre-designed organic structure-directing agents [36,37]. On the other hand, the advancement of computer simulation techniques has improved the ability of researchers to hypothetically predict the zeolite structures and obtain structure solutions of complex zeolite structures [36]. The advancement in structures determining and synthesis resulted in discovering new zeolite framework [38]. The international zeolite association approved 50 new framework types since 2007. Some interesting structures having extra-large pores (16-, 20-, and 30-rings) and odd-ring numbers (11- and 15-rings) [36].

The synthesis of zeolites is carried out under hydrothermal conditions utilizing the raw materials shown in Table 2-2 below.

Table 2-2: Synthesis raw materials [24]

Sources	Function
Silicon source	Primary building units of the framework
Aluminium source	
Template	Structure directing agent
Solvent(water)	Acts as a mineralizer
Alkali cation	Works as a counter ion to balances the charge of the framework

Zeolite synthesis is affected by many factors and includes the gel composition, temperature, mineraliser, cation source, solvent, silica and alumina sources, and aging.

Batch composition

The composition of the reactants in the synthesis gel is a key factor in determining the typology of the zeolite. For example, varying the amount of Na_2O, Al_2O_3 and SiO_2 in the gel can lead to the formation of different zeolites although the crystallization conditions are still the same. Figure 2-6 illustrates the different zeolite which could be formed using different gel compositions. Increasing the SiO_2/Al_2O_3 leads to the formation of more siliceous zeolites such as ZSM-5 and mordenite [3].

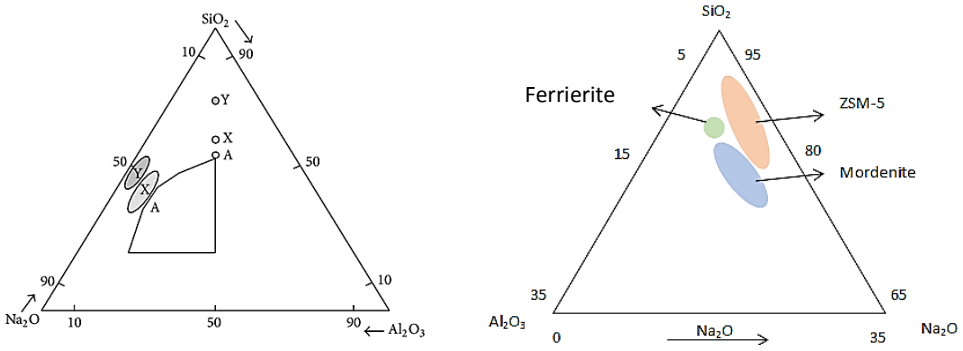

Figure 2-6: Different zeolites synthesis ternary diagrams for starting components [24]

Silica and alumina sources

The physical and chemical nature of the reactants can affect the crystallization significantly. Colloidal silica, sodium silicate and tetraethyl orthosilicate are some of the commonly used silica sources which affect the synthesis in many ways. It was reported that the silicon source surface area can affect the crystal size and crystallization rate of the zeolite. Low surface area sources are difficult to dissolve where the opposite applies to high surface area sources leading to a higher nucleation rate favouring the formation of small crystals. Instead, low surface area source favours the formation of large crystals. The source of alumina can influence the synthesis too. However, the effects are not critical compared to the silica source. Sodium aluminate, aluminium nitrate and aluminium hydroxide are usually used as alumina source in zeolite synthesis [24].

Cation source and templates

In general, an alkali cation such as Na^+ is used to balance the negative charge of the zeolite framework and works as a template or structure directing agent throughout the nucleation and the crystallization processes. Templates can either be organic or

inorganic types. They are implemented to form a certain structure as a result of their geometry [24]. The main sources of inorganic cations are usually alkali metal and alkaline hydroxides. Organic templates are frequently used in the synthesis of more siliceous zeolites such as ZSM-5 with TPAOH and TPABR being the most commonly used organic templates [16]. An important role of organic templates is to enhance the hydrothermal stability of the zeolite by prohibiting the water molecules from entering the pores [39].

Solvent source

Water is the most commonly used solvent in zeolite synthesis. It plays a key role in dissolving the reactants in the presence of a mineraliser (OH^-). The mineraliser enhances the solubility of amorphous silica particles. It also creates a basic environment which boosts the crystal growth rates and reduces the nucleation time. The crystallization time can be altered by controlling the hydroxide concentration in the gel mixture. Increasing the hydroxide content can result in decreasing the SiO_2/Al_2O_3 ratio of the formed crystals. However, increasing the hydroxide content further can lead to the leaching of some alumina from the gel or the solid into the solution [40].

Temperature

Different synthesis temperatures can lead to the formation of different zeolite frameworks. Although it has a significant effect on the crystallization process, nucleation rate is less affected. consequently, It was found that increasing the synthesis temperature results in the formation of large crystals [35].

2.6 Zeolite crystallization

During zeolite synthesis, amorphous phase containing all the synthesis raw materials mixed (Si-source, Al-source, cation and water) forms crystalline aluminosilicate through a sequence of complex chemical reactions. The crystallization mechanism via hydrothermal synthesis was extensively discussed in the literature [41]. Monomers and oligomers are provided by the mineralizing agent formed by dissolving silica and alumina sources in water. These monomers and oligomers arrange into intermediate structure which is followed by the formation of a crystalline phase. Ageing of the gel at room temperature is a crucial step to accelerate the crystallization [41,42].

Crystallization of zeolites involves three steps which are supersaturation, nucleation and crystal growth. Supersaturation occurs during ageing process where the aluminosilicate precursor species concentration increase as the amorphous solid phase is given longer time to dissolve. Aluminosilicate precursor species chemically aggregate which triggers the nucleation process and nucleation is either homogenous or heterogeneous. Heterogeneous nucleation comprises the addition of crystals to the gel via seeding method. This helps in decreasing the crystallization time and growing crystals with high surface area [41,43].

2.7 References

1. Bekkum H, Flanigen E, Jacobs P, Jansen J. Introduction to zeolite science and practice. 2nd ed. Vol 137. Amsterdam; Boston: Elsevier; 2001. p. 11-35.

2. Breck DW. Zeolite molecular sieves: structure, chemistry, and use. New York: Wiley; 1974. p. 1-10

3. Xu R, Pang W, Yu J, Huo Q, Chen J. Chemistry of zeolites and related porous materials : synthesis and structure. Hoboken, NJ: Wiley; 2007. p. 1-18.

4. Cundy CS. Synthesis of zeolites and zeotypes. In: ĈejkaH J, Bekkum V, editors. Zeolites and ordered mesoporous materials: Progress and prospects. Amsterdam: Elsevier; 2005. p. 65–90.

5. Flanigen E, Broach R, Wilson S. Introduction. In: Kulprathipanja S, editor. Zeolites in industrial separation and catalysis. Wiley-VCH Verlag GmbH & Co. KGaA; 2010. p. 1–26.

6. Clough M, Pope J, Xin Lin L, Komvokis V, Pan S, Yilmaz B. Nanoporous materials forge a path forward to enable sustainable growth: Technology advancements in fluid catalytic cracking. Microporous and Mesoporous Materials. 2016;1–14.

7. Vermeiren W, Gilson J. Impact of zeolites on the refining and petrochemical industry. Topics in Catalysis. 2009;52:1131–1161.

8. Van Der W, Bekkum H. Zeolite Beta and its uses in organic reactions. In: Sherrington DC, Kybett AP, editors. Supported catalysts and their applications.

1967. p. 27–37.

9. Richardson J. Principles of catalyst development. Boston, MA: Springer US; 1989. p. 69-82

10. Bartholomew C, Farrauto R. Fundamentals of industrial catalytic processes. Hoboken, NJ, USA: John Wiley & Sons, Inc.; 2006. p. 68-70.

11. Jha B, Singh D. Fly ash zeolites. Singapore: Springer Singapore; 2016. Advanced Structured Materials series. no. 78.

12. Kovo A. Development of zeolites and zeolite membranes from ahoko nigerian kaolin. PhD Thesis. The Universit of Manchester; 2011.

13. Pálinkó I, Kónya Z, Kukovecz Á, Kiricsi I. Zeolites. In: Vajtai R, editor. Springer Handbook of Nanomaterials. Berlin, Heidelberg: Springer Berlin Heidelberg; 2013. p. 819–858.

14. McCusker L, Olson D, Baerlocher C. Atlas of zeolites structures. Amsterdam: Elsevier; 2007.

15. Chen N, Garwood W, Dwyer F. Shape selective catalysis in industrial applications. 2nd ed. New York: Marcel Dekker, Inc; 1996. p. 27.

16. Thomas J, Thomas W. Principles and practice of heterogeneous catalysis. Weinheim, Germany: VCH; 1997.

17. Shaikh I, Shaikh R, Shaikh A, War J, Hangirgekar S, Shaikh AL, et al. H-ZSM-5 zeolite synthesis by sourcing silica from the wheat husk ash: characterization and application as a versatile heterogeneous catalyst in organic transformations including some multicomponent reactions. Journal of Catalysis. 2015;2015:1–14.

18. McCusker L, Baerlocher C. Zeolite structures. In: Bekkum H, Flanigen E, Jacobs P, Jansen J, editors. Introduction to zeolite science and practice. 2001. p. 37–67.

19. Chen N, Garwood W. Industrial application of shape-selective catalysis. Catalysis Reviews. 1986 Jun;28(2–3):185–264.

20. Weitkamp J, Puppe L. Catalysis and zeolites : fundamentals and applications. Berlin: Springer; 1999. p. 347.

21. Csicsery S. Shape-selective catalysis in zeolites. Zeolites. 1984;4(3):202–213.

22. Csicsery S. Catalysis by shape selective zeolites-science and technology. Pure and Applied Chemistry. 1986;58(6):841–856.

23. Dyer A. Zeolite molecular sieves. Advanced Materials. 1989 Jan 1;1(7):149.

24. Maxwell I, Stork W. Hydrocarbon processing with zeolites. In: Bekkum H, Flanigen E, Jacobs P, Jansen J, editors. Introduction to zeolite science and practice. 2nd ed. Amsterdam; New York: Elsevier; 2001.

25. Boronat M, Corma A. Factors controlling the acidity of zeolites. Catalysis Letters. 2015;145(1):162–172.

26. Deka R. Acidity in zeolites and their characterization by different spectroscopic methods. Indian Journal of Chemical Technology. 1998;5(3):109–123.

27. Stöcker M. Gas phase catalysis by zeolites. Microporous and Mesoporous Materials. 2005;82(3):257–292.

28. Almutairi S. The role of Lewis and Brønsted acidity for alkane activation over zeolites. PhD. Technische Universiteit Eindhoven; 2013

29. Huang J, Jiang Y, Marthala V, Thomas B, Romanova E, Hunger M. Characterization and acidic properties of aluminum-exchanged zeolites X and Y. The Journal of Physical Chemistry C. 2008;112(10):3811–3818.

30. Zeolites [Internet]. [cited 2017 Sep 1]. Available from: http://www.catalysis-ed.org.uk/petrol/petrol3_popup.htm

31. Weckhuysen B, Yu J. Recent advances in zeolite chemistry and catalysis. Chemical Society Reviews. 2015;44(20):7022–7024

32. Olsbye U, Svelle S, Lillerud KP, Wei ZH, Chen YY, Li JF, et al. The formation and degradation of active species during methanol conversion over protonated zeotype

catalysts. Chemical Society Reviews. 2015;44(20):7155–7176

33. Beale AM, Gao F, Lezcano-Gonzalez I, Peden CHF, Szanyi J. Recent advances in automotive catalysis for NO_x emission control by small-pore microporous materials. Chemical Society Reviews. 2015;44(20):7371–7405

34. Vermeiren W, Gilson J. Impact of zeolites on the petroleum and petrochemical industry. Topics in Catalysis. 2009;52(9):1131–1161.

35. Barrer R. Hydrothermal chemistry of zeolites. London; New York: Academic Press; 1982.

36. Li J, Corma A, Yu J. Synthesis of new zeolite structures. Chemical Society Reviews. 2015;44(20):7112–7127

37. Moliner M, Rey F, Corma A. Towards the rational design of efficient organic structure-directing agents for zeolite synthesis. Angewandte Chemie International Edition. 2013;52(52):13880–13889.

38. Li Y, Yu J. New stories of zeolite structures: Their descriptions, determinations, predictions, and evaluations. Chemical Society Reviews. 2014;114(14):7268–7316.

39. Kaucic V, Gaspersic S, Hocevar S. Synthesis of ZSM-5 and ZSM-11 zeolites with TBA and TBP cations and their structural characterization. In: Jacobs P, Santen R, editors. Zeolites: facts, figures, future: Proceedings of the 8th international zeolite conference; 1989 July 10-14; Amsterdam, The Netherlands. Elsevier; 1990. p. 311-320

40. Szostak R. Molecular sieves : principles of synthesis and identification. London: Blackie Academic & Professional; 1998. p. 68-70.

41. Knozinger H, Weitkamp J, Ertl G. Preparation of solid catalysts. Wiley VCH; 2008. p. 262-279

42. Cundy C, Cox P. The hydrothermal synthesis of zeolites: precursors, intermediates and reaction mechanism. Microporous and Mesoporous Materials. 2005;82(1–2):1–78.

43. Occelli M, Kessler H. Synthesis of porous materials zeolites, clays, and nanostructures. New York: Marcel Dekker; 1997.

Chapter 3 Toluene disproportionation

3.1 Introduction

As discussed in chapter one, toluene disproportionation is one of the implemented technologies in the industry to meet the demand for p-xylene. Several types of acidic catalysts have been studied for the toluene disproportionation reaction. In the initial stages of alkylation processes, liquid acid catalysts, such as Friedel-Crafts catalysts, hydrofluoric and sulfuric acid were employed [1]. Although these catalysts were efficient, they were corrosive, toxic and difficult to separate and regenerate [2]. Nowadays different acidic zeolites replaced the previous catalysts, such as, mordenite, zeolite Y, and ZSM-5 [3]. In terms of the activity, selectivity and resistance to ageing, synthetic zeolites are better than amorphous silica-alumina and Fredel-Crafts catalysts. However, large-pore zeolites like faujasite (X and Y) and mordenite allow some undesired reactions to take place such as transalkylation of xylenes that will lead to a decrease in the selectivity and the stability of the catalyst [3].

In the 1980s, Mobil developed ZSM-5 zeolite catalyst that offered an excellent performance because of the 10 membered rings channel system and pore size (0.51-0.58 nm) almost matching the size of the main product and reactant molecular diameters (toluene, benzene and xylenes) (Table 3-1). Furthermore, ZSM-5 favours the diffusion of para-xylene molecules over ortho and meta- xylenes. This is a very significant factor making ZSM-5 stand out from the other zeolite catalysts in terms of performance [4]. Nevertheless, for disproportionation of toluene, the xylene isomers produced are usually close to the thermodynamic equilibrium with 24% ortho-xylene, 53% meta-xylene and 23% para-xylene over unmodified ZSM-5 zeolite because of the acid sites situated on the catalyst external surface allowing the isomerization of p-xylene to o-xylene and m-xylene to take place [5].

Table 3-1: Kinetic diameters of molecules close to the pore size of ZSM-5 [6]

Component	Kinetic diameter (Å)
Benzene	5.8
Toluene	5.8
p-xylene	5.8
m-xylene	6.8
o-xylene	6.8

3.2 Toluene disproportionation industrial processes

There are several toluene disproportionation processes available in industry. Among them, the toluene disproportionation process version 3 (TDP-3^{SM}) by Mobil which operates at higher space velocity and lower hydrogen to hydrocarbon ratio compared to the earlier versions. Furthermore, the process showed the closest value of xylene to benzene ratio (1.1:1) to the theoretical number of unity [7].

Fina Oil developed another process in 1980 called T2BX^{SM}. Low WHSV was applied with higher pressure compared to Mobil's process, producing significant amount of C_9 aromatics which are utilized as a stock for gasoline blending [8].

Three p-xylene selective technologies were developed by Mobil and UOP. Mobil selective toluene disproportionation process (MSTDP) is among them [9]. This process involved the use of pre-coked ZSM-5 which enhanced the selectivity towards p-xylene. The first commercial demonstration of the technology in 1988-1990 showed high selectivity towards p-xylene between 85 and 95%. The catalyst life cycle was 500 days [10]. Figure 3-1 shows a simple flow diagram for the MSTDP process.

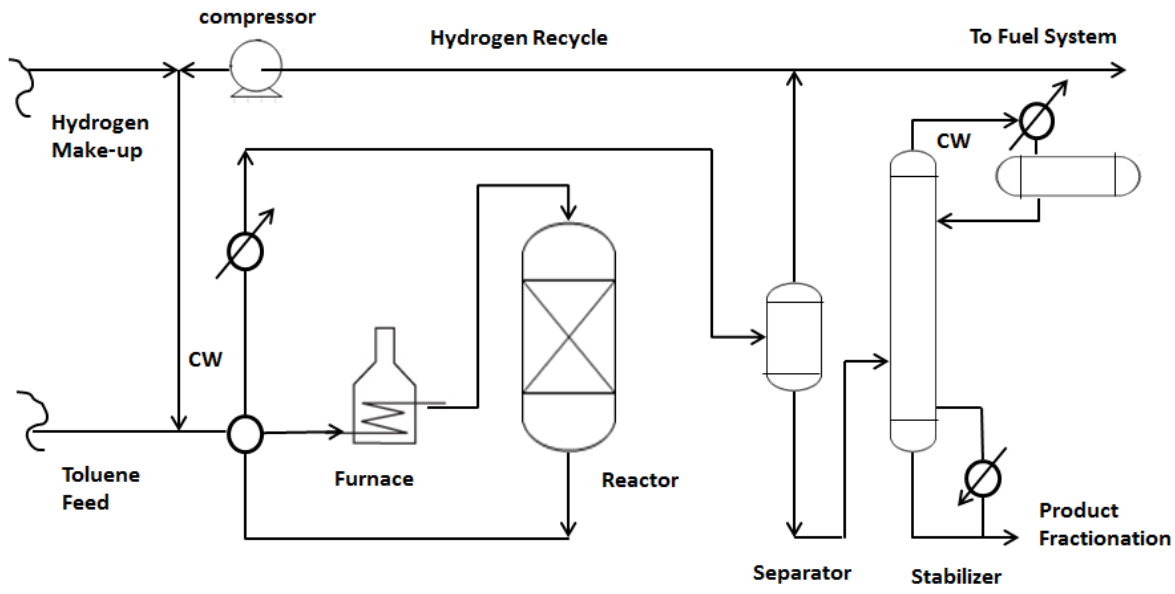

Figure 3-1: Flow diagram for Mobil Selective Toluene Disproportionation [11]

Mobil's Toluene to p-Xylene (MTPX) process and PX-Plus XP process by UOP are the other two p-xylene selective processes. Limited details of the PX-Plus XP process were disclosed to the public [12]. The key factor in this technology is the novel catalyst which offers

improved yields, excellent stability and ease of operation. This technology showed a very high selectivity to para-xylene reaching 90 % and more and also offers higher total xylene yields and higher benzene to xylene ratio [7]. According to the literature a silica modified ZSM-5 catalyst was utilized for the MTPX process [13]. On the other hand, the technique used to modify the catalyst in PX-Plus XP process was not revealed. The PX-Plus XP process is composed of three units; selective toluene disproportionation via PX-Plus unit, recovery of recycled toluene and benzene and finally the single stage crystallization to separate the p-xylene. All three discussed processes yield a mixture of xylene with selectivity towards p-xylene that is higher than thermodynamic equilibrium value. Table 3-2 presents the available details of all discussed processes.

Table 3-2: Summary of toluene disproportionation commercial processes [14]

	Process name				
	TDP-3	MSTDP	MTPX	PX-Plus	T2BX
Catalyst	ZSM-5	Pre-coked ZSM-5	Silica modified ZSM-5	Not disclosed	Not disclosed
Reaction conditions					
Reactor type	Fixed bed	Fixed bed	Fixed bed	Fixed bed	Fixed bed
Temperature (°C)	435	455-470	420	-	390-495
Pressure (bar)	27.5	20-41	20-41	-	48
H_2/HC (mol)	1-2	2-4	2-4	-	4
WHSV (h^{-1})	6	2-4	-	-	1.2-2.3
Conversion	45-50	30	30	30	44
Product selectivity (%)					
C_1-C_5	2.7	6.6	3.7	5.3	8.1
Benzene	42.3	44.9	44.7	46.4	35.0
Xylene	50.4	43.5	48.0	44.7	40.8
Ethylbenzene	1.3	2.5	1.6	1.7	13.7
C_9 aromatics	3.3	2.5	1.6	1.7	13.7
p- Selectivity (%)	25	82	90	90	25
B/X (mol)	1.1	1.3	1.2	1.4	1.1

3.3 Toluene disproportionation reaction mechanism

The product distribution of toluene disproportionation analysed by chromatography analysis revealed the presence of lower alkanes, benzene, xylenes, ethylbenzene and trimethylbenzenes. Accordingly, many researchers have concluded that toluene disproportionation over zeolite catalyst involves primary and secondary reactions shown in Figure 3-2. The obtained components in the product stream indicate that the disproportionation of toluene is the main and primary reaction. Yet, secondary reactions can take place. These reactions include the disproportionation of xylenes to form trimethylbenzenes and toluene, paring reactions to form ethylbenzene, benzene, and lower alkanes. Also, the formation of lower alkanes by benzene hydrocracking [15–17].

Primary reaction

Toluene disproportionation

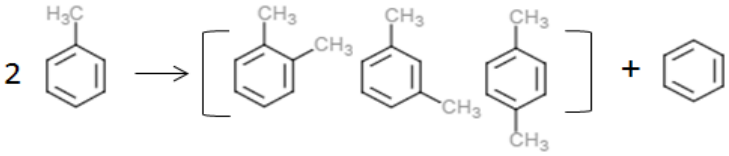

Secondary reactions

Xylene disproportionation

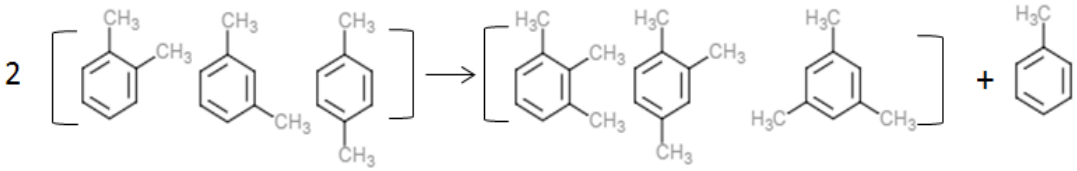

Paring reactions

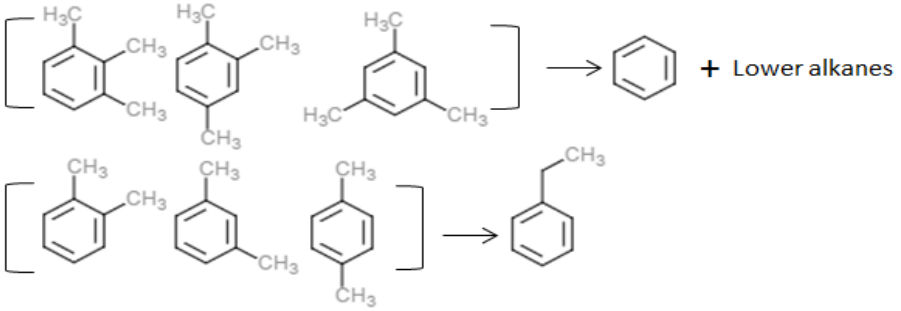

Hydrocracking

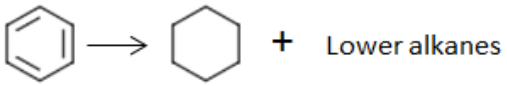

Figure 3-2: Primary and secondary reactions included in TDP [15]

Voloshina et al. confirmed a detailed mechanism for toluene disproportionation and discussed two different reaction pathways [18]. The first one is the mechanism of methyl transfer which requires the formation of methoxy group on the zeolite surface. The other one is the diphenyl methane mechanism [19,20]. In toluene conversion, primary products were shown to be para-xylene and benzene evidenced in short residence time reactions [20].

Protonation of toluene at the methyl group is considered as the first step of the reaction as the only other route possible is the elimination of hydride ion from the methyl group which requires extremely extensive energy. The carbon atom of the methyl group is characterised by excess electron density allowing the protonation to occur [18,21]. This leads to a carbocation process with pentacoordinate carbon atom:

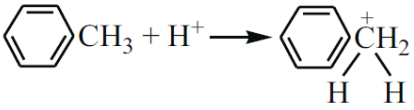

(1)

The loss of a hydrogen molecule in this carbocation can lead to a benzyl carbocation. This is likely to occur if the catalyst has a dehydrogenating metal in the zero-valent state or in presence of Lewis acid sites [22]. Otherwise step (1) carbocation will react with the CH group of the succeeding toluene molecule in the para position bearing some negative charge and form a binuclear activated complex or intermediate assumed to be dominant over ZSM-5 as transition state since it fits well in the zeolite channels [18].

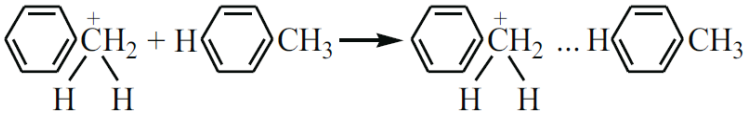

(2)

The carbocation step in the transition state is considerably different than the initial carbocation step. According to Haag and Dessau during the transition state the bond between CH_4^+ and the benzene ring will be weakened promoting the α-scission step [18].

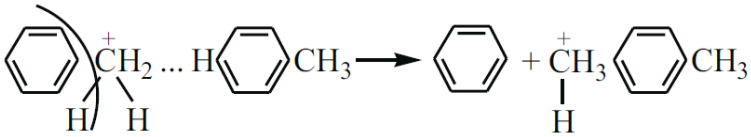

(3)

Finally, the proton will be returned to the catalyst by the carbocation of step (3) promoting the formation of para-xylene [18].

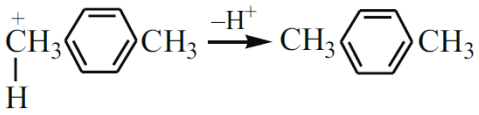

(4)

The formation of ethylbenzene can take place if the second toluene molecule inside the channels had the opposite orientation as the carbon atom of the toluene methyl group bears a negative charge [18].

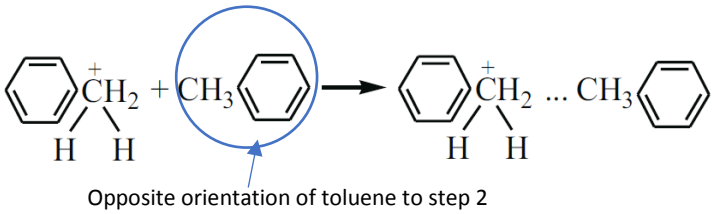

(5)

As seen in step (3), a α-scission step follows. However, this time forming an intermediate for ethylbenzene.

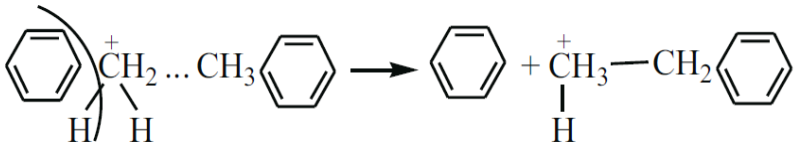

(6)

Returning the proton to the catalyst as in step (4), the neutral product is formed. Also, it is possible for para-xylene intermediate to form through the intermediate of ethylbenzene from step (6) [18]

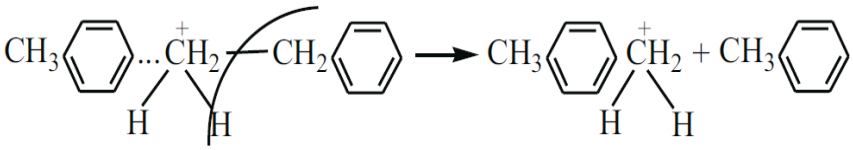

(7)

As para-xylene is produced in higher percentage in C_8 products compared to the ethylbenzene, step (7) is considered to be highly favourable [23].

This proposed mechanism does not take the carbocation of methyl diphenyl methane (MDPM) into consideration which was suggested to be as an intermediate by Xiong et al [19]. The suggestion of MDPM to be an intermediate was based on experimental observations where the addition of diphenyl methane (DPM) to the toluene feedstock increased the toluene conversion. Voloshina et al. argued that probably additional acid

sites are utilized by DPM and eventually initiate a new conversion cycle via the formation of a benzyl carbocation without neither the participation of the catalyst acid sites nor additional contribution of DPM in the reaction [18]. However, toluene conversion dropped back to the initial value after the feeding of DPM was stopped. Thus, another interpretation of DPM role had to be considered. It was speculated that DPM can be considered as a simple coke molecule and it is well established in the literature that carbonium-ion conversions of hydrocarbons are always accompanied by coke formation reactions [24,25]. They compensate the lack of direct contact between the conversion intermediates and the acid sites by enabling hydrogen movements through all reaction chains. Therefore, Voloshina and co-workers concluded that DPM worked as co-catalyst leading to an increase in toluene conversion [18].

3.4 Development of selective toluene disproportionation

Although it is understood that p-xylene is primary product leaving the pore mouth of ZSM-5 zeolite, isomerization takes place on the external surface. This leads to producing xylene isomers in their thermodynamic equilibrium values (24% p-, 54% m- and 22% o-) through toluene disproportionation over ZSM-5. However, it was suggested that deactivating the external acid sites of the zeolite as well as increasing the diffusional path by increasing the crystal size, are crucial factors to exhibit higher p-xylene selectivity than the thermodynamic equilibrium value [26–29]. Deactivation of the external surface will inhibit the secondary isomerization on the surface while the longer diffusion path will increase the diffusion resistance on the undesired isomers where the p-xylene diffusion rate is 1000 times higher than the rest of the isomers [30]. Therefore, increasing the diffusion resistance will generate more diffusion superiority for p-xylene by restricting o-xylene and m-xylene. Olson and Haag investigated the isomerization rate and diffusion rate to improve p-xylene selectivity and they suggested the following criteria [31]:

$$D_p >> D_{m,o} \qquad \text{Eq 3-1}$$

$$K_I \geq D_{m,o} / r^2, \qquad \text{Eq 3-2}$$

$$K_D \leq D_T / r^2, \qquad \text{Eq 3-3}$$

$$(K_I / K_D)\ observed \leq 1, \qquad \text{Eq 3-4}$$

Where D_p, $D_{m,o}$ and D_T are the diffusivities of p-xylene, m-xylene and o-xylene and toluene, respectively. K_I and K_D are the isomerization and disproportionation rate constants, respectively, and r is the crystal size. The intrinsic kinetic rate of isomerization reaction to the disproportionation reaction is calculated to be around 5000 [32]. Alternatively, the observed ratio of K_I/K_D relies on the constraint index. For instance, employing ZSM-5 zeolite in the reaction decreased the K_I/K_D to 360 and it was decreased furthermore to about 2 when using large crystals ZSM-5 [28].

The relationship between p-xylene selectivity and o-xylene diffusion time over large and small crystals ZSM-5 zeolite modified with coke, silica, magnesium, zinc, calcium and boron was investigated by Olson et al. [31] as illustrated in Figure 3-3. The diffusivity was investigated based on the time required to absorb 30 % o-xylene at 120 ˚C. It is observable from the graph that p-xylene selectivity was increased beyond 50 min diffusion time $t_{0.3}$ and large crystal size provided higher p-xylene selectivity than small crystals. The effect of crystal size is furtherly discussed in chapter 6.

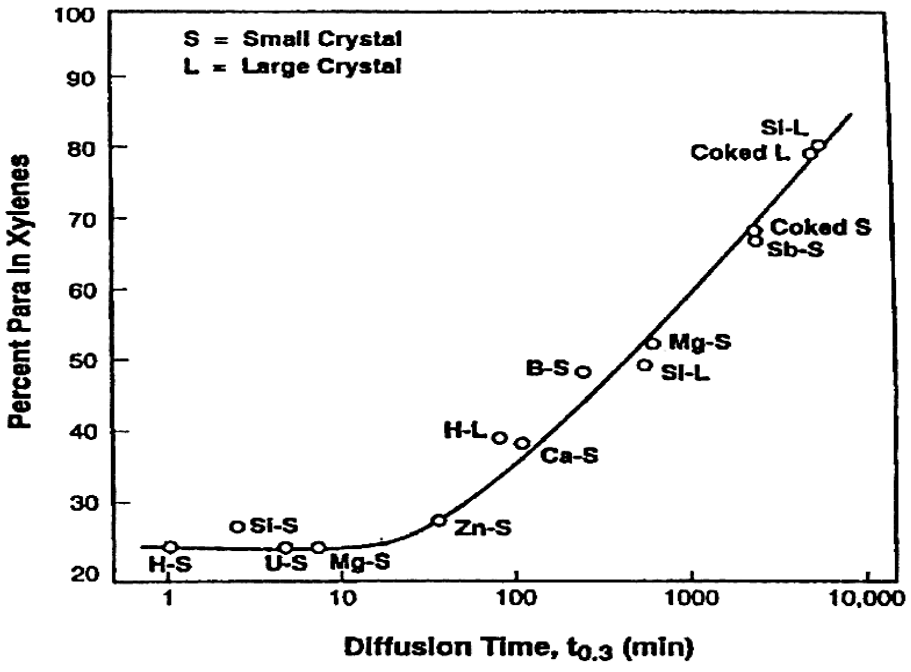

Figure 3-3: Relationship between p-xylene selectivity in toluene disproportionation against time to adsorb 30 % o-xylene at 120 °C [31].

Pre-coking ZSM-5 was one of the earliest techniques used to enhance p-xylene selectivity [33–37]. It was proposed that coke selectively forms on the external surface of the zeolite as shown in Figure 3-4. Therefore, the external acid sites were deactivated and the

isomerization reaction was inhibited. Conversely, Chen et al. suggested that during early time on stream coke forms preferentially on Brønsted acid sites located inside the channels of ZSM-5 [38]. Fang et al. [33] developed a five-stage coking procedure to demonstrate that the nature and location of coke can be varied as shown in Figure 3-5 and it can be observed that it is in agreement with Chen theory were coke initially formed inside the channels.

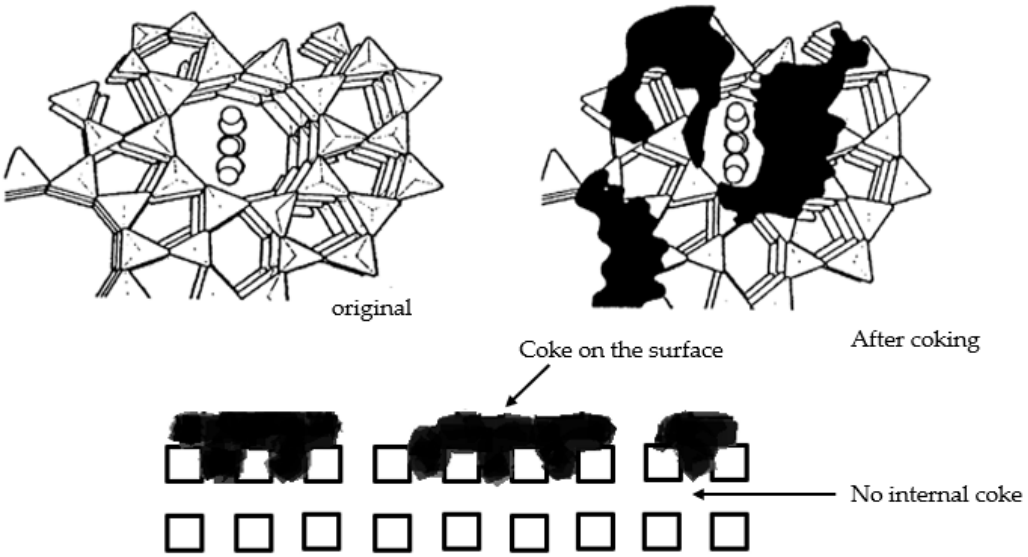

Figure 3-4: Selective coke deposition model modified from [31]

Fang's method involved switching between two different carrier gases, hydrogen and nitrogen while temperature was varied between 480 – 540 ˚C (Figure 3-5). The p-xylene selectivity was enhanced in stage III after 60 hours on stream. It was suggested that during stage I, coke was deposited inside the channels. The carrier gas was switched to hydrogen in stage II which resulted in stripping out the internal coke to the external surface. Stage III used nitrogen and time on stream about 70 hours which resulted in a severe drop in the activity of the catalysts as coke was heavily deposited inside the channels and on the external surface. As in stage II the carrier gas was switched to hydrogen in stage IV and the temperature was increased to 540 ˚C which restored the catalysts activity and high p-xylene selectivity was achieved (50 %). The work of Fang and colleagues illustrated that p-xylene selectivity was improved to 50 % by covering the external surface acid sites with coke. They concluded that in the presence of N_2 as a carrier gas soft volatile coke deposits inside the channels resulted in a decrease in toluene

conversion. However, switching the carrier gas to H_2 removed the internal soft coke. The coke deposited on the external surface during the use of H_2 was mostly hard coke and not easy to remove in H_2 treatment.

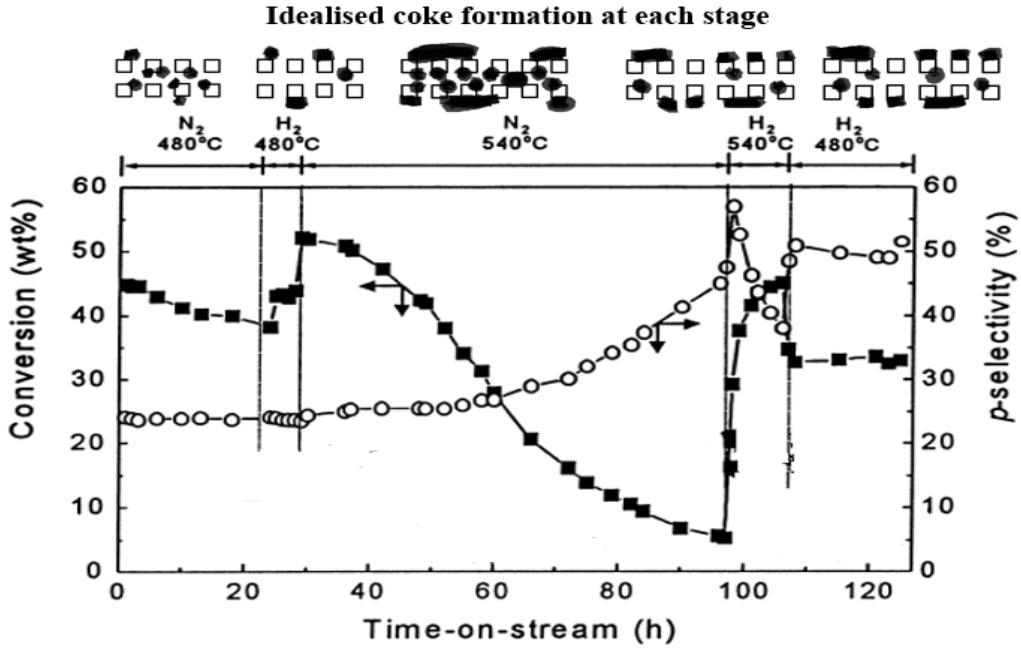

Figure 3-5: Toluene conversion (■) and p-xylene selectivity (○) in toluene disproportionation over ZSM-5 with five stage coke selectivation method; WHSV 6.5 h^{-1}, Pressure 27.6 bar and H_2/HC = 4/1 modified from [33]

Deposition of silica on the external surface of ZSM-5 zeolite is another type of modification implemented in industry. This modification can be achieved either by in situ or ex situ silica impregnation. Silica modification of the catalyst can be performed through in situ technique using chemical vapour deposition method (CVD) [35,39–43]. Moreover, in situ silica deposition can be performed as a separate treatment or simultaneously fed with the reactants. In the case of toluene disproportionation, toluene is co-fed with the silica agent and after reaching the desired p-xylene selectivity and toluene conversion, the silica agent is discontinued. This technique can be followed by ex situ silica modification to optimize the modification through either CVD or chemical liquid deposition (CLD). CLD is an ex situ treatment of the zeolite where mixing the zeolite with a solution containing the desired amount of silica agent was followed by drying and calcination [15,44–46].

Chang et al. [47] impregnated ZSM-5 with different silica compounds such as dimethylphenylmethylpolysiloxane, phenylmethylsilicone (PMS) and dimethylsilicone

(DMS) to increase p-xylene selectivity. Selectivity towards p-xylene achieved by using PMS (86 %) was higher compared to DMS (57 %). However, both maintained a toluene conversion around 30 %. Moreover, it was determined that silica impregnation was a better technique than pre-coking in terms of retaining catalyst activity.

Weber et al. [46] compared the effects of CVD and CLD modification of ZSM-5 (Si/Al = 34) on n-hexane, p-xylene and o-xylene adsorption rates as shown in Table 3-3. The catalyst was mixed for 21 hours with a solution of n-hexane and 5 vol. % tetraethyl orthosilicate (TEOS) at ambient temperature. This was equivalent to 11 % wt. SiO_2 /g ZSM-5. By comparison, the CVD treatment was performed on one gram of ZSM-5 at 400 °C for 8 hours with TEOS using a WHSV of 0.18 h^{-1}.

Table 3-3: Adsorption capacity data over parent and modified ZSM-5 [46]

catalyst	Adsorption capacity (wt. %)		
	n-hexane	p-xylene	o-xylene
ZSM-5 parent	10.3	3.0	2.7
ZSM-5 (CLD) modified	9.7	3.3	2.3
ZSM-5 (CVD) modified	9.6	2.9	0.7

The data presented in Table 3-3 demonstrated a big drop in o-xylene adsorption capacity over the CVD modified catalyst. This decrease was thought to come about because the deposition was fast and less selective leading to serious pore blocking while leaving the external surface of the catalyst non-uniformly covered. However, both modified catalysts were subjected to 4-methylquinoline TPD tests and the data showed similar acidity results [46]. Furthermore, the CLD modification can be improved by increasing the amount of silica deposited and the number of deposition cycles.

Das et al. [48] carried out in situ silica CVD modification over ZSM-5 zeolite however at a much lower catalyst bed temperature (230 ˚C) while feeding a toluene: methanol solution containing 6.5% TEOS (approximately equivalent to 16 wt. % SiO_2/g ZSM-5). Toluene disproportionation was performed over this catalyst at 500 ˚C and very slow flowrate of toluene (WHSV = 0.87 h^{-1}) showed 88 % p-xylene selectivity and 23 % toluene conversion.

In another study, Zhu et al. [44] investigated the effect of silica CLD modification. ZSM-5 zeolite with Si/Al ratio 24 was modified with polydimethylsiloxane (PDMS). A mixture of hexane and 10 wt. % PDMS to ZSM-5 were stirred for 4 hours. Then, the catalyst was dried and finally calcined at 550 ˚C. The process was repeated four times to achieve four deposition cycles. Toluene disproportionation was carried out at 430 ˚C and a pressure of 30 bar. Selectivity to p-xylene was 96 % with toluene conversion of 27 % wt.

It can be concluded from the studies above that both CVD and CLD silica modifications can improve p-xylene selectivity by deactivating the external acid sites and narrowing the pores. However, CLD could be more favourable industrially as CVD method suffers from poor reproducibility and potential as well as energy cost and more complex scalability.

The effectiveness of the CLD method on p-xylene selectivity and the mechanism of silica deposition on the acid sites of ZSM-5 are discussed further in chapter 7.

In conclusion, ZSM-5 zeolite was chosen for this work because it exhibits shape selectivity towards p-xylene as a result of the straight and sinusoidal channels having pore sizes around (0.51-0.56) nm which are close to the kinetic diameter of para-xylene (0.58 nm). On the other hand, the other xylene isomers (ortho- and meta-) possess larger kinetic diameters (0.68 nm) hindering their formation and slowing their diffusion through the channels favouring the production of p-xylene. However, the external acid sites should be deactivated using different modifications to suppress the fast isomerisation of p-xylene to the other isomers on the surface. Different selective toluene disproportionation processes are already implemented in industry including MSTDP, MTPX by Mobil and PX-Plus by UOP. These processes deliver high p-xylene selectivity (80 – 90%) and sensible toluene conversion (20-30%) using modified ZSM-5 zeolite. However, it was mentioned earlier in this chapter that demand will outgrow supply in the next ten years and plants are operating at maximum capacity. This work addresses the use of different modification techniques to ZSM-5 zeolite in attempt to achieve high p-xylene selectivity and industrial toluene conversion.

3.5 References

1. Gerritsen LA, Jong W, Berg V, Aneke L. The disproportionation of toluene over a HY / B -AIF3 / Cu catalyst. Journal of Catalysis. 1979;6(59):26–36.

2. Weitkamp J, Traa Y. Isobutane/butene alkylation on solid catalysts. Where do we stand?. Catalysis Today. 1999;49:193–199.

3. Hegedus LL, Aris R. Catalyst design : progress and perspectives. New York: Wiley; 1987.

4. Shah DB, Guo CJ, Hayhurst DT. Effect of structural heterogeneity on the diffusion of aromatic hydrocarbons in large silicalite crystals. Studies in Surface Science and Catalysis. 1993;80:575–582.

5. Ashraf MT, Chebbi R, Darwish NA. Process of p-Xylene production by highly selective methylation of toluene. Industrial and Engineering Chemistry Research. 2013;52:13730–13737.

6. Jae J, Tompsett GA, Foster AJ, Hammond KD, Auerbach SM, Lobo RF, et al. Investigation into the shape selectivity of zeolite catalysts for biomass conversion. Journal of Catalysis. 2011;279(2):257–268.

7. Viswanathan B, Sivasanker S, Ramaswamy A V. Catalysis : principles and applications. New Delhi: Narosa Publishing House; 2007. p. 245-246.

8. Hattori H, Ono Y. Solid acid catalysis : from fundamentals to applications. Singapore: Pan Stanford Publishing; 2015. p. 356-357.

9. China Petroleum & Chemical Corporation. Process for selective disproportionation of toluene and disproportionation and transalkylation of toluene and C9+ aromatics. US; US6774273 B2, 2004.

10. Weitkamp J, Puppe L. Catalysis and zeolites : fundamentals and applications. Berlin: Springer; 2010. p. 520-521.

11. Chen NY, Degnan Jr. TF, Smith CM. Molecular transport and reaction in zeolites : Design and application of shape selective catalysts. New York, NY; Weinheim; Cambridge: VCH; 1994. p. 284.

12. Welfare H. Synthetic zeolites and other microporous oxide molecular sieves. Proceedings of the National Academy of Sciences of the United States of America;

1999;96:3471–3478.

13. Rase HF. Handbook of commercial catalysts : heterogeneous catalysts. Boca Raton: CRC Press; 2000. p. 31.

14. Tsai T. Disproportionation and transalkylation of alkylbenzenes over zeolite catalysts. Applied Catalysis A General. 1999;181(2):355–398.

15. Ali MA, Ali SA, Al-Nawad K. Disproportionation of toluene: enhanced para-xylene selectivity over modified HZSM-5. Current Catalysis. 2013;2(2):96–110.

16. Kareem A, Chand S, Mishra IM. Disproportionation of toluene to produce benzene and p- Xylene - A Review. Journal of Scientific and Industrial Research (India). 2001;60(4):319–327.

17. Fechete I, Dumitriu E, Caullet P, Lutic D, Kessler H. Synthesis and physicochemical characterisation of (Si, Ga) -MCM-22 zeolite . Toluene disproportionation reaction. Scientific Study and Research. 2007;(4):355–368.

18. Voloshina YG, Patrilyak LK, Ivanenko V V., Patrilyak KI. Mechanism for selective para-disproportionation of toluene on pentasil-based catalysts. Theoretical and Experimental Chemistry. 2009;45(4):263–266.

19. Xiong Y, Rodewald PG, Chang CD. On the mechanism of toluene disproportionation in a zeolite environment. Journal of American Chemical Society. 1995;117(37):9427–9431.

20. Čejka J, Wichterlová B. Acid-catalyzed synthesis of mono- and dialkyl benzenes over zeolites: active sites, zeolite topology, and reaction mechanisms. Catalysis Reviews. 2002;44(3):375–421.

21. Demuth T, Raybaud P, Lacombe S, Toulhoat H. Effects of zeolite pore sizes on the mechanism and selectivity of xylene disproportionation - A DFT study. Journal of Catalysis. 2004;222(2):323–337.

22. Patrilyak LK, Manza IA, Vypirailenko VI, Korovitsyna AS, Likhnevskii R V. Study of the mechanism of hexane isomerization under micropulse conditions. Theoretical and

Experimental Chemistry. 2003;39(4):263–267.

23. Voloshina YG, Ivanenko V V., Patrilyak LK, Patrilyak KI, Manza IA, Ionin VA. Peculiarities of disproportionation of toluene on acidic pentasil zeolites. Theoretical and Experimental Chemistry. 2009;45(2):118–121.

24. Wang B, Manos G. A novel thermogravimetric method for coke precursor characterisation. Journal of Catalysis. 2007;250(1):121–127.

25. Magnoux P, Guisnet M. Coking, ageing and regeneration of zeolites. Applied Catalysis. 1988 Apr;38(2):341–352.

26. Chen NY, Kaeding WW, Dwyer FG. Para-directed aromatic reactions over shape-selective molecular sieve zeolite catalysts. Journal of American Chemical Society. 1979;101(22):6783–6784.

27. Kaeding WW, Chu C, Young LB, Butter SA. Shape-selective reactions with zeolite catalysts. II. Selective disproportionation of toluene to produce benzene and p-Xylene. Journal of Catalysis. 1981;69(2):392–398.

28. Young LB, Butter SA, Kaeding WW. Shape selective reactions with zeolite catalysts III. Selectivity in xylene isomerization, toluene-methanol alkylation, and toluene disproportionation over ZSM-5 zeolite catalysts. Journal of Catalysis. 1982;76(2):418–432.

29. Ratnasamy P, Babu GP, Chandwadkar AJ, Kulkarni SB. Influence of crystal size of HZSM-5 on activity and shape selectivity in xylene isomerization. Zeolites. 1986;6(2):98–100.

30. Al-Khattaf S. Xylenes reactions and diffusions in ZSM-5 zeolite-based catalyst. Industrial and Engineering Chemistry Research. 2007;46(1):59–69.

31. Olson DH, Haag WO. Structure-selectivity relationship in xylene isomerization and selective toluene disproportionation. American Chemical Society journal. 1984;248:275–307.

32. Venuto PB. Organic catalysis over zeolites: A perspective on reaction paths within

Microporous and Mesoporous Materials. 1994;2(5):297–411.

33. Fang L, Liu S, Wang I. Enhanced para-selectivity by selective coking during toluene disproportionation over H–ZSM-5 zeolite. Journal of Catalysis. 1999;185(1):33–42.

34. Chen W, Bauer F, Bilz E, Freyer A, Huang S, Lai C, et al. Acidity characterization of H-ZSM-5 catalysts modified by pre-coking and silylation. Studies in Surface Science and Catalysis. 2004;154: 2269-2274.

35. Chen W, Tsai T, Jong S, Zhao Q, Tsai C, Wang I, et al. Effects of surface modification on coking, deactivation and para-selectivity of H-ZSM-5 zeolites during ethylbenzene disproportionation. Journal of Molecular Catalysis A, Chemical. 2002;181(1–2):41–55.

36. Uguina M, Serrano D, Van Grieken R, Venes S. Adsorption, acid and catalytic changes induced in ZSM-5 by coking with different hydrocarbons. Applied Catalysis A, General. 1993;99(2):97–113.

37. Kaeding WW, Chu C, Young L, Weinstein B, Butter S. Selective alkylation of toluene with methanol to produce para-xylene. Journal of Catalysis. 1981;67(1):159–174.

38. Chen W, Jong S, Pradhan A, Lee T, Wang I, Tsai T, et al. Coking and deactivation of H-ZSM-5 zeolites during ethylbenzene disproportionation: formation and location of coke. Journal of the Chinese Chemical Society. 1996;43(4):305–313.

39. Niwa M, Kawashima Y, Hibino T, Murakami Y. Mechanism of chemical vapour deposition of silicon alkoxide on mordenites. Journal of the Chemical Society, Faraday Transactions. 1988;84(12):4327–4336.

40. Manstein H, Möller K, Böhringer W, O'Connor C. Effect of the deposition temperature on the chemical vapour deposition of tetraethoxysilane on ZSM-5. Microporous and Mesoporous Materials. 2002;51(1):35–42.

41. Weber R, Möller K, Unger M, O'Connor C. The chemical vapour and liquid deposition of tetraethoxysilane on the external surface of ZSM-5. Microporous and Mesoporous Materials. 1998;23:179–187.

42. Hibino T, Niwa M, Murakami Y. Inactivation of external surface of mordenite and ZSM-5 by chemical vapor deposition of silicon alkoxide. Zeolites. 1993;13(7):518–523.

43. Shaikh R, Hegde S, Behlekar A, Rao B. Enhancement of acidity and paraselectivity by the silynation in pentasil zeolites. Catalysis Today. 1999;49(1):201–209.

44. Zhu Z, Xie Z, Chen Q, Kong D, Li W, Yang W, et al. Chemical liquid deposition with polysiloxane of ZSM-5 and its effect on acidity and catalytic properties. Microporous and Mesoporous Materials. 2007;101:169–175.

45. Zheng S, Heydenrych H, Röger H, Jentys A, Lercher J. On the enhanced selectivity of HZSM-5 modified by chemical liquid deposition. Topics in Catalysis. 2003;22(1–2):101–106.

46. Weber R, Möller K, O'Connor C. The chemical vapour and liquid deposition of tetraethoxysilane on ZSM-5, mordenite and beta. Microporous and Mesoporous Materials. 2000;35–36:533–543.

47. Mobil Oil. Catalyst and process for the selective production of para-dialkyl substituted benzenes. US; US5243117 A, 1993.

48. Das J, Bhat Y, Halgeri A. Selective toluene disproportionation over pore size controlled MFI zeolite. Industrial and Engineering Chemistry Research. 1994;33(2):246–250.

Chapter 4 Experimental methodology and characterization techniques

4.1 Introduction

Materials and chemicals used for zeolite synthesis, post modification and toluene disproportionation experiments are listed, and various techniques utilized to characterize the parent and modified catalysts are reviewed in this chapter. The in-house syntheses of ZSM-5 zeolites with different crystal sizes and Si/Al ratios are described along with its different post modification methods used. In this study, toluene disproportion was performed over different parents and modified ZSM-5 zeolites in a fixed bed reactor at atmospheric and 10 bar pressures to achieve high p-xylene selectivity and satisfactory toluene conversion. Temperature was kept constant at 475 °C and a range of toluene weight hourly space velocity (WHSV) (3 - 80) h^{-1} was investigated.

4.2 Materials

Commercial ZSM-5 zeolites as well as several materials used in this study to synthesize and modify zeolite catalysts for toluene disproportionation reaction are listed in Table 4-1.

Table 4-1: Materials used in the zeolite synthesis, post modifications and catalytic testing

Material	Supplier
Commercial ZSM-5 Zeolite	
NH_4ZSM-5 (SiO_2/Al_2O_3 = 50)	Alfa Aesar
Chemicals used for the In - house synthesis of Na-ZSM-5	
Sodium Aluminate ($NaAlO_2$)	Sigma-Aldrich
Sodium Hydroxide (NaOH) ≥ 98 %	Sigma-Aldrich
Tetrapropyl ammonium hydroxide (TPAOH) (1 M in aqueous solution)	Sigma-Aldrich
Tetrapropyl ammonium bromide (TPABr) ≥ 98 %	VWR
Ludox AS-40 (40 wt. % in H_2O)	Sigma-Aldrich
Chemicals used for the post - synthesis modification of ZSM-5 zeolites	
Ammonium nitrate (NH_4 NO^-_3) 99.99 %	Sigma-Aldrich
Tetraethyl orthosilicate (TEOS) 99.99 %	Sigma-Aldrich
3-Aminopropyl triethoxysilane (APTES) 99 %	Sigma-Aldrich
Cyclohexane 99.9 %	Sigma-Aldrich
Phosphoric acid (H_3PO_4) 85 wt. % in H_2O	Sigma-Aldrich
Lanthanum nitrate hexahydrate ($La(NO_3)_3 \cdot 6H_2O$) 99.99 %	Sigma-Aldrich

4.3 Catalyst preparation

4.3.1 Hydrothermal synthesis of ZSM-5 zeolite

4.3.1.1 ZSM-5 with 5 µm crystal size

NaZSM-5 (Si/Al=16) was synthesized using feedstock and seeding gels in order to produce the ZSM-5 with 5 µm crystals as shown in Figure 4-1 [1]. The seeding gel was prepared using colloidal silica (Ludox AS-40), sodium Hydroxide, tetrapropylammonium hydroxide (TPAOH) and deionised water according to a gel molar ratio of Na_2O: 3 TPAOH: 60 SiO_2: 1200 H_2O. Aging of the seeding gel was performed at 100 °C overnight. The feedstock was prepared by mixing sodium aluminate ($NaAlO_2$), sodium hydroxide (NaOH) and colloidal silica in deionised water according to the gel composition 6 Na_2O: 2 Al_2O_3: 60 SiO_2: 1916 H_2O. The seeding gel was added to the feedstock gel and poured into a PTFE-lined autoclave. The autoclave was placed in an oven at 180 °C for 24 hrs. The autoclave was then cooled, and the resulted solid was washed, filtered and dried at 120 °C. Then, heated in a muffle furnace slowly at a rate of 3 °C/min to 550 °C and held for 8 hours to remove the template. The synthesised zeolite was ion exchanged as discussed in section 4.3.2.1. Finally, the ammonium form of ZSM-5 was calcined at 550 °C for 8 hours to generate H-ZSM-5.

4.3.1.2 ZSM-5 with 50 µm and 100 µm crystal size

The synthesis was performed in a PTFE-lined autoclave at 170 °C for 10 days following Chen et al. procedure [2] – shown in Figure 4-2. The materials used in the synthesis are colloidal silica (Ludox AS-40), $Al(OH)_3$, tetrapropylammonium bromide (TPABr), NaOH, potassium hydroxide (KOH), ammonium carbonate [NH_4HCO_3 . NH_2COONH_4] and distilled water. To obtain $NaAlO_2$ solution, the required amount of $Al(OH)_3$ was mixed with NaOH and distilled water and placed in an autoclave which was kept in an oven at 170 °C overnight. NaOH and KOH were dissolved in 80 % of the water amount required for the synthesis. Ludox was added drop wise to this solution and kept stirring for 1 hour. The $NaAlO_2$ solution was added to 10 % of the water used in this synthesis and the ammonium carbonate was diluted in the final 10 % of the water. After that, the TPABr, $NaAlO_2$ and ammonium carbonate were added to the silicate solution. The obtained gel with molar ratios (51 SiO_2: $NaAlO_2$: 9 NaOH: 0.5 KOH: 12 TPABr: 9 NH_4HCO_3 NH_2COONH_4: 1300 H_2O) was aged overnight at room temperature. Then, transferred to

an autoclave and placed in the oven at 170 °C under autogenous pressure for 10 days. The final product was filtered, washed with distilled water, dried and then calcined at 550 °C in a muffle furnace for 8 hours. The 100 µm crystals were generated while the intention was to reproduce ZSM-5 with (50 µm). However, old silica source was used, and it could be that the silica particles were not well dissolved in the solution. This allowed the soda (Na_2O) to make the crystals grow faster during the earlier days of the synthesis. Finally, the undissolved silica particles were used at the end of the synthesis which allowed the crystals to grow further.

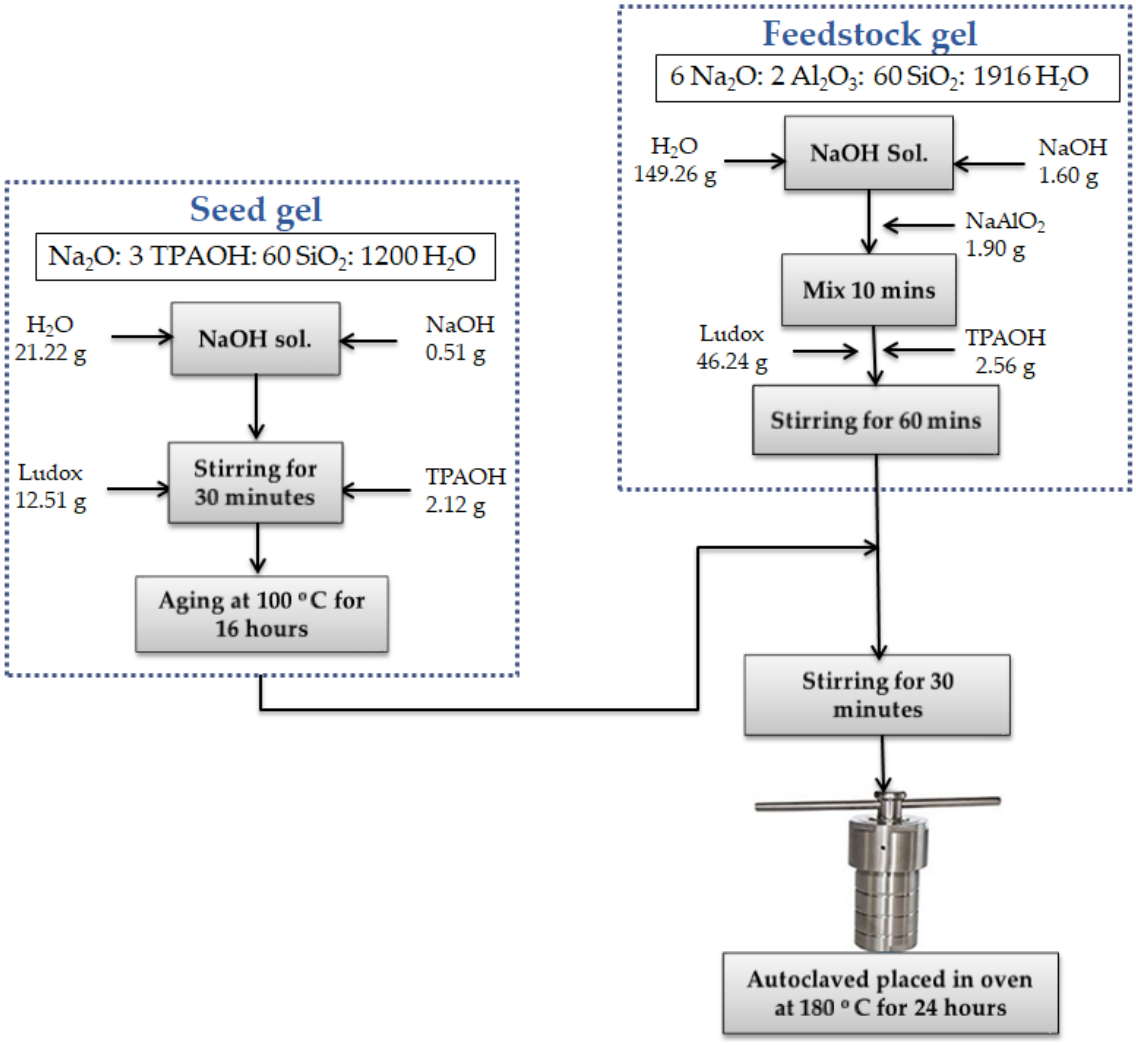

Figure 4-1: Schematic of synthesis procedure for ZSM-5 (5 µm)

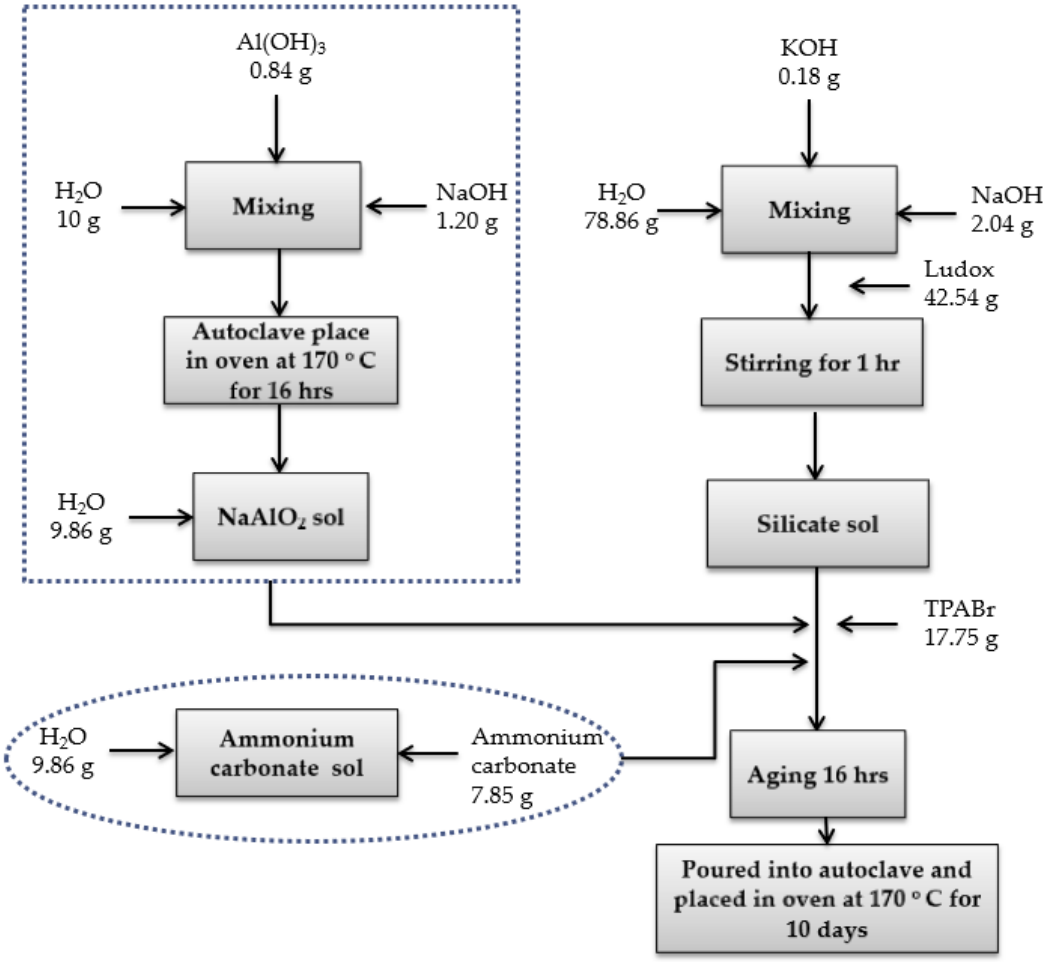

Figure 4-2: Schematic of synthesis procedure for ZSM-5 (50 µm) and (100 µm)

4.3.2 Post modification techniques

Different post modification methods of zeolites were proposed to achieve higher selectivity towards p-xylene whilst maintaining toluene conversion. Usually the purpose of zeolite modification for toluene disproportionation reaction is to passivate the external acid sites located on the surface of the ZSM-5 zeolite to suppress the isomerization of the product, p-xylene. In addition, narrowing the pores is another possible outcome of the zeolite modification which imposes more constraints on the diffusivity of m-xylene and o-xylene [3]. To increase the selectivity towards p-xylene, ZSM-5 was modified in several ways following the literature. Pre-coking, chemical liquid deposition of organosilicon compounds such as (tetraethyl orthosilicate) and the addition of different elements and metals such as phosphorus and lanthanum were used to passivate the external undesirable acid sites and narrow the pores of the zeolite to increase the selectivity towards p-xylene [4].

4.3.2.1 Ion exchange

Ion exchange is performed by mixing the zeolite in a salt solution to generate the Brønsted acid sites in zeolites. After synthesis, the sodium ions should be exchanged with ammonium ions and then calcined at elevated temperature to transform the zeolite to the hydrogen form.

All synthesized zeolites in this study were obtained in the Na^+ or K^+ form and had to be ion exchanged with ammonium nitrate solution to attain the ammonium form. Each zeolite (typically 1 g) was mixed with 100 ml of 1 M NH_3NO_3 (aq) and stirred at 40 °C for three hours. The ion exchange process was repeated three times and finally each catalyst was filtered, washed with deionised water and dried overnight at 100 °C.

4.3.2.2 Silylation

Silylation is the process of impregnating the surface of the catalyst with an amorphous silica layer using an organosilicon compound. It is carried out by either chemical liquid deposition (CLD) or chemical vapour deposition (CVD) [5]. Different silylation agents can be used to modify the zeolite such as tetraethyl orthosilicate (TEOS), 3-aminopropyltriethoxysilane (APTES) and polysiloxanes. In this study, different ZSM-5 zeolites were silylated by CLD method using different amounts of the silylation agent based on the required loading amount of SiO_2 as wt. % to one gram of zeolite.

For example, commercial ZSM-5 zeolite (Si/Al=25 and crystal size 0.5 µm, 10g) was suspended in a solution of cyclohexane (100 ml) and TEOS (3.7 ml) to obtain a modified catalyst with 10 wt. % SiO_2. The regents were mixed in a three-neck round flask fitted with a reflux condenser and stirred under reflux at 40 °C for 7 hours. After that, the temperature was raised up to 100 °C and the reflux condenser was removed to evaporate the cyclohexane. Then, the remaining slurry was placed in an oven at 100 °C and dried overnight. Finally, the modified catalysts were calcined by heating 3 °C/ min up to 550 °C and holding for 6 hours in a muffle furnace. The discussed procedure is repeated twice to attain two silylation cycles. In this study different SiO_2 loading were utilized (X = 10, 30 and 45 wt. %) – see chapter 6 for further information.

4.3.2.3 P and metal loading

Incorporation of different elements such as phosphorus, magnesium and lanthanum in ZSM-5 have been shown can lead to higher p-xylene selectivity [6–9]. These different elements can be loaded on the surface of the zeolite and into the pore structure with the aim of changing the nature of zeolite acidity and narrowing the pore mouths and channels.

Phosphorus was impregnated on ZSM-5 by an aqueous solution of phosphoric acid (HP_3O_4). Catalysts with different loading levels of P (0.75, 1.5 and 3 wt. %) were prepared. For example, to obtain (1.5 wt. % P-ZSM-5) 10 g of commercial ZSM-5 was mixed with water (100 ml) for one hour. Then, H_3PO_4 (0.34 ml) was added to the mixture which was stirred at 60 °C for further one hour. After that, the water was evaporated and the catalyst was dried in the oven overnight. Finally, it was calcined at 550 °C at a rate of 2 °C/ min for 4 hours.

Lanthanum was impregnated on the ZSM-5 zeolite to achieve (5 and 10 wt. % La ZSM-5) by mixing the zeolite with a nitrate solution of La for 3 hours. For example, 5 g of synthesized ZSM-5 (5 µm crystals) were mixed with deionized water (50 ml) and lanthanum nitrate hexahydrate (0.78 g) to get 5 wt. % La-ZSM-5. Then, the solution was evaporated and the catalysts were dried at 100 °C. Finally, the catalysts were calcined at 550 °C for 4 hours.

4.4 Catalyst characterization

4.4.1 X-ray diffraction (XRD)

XRD is one of the most essential characterization techniques used in the identification of zeolites during synthesis and after post synthetic modifications. It is mainly used to identify the crystalline zeolite phase by the generated diffraction patterns. Different zeolites with different topologies and structures show diffraction patterns which are distinct from each other [10, 11]. XRD can also determine whether the powder sample is amorphous or crystalline.

When an X-ray beam of a wavelength, $\boldsymbol{\lambda}$, is projected at the atoms of a powder sample, will diffract at an angle producing distinctive diffraction pattern. Electrons in an atom can scatter lights. Atoms in a crystal are arranged in a periodic array allowing them to diffract

light while amorphous materials don't have a periodic array and no diffraction pattern will be produced. Different atom arrangements will result in different patterns. Intensities, positions, shapes and widths of the peaks provide key information on the sample.

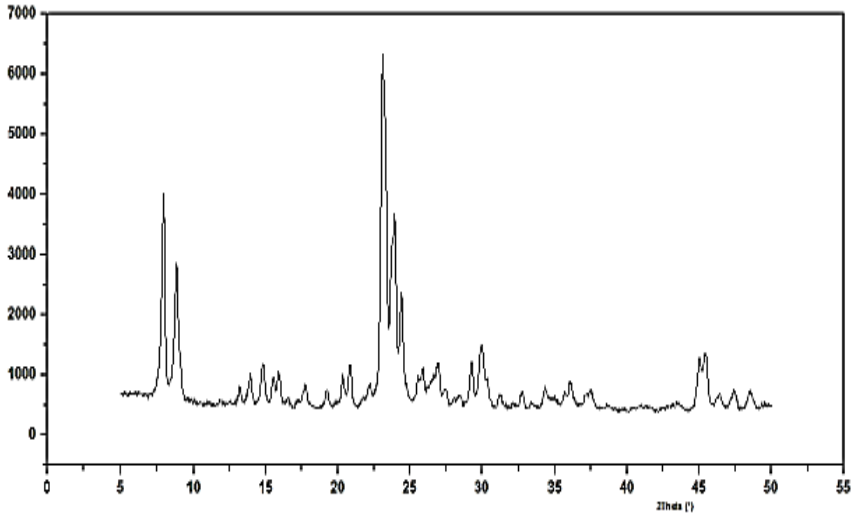

Figure 4-3: XRD pattern of a ZSM-5 zeolite [12]

Bragg formulated the most useful law in powder diffraction. Bragg's law relates the spacing between two planes d_{hkl} to the diffraction angle 2ϑ between the incoming and the outgoing beams [11, 13]:

$$n\lambda = 2d\sin\theta \qquad \textit{Eq. 4-1}$$

Where n is the diffraction order (n=1, 2,….), λ is the wavelength of the incident X-ray beam (λ = 1.54178 Å for Cu Kα), θ_{hkl} is the Bragg angle between the X-ray beam and the crystal planes and d_{hkl} is the interplanar distance for a set of planes, as shown in Figure 4-4

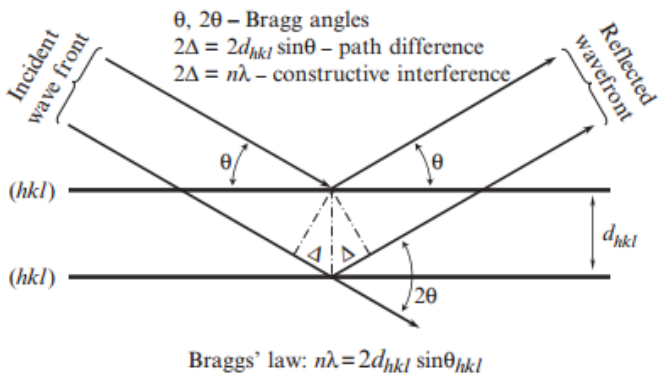

Figure 4-4: Illustration of Bragg's law basic principal [13]

X-ray powder diffractometer components are illustrated in Figure 4-5 . It is composed of an X-ray source, detector, a collimator working as a filter and a sample holder [14]. X-rays are generated by accelerating electrons to a very high speed. An X-ray tube is usually used to produce X-rays. The tube has an anode and a cathode which includes a filament that is heated by an electrical current to produce electrons. The emitted electrons are accelerated by a high electric potential [15].

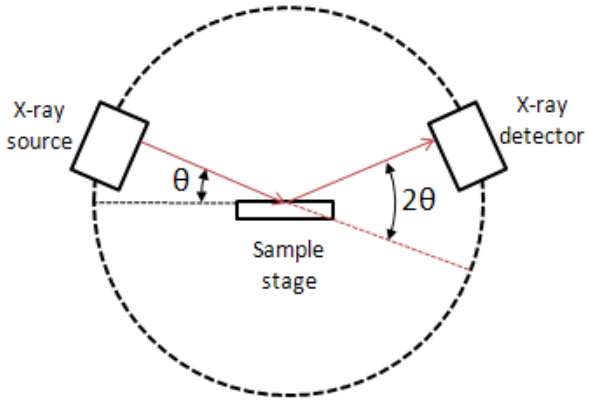

Figure 4-5: Schematic diagram of XRD diffractometer components [16]

Determining the degree of crystallinity can be measured by comparing the sample with a standard material [17]. A standard method for calculating the crystallinity of ZSM-5 zeolites uses several selected peaks of the X-ray diffraction pattern by comparing their major peaks to the reference ZSM-5 that has been approved by ASTM international [18]. This ASTM (D5758) method includes two procedures that can be implemented. Procedure one is called integrated peak area method which compares the sum of integration of peaks in the 22.5 to 25 2θ range for the modified and reference samples. On the other hand, Procedure two compares the absolute peak heights at 24.3 2θ of the modified samples with the reference [18].

ZSM-5 Zeolite samples were evaluated using Philips X'Pert Pro PW 3719 diffractometer. A 2θ interval between 5° and 90° was used with a step size of 0.0407° and a step time of 64 seconds. The instrument was operated at a 40 KV tension and a current of 30 mA. Each run takes about 35 minutes to complete. The samples were grinded into fine powder prior to placing them over the sample holders. After packing the samples, they were lightly compressed on the sample holder to make them flat. The generated XRD patterns were saved and analysed using X' Pert HighScore Plus software. The obtained XRD

patterns were compared with the established ones in the literature. Furthermore, the modified samples patterns were compared with the parent zeolite to quantify the relative crystallinity according the ASTM method discussed above [18] using the following equation:

$$\textbf{\textit{Relative crystallinity}}\ \% = \frac{S_s}{S_r} \times 100 \qquad \textit{Eq. 4-2}$$

Where S_s is the peak area of the ZSM-5 sample and S_r is the peak area of the reference ZSM-5

4.4.2 Scanning Electron Microscopy (SEM) and Energy Dispersive X-ray Analysis (EDX)

Different electron microscopy techniques are available to be used as characterization tool, such as scanning electron microscopy (SEM), transition electron microscopy (TEM) and scanning transition electron microscopy (STEM) [19]. Chemical information from the sample can be acquired through an energy dispersive X-ray spectroscopy device (EDX) when attached to the microscope.

SEM is a very important characterization technique in the field of zeolites. It can be used to obtain the size and morphology of the zeolite crystals [20-22]. An electron source (tungsten filament), lenses, scanning coil, sample chamber and a detector are key components required for a scanning electron microscope to operate [20] as shown in Figure 4-6. Two types of electron detectors are used to collect the electrons emitted by the sample which are secondary electron detector (SE) and backscattered electron detector (BSE) [20].

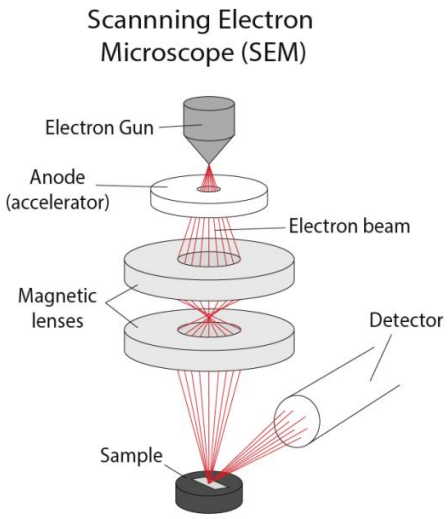

Figure 4-6: SEM key components [23]

Energy dispersive X-ray spectroscopy (EDS or EDX) provides information on the chemical composition of a sample. The technique allows for the detection of elements with atomic numbers from 4 to 92 [24]. Figure 4-7 shows an example of ZSM-5 zeolite EDX spectrum.

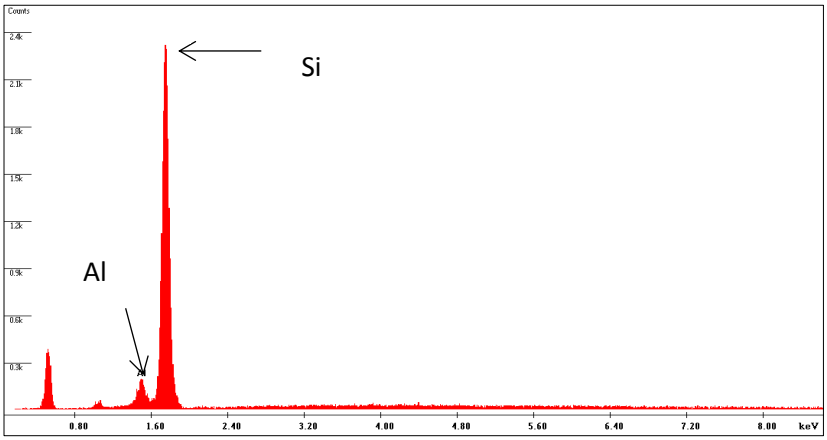

Figure 4-7: Example EDX spectrum for a zeolite sample

The principal behind EDX is that a beam of electrons bombards the solid powder sample resulting in emitted X-rays [24]. A primary electron beam ionizes the atoms generating holes on the core shells. The holes will be filled with electrons dropping from outer shells causing them to release some of their energy in X-rays form [25]- as shown in Figure 4-8.

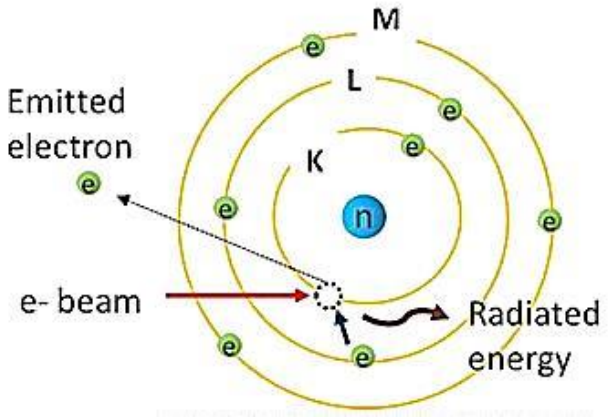

Figure 4-8: Illustration of the EDX principal [26]

In this research, samples were analysed using a Philips XL30 FEGSEM fitted with several types of detectors including (Bruker) energy dispersive spectroscopy (EDX). The zeolite powder sample was mixed with acetone then few drops of the mixture dropped on the sample holder and left to dry off. Instead, for EDX analysis the zeolite powder was sprinkled with spatula and pressed lightly on carbon tapes on the holders. Then, sample holders were coated with gold by a sputtering coater under vacuum to reduce imaging

distortion and drift caused by charging effects. SEM and EDX analyses were performed to investigate the morphology, crystal size and silicon to aluminium ratio (Si/Al).

4.4.3 Fourier transform infrared (FTIR)

Infrared spectroscopy (IR) has been used widely to investigate and characterize zeolite structure. It can provide information on the zeolite framework, surface properties, adsorption and catalysis[10]. IR is divided into three regions in terms of wavelength. The near IR (> 3000 cm^{-1}) delivers knowledge on the adsorbed molecules such as water, gas and organic molecules. Mid IR (4000-400 cm^{-1}) is the most important region in investigating zeolite. It provides essential information on OH groups situated on the surface of the zeolite as well as framework vibrations. Finally, to investigate framework oxygen and cations in the zeolite structure the far IR (400-30 cm^{-1}) is studied [10]. IR adsorption bands in zeolites have been studied intensively and identified. A band at 3750-3745 cm^{-1} is assigned to the terminal sailanol groups (Si-OH). A vibrational band resulting from framework OH groups vibration, which are associated with the Brønsted acidity in zeolites, can be found in the region between 3600 and 3550 cm^{-1} as seen in Figure 4-9. Furthermore, a weak band assigned to the internal sailanol groups appears at approximately 3700 cm^{-1} [27]. Datka et al. studied the effect of Si/Al ratio on the acidity of NaH-ZSM-5 and NaH-ZSM-11 using FTIR and concluded that there is a linear relationship between the number of Brønsted acid sites and the activity of the zeolite where more Brønsted acidity provided higher activity [28].

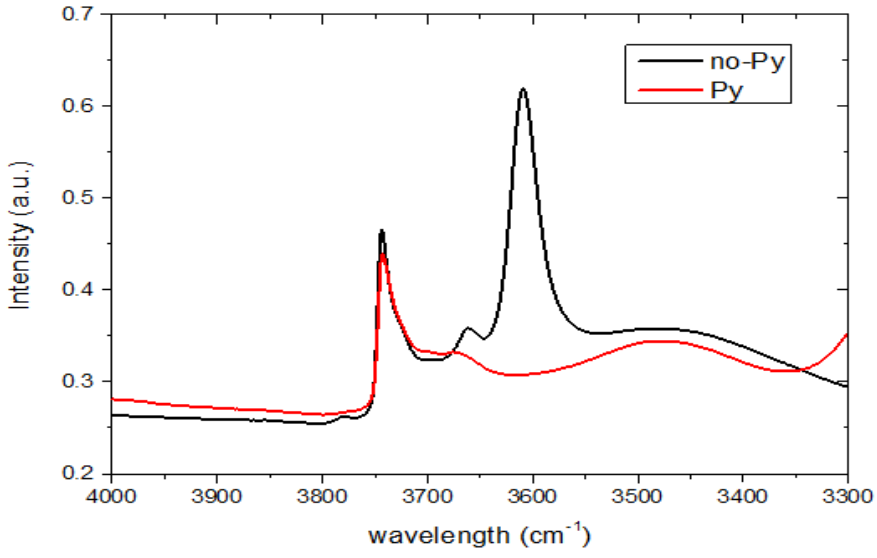

Figure 4-9: ZSM-5 Zeolite FTIR spectrum in the OH stretching region.

Only hydroxyl groups can be detected by direct IR spectroscopy. Determining the Lewis acidity needs the help of probe molecules. Different probe molecules having different vibrational spectroscopic properties can be used. Some probe molecules are employed to measure the concentration of acid sites such as pyridine, by forming a chemical bond with hydroxyl groups [29]. Knozinger, Paukshtis and Yurchenko reported that using the appropriate probe molecule can be accomplished by choosing a molecule having a similar size to the reactant molecule to simulate the interaction of the reactant molecule with the zeolite. The probe molecule should be basic and have negligible acidic properties. It should be selective to a certain type of acid sites to be able to determine protonic and non-protonic sites [30]. Pyridine is extensively used as probe molecule in zeolite analysis providing fruitful quantitative information on Brønsted and Lewis acid sites [31]. Pyridine interacts with Brønsted acid sites to produce pyridinium ion and at the same time interacts with Lewis acid site to produce a characteristic adsorption peak as shown in Figure 4-10. Moreover, it has high thermal stability and can determine Lewis acid sites with different strengths [32]. Pyridine adsorption reveals characteristic IR bands at around 1450 and 1540 cm^{-1} attributed to Lewis and Brønsted acid sites, respectively. Moreover, the bands corresponding to the acidic hydroxyl groups can be identified by pyridine adsorption leading to the disappearance of the OH stretch bands [28]. Pyridine and ammonia were compared in terms of their accessibility to the acid sites by Jia and co-workers and concluded that all hydroxyl groups were accessible to pyridine [28].

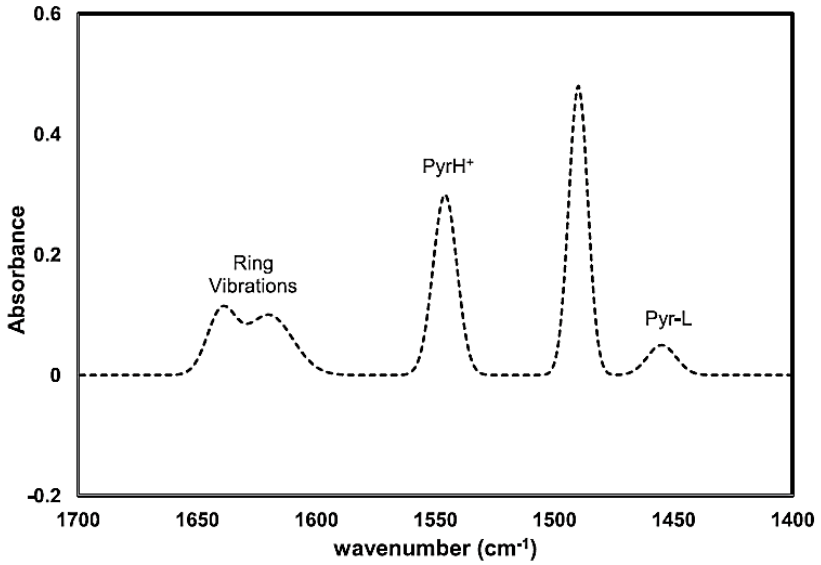

Figure 4-10: FTIR spectrum of H-ZSM-5 after Pyridine adsorption [33].

An FTIR spectrometer consists of six main components which are a radiation source, interferometer, sample cell, detector, amplifier, A/D convertor and a computer. The infrared light projected from the source goes through an interferometer to the sample and detected by a detector. Finally, the detected signal is transferred into a digital signal [34,35]. Michelson interferometer shown in Figure 4-11 is the most widely used in FTIR spectroscopy which requires two mirrors and a beam splitter [35, 36].

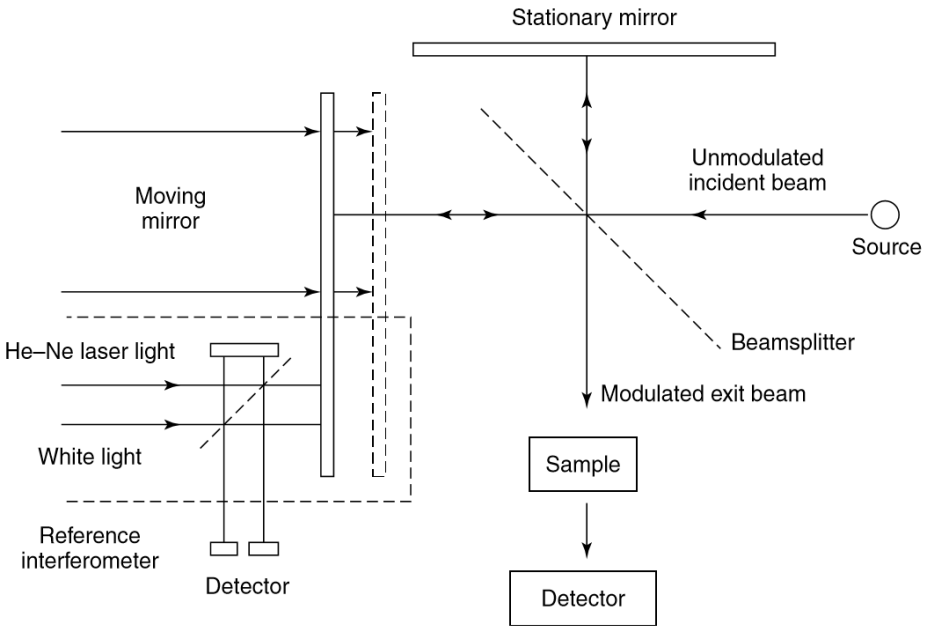

Figure 4-11: Michelson interferometer schematic diagram [35].

To perform a FTIR experiment on a zeolite sample, about 10 mg of a solid sample should be pressed into rigid discs. The disc width should be controlled by controlling the weight of the pressed sample as the width can affect the intensity of the transmitted IR resulting in shifting some bands. The diameter of the sample disc should be around 1 cm. After that, the disc is fitted into the sample holder which can accommodate two discs. The chamber containing the sample holder or cell (Figure 4-12) has cooper chain to lower the sample into the IR range where silicon windows are fitted allowing the samples to be exposed to the IR radiations. Using the cooper chain, the samples can be raised to the heating zone as well. The chamber has a liquid injection system to introduce a probe molecule, such as pyridine, to the zeolite discs.

The characterization of the samples was carried out using transmittance FTIR measurements in the 5000-900 cm^{-1} spectral range. Pyridine (a probe molecule) was used

for monitoring the relative quantities of both Brønsted acid sites (BAS) and Lewis acid sites (LAS). FTIR spectra were collected and analysed using a Thermo iS10 spectrometer accumulating 64 scans at 4 cm^{-1} resolution. The zeolite samples were pressed into self-supported discs and activated under vacuum at a rate of 1 /min up to 450 ^{o}C and held for 5 hours. Their acidic properties were evaluated using adsorption of pyridine (py), which was admitted into the transmittance cell at 150^{o}C in a stepwise manner (typically 1 – 2 injections of 1 µL of py) until no changes were observed in the spectra. The saturated sample was then evacuated at 150^{o}C to remove physically adsorbed pyridine and the FTIR spectrum collected. The intensity of the py-H^{+} and py-LAS peaks at ~ 1540 and 1450 cm^{-1} were used to compare the number of active sites in the samples.

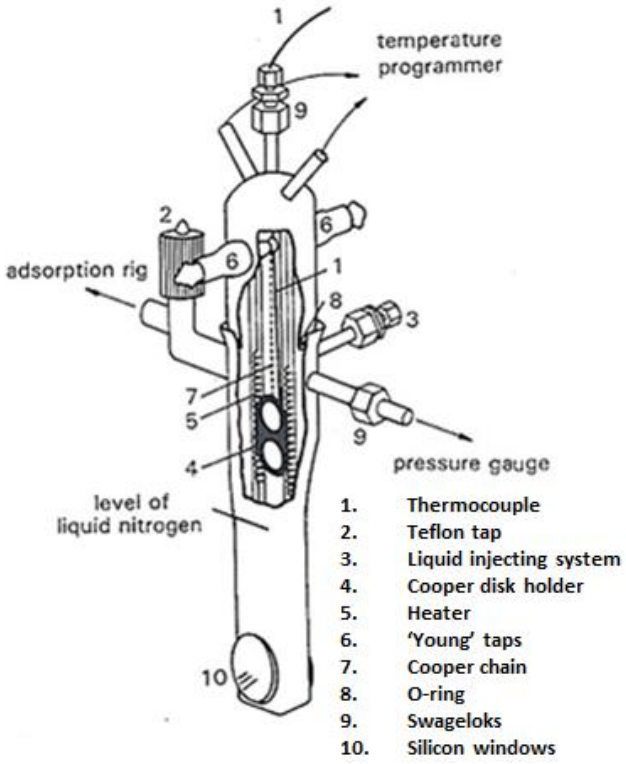

Figure 4-12: FTIR sample chamber schematic [37]

4.4.4 BET Surface area and pore volume

Characterization of the textural properties for zeolites is crucial to optimise its applications. Surface area and porosity (pore volume, pore size and pore size distribution) are very important properties in designing a heterogeneous catalyst. Surface area determines the accessibility of active acid sites and porosity controls selectivity in reactions. Physical adsorption of nitrogen (N_2) is a widely-used method to study the

surface area and porosity of zeolites [38]. In order to calculate the surface area and porosity, proper theoretical model for gas adsorption mechanics has to be applied [38].

Physisorption is the adsorption of gas molecules on the surface of the catalyst at a pressure less than the vapour pressure [39]. The attraction between the adsorbed molecules and the surface is week. Usually adsorption experiments are made at a temperature less than the triple point but above the freezing point [39]. In this case, the adsorbate will have the characteristics of a liquid phase and not a solid phase which is normally assumed by adsorption theories. The adsorption isotherm can be measured by measuring the adsorbed amount against the adsorptive pressure at constant temperature [39,40].

Brunauer et al, classified the adsorption isotherms into six categories and three of them are associated with adsorption on porous materials and can be seen in Figure 4-13 [40,41]. Type (I) represents the physisorption on microporous materials such as ZSM-5 zeolite. Type (IV) and (V) demonstrate the characteristic of materials containing mesoporousity at high and low adsorption energy, respectively. These types of curves contain hysteresis loops as a result of mesoporousity. The adsorption on mesoporous solids is carried out by adsorption of multilayers followed by capillary condensation. Some pore openings lead to small channels inside the zeolites where during desorption they will empty at their corresponding pressure which is lower than what needed for emptying larger ones resulting in the hysteresis loop [42, 43]. In this thesis, the analysis were done based on adsorption isotherms using Micromeritics Gemini 2365 which doesn't provide desorption isotherm analysis. So no pore size distribution was obtained.

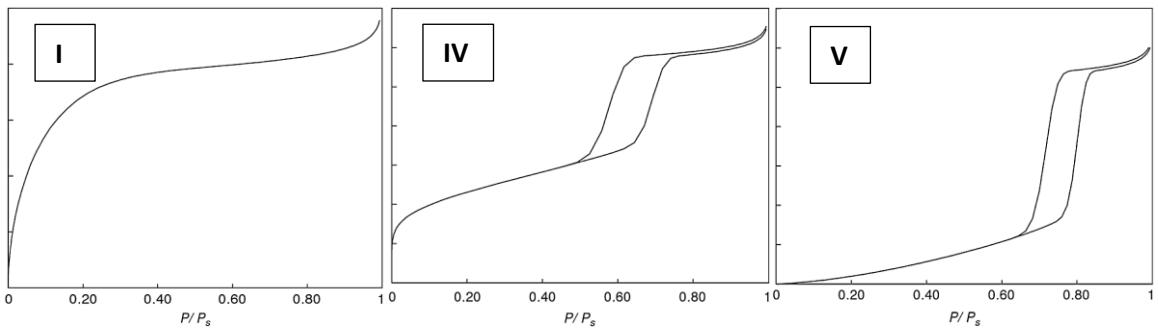

Figure 4-13: Different types of adsorption isotherms [40]

The amount of gas adsorbed on a microporous material is proportional to the sample mass, operation temperature, vapour pressure and the nature of both gas and the tested material. Bruner-Emmett-Teller (BET) is commonly used method in microporous materials surface area measurements using the following equation [44].

$$\boldsymbol{1/[n((P_0/P)-1)] = (1/n_m\, C) + [(C-1)/n_m C](P/P_0)} \qquad \textit{Eq. 4-3}$$

Where n is the adsorbed amount at a pressure P, n_m is the monolayer capacity, C is a constant representing the interaction between the adsorbent (solid) and adsorbate (gas) and P_0 is the saturation vapour pressure.

When P/n (P_0-P) is plotted versus P/P_0 from the above equation, n_m is obtained as 1/ (slope + intercept) and the total surface area can be calculated from the following equation.

$$\boldsymbol{S = n_m L\sigma} \qquad \textit{Eq. 4-4}$$

where L is Avogadro's number and σ is the average area occupied by every molecule in the entire monolayer (16.2 x 10^{-20} m^2 for N_2) [45].

The standard curve shown in Figure 4-14 can be used to measure the porosity of microporous zeolites. Two linear regions should be obtained when plotting the adsorbed amount versus **F** (P/P_0) [40]. The slope of the lower line labelled (L) is proportional to the surface area. The slope of the obtained upper linear region (H) is proportional to the area outside the pores and the pore openings. Finding the intercept of this line (n/n_m), which is the amount of adsorbed molecules that can fit in the micropores gives an indication of pore volume [40].

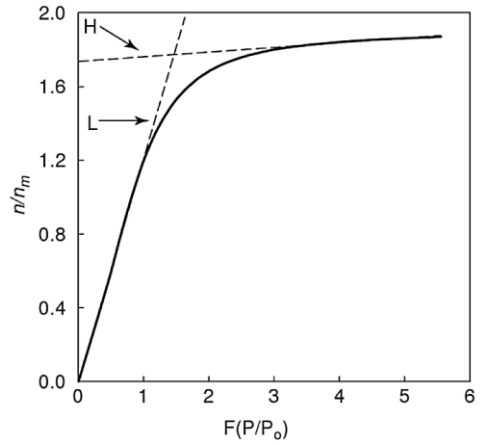

Figure 4-14: A standard plot of type I isotherm for porosity measurement [40]

Catalyst samples BET surface area was determined using a Micromeritics Gemini 2365 surface area analyser. The measurements were carried out by nitrogen adsorption at -196 °C using ~ 0.2 g of sample, purged for 18 h at 100 °C under a constant flow of helium (99.9 %) using a Micromeritics Flowprep060.

4.4.5 Solid state nuclear magnetic resonance (NMR):

Valuable information on the type and number of neighbouring atoms and bonding characteristics can be acquired from the produced chemical shift (δ). A reference material, such as adamantane, can be utilized as a chemical shift standard before running the NMR experiment on the required sample. Silicon and aluminium atoms in zeolites can be measured through their natural occurring isotopes ^{29}Si and ^{27}Al which are normally used to investigate zeolite framework [46,47].

In general, the ^{27}Al MAS NMR spectra of zeolite materials show a large peak at about 60 ppm attributed to the tetrahedral framework aluminium. Peaks at 30 and 0 ppm might appear due to the extra-framework aluminium and octahedral framework aluminium species, respectively [48]. The peak intensities (I_{60} and I_0) can be used to calculate the framework (Si/Al) ratio through the following equation [46].

$$\left[Si/Al\right]_{fr} = \left[Si/Al\right]_{tot}{}^{[I_{60}+I_0]}/_{I_{60}} \qquad \textit{Eq. 4-5}$$

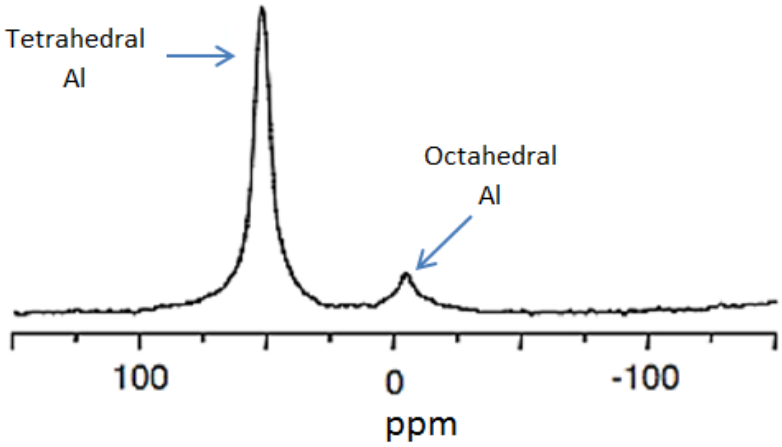

Figure 4-15: Chemical shifts of ^{27}Al species in zeolites [48]

Silicon species in the zeolite framework can exist in five different environments of Si (nAl) units, where n is 0, 1, 2, 3 or 4 indicating the number of coordinated Al atoms in the first

coordinated SiO_2 sphere for the given peak (Figure 4-16) [46]. ^{29}Si MAS NMR spectra, which usually consist of five peaks, are used to investigate the silicon species. It was concluded that decreasing the Al-atoms leads to an increase in the intensities of Si-peaks. On the other hand, replacing Si-atoms with Al-atoms will shift the peaks to low field with less negative values of (δ) as illustrated in Figure 4-17 [46]. Using the Lowenstein's equation the framework tetrahedral Si and Al molar ratio can be calculated from the ^{29}Si MAS NMR spectra, where *I* is the peak intensity of a signal corresponding to the Si (nAl) units [49].

$$\left[{}^{Si}/_{Al}\right] = \frac{I_4+I_3+I_2+I_1+I_0}{I_4+(0.75)I_3+(0.5)I_2+(0.25)I_1} \qquad \textit{Eq. 4-6}$$

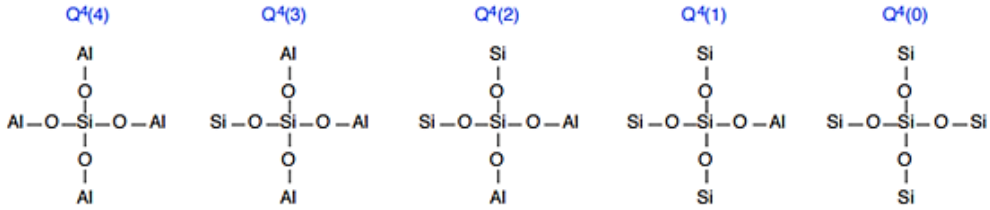

Figure 4-16: Five different Si(nAl) environments [50]

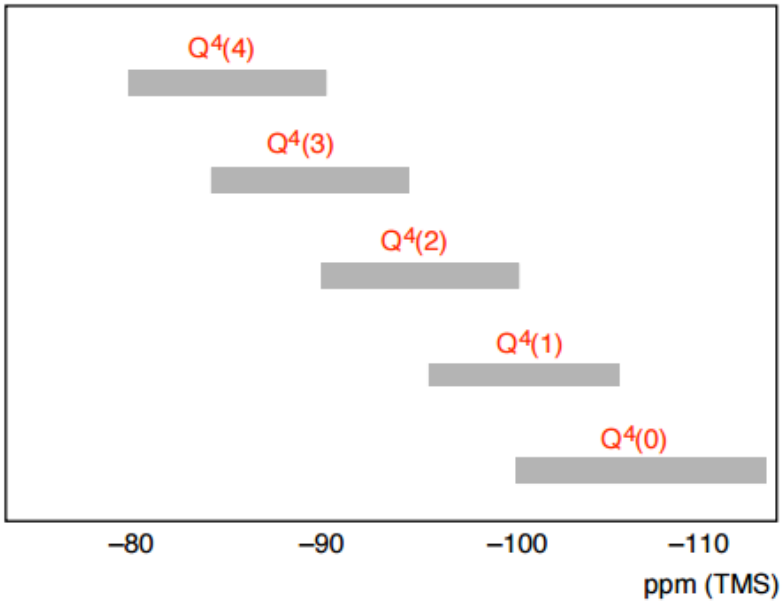

Figure 4-17: ^{29}Si chemical shift values of Si(nAl) units [50]

To perform a NMR experiment, the zeolite powder is loaded (typically and pressed carefully into a zirconia rotor and inserted in a large magnetic field ($B_\circ$) inside the coil. The rotor is positioned at a magic angle of about 54.73° in respect to the direction of the

magnetic field applied. Adamantane is used as an external reference to calibrate the chemical shift.

Bruker Avance III-400 spectroscopy was used to analyse the parent and modified ZSM-5 samples. About 0.1 g of zeolite powder was pressed down in the zirconia rotor. A total time of 2 hours and 45 minutes was the run time for each ^{27}Al MAS NMR test based on the following operating conditions: 100 scans, a spinning rate of 10 kHz, relaxation time 5 seconds and an acquisition time of 0.00824 S. Each ^{29}Si MAS NMR test was completed in about 11 hours and the operating conditions were: 1000 scans, a spinning rate of 10 kHz, relaxation time 40 seconds and acquisition time of 0.02135 S.

4.4.6 Inductively Coupled Plasma (ICP-OES):

Inductively coupled plasma optical emission spectroscopy-ICP-OES is one of the common techniques utilised to determine the chemical composition of porous materials and detect traces of metals and elements [51, 52].

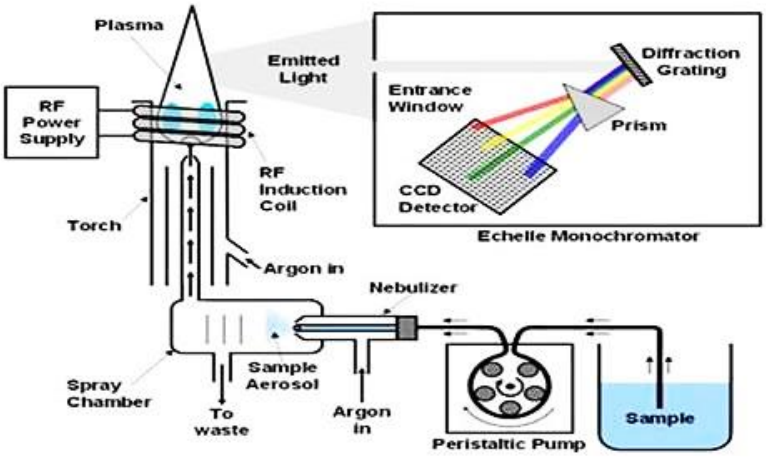

Figure 4-18: Schematic diagram of ICP-OES instrument [53]

Analyses of different zeolite samples were carried out by outsourcing to Medac Ltd who used a Varian Vista MPX ICP-OES where the plasma was produced using argon gas at around 8000 K. Each sample was digested using a combination of hydrofluoric acid (HF) and nitric acid (HNO_3) then, introduced to the instrument torch as an aqueous solution. Acid digestion was required to solubilise all the elements within the zeolite. The weight of samples used was 7 mg for Al and Si analysis and 12-15 mg used for other elements. The standards were used to generate a calibration curve for each element to be determined.

The metal concentration in the tested sample is calculated by running the sample solution and comparing values against the calibration curve. The accuracy of measurement was quoted at 0.3 wt. % for Al and Si.

4.4.7 Thermogravimetric analysis (TGA):

Thermogravimetric analysis technique is employed to measure the change in mass over a range of temperatures or a period of time in a controlled environment. The change in weight can be utilised to determine the thermal stability and composition of a material and the weight loss can occur due to decomposition, reduction or evaporation. The sample can also gain weight due to oxidation or absorption. The TGA instrument, as shown in Figure 4-19, consists of a sample pan, reference pan, microbalance and a controllable furnace [54].

Zeolite powders were analysed using a Q5000IR TA Instrument TGA and controlled by TA universal software. The obtained curve from the TGA is used to study the amount of coke deposited on the spent zeolite as well as the moisture content. From the curve, information on at what temperature the coke was burned can be obtained, which could help in understanding the nature of coke, soft or hard coke.

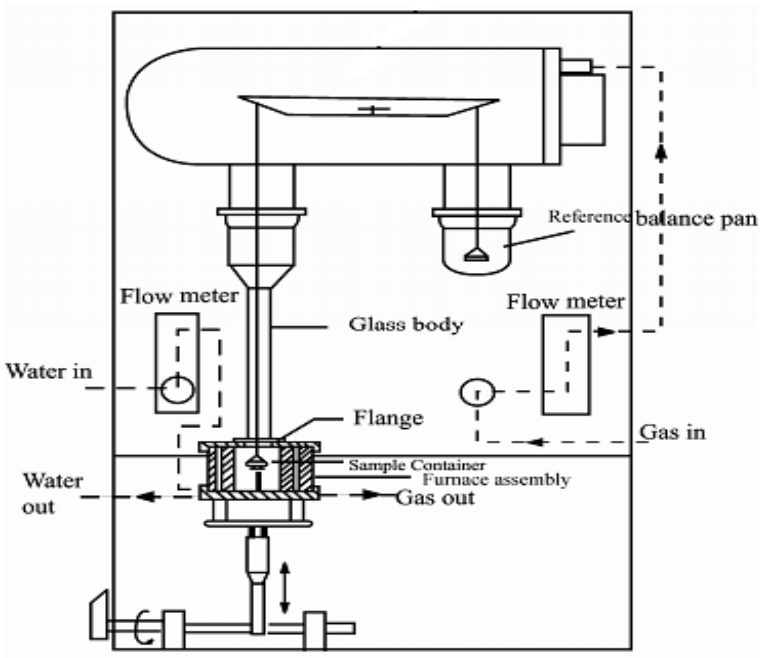

Figure 4-19 TGA instrument schematic [55].

A small amount of sample (typically 10 - 20 mg) was loaded into a ceramic pan that was connected to a microbalance detecting the weight loss. Temperature was monitored by a

thermocouple located inside the furnace. Air was passed on the samples with a flowrate of 25 ml/min. The samples were heated at a rate of 5 °C/ min to 650 °C and kept isothermal for 2 hours.

4.4.8 Gas chromatography (GC) analysis:

Chromatography analysis is a common technique used to identify the individual components of a mixture of volatile organic compounds sample. The sample is carried by gas (mobile phase) such as He, H_2 or N_2, through a specific column inside a temperature controlled oven [56].

Liquid quantitative analyses were carried out by Varian 3400 GC equipped with a (30 m X 0.32 mm i.d. X 1 µm) Stabilwax column and FID (flame ionization detector). Helium gas with 99.99% purity was used as a carrier gas with a split ratio of 100: 1. Injector and detector temperatures were set at 240 °C. To insure a proper separation of the involved compounds, a temperature program was set where the oven temperature was set at 60 °C, held for 5 minutes and ramped 5 °C/min up to 190 °C.

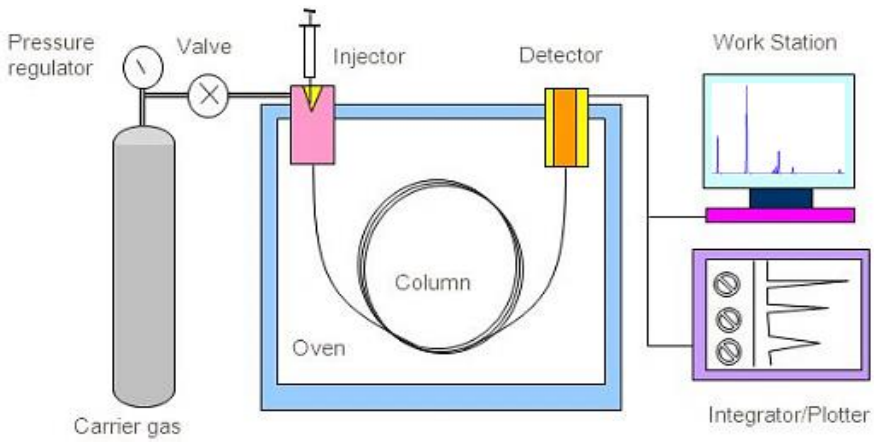

Figure 4-20: Schematic diagram of GC [56]

The calibration of the GC was done by mixing benzene, toluene, ethylbenzene, p-xylene, m-xylene, o-xylene and trimethyl benzenes to identify the peak retention time of each component allowing for qualitative and quantitative analysis of the reaction products. An example of prepared standard chromatograms can be seen below in Figure 4-21.

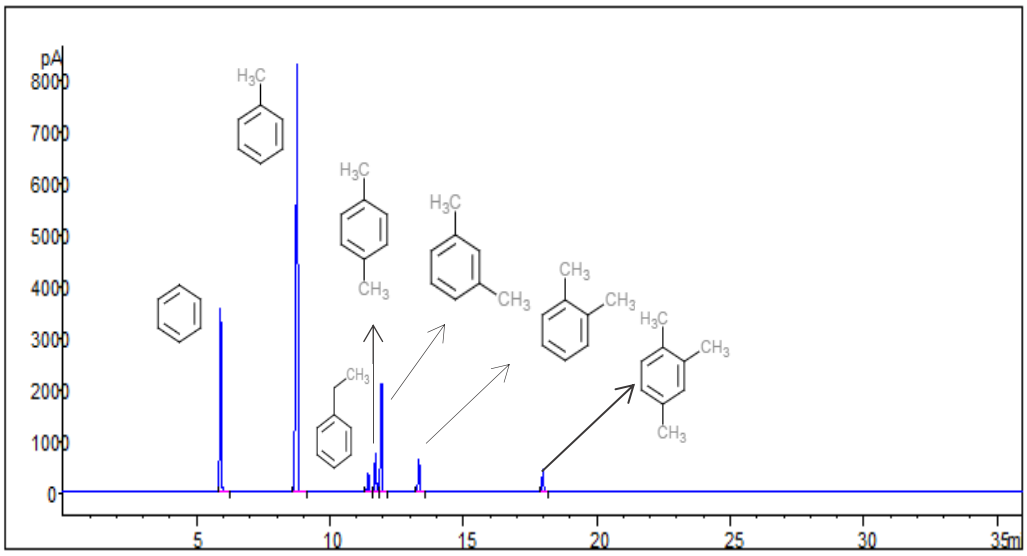

Figure 4-21 GC standard mixture chromatogram

Table 4-2: Standard mixture for GC calibration

Component	Retention time (min)	(wt. %)	GC (wt. %)	Error (%)
Benzene	5.91	20	19.10	3.4
Toluene	8.78	56	57.02	2.0
Ethylbenzene	11.44	2.5	2.32	6.0
p-xylene	11.71	4	3.76	6.0
m-xylene	11.94	11	11.69	6.0
o-xylene	13.34	4	3.80	5.0
1,2,4 Trimethylbenzene	17.98	2.5	2.31	6.6

4.5 Experimental set up

4.5.1 Toluene disproportionation reaction unit

The experimental setup of toluene disproportionation rig is shown in Figure 4-22. The unit consists of gas supply, calibrated gas flow controller to control the gas flow, a HPLC pump to feed toluene, a fixed bed reactor surrounded by a vertical furnace controlled by a Carbolite temperature controller, heat exchanger to cool the products using cooling water and a back-pressure regulator (BPR) to control the system pressure.

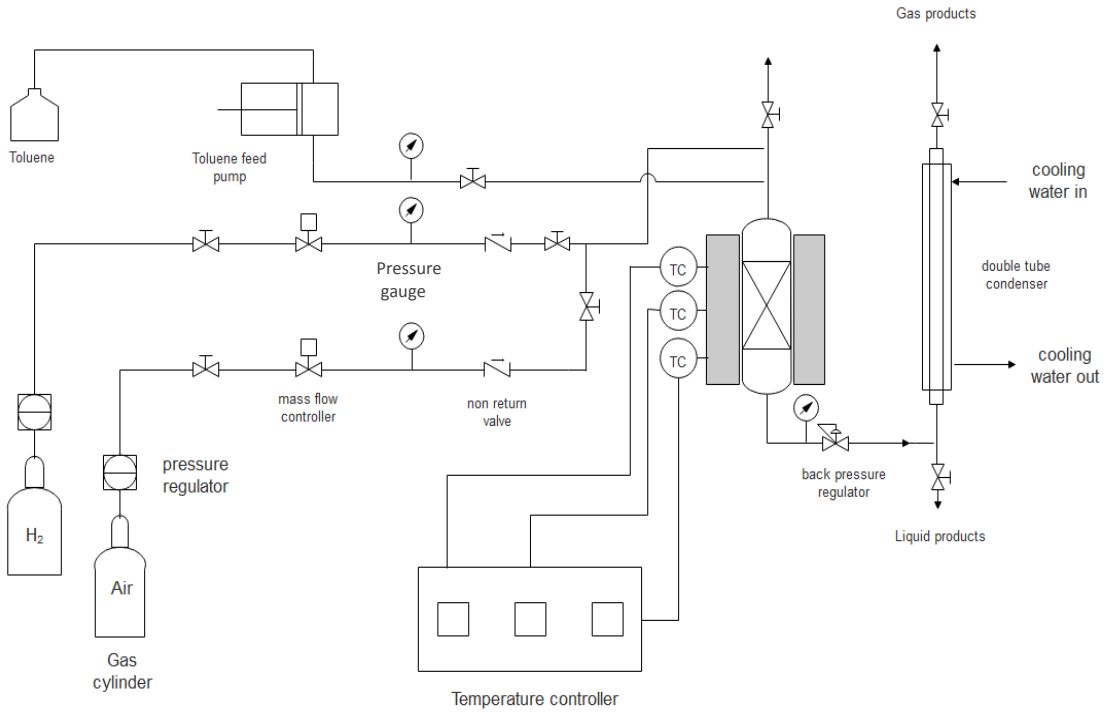

Figure 4-22: Simple schematic of toluene disproportionation unit

The reactor is made of stainless steel with an inner diameter of 1 cm and 55 cm long. The reactor is heated by a furnace consisted of three controlled independent heating zones. The reactor design and specifications are illustrated in Figure 4-23 and Table 4-3. The condenser was designed to make sure of optimum mass balance by cooling any products in the gas phase to be collected as liquid product from the sampling point. Cold water was passed through condenser in a counter-current configuration to the product stream. The pressure of the system was controlled through a manual back pressure regulator fitted with a pressure monitoring gauge supplied by Swagelok. The liquid feed toluene (99.9 wt. %, Sigma Aldrich) was fed through the HPLC pump, Jasco PU-980 (flow rate 0.01 – 5 ml/min). The carrier gases (H_2, Air, N_2 99.99 % purity, supplied by BOC Company) were fed to the reactor from gas cylinders and the flow rate was controlled by Brooks mass flow controllers (MFC). Toluene and hydrogen were mixed at the inlet of the reactor. The feed mixture goes down the reactor in a co-current flow mode. The rig was commissioned by calibrating the HPLC pump and the MFCs.

4.5.2 Catalyst loading and activation

All catalysts tested for toluene disproportionation were pressed into pellets under a 5 ton/cm^2 for one minute, crushed and sieved to a particle size of 250-425 µm. The

reactor was filled with glass beads at the top and bottom with one gram of the catalyst sandwiched in between. The catalyst was separated from the glass beads with two layers of glass wool as shown in Figure 4-23. After loading the reactor, catalyst activation is done in situ at 550 °C for 4 hours at a heating rate of 2 °C min^{-1}.

Table 4-3: Reactor design and specifications

Description	Specification
Body material	Stainless steel -316
Reactor length	55.0 cm
Internal diameter	1.00 cm
External diameter	1.30 cm

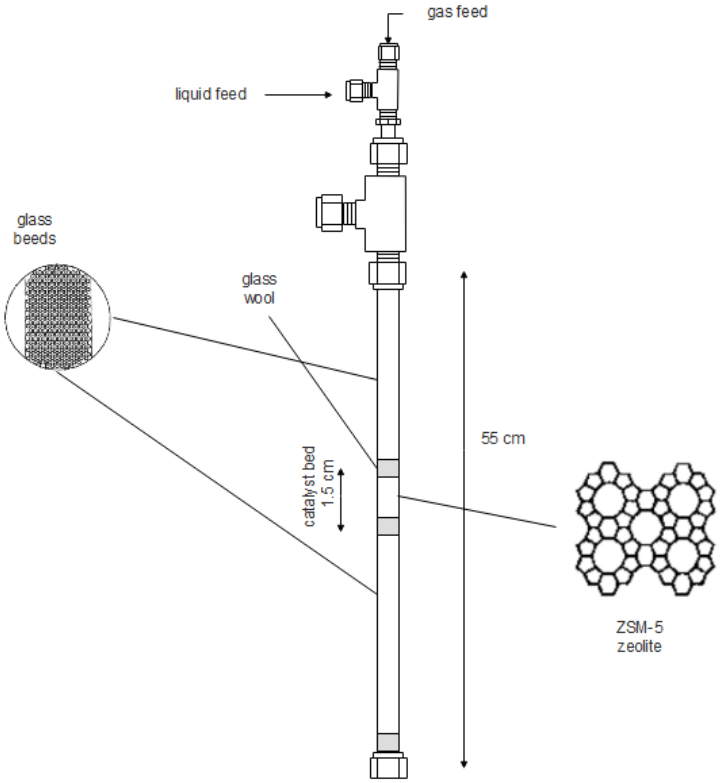

Figure 4-23: Reactor configuration and loading

After setting the carrier gas flow rate to the required value and the temperature was stabilised, the flow rate on the HPLC pump was set according to the required WHSV to feed toluene to the reactor. Both carrier gas and toluene were mixed at the inlet of the reactor and passed through the reactor. Firstly, samples were taken at a WHSV (3 h^{-1}). Then, the WHSV was changed to 30 h^{-1} by changing the toluene flow rate and sample was

taken when steady state was reached. After that, it was changed to 70 h^{-1} and finally the flow rate was adjusted to achieve a WHSV of 83 h^{-1}, where WHSV was calculated following Equation 4-10. Two different hydrogen pressures (1 and 10 bar) were used to evaluate toluene disproportionation over parent and modified zeolites. Liquid samples were collected in GC vials and analysed by Varian 3400 GC. The overall mass balance after each experiment was calculated and was 90 ± 5 %. After each reaction, the reactor was purged with hydrogen overnight while dropping the temperature down to room temperature. Then, the catalyst was reactivated in air at 550 °C if testing was required at different pressures, temperatures and WHSVs.

Table 4-4: TDP reaction conditions

Temperature (°C)	475
Pressure (bar)	1 - 10
Toluene WHSV (h^{-1})	3 - 83
Toluene flow rate (ml min^{-1})	0.06 – 1.6
H_2 flowrate (ml min^{-1})	30
Catalyst weight (g)	1

The conversion of toluene (wt. %), yield of p-xylene (wt. %), selectivity of p-xylene in xylene isomers (%) and WHSV were calculated using the following equations:

$$\boldsymbol{X_T = \frac{W_{T0} - W_T}{W_{T0}} \times 100} \qquad \textit{Eq. 4-7}$$

$$\boldsymbol{S_P = \frac{W_{PX}}{W_X} \times 100} \qquad \textit{Eq. 4-8}$$

$$\boldsymbol{Y_P = \frac{W_{PX}}{W_{total\ products}} \times 100} \qquad \textit{Eq. 4-9}$$

$$\boldsymbol{WHSV = \frac{Toluene\ feed\ (g\ h^{-1})}{weight\ of\ catalysts\ (g)}} \qquad \textit{Eq. 4-10}$$

Where W_{T0} is the weight of toluene in the feed, W_T is the weight of toluene in the product, S_P is p-xylene selectivity in the xylene isomers. W_{PX} is the weight of p-xylene, W_X is the weight of total xylene and Y_p is p-xylene yield in the total products.

4.6 Unit calibration

Major equipment of the reaction unit such as the liquid pump, mass flow controller and furnace temperature controller were calibrated.

4.6.1 HPLC liquid pump (Jasco pump)

To calibrate the pump, different toluene flowrates were set and at each flowrate a sample was collected. The sample was timed (10 minutes) and weighed to measure the actual volumetric and mass flowrate according to the set points values and this calibration was performed every month to make sure that the pump is accurate – see Table 4-5. The slowest flow rate showed a 4 % error and the set point had to be adjusted to get the exact required value. On the other hand, all other faster set points produced almost accurate flowrates.

Table 4-5 Calibration of HPLC pump

Pump set point (ml/min)	Actual flow (g/10 mins)	Actual flow (ml/min)	Error (%)
0.06	0.50	0.057	4 %
0.1	0.87	0.100	0
0.2	1.74	0.201	0.5%
0.5	4.35	0.501	0.2%
1.0	8.70	1.00	0

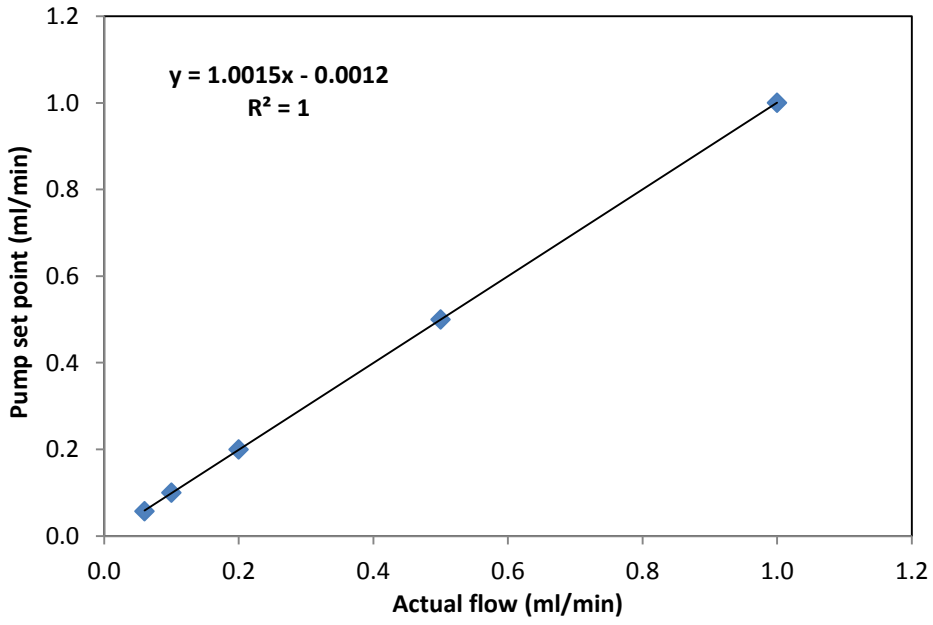

Figure 4-24: HPLC pump calibration

4.6.2 Mass flow controller

The H_2 mass flow controller was calibrated by changing the valve opening in the controller and measuring the resulted flowrate using a gas bubble meter at the gas sampling point. The procedure was repeated 3 times for valve opening percentage and the average was calculated (Table 4-6). The calibration was performed to know the required valve opening to reach 30 ml/min hydrogen flow.

Table 4-6: Mass flow controller calibration

Valve opening %	Flow (ml/min)
0	0.00
1	33.0
1.5	36.5
2	39.0
3	45.0
5	58.0
10	88.0
15	120

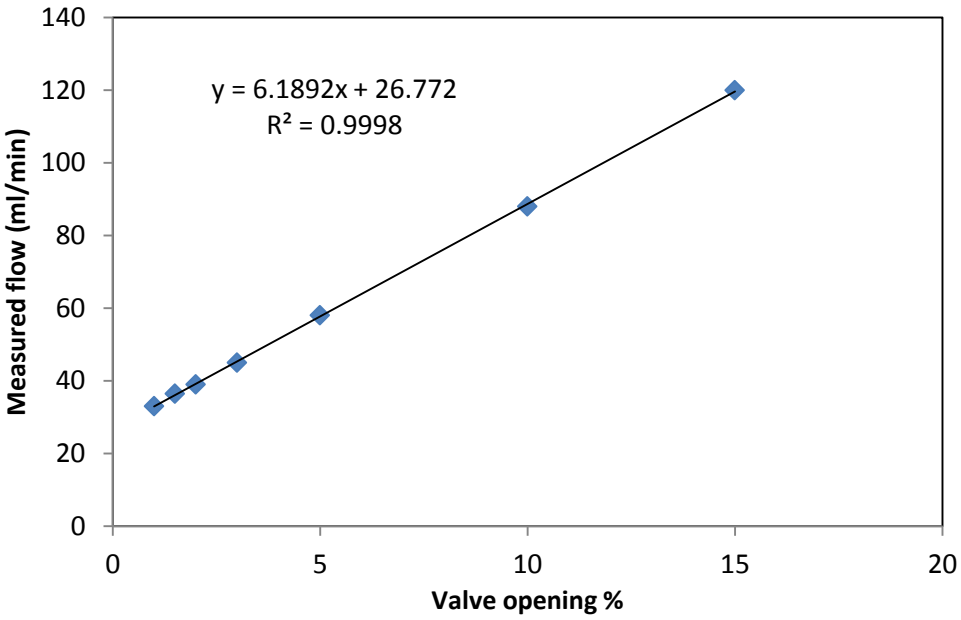

Figure 4-25: Hydrogen mass flow controller calibration

4.6.3 Furnace temperature controller

The furnace surrounding the reactor tube is made of three heating zones (top, middle and bottom) controlled by an electrical controller. A ceramic thermo-well was fitted inside the reactor and a thermocouple was inserted inside the thermo-well. The

actual temperature was measured moving the thermocouple down through the full length of the reactor and the set point was adjusted accordingly.

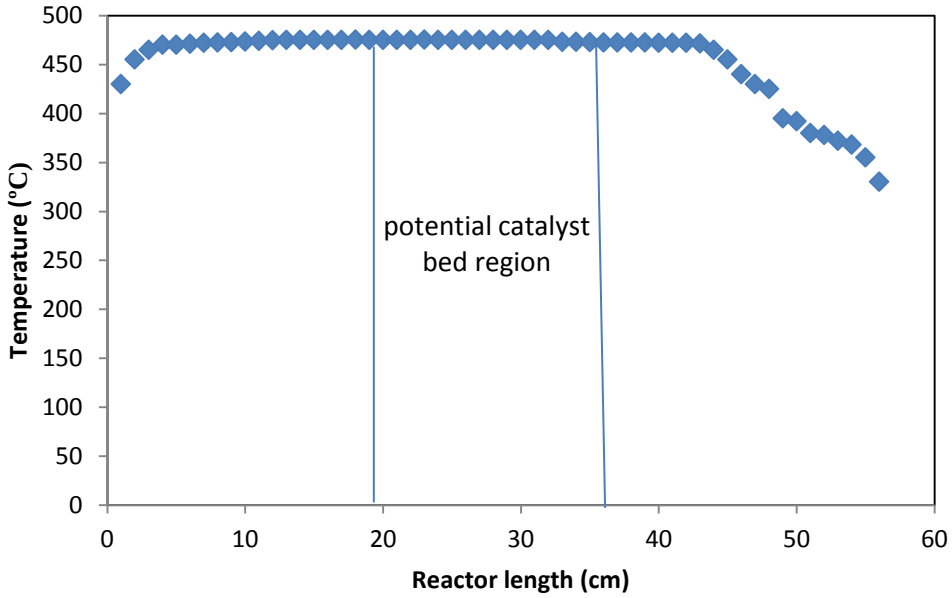

Figure 4-26: Calibration of furnace temperature

4.7 Repeatability

To establish confidence in the obtained results, error should be minimized to be able to produce similar results. Verifying the attained experimental data can be done through two methods, repeatability and reproducibility. Repeatability is the variations in measurements obtained by repeating catalytic run on the same catalyst sample using the same set of operating conditions (such as temperature, pressure and flowrate). On the other hand, reproducibility is defined as the difference in the obtained results from experiments conducted on different samples of the same catalyst.

Several experiments were repeated two or three times with the same method and operating parameters to validate the results and ensure their repeatability. In addition, three samples of commercial parent ZSM-5 with crystal size 0.5 µm were loaded into three reactor tubes and tested separately under the same operating conditions. The toluene conversion with time on stream is shown in Figure 4-27. The conversion was stable in all runs for over three hours. The variation in the results obtained through the different experiments is very small and less than 3 %. The average standard deviation for samples at different time on stream was calculated to be ($\sigma = 0.33$).

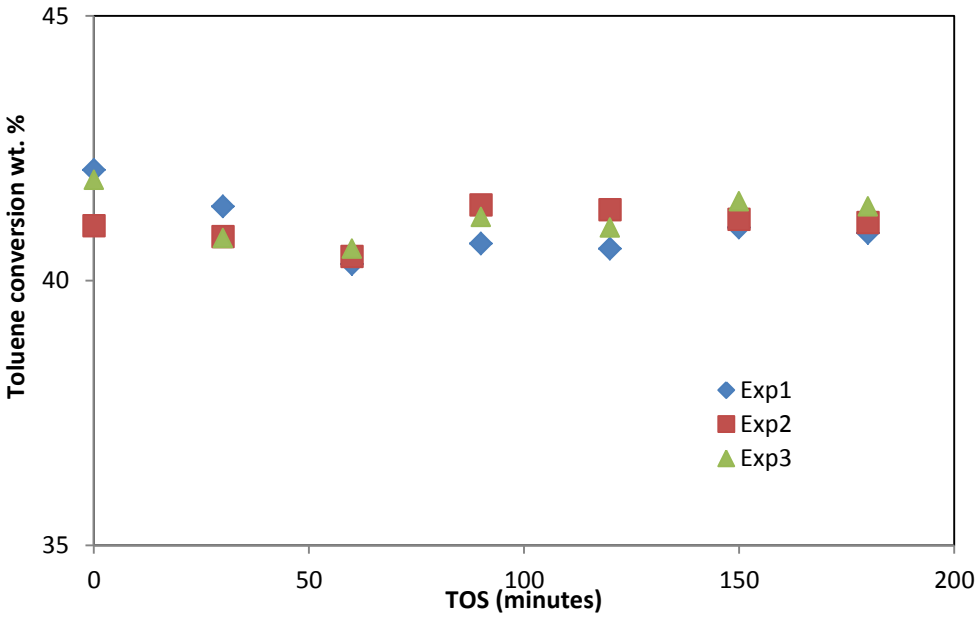

Figure 4-27: Reproducibility of parent ZSM-5 experiment

The variation in p-xylene selectivity for the three different experiments was only around 1 %. The product selectivity was plotted against various toluene conversions at different WHSVs including error bars. The error bars showed how small are the variation in conversion and selectivity between the different experiments with a 0.8 wt. % error in conversion, which is difficult to show on the graph as result of the wide range of conversion.

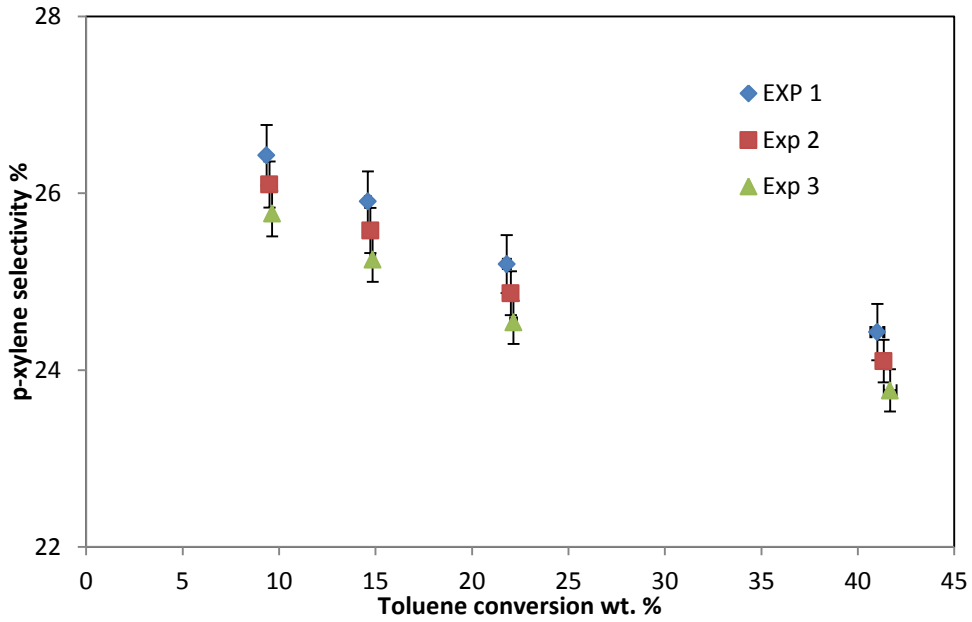

Figure 4-28: Toluene disproportionation over parent ZSM-5

4.8 References

1. Rallan C, Al-Rubaye R, Garforth A. Generation of catalytic films of alumina and zeolites on FeCralloy rods. Chemical Engineering Transactions. 2015;43:907–912.

2. Chen SZ, Huddersman K, Keir D, Rees LVC. Synthesis of large uniform crystals of ZSM-5. Zeolites. 1988;8(2):106–109.

3. Zheng S. Surface modification of HZSM-5 zeolite. PhD Thesis. Institute for Technical Chemistry II of the Technical University of Munich; 2002.

4. Chen W, Bauer F, Bilz E, Freyer A, Huang S, Lai C et al. Acidity characterization of H-ZSM-5 catalysts modified by pre-coking and silylation. Studies in Surface Science and Catalysis. 2004; 2269-2274.

5. Weber R, Möller K, O'Connor C. The chemical vapour and liquid deposition of tetraethoxysilane on ZSM-5, mordenite and beta. Microporous and Mesoporous Materials. 2000;35–36:533–543.

6. Kaeding W, Chu C, Young L, Weinstein B, Butter S. Selective alkylation of toluene with methanol to produce para-Xylene. Journal of Catalysis. 1981;67(1):159–174.

7. Meshram NR. Selective toluene disproportionation over ZSM-5 zeolites. Journal of Chemical Technology and Biotechnology. 1987;37(2):111–122.

8. Zhang L, Gao J, Hu J, Li W, Wang J. Lanthanum oxides-improved catalytic performance of ZSM-5 in toluene alkylation with methanol. Catalysis Letters. 2009;130(3–4):355–61.

9. Uguina M , Sotelo J, Serrano D, Grieken R. Magnesium and silicon as ZSM-5 modifier agents for selective toluene disproportionation. Industrial and Engineering Chemistry Research. 1992;31(8):1875–1880.

10. Burton A. Powder diffraction in zeolite science. In: Chester A, Derouane E, editors. Zeolite characterization and catalysis. Springer Netherlands; 2009. p. 1-64.

11. Jenkins R, Snyder R. Introduction to x-ray powder diffractometry. Winefordner J, editor. John Wiley & Sons, Inc; 1996.

12. Treacy M, Higgins J, editors. Collection of simulated XRD powder patterns for zeolites. 4th ed. Elsevier. 2001. p. 239.

13. Pecharsky V, Zavalij P. Fundamentals of powder diffraction and structural characterization of materials. 2nd ed. Springer US; 2009. p.148.

14. Ooi L. Principles of x-ray crystallography. New York: Oxford university press Inc; 2010.p. 148.

15. Lee M. X-ray diffraction for materials research: from fundamentals to applications. Oakville, Canada: Apple academic press, Inc; 2016. p. 15.

16. Arora S. Component parts of an X-ray diffractometer [Internet]. xrd.co; 2016 [cited 2017 Jan 22]. Available from: http://xrd.co/category/x-ray-diffractometer/

17. Van Koningsveld H, Bennett J. Zeolite structure determination from X-ray diffraction. In: Karge H, Weitkamp J, editors. Structures and structure determination. Germany: Springer-Verlag Berlin Heidelberg; 1999. p. 1-29.

18. ASTM International. ASTM D5758-01(2015) Standard test method for determination of relative crystallinity of zeolite ZSM-5 by X-ray diffraction; 2015. Available from https://doi.org/10.1520/D5758-01R15

19. Wan W, Xiao C, Zou X. Structural characterization of zeolites and mesoporous zeolite materials by electron microscopy. In: García-Martínez J, Li K, editors. Mesoporous zeolites: Preparation, characterization and applications. Weinheim, Germany: Wiley-VCH Verlag GmbH & Co. KGaA; 2015. p. 425-460.

20. Scheu C, Kaplan WD. Intorduction to scanning electron microscopy. In: Dehm G, Howe J, Zweck J, editors. In-situ electron microscopy: Applications in physics, chemistry and materials science. Weinheim, Germany: Wiley-VCH Verlag GmbH & Co. KGaA; 2012. p. 1-37.

21. How an SEM works [Internet]. [cited 2017 Jan 24]. Available from: http://www.nanoscience.com/technology/sem-technology/how-sem-works/

22. University of Turku. Scanning electron microscope (SEM) [Internet]. Finland; [cited

2017 Jan 23]. Available from: http://www.utu.fi/fi/yksikot/sci/yksikot/fysiikka/laboratoriot/materiaali/materiaalitiede/tutkimusmenetelmat/sem/Sivut/home.aspx

23. University of Cambridge. The Scanning electron microscope [Internet]. [cited 2017 Jan 24]. Available from: http://www.eng-atoms.msm.cam.ac.uk/RoyalSocDemos/SEM

24. Heath J. Energy dispersive spectroscopy. 2nd ed. Sussex, Uk: John Wiley & Sons Ltd; 2015.p. 9-11.

25. Cao G, Wang Y. Nanostructures and nanomaterials: Synthesis, properties, and applications. 2nd ed. Singapore: World Scientific Publishing Co Pte Ltd; 2011. p. 457.

26. Schematic of the principle of EDS [Internet]. [cited 2017 Jan 22]. Available from: http://www.faantech.com/EDAX.html

27. Huang M, Adnot A, Kaliaguine S. Silylation of H-ZSM-5: an X-ray photoelectron and infrared spectroscopy study. J Chem Soc Faraday Trans. 1993;89(23):4231.

28. Datka J, Tużnik E. Infrared spectroscopic studies of acid properties of NaHZSM-5 zeolites. Journal of Catalysis. 1986 Nov;102(1):43–51.

29. Damjanović L, Auroux A. Determination of acid/base properties by temperature programmed desorption (TPD) and adsorption calorimetry. In: Chester A, Derouance E, editors. Zeolite chemistry and catalysis. Dordrecht: Springer Netherlands; 2009. p. 107–167.

30. Knözinger H. Infrared spectroscopy as a probe of surface acidity. In: Joyner R, van Santen R, editors. Elementary reaction steps in heterogeneous catalysis. Dordrecht: Springer Netherlands; 1993. p. 267–285.

31. Buzzoni R, Bordiga S, Ricchiardi G, Lamberti C, Zecchina A. Interaction of pyridine with acidic (H-ZSM5, H-β, H-MOR zeolites) and superacidic (H-Nafion Membrane) systems: An IR investigation. Langmuir. 1996;12(4):930–940.

32. Karge H, Hunger M, Beyer H. Characterization of zeolites — infrared and nuclear magnetic resonance spectroscopy and X-ray diffraction. In: Weitkamp J, Puppe L, editors. Catalysis and zeolites. Berlin, Heidelberg: Springer Berlin Heidelberg; 1999. p. 198–326.

33. Sandoval-Díaz L, González-Amaya J, Trujillo C. General aspects of zeolite acidity characterization. Microporous and Mesoporous Materials. 2015;215:229–243.

34. Hsieh H. FTIR instrumentation [Internet]. Lab Servis. 2012 [cited 2017 Feb 14]. Available from: http://www-ec.njit.edu/~hsieh/ene669/FTIR.html

35. Stuart B. Infrared spectroscopy: Fundamentals and applications. Chichester, UK: John Wiley & Sons, Ltd; 2004. p. 18-19.

36. Wartewig S. IR and raman spectroscopy: Fundamental processing. Weinheim, FRG: Wiley-VCH Verlag GmbH & Co. KGaA; 2003. p.35-36.

37. Makarova MA, Zholobenko VL, Al-Ghefaili KM, Thompson NE, Dewing J, Dwyer J. Brønsted acid sites in zeolites. FTIR study of molecular hydrogen as a probe for acidity testing. Journal of the Chemical Society, Faraday Transactions. 1994;90(7):1047–1054.

38. Thommes M. Textural characterisation of zeolites and ordered mesoporous materials by physical adsorption. Studies in Surface Science and Catalysis. 2007;168:495–523.

39. Lowell S, Shields J. Powder surface area and porosity, 2nd ed. London, UK: Chapman and Hall Ltd.

40. Condon J. Surface area and porosity determinations by physisorption. Amsterdam: Elsevier; 2006. p. 1-3.

41. Al-rubaye R. Generation and characterisation of catalytic films of zeolite Y and ZSM-5 on FeCrAlloy metal. PhD Thesis. The University of Manchester. 2013.

42. Llewellyn P, Bloch E, Bourrelly S. Surface area/porosity, adsorption, diffusion. In: Che M, Védrine J, editors. Characterization of solid materials and heterogeneous

catalysts: From structure to surface reactivity. 2012. p. 853–879.

43. Bonardet J, Fraissard J, Unger K, Kumar D, Ferrero M, Ragle J, et al. The use of 15^N NMR for the understanding of nitrogen physisorption. Studies in Surface Science and Catalysis. 1994;87(C):319–326.

44. Fagerlund G. Determination of specific surface by the BET method. Materials and Structures. 1973;6(3):239–245.

45. Bartholomew C, Farrauto R. Fundamentals of industrial catalytic processes. Hoboken, NJ, USA: John Wiley & Sons, Inc.; 2005. p. 125.

46. Jentys A, Lercher J. Techniques of zeolite characterization. In: Bekkum H, Flanigen E, Jacobs P, Jansen J, editors. Introduction to zeolite science and practice. 2001;137: p. 345–386.

47. Bartholomew C, Farrauto R. Fundamentals of industrial catalytic processes. Hoboken, NJ, USA: John Wiley & Sons, Inc.; 2005. p. 175-177.

48. Gola A, Rebours B, Milazzo E, Lynch J, Benazzi E, Lacombe S, et al. Effect of leaching agent in the dealumination of stabilized Y zeolites. Microporous and Mesoporous Materials. 2000;40(3):73–83.

49. Chiyoda O, Davis M. Hydrothermal conversion of Y-zeolite using alkaline-earth cations. Microporous and Mesoporous Materials. 1999;32(3):257–264.

50. Ashbrook S. NMR of microporous materials. Presentation presented at; 2008; Cape Town, South Africa.

51. Inductively-coupled plasma (ICP) excitation source [Internet]. [cited 2017 Mar 1]. Available from: http://elchem.kaist.ac.kr/vt/chem-ed/spec/atomic/emission/icp.htm

52. Al-Zaidi, B. The effect of modification techniques on the performance of zeolite-Y catalysts in hydrocarbon cracking reactions. PhD Thesis. The University of Manchester. 2011.

53. Inductively coubpled plasma-optical emission spectrometer (ICP-OES) [Internet].

[cited 2017 Mar 1]. Available from: http://www.rohs-cmet.in/content/icp-oes

54. Redfern J, Coats A. Thermogravimetric analysis. Analyst. 1963;88:906-924.

55. Thermogravimetric analysis [Internet]. [cited 2017 Mar 2]. Available from: http://www.expertsmind.com/topic/thermogravimetric-analysis/recorder-911730.aspx

56. Littlewood A. Gas chromatography: Principles, techniques, and applications. 2nd ed. London: Academic Press, INC; 1970.

Chapter 5 Effect of crystal size and acidity of ZSM-5 on toluene conversion and p-xylene selectivity

5.1 Introduction to the effect of large crystals

Intracrystalline diffusion limitations can have a major effect on catalyst performance. Varying the zeolite crystal size can lead to noticeable changes in the product selectivity and reaction rate. The literature provides many examples of hydrocarbon reactions with significant effects on the reaction rate imposed by the intracrystalline molecular transport such as the cracking of n-hexane where the yield of the cracking products decreased with increasing the crystal size [1]. The effect of increasing the crystal size of ZSM-5 can be best demonstrated by the increase in para-xylene selectivity in toluene disproportionation and alkylation of toluene with methanol. The desired para-xylene isomer diffuses much faster than ortho- and meta-xylenes in the channels, hint increasing the crystal size will lead to more p-xylene in the product [2–4]. Performing toluene disproportionation over ZSM-5 zeolite produces different aromatic hydrocarbons which have kinetic diameters very close to or larger than the pore size. Therefore, the diffusion of these molecules will be severely restricted favouring the formation of p-xylene because of its smaller diameter resulting in a diffusion rate which is 1000 times greater than o-xylene and m-xylene diffusion rates [5]. At the same time, the other isomers will isomerise to para-xylene in order to diffuse through the channels. Olson and Hagg found a unique relationship between p-xylene selectivity and o-xylene diffusion time determined by adsorption measurements. They suggested that limiting the diffusion of o-xylene by reducing the diffusion rate as a result of catalyst modifications or increasing the crystal size will improve p-xylene selectivity [6].

Uguina et al. [3] carried out toluene disproportionation over ZSM-5 zeolite with 7 and 14 µm crystal sizes having a Si/Al ratio of 29 and 31, respectively. They observed that increasing the crystal size showed only a slight increase in the p-xylene selectivity from (22 to 25 %) which was not much higher than the thermodynamic equilibrium value. In contrast, Chen performed the alkylation of toluene with methanol over ZSM-5 zeolites with 0.1 and 7 µm crystal size having Si/Al ratio of 70. After modification with silica, the large crystals showed excellent p-xylene selectivity of around 70% while the modified small crystals showed slightly higher p-xylene selectivity than the thermodynamic equilibrium around 26%. Furthermore, the unmodified large crystals improved the p-xylene selectivity to 50 % [7]. As diffusion constraint was increased by the large crystals,

p-xylene selectivity was enhanced. Ducarme et al. [8] studied the deactivation and shape selectivity of three ZSM-5 zeolites with (0.3, 0.5 and 2) µm crystals with Si/Al ratio 10, 23 and 48, respectively. The p-xylene selectivity increased with crystal size as expected. In terms of deactivation behaviour, it was determined that the deactivation rate by coke was higher when decreasing the crystal size and/or the content of aluminium on the surface. However, pressing 1 to 5 µm crystals into dense aggregates using a press instrument slowed the deactivation process. Thus, the intercrystalline void volume is a key factor in the deactivation properties [8]. Ratnasamy et al. [4] studied the influence of ZSM-5 crystal size on the activity and selectivity towards p-xylene in xylene isomerization reaction. They tested ZSM-5 catalysts with 8, 13 and 16 µm which showed a decrease in activity with crystal size increase, it was decreased by a factor of 3 when increasing the crystal size from 8 to 16 µm. However, the ratio of p-xylene to o-xylene increased from 1.2 to 2.5 and hence more p-xylene formed.

Wei et al. [9] have observed that for the zeolite to be para-selective diffusion limitations should be increased. He established a key parameter controlling para-selectivity, $\emptyset = \mathrm{L}\,(\,K_1/D_o)^{1/2}$ where L is the pore length which is directly related to the crystal size, K is the intrinsic isomerization rate constant and D is the diffusivity. They observed from the equation that the higher the value of Ø, the higher p-xylene selectivity achieved. It can be concluded from the equation that increasing the crystal size should result in higher p-xylene selectivity.

Van Vu et al. studied the effect of crystal size on toluene conversion and p-xylene selectivity in the alkylation of toluene reaction using ZSM-5 zeolites with crystal sizes ranging from 5 to 30 µm. It was concluded from the experimental results that increasing the crystal size increased the p-xylene selectivity as seen in Figure 5-1. Again as in Ducarme's study the toluene conversion decreased with increasing the crystal size which can be attributed to the diffusion limitation induced on the reactants and products [10,11].

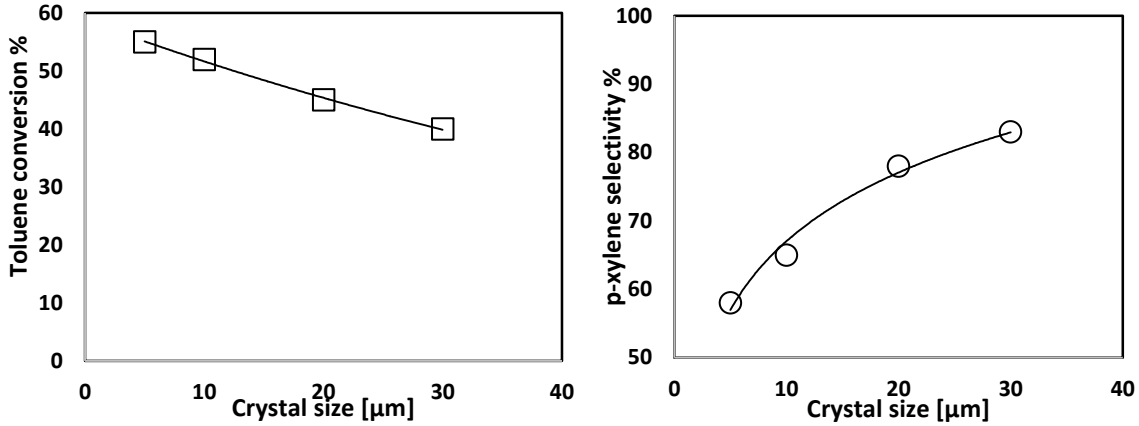

Figure 5-1: Effects of crystal size in toluene alkylation reaction [11]

From the discussion above it can be concluded that p-xylene formation in the pores will increase as a result of increased diffusion limitations. However, the number of acid sites on the external surface correlated with the amount of aluminium should be considered. Acid sites on the surface allow the isomerization of p-xylene decreasing the p-xylene selectivity to the thermodynamic equilibrium value (24 %) in the final products. Research has shown that the xylene isomerization intrinsic rate is 5000 times greater than toluene disproportionation rate [12]. To suppress the undesired isomerization on the surface, the external acid sites should be deactivated by different surface modifications such as the addition of silica layer, discussed in chapter 6. It is important to understand the aluminium distribution in ZSM-5 large crystals to comprehend the outcomes of any performed modification on their surface. Muller et al. studied the aluminium distribution in ZSM-5 large crystals by employing electron microscopy analysis and they observed that the aluminium content was enriched at the rims of the crystals (Figure 5-2) [13]. This was explained by considering the synthesis where initially an Al-rich gel was formed and settled towards the bottom of the autoclave which resulted in the ZSM-5 crystals nucleating from the Si-rich solution. Towards the end of the crystallization process more Al will be incorporated into the framework, explaining the higher content in the rim of the ZSM-5 [14,15] .

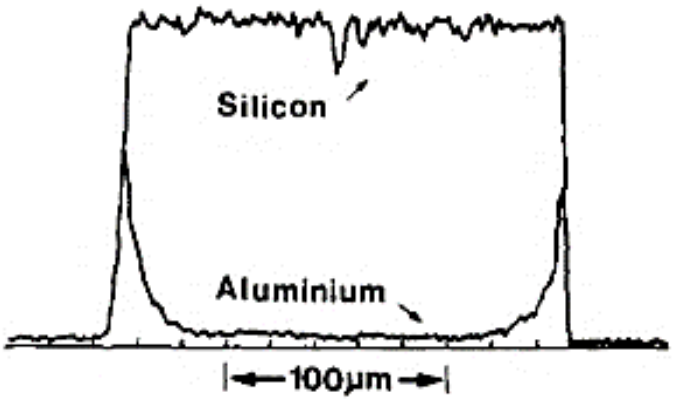

Figure 5-2: Aluminium distribution in large ZSM-5 crystal [13]

In this chapter, the effects of ZSM-5 zeolites with different silicon to aluminium ratio and crystal size have been evaluated in toluene disproportionation reaction in a fixed bed reactor. The behaviour of the catalysts in terms of p-xylene selectivity, p-xylene yield, toluene conversion and product distribution is discussed. The effect of different reaction parameters was investigated in this study, such as pressure and contact time, to maximize the p-xylene selectivity while maintaining industrially sensible conversions. Different characterization techniques were used to study the crystallinity, morphology and acidity of the catalysts.

5.2 Experimental

5.2.1 Catalyst preparation

Different ZSM-5 catalysts were evaluated in this chapter having different crystal sizes and Si/Al ratios. All large crystals zeolites were hydrothermally synthesized in house. The hydrothermal synthesis procedures were explained in section 4.3.1. The synthesized zeolites had to be calcined at 550 °C for 6 hours to remove the template (TPABr or TPAOH) and then, ammonium ion exchanged. Finally, all zeolites were calcined by ramping the temperature from ambient to 550 ˚C at a rate of 2 °C/min and held for 6 hours to produce the acidic H-form. Characteristics of ZSM-5 catalysts tested are listed in Table 5-1.

Table 5-1: Tested ZSM-5 zeolites characteristics

Catalyst	Crystal size (µm)	Si/Al	source	Sample ID
Small ZSM-5	0.5	26	Alfa-Aesar	SZ-0.5
Large ZSM-5	5	16	In house synthesis	LZ-5
Large ZSM-5	50	58	In house synthesis	LZ-50
Large ZSM-5	100	64	In house synthesis	LZ-100

The hydrothermal synthesis of zeolites was intended for making ZSM-5 catalysts with different crystal sizes and similar Si/Al ratios. Unfortunately, the synthesis was difficult to control leading to a range of bulk Si/Al ratios. The Si/Al ratio will affect the acidity, affecting the conversion of toluene and product distribution and will be discussed further in the results. Although the synthesis was unpredictable on the final bulk Si/Al, the crystal size allowed for toluene disproportionation to be carried over a wide crystal size range.

5.2.2 Catalyst characterization

5.2.2.1 X-Ray diffraction (XRD)

XRD X'Pert Philips instrument was used to study the structure by comparing the obtained patterns of the commercial and synthesized ZSM-5 zeolites to the literature. Samples were analysed according to the procedure described in section 4.4.1. Overall the XRD patterns indicated good crystallinity. The commercially synthesized ZSM-5 showed the least intense XRD peaks. The reflection peak for the length 100 µm crystals also appeared lower than those of 5 and 50 µm. These results are semi quantitative only as no silicon standard was used to allow quantitative crystallinity determination.

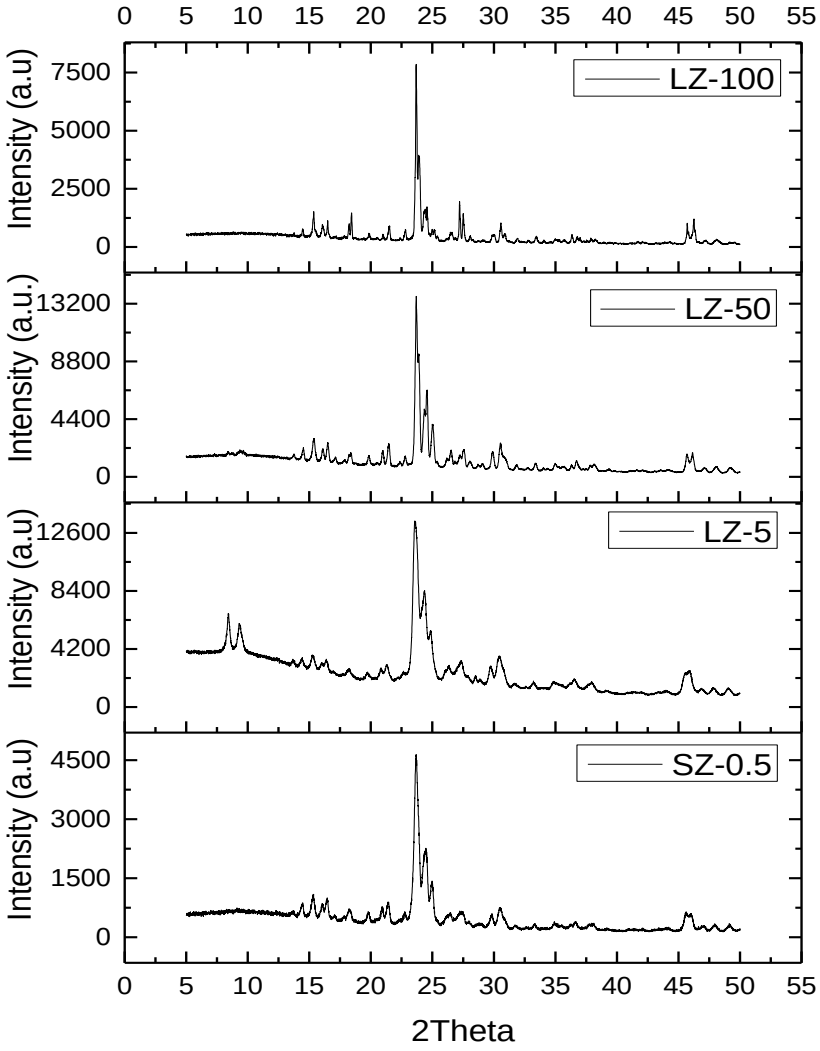

Figure 5-3 XRD patterns for different ZSM-5 zeolites with varying crystal size

5.2.2.2 Scanning electron microscopy (SEM)

SEM was utilized to understand the morphology of the crystals (agglomerates, single or twinning crystals) while EDX was used to measure the Si/Al ratio. All samples were analysed following the procedure in section 4.4.2. The SEM pictures below for the different ZSM-5 catalysts show the difference in morphology and crystal size ranging from 0.5 to 100 µm. The commercial ZSM-5 showed agglomerates of crystals while the synthesized ones showed different morphologies. The 5 µm showed spherical crystals and the 50 and 100 µm displayed elongated hexagonal crystals as seen in Figure 5-4. Different synthesis routes were followed to synthesize the 5, 50 and 100 µm which can explain the difference in crystal size, morphology and Si/Al ratio. The 5 µm crystals were synthesized

using aged feedstock gel and a seeding gel, which helps in reducing the crystallization period (24 hrs), while the 50 and 100 µm were synthesized using one overall gel. The synthesis procedure of the large crystals (50 and 100 µm) involved a crystallization period of 10 days which might have led to large crystals. Similar observations were reported by Shiralkar et al. where they found that increasing the crystallization time from 96 to 169 hours increased the crystal size from 1 to 3.5 µm [16]. Furthermore, it was suggested in the literature that the lower amount of aluminium in the synthesis gel mixture the larger the produced crystals as the addition of aluminium into ZSM-5 was found to disrupt the process. It was shown that aluminium increases the activation energy required for nucleation and crystal growth [17]. This reveals that Si/Al ratio can affect the size of the synthesized crystals which was confirmed by Shirazi et al. where they varied the Si/Al ratio in ZSM-5 synthesis (Si/Al=10 to 50) resulting in ZSM-5 zeolite with crystal sizes from 1-9 µm [17]. In this thesis, the 50 and 100 µm had Si/Al ratio above 50 as seen in Table 5-2 while the 5 µm had Si/Al ratio of 16 and, although it is lower than the commercial ZSM-5 (Si/Al=25). The commercial zeolites are usually prepared in large batches where agitation is used resulting in small aggregated crystals with irregular shapes.

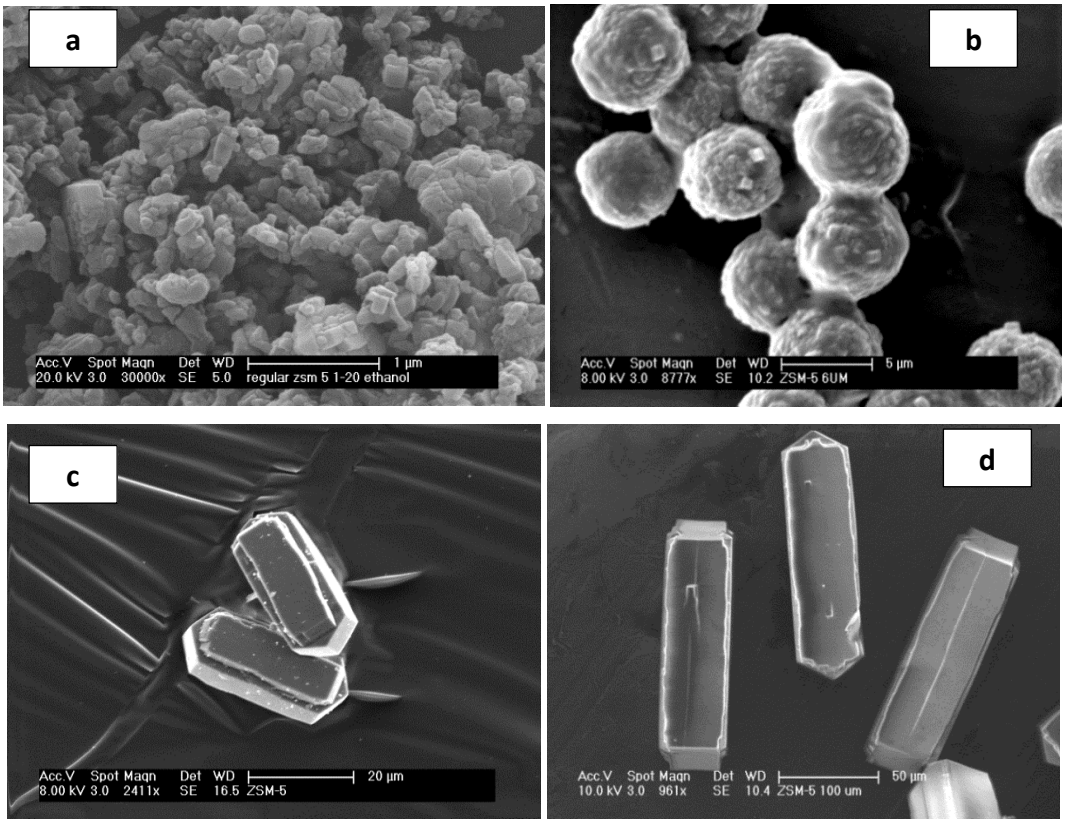

Figure 5-4: ZSM-5 with different crystal sizes (a) 0.5 µm (b) 5 µm (c) 50 µm (d) 100 µm

5.2.2.3 Energy Dispersive X-ray (EDX) and inductively coupled plasma optical emission (ICP-OES)

EDX was employed to investigate the Si/Al ratio by taking six spots (3 nm) on each sample and the results were averaged and only used as indication of Si/Al ratio. At the same time ICP-OES was used to obtain the Si/Al ratio of each catalyst as well. First, 7-10 mg of each sample was digested with HF acid. Then, they were sprayed into the instrument chamber. The ICP-OES analyses were performed in Medac Ltd and the quoted error in Al and Si wt. % is ± 0.3 wt. %. Si/Al ratios of the zeolites by EDX and ICP can be found in Table 5-2. The obtained Si/Al by ICP and EDX were similar for SZ-0.5, LZ-5 and LZ-100. On the other hand, EDX showed lower Si/Al ratio than ICP for LZ-50. This means that LZ-50 had less aluminium near the surface as EDX analysis cannot reach deep enough. In contrast ICP measures the bulk Si/Al ratio.

5.2.2.4 Pyridine - Fourier-transform infrared spectroscopy (py-FTIR)

The BAS and LAS of the parent and silylated ZSM-5 were investigated by pyridine adsorption. The samples were pressed into discs and activated at 450 ^{o}C for 5 hours. The region 3500 – 3900 cm^{-1} shows the bridging hydroxyl group (3610 cm^{-1}) and the SiOH (3745 cm^{-1}). All the bridging OH-groups of the ZSM-5 zeolites with different crystal sizes were accessible to pyridine as seen in Figure 5-5 while ZSM-5 with 5 µm crystal size (Si/Al=16) had the highest number of bridging hydroxyl groups.

FTIR Pyridine adsorption was used to understand the type (Brønsted and Lewis acidity) and the amount of acidity of each catalyst. Pyridine was introduced to the cell at 150 ^{o}C and the sample was evacuated at the same temperature to remove physically adsorbed pyridine. BAS and LAS peaks can be found at 1455 and 1545 cm^{-1}, respectively.It is noticeable from Figure 5-6 that the ZSM-5 zeolite with 5 µm crystals has the highest acidity in terms of Brønsted and Lewis acid sites which is related directly to having higher aluminium content as the Si/Al ratio is about 16. Whereas, the other catalysts have lower acidity as they contain lower aluminium. In terms of the ratio of BAS to LAS, all the catalysts differ from each other's and LZ-5 had the highest amount of LAS which could mean higher amount of extraframework aluminium as can be seen in Table 5-2. The level of acidity from FTIR correlated well with the Si/Al (from ICP-OES) with the highest Si/Al having the lowest total acidity (Brønsted + Lewis).

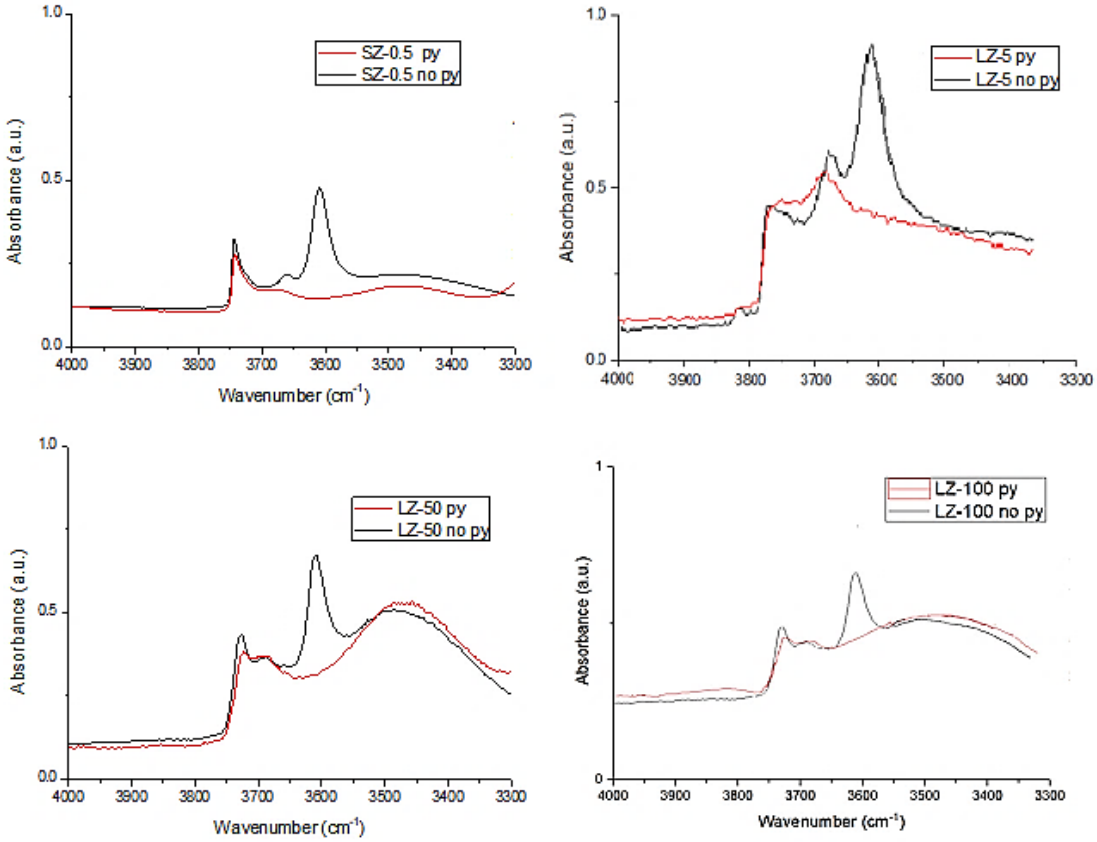

Figure 5-5: FTIR spectra in the hydroxyl region with and without pyridine

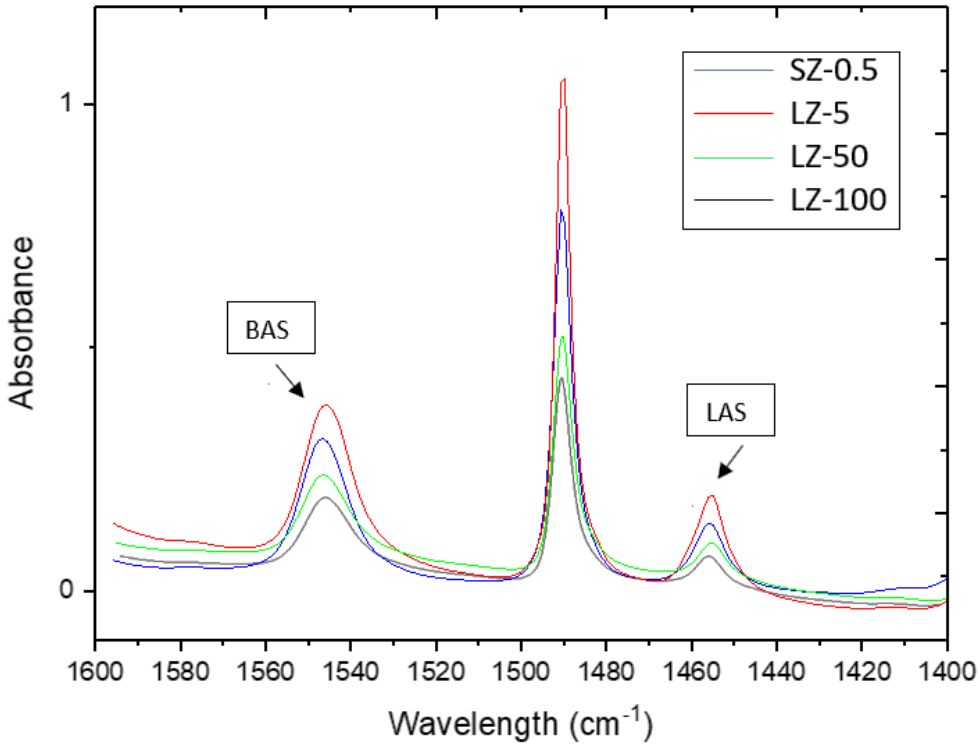

Figure 5-6: BAS and LAS of ZMS-5 zeolites with different crystal sizes

It is well known in the literature that the hydrocarbon reactions occur on Brønsted acid sites. It was detected through various characterization techniques that Si/Al ratio is an important factor in determining the strength and nature of ZSM-5 acidity. These studies have revealed that the number of acid sites per unit cell is directly proportional to the number of aluminium atoms per unit cell. In addition, Meshram et al. [18] showed that conversion in toluene disproportionation increased as the number of acid sites increased. In addition, the Brønsted acid sites strength increased with aluminium content (lower Si/Al). However, decreasing the number of strong acid sites can suppress toluene dealkylation or cracking reactions keeping benzene to xylene ratio around 1. Also, their results suggested acid sites generated by lattice aluminium located in the channels are mostly used for toluene disproportionation reaction. It can be observed from Table 5-2 that the lower the Si/Al ratio the higher the number of Brønsted and Lewis acid sites.

Table 5-2: ZSM-5 Zeolites Acidity and Si/Al measurements

Catalyst	Si/Al (EDX)	Si/Al (ICP)	BAS (mmol/g)	LAS (mmol/g)	BAS/LAS
SZ-0.5	29.6	26.3	0.310	0.079	3.92
LZ-5	16.4	15.9	0.368	0.172	2.15
LZ-50	30.0	58.2	0.185	0.060	3.08
LZ-100	55.4	64.3	0.152	0.046	3.30

5.2.2.5 BET surface area and pore volume measurements by N_2 adsorption

BET was utilized to measure the surface area of the commercial and synthesized ZSM-5 zeolites. Furthermore, the pore volumes and external surface areas were obtained. The surface area is an important characteristic of the zeolites in this study. As having a large surface area could mean higher possibility for the isomerization reaction to take place as more acid sites will be available. During this study, Micromeritics Gemini 2365 surface area instrument was used.

ZSM-5 with the smallest crystal size (0.5 µm) had the highest surface area while surprisingly the zeolite with crystal size 5 µm had the lowest surface area amongst all samples. In terms of pore volume, all samples had about the same pore volume with the

100 µm crystals showing the lowest value (0.079 cm^3/g). Shirazi et al. synthesized ZSM-5 zeolites with a crystal size range (1 - 9) µm and Si/Al ratio (10 – 50). Furthermore, they studied the relationship between Si/Al ratio and the BET surface area in ZSM-5 zeolites and it was observed that having lower Si/Al ratio will lead to lower surface area [17]. Also, smaller crystals had lower surface area than large crystals. The observed relationship between Si/Al and surface area in this study can explain the 5 µm crystals having the lowest surface area as they have the lowest Si/Al ratio that is around 16. However, no correlation was found between crystal size and surface area. Table 5-3 shows the data obtained for the used catalysts.

Table 5-3: ZSM-5 Surface area and pore volume measurements

Catalyst	BET surface area (m^2/g)	Pore volume (cm^3/g)	External surface area (m^2/g)
SZ-0.5	338	0.113	151
LZ-5	280	0.110	93.1
LZ-50	320	0.090	181
LZ-100	316	0.079	206

5.2.3 Catalytic evaluation

All ZSM-5 catalysts with different crystal sizes were tested for toluene disproportionation. Firstly, the reaction was performed at a toluene weight hourly space velocity (WHSV) of 3 h^{-1} for 2 hours as time on stream to observe initial activity and stability. In addition, to ensure that steady state was reached and indicated by no fluctuation in the conversion. Then, the catalyst was tested as the WHSV was increased to 30, 70 and finally 80 h^{-1}. The WHSV was changed during the experiments to study the effect of residence time on toluene conversion, p-xylene selectivity and p-xylene yield. Furthermore, all catalysts were tested at two different pressures, 1 and 10 bar.

5.2.3.1 Effect of crystal size on p-xylene selectivity and conversion at WHSV=3 h^{-1}

All four ZSM-5 catalysts were tested at a 3 h^{-1} WHSV over 2 hours to study the stability with time. It was expected that increasing the crystal size will increase the p-

xylene selectivity as a result of diffusion limitations imposed by the increase in crystal size. After 2 hours on stream, ZSM-5 zeolites with 0.5 and 5 µm showed similar conversion and para-selectivity around 25% in line with the thermodynamic equilibrium value. As expected, the much larger crystals of ZSM-5 (50 and 100 µm) showed a clear improvement over the thermodynamic value where both catalysts reached approximately 35 % p-xylene selectivity at much reduced conversion.

The lower toluene conversion can be attributed to both the reduced acidity and the limited diffusion caused by the longer diffusion path. With half the Brønsted and Lewis acidity of the 0.5 µm commercial ZSM-5 (Table 5-2), it was expected that reduced conversion would result. It is well known in zeolites that acid sites are related to the framework aluminium content which affects the catalytic properties and acid sites distribution [19]. It was likely that LZ-50 and LZ-100 was going to deliver low toluene conversion due to the fewer available acid sites. In addition, LZ-100 had lower pore volume (Table 5-3) which could affect the conversion.

Figure 5-7 shows the catalytic evaluation of toluene disproportionation over ZSM-5 with crystal size (0.5, 5, 50 and 100) µm at WHSV 3 h^{-1} for 2 hours. Time zero minutes is defined as the appearance of the first drop of product from the separator which usually takes 2 hours from the starting of the pump.

The difference in conversion obtained by small and large crystals can be ascribed to the crystals size and the imposed diffusion limitations in addition to the Si/Al difference. Another reason could be the difference in uniformity of the aluminium distribution in the small and large crystals. It was concluded in the literature that aluminium in large crystals is not uniformly distributed and is enriched at the rim of the crystals [13].

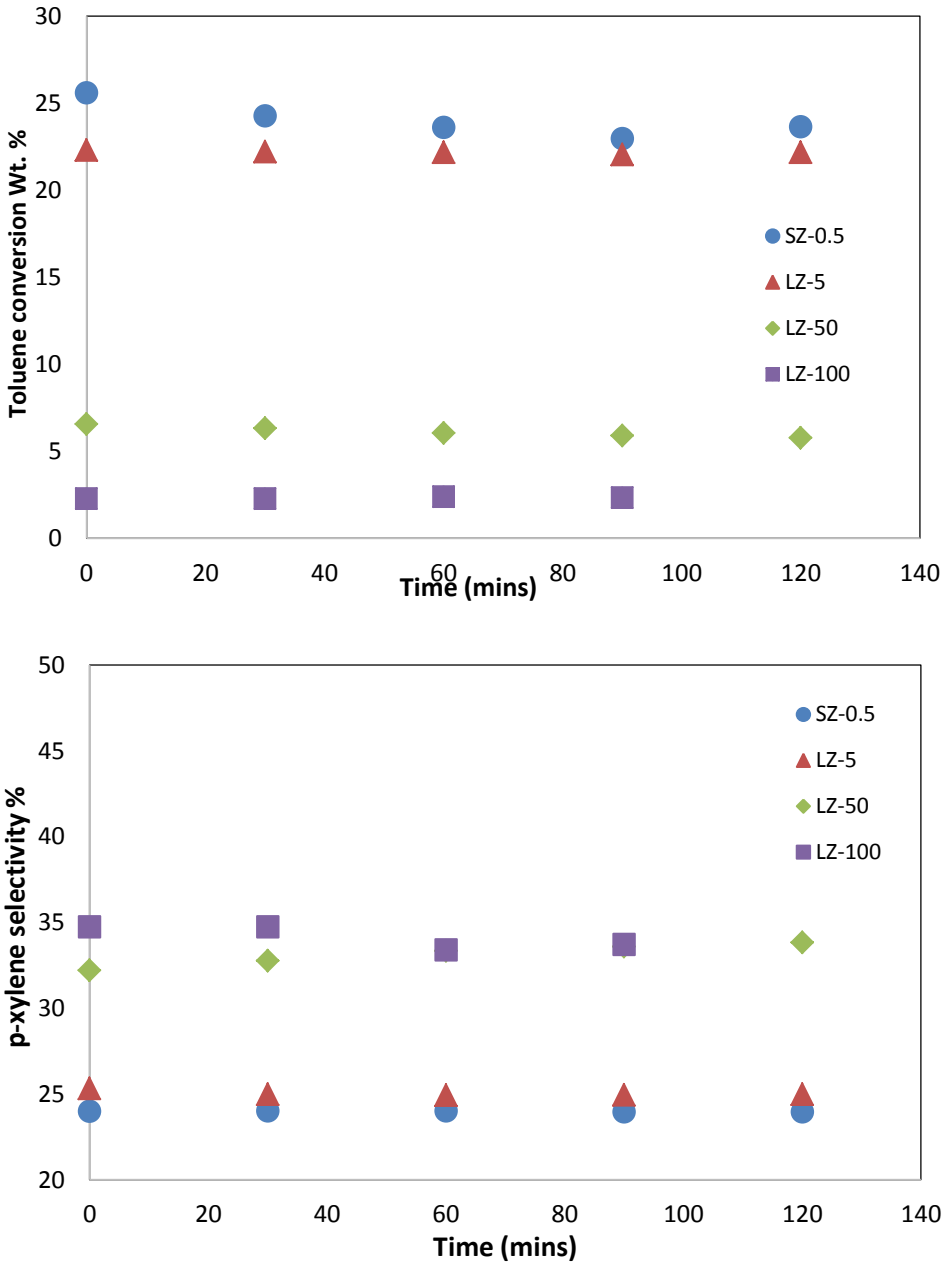

Figure 5-7: Effect of crystals size on toluene conversion and p-xylene selectivity at WHSV 3 h^{-1}

5.2.3.2 *Effect of crystal size on para-xylene selectivity and toluene disproportionation at varying WHSV*

Increasing the WHSV reduces the contact time between the reactants/products and the acid sites of the zeolite. As contact time decreases (i.e. the higher the WHSV), the lower the conversion. In terms of p-xylene selectivity, it increased noticeably with increasing WHSV (Figure 5-8) reaching its highest value for all catalysts at the highest WHSV (83 h^{-1}). A drop in toluene conversion was accompanied by increase in p-xylene selectivity. LZ-50 and LZ-100 showed the highest p-xylene selectivity with all WHSV values

but at the same time the conversion was the lowest amongst the other catalysts. Amongst the four catalysts, LZ-5 delivered the best results in terms of the combination of toluene conversion, p-xylene selectivity and p-xylene yield.

Based on the obtained results it can be concluded that crystal size plays a key role in increasing the p-xylene selectivity in the xylene mixture. As the diffusion path increases, greater diffusion limitations will be imposed on the isomers with larger kinetic diameters requiring them to isomerize to the favourable para isomer, which have a smaller kinetic diameter, to be able to diffuse through the channels. These findings are in agreement with the literature results at atmospheric pressure [20].

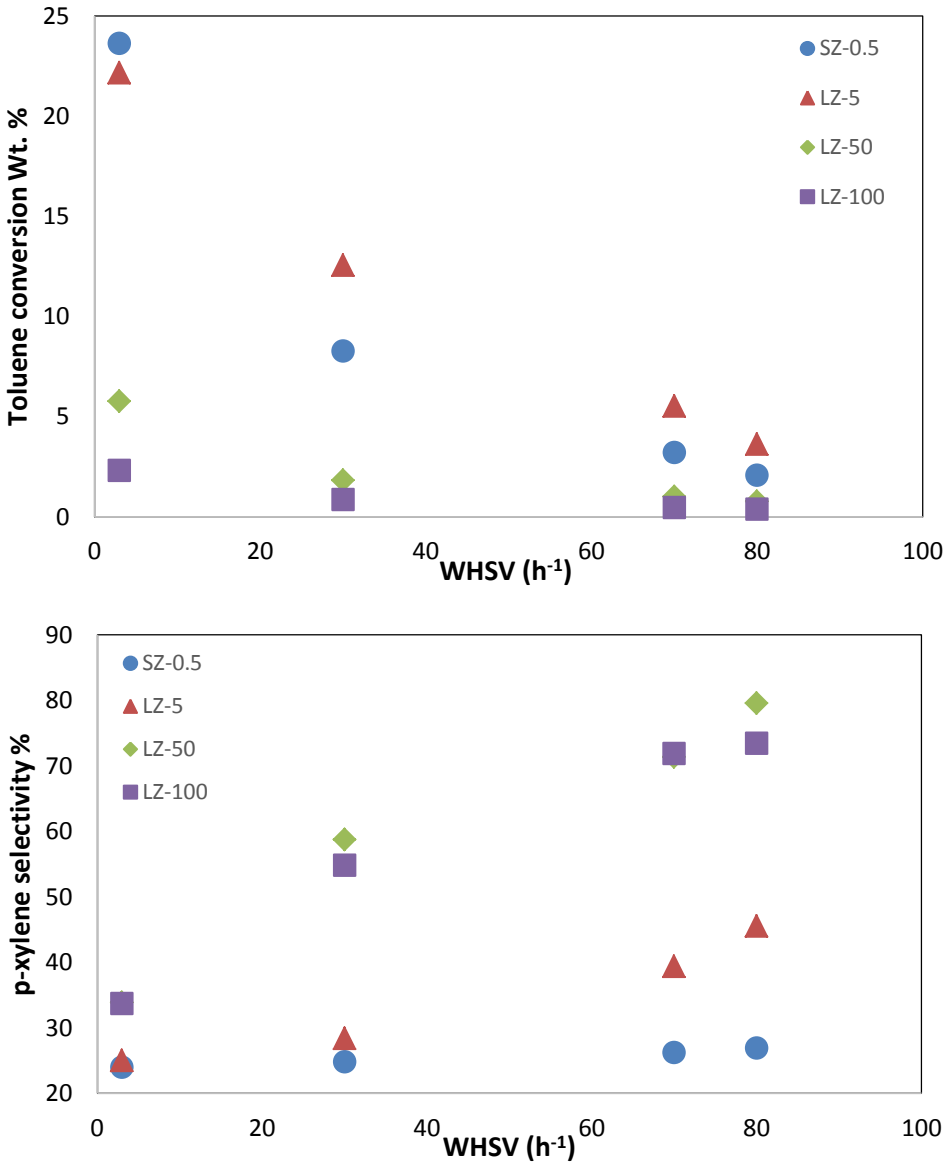

Figure 5-8: Effect of WHSV on toluene conversion and p-xylene selectivity over ZSM-5 with different crystal size at 1 bar

To optimise the toluene disproportionation process, it is essential to find the right balance between these three important variables, conversion, selectivity to para isomer in the xylene isomers and yield of p-xylene (wt. %) in the total products. LZ-5 showed the highest toluene conversion at all WHSVs except for WHSV 3 h^{-1} resulting in the highest p-xylene yield amongst all other tested catalysts (Figure 5-9).

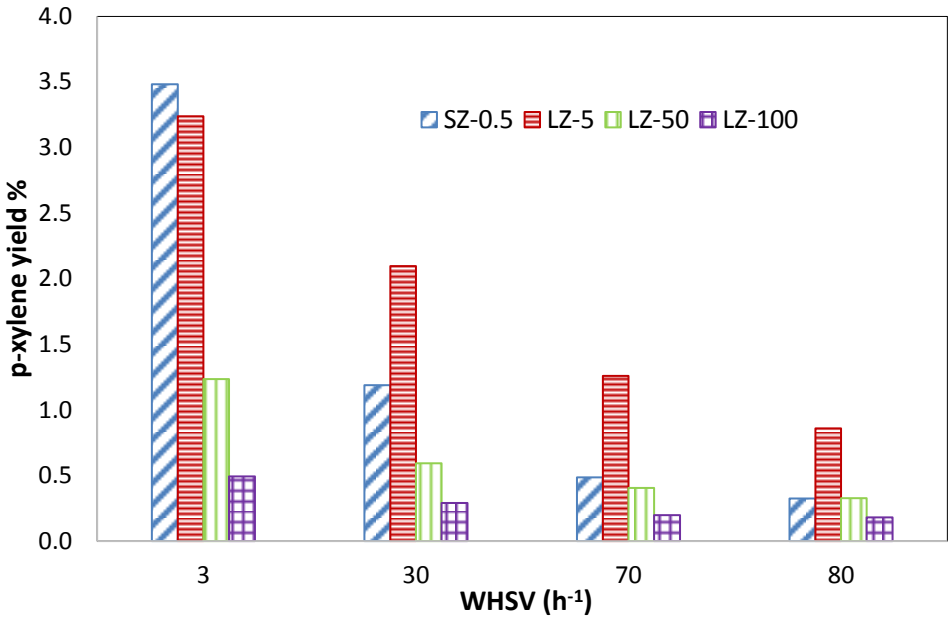

Figure 5-9: p-xylene yield over different crystal size at various WHSV

5.2.3.3 Effect of pressure on p-xylene selectivity and toluene conversion

Increasing the reaction pressure should increase the conversion of feed over the catalyst by allowing more molecules to react with the available acid sites in the channels and on the surface of the tested catalysts [21]. Pressure induces more and longer contact between the zeolite and toluene molecules meaning higher chance of feed molecules reacting over the available acid sites within ZSM-5. Increasing the pressure to 10 bar using hydrogen showed significant increase in the conversion of toluene. The effects induced by increasing the pressure to 10 bar can be clearly seen in Figure 5-10 compared with the results at 1 bar in the previous section. Noticeably performing the reaction at high pressure increased the toluene conversion. In the case of large crystals catalysts, the selectivity increased with increasing WHSV (h^{-1}). However, it is lower than the values achieved at atmospheric pressure. The observed results indicate a trade-off between conversion and selectivity.

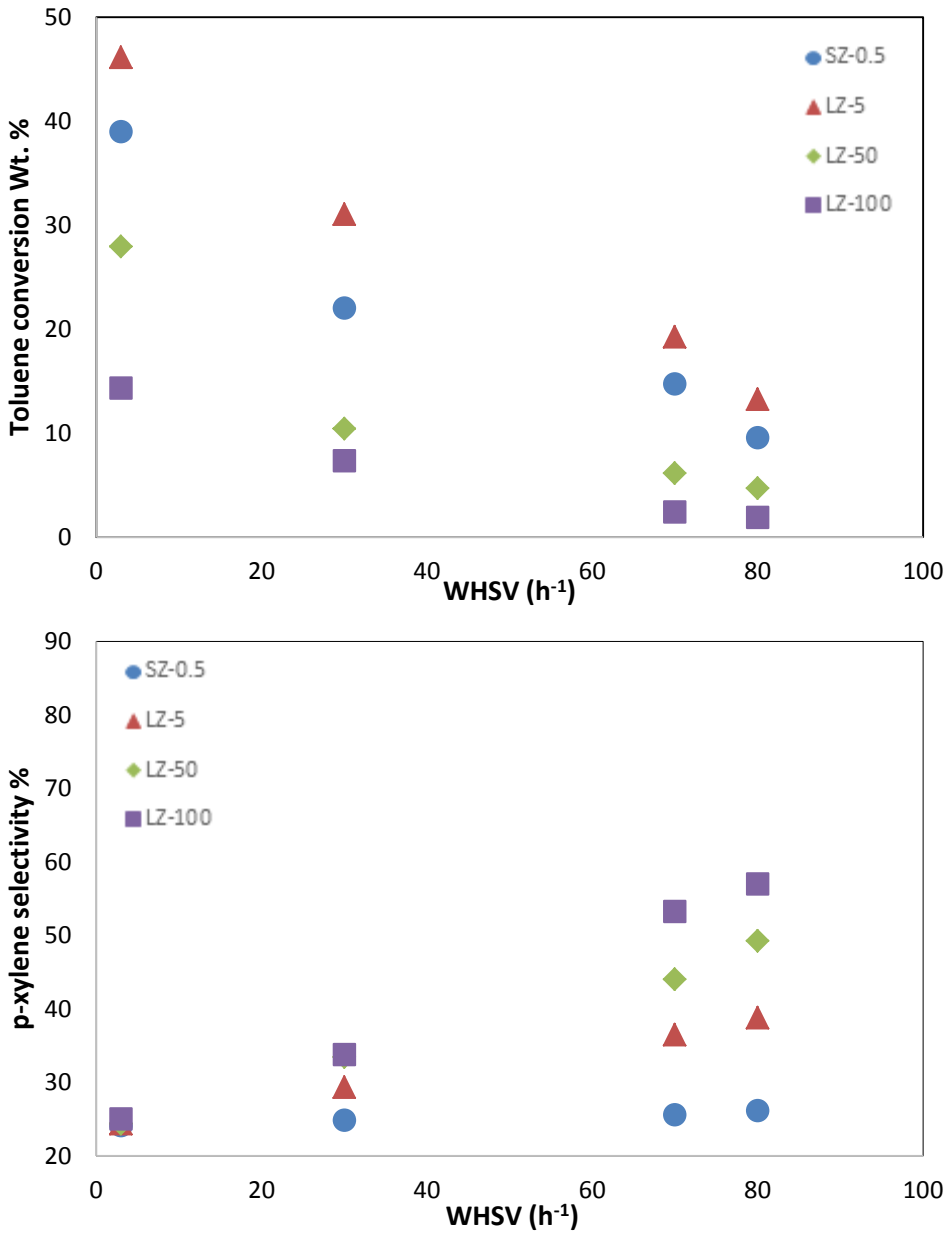

Figure 5-10: Conversion and p-xylene selectivity over varying crystal sizes as a function of WHSV at elevated pressure (10 bar)

Increasing the pressure almost doubled the conversion for all samples and dropped the selectivity back to the thermodynamic equilibrium value (24 %) at WHSV 3 h^{-1}. Although increasing WHSV of toluene increased the selectivity for all samples, conversion dropped consequently while still being higher than the conversion achieved at atmospheric pressure.

LZ-5 produced the highest conversion at about 46 % at the lowest WHSV. This achieved conversion can be attributed to the higher aluminium content in this catalyst and more acid sites were available to be utilized during the reaction as illustrated in Table 5-2.

Based on this, LZ-5 performed better in terms of toluene conversion even when the WHSV was varied from (3 to 83 h^{-1}). LZ-50 and LZ-100 delivered the highest p-xylene selectivity 50 % and 60 %, respectively at the lowest residence time. Conversely, they showed the lowest conversion which was around 5 % and 2 %, respectively.

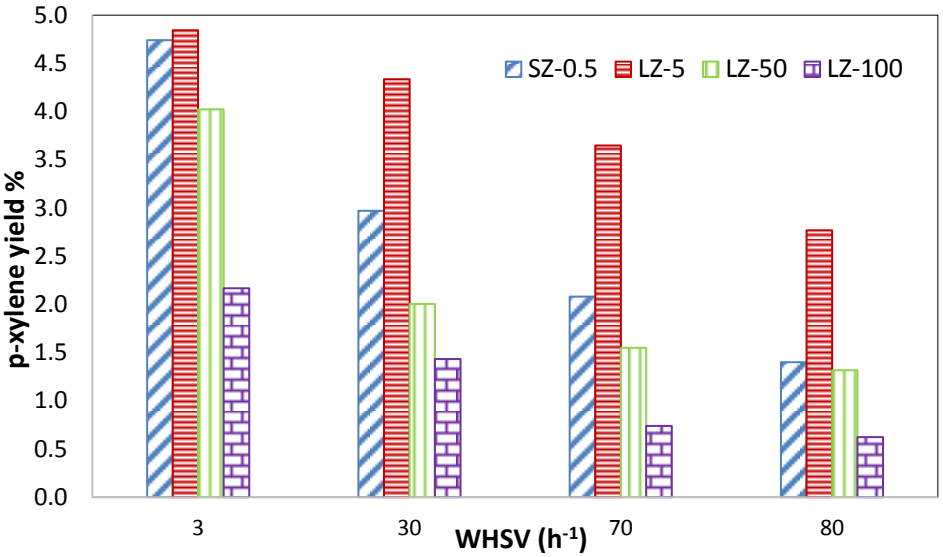

Figure 5-11: Effect of pressure on p-xylene yield

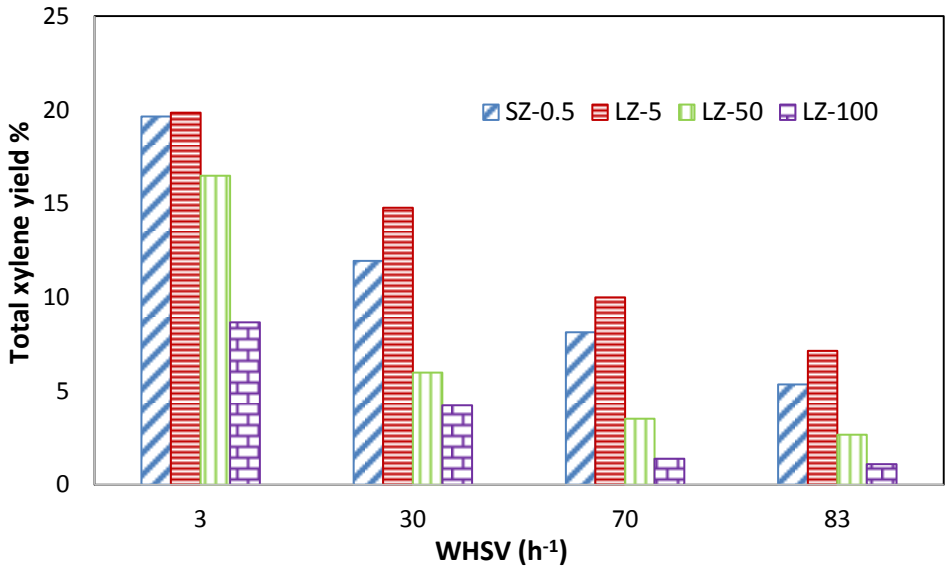

Figure 5-12: Effect of pressure on total xylene yield

As stated earlier that LZ-5 showed the best results in terms of conversion and p-xylene selectivity, the same conclusion was reached when the catalysts were tested at 10 bar. For example, a conversion of around 15 % was achieved alongside 40 % p-xylene

selectivity at 83 h^{-1} WHSV. In terms of p-xylene yield, as it was expected the highest value was obtained by LZ-5 catalyst because of its high toluene conversion (Figure 5-11). The yield of p-xylene was increased by 36 % and 50 % for SZ-0.5 and LZ-5, respectively. On the other hand, the yield attained over LZ-50 and LZ-100 was three to four times the yields achieved with atmospheric pressure. In terms of total xylene yield, LZ-5 delivered the highest yield at all WHSVs (Figure 5-12).

5.2.3.4 Effect of crystal size on the catalytic activity

The observed reaction rate constant (k_{obs}) was calculated for all four ZSM-5 catalysts to investigate the effect of diffusion path and Si/Al ratio on the activity at varying WHSVs (30, 70 and 83) h^{-1}. Figure 5-13 shows that all catalysts showed first order behaviour at WHSVs (30 – 83 h^{-1}) and LZ-5 had the highest activity which could be attributed to having the highest aluminium (lowest Si/Al) content compared to other catalysts (Table 5-2). The very large crystals (LZ-50 and LZ-100) showed very low rate constants values with LZ-100 having the lowest value as seen in Table 5-4. The low values of rate constants observed by the large crystals can be attributed to the diffusion constraints imposed by the longer diffusion path as well as the higher Si/Al ratio exhibited (Table 5-2). Increasing the pressure to 10 bar increased the activity which is displayed by the increase in the observed kinetic rates of all four catalysts.

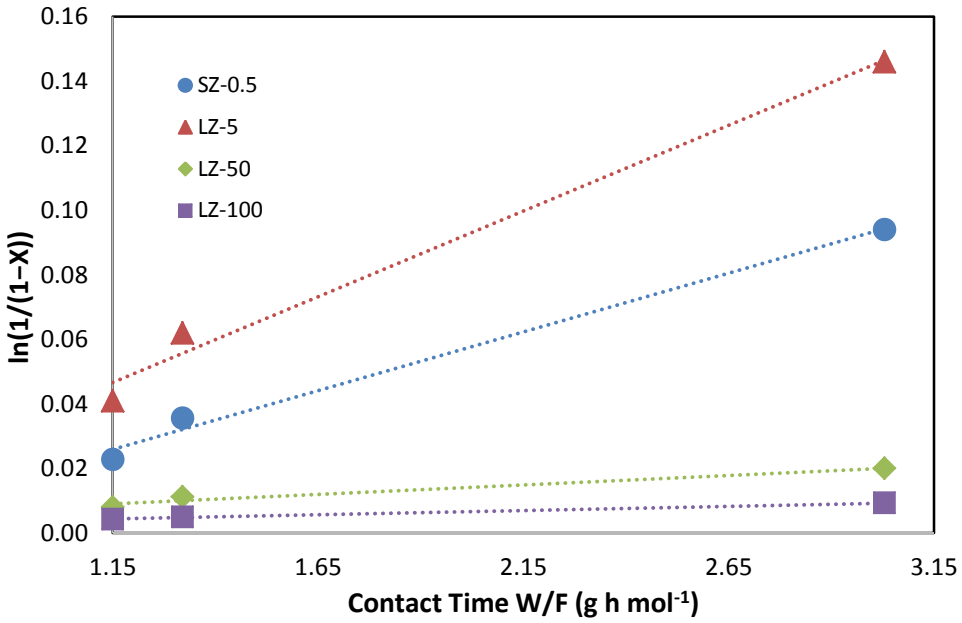

Figure 5-13: First order plot for different ZSM-5 zeolites at 1 bar against W/F

Table 5-4: Observed rate constant at different pressure

Catalyst	(k_{obs}) observed Rate Constant	
	At 1 bar	At 10 bar
SZ-05	0.036	0.075
LZ-5	0.053	0.123
LZ-50	0.006	0.034
LZ-100	0.003	0.033

5.2.3.5 Effect of crystal size on product distribution

The difference in crystal size and Si/Al ratio in the tested ZSM-5 zeolites affected the product distribution with varying the WHSV (h^{-1}). Figure 5-14 and Table 5-5 illustrate the difference in the product distribution at two different WHSVs, 3 and 30 h^{-1}. LZ-5 showed the lowest amount of toluene in the product stream, meaning the highest conversion amongst the four catalysts was achieved. Small amount of ethylbenzene was observed in the products obtained over LZ-5 due to the high conversion. C_{10} and C_9 products were produced in negligible amounts and the highest amount were produced over LZ-5. Increasing the WHSV resulted in very small amount of ethylbenzene and no C_{10} in the products.

Table 5-5: Effect of crystal size on product distribution at 10 bar and varied WHSV

	Catalyst	Benzene	Toluene	Et-Benzene	p-xylene	m-xylene	o-xylene	C_9	C_{10}
WHSV (3 h^{-1})	SZ-0.5	17.03	61.01	0.04	4.74	10.47	4.43	0.68	0.06
	LZ-5	23.27	53.86	0.65	4.84	10.37	4.63	1.16	0.14
	LZ-50	10.93	72.05	0.11	4.02	8.55	3.91	0.36	0.02
	LZ-100	5.49	85.66	0.03	2.17	4.54	1.95	0.15	0.02
WHSV (30 h^{-1})	SZ-0.5	9.94	77.99	0.00	2.97	6.22	2.75	0.22	0.00
	LZ-5	14.71	68.94	0.29	4.33	7.61	2.83	0.53	0.53
	LZ-50	4.30	89.59	0.00	2.00	2.93	1.05	0.10	0.00
	LZ-100	3.02	92.67	0.00	1.43	2.02	0.79	0.07	0.00

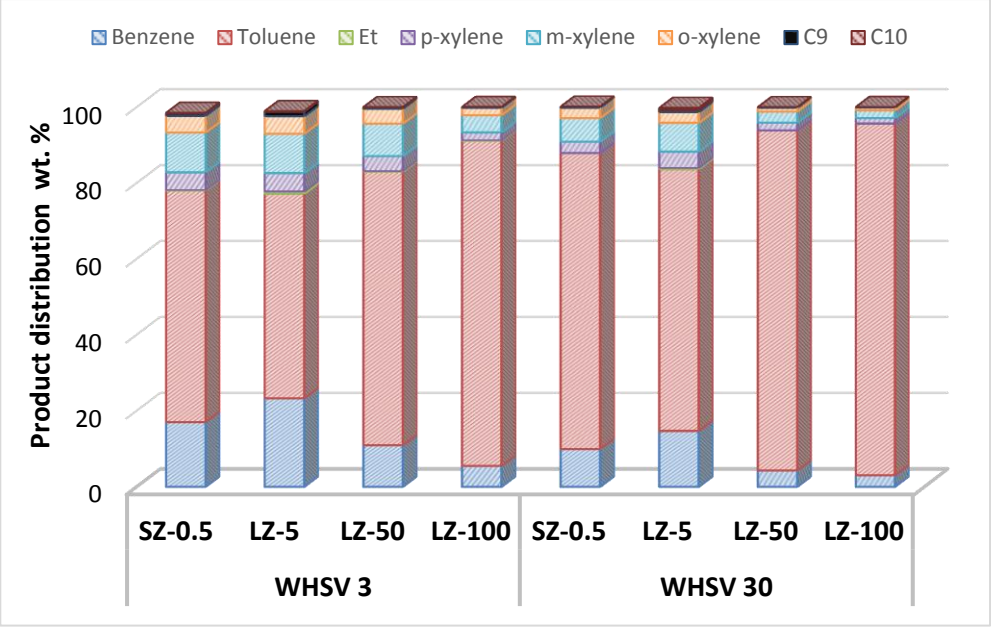

Figure 5-14: Effect of crystal size on product distribution at 10 bar

In general, the toluene conversion decreases with increasing the crystal size of ZSM-5, especially when the crystal size is very large (50 and 100) µm. It can be observed from Figure 5-7 that at atmospheric pressure ZSM-5 with 0.5 µm achieved the highest conversion. This observation is in line with the literature, where Wan et al. studied the effect of different crystal size of ZSM-5 for methanol to gasoline conversion and found that small crystals provided higher conversion [22]. Increasing the pressure showed that the 5 µm and 0.5 µm crystals gave similar levels of conversion being higher over the 5 µm. This can be attributed to the lower Si/Al ratio of the 5 µm crystals. In terms of p-xylene selectivity, the selectivity increased as expected because of the diffusion limitations imposed on the ortho- and meta- isomers by the longer diffusion path created with the increase in the crystal size. It will be more difficult for the larger molecules (o- and m-) to travel through the long channels. They will either stay inside the channels or rearrange to form p-xylene.

Every tested ZSM-5 catalyst delivered different benzene to xylene ratio as shown in Figure 5-15. This variation can be attributed to the different Si/Al ratios and crystal size exhibited by each catalyst. The larger the crystals size the lower the ratio of benzene to xylene. However, LZ-5 showed the highest value at the lowest WHSV and this can be attributed to the higher toluene conversion achieved because of the higher aluminium content of this catalyst. Increasing the WHSV resulted in decreasing the benzene to xylene ratio as the

conversion dropped. Das et al. observed a similar trend, they reported that increasing space velocity showed lower values of benzene to xylene and lower conversion as contact time lowered at high WHSVs [23].

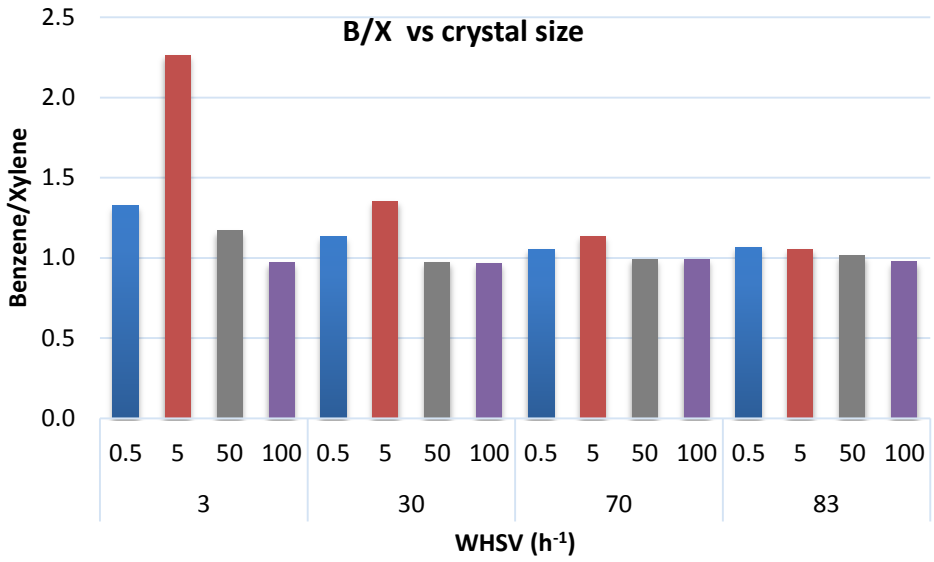

Figure 5-15: Effect of crystal size on benzene to xylene ratio at 10 bar

5.2.3.6 Deactivation behaviour of the different catalysts at 10 bar

SZ-0.5, LZ-5 and LZ-100 were tested for 50 hours at a WHSV 30 h^{-1} to study how the crystal size effected toluene conversion and p-xylene selectivity over extended operation (> 50 hrs) (Figure 5-16). The conversion dropped with time over all three catalysts. As expected, conversion decreased rapidly initially and then more slowly after 12 hours or less for the large crystals (LZ-5 and LZ-100). The smaller crystal size continued to deactivate up to 40 hours and then stabilized. The most interesting result was the significant improvement in the p-xylene selectivity of LZ-100 increasing from around 34% to 55% after 30 hours on stream. SZ-0.5 did not show any improvement in selectivity and remained at around the thermodynamic equilibrium value throughout the whole run. Similarly, LZ-5 observed only a minor improvement on thermodynamic equilibrium value (27.5 % after 50 hours on stream).

Velasco et al. observed a similar behaviour over ZSM-5 [24]. However, their observation was based on ethylbenzene disproportionation over ZSM-5 (Si/Al = 42 and crystal size of 4.4 µm) at 300^{o}C and atmospheric pressure. They found that there was a rapid

deactivation during the first 3 hours on stream.

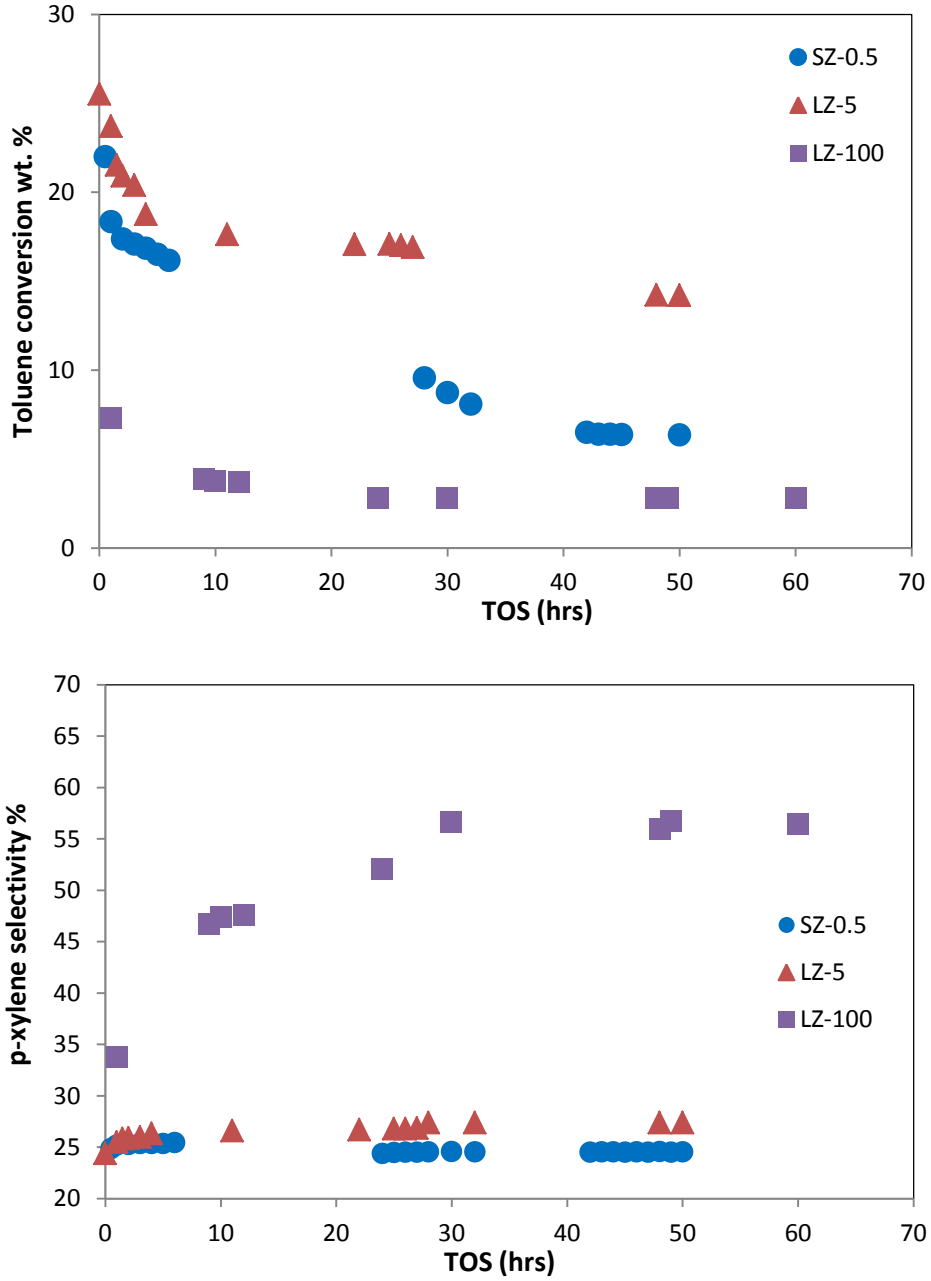

Figure 5-16: Deactivation behaviour over ZSM-5 zeolites with different crystal size

After the reaction, the coke content was determined for all three catalysts using TGA (see section 4.4.7 for method). LZ-100 had the highest amount of coke while SZ-0.5 with the smallest crystal size possessed least coke formation amongst all tested zeolites. This is believed to be a result of the higher BET surface area and shorter diffusion path, providing more chances for larger molecules to exit the pores. The low pore volume observed for LZ-100 could lead to the formation of higher coke on the large crystals. Similar results were reported by Wan et al., where they showed that the longer the

diffusion path the more coke formation observed on the catalyst as it is more difficult for large molecules to diffuse through [22]. Figure 5-17 shows the TGA weight loss curves of all spent catalysts as weight percent after performing toluene disproportionation for 50 hours at a WHSV 30 h^{-1}.

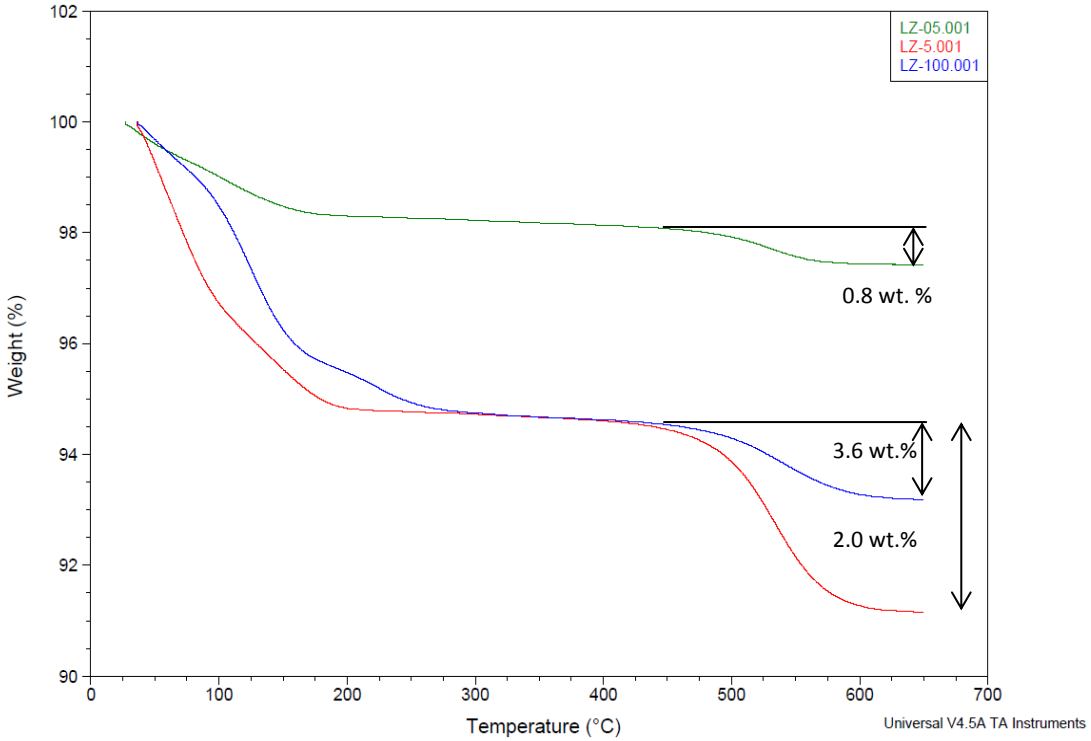

Figure 5-17: TGA curves for ZSM-5 with different crystal sizes after 50 hours on stream

The weight loss for each zeolite is shown in Table 5-6 and the smallest crystal size (0.5 µm) had the lowest amount of coke. However, in this case LZ-5 (5 µm) had the largest amount of coke as it was the lowest in Si/Al, with more acid sites (Table 5-2) than LZ-100 (100 µm).

Table 5-6: Coke analysis after deactivation studies

Catalyst	Si/Al	X (50h)	S_P (50 h)	Coke wt. %
LZ-0.5	26.3	7.2	24.5	0.85
LZ-5	15.9	14.2	27.5	3.61
LZ-100	64.3	2.8	56.7	2.00

5.3 Conclusions

Four different ZSM-5 zeolites with different crystal sizes synthesized in house were tested for toluene disproportionation to investigate the effect of crystal size on p-xylene selectivity and toluene conversion. The effects of different key operating parameters such as residence time and reaction pressure were studied in order to optimize the conversion and selectivity of toluene disproportionation. Increasing the crystal size improved p-xylene selectivity and inversely decreased the conversion, especially with the very large crystals (50, 100) µm. In terms of residence time, conversion decreased with increasing WHSV. On the other hand, p-xylene selectivity was enhanced. The increase in selectivity was only observable with large crystals (5, 50, and 100) µm indicating that the increase was due to the combination of crystal size and residence time. Increasing the pressure from atmospheric to 10 bar increased the conversion of toluene at the cost of p-xylene selectivity. The highest conversion was reached over the 5 µm (LZ-5) while the best p-xylene selectivity was achieved over the 100 µm (LZ-100) alongside very low conversion. It was concluded that LZ-5 delivered the best results in terms of p-xylene selectivity and conversion combination. Figure 5-18 below summarizes toluene conversion against p-xylene selectivity at 10 bar for all tested catalysts in this chapter.

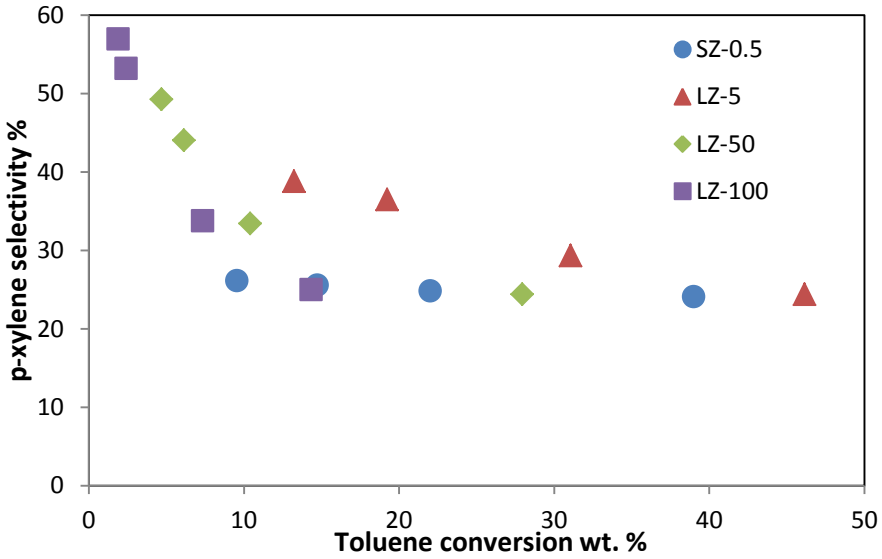

Figure 5-18: Toluene conversion vs p-xylene selectivity over ZSM-5 with different crystal sizes

It can be concluded from this chapter that increasing the diffusion limitation by increasing the diffusion path length (crystal size) is a key factor in increasing the selectivity towards p-xylene. To furtherly optimize the selectivity, the external acid sites should be

deactivated to suppress the isomerization occurring on the zeolite surface. The next chapter discusses ZSM-5 zeolite surface deactivation by depositing amorphous silica layer using chemical liquid deposition method (CLD).

5.4 References

1. Herrmann C, Haas J, Fetting F. Effect of the crystal size on the activity of ZSM-5 catalysts in various reactions. Applied Catalysis. 1987;35(2):299–310.

2. Bhat YS, Das J, Rao KV, Halgeri AB. Inactivation of external surface of ZSM-5: Zeolite morphology, crystal Size, and catalytic activity. Journal of Catalysis. 1996;159(2):368–374.

3. Uguina M, Sotelo J, Serrano D. Toluene disproportionation over ZSM-5 zeolite. Effects of crystal size, silicon-to-aluminum ratio, activation method and pelletization. Applied Catalysis. 1991;76(2):183–198.

4. Ratnasamy P, Babu G, Chandwadkar A, Kulkarni Sb. Influence of crystal size of HZSM-5 on activity and shape selectivity in xylene isomerization. Zeolites. 1986;6(2):98–100.

5. Csicsery SM. Shape-selective catalysis in zeolites. Zeolites. 1984;4(3):202–213.

6. Olson D, Haag W. Structure-selectivity relationship in xylene isomerization and selective toluene disproportionation. American Chemical Society Symposium Series. 1984;248:275–307.

7. Chen N. Reactions of mixtures of toluene and methanol over ZSM-5. Journal of Catalysis. 1988;114(1):17–22.

8. Ducarme V, Vedrine J. ZSM-5 and ZSM-11 zeolites: influence of morphological and chemical parameters on catalytic selectivity and deactivation. Applied Catalysis. 1985;17(1):175–184.

9. Wei J. A mathematical theory of enhanced para-xylene selectivity in molecular sieve catalysts. Journal of Catalysis. 1982;76(2):433–439.

10. Van Vu D. MFI zeolite catalysts for selective production of para-xylene and light

olefins. PhD Thesis. Osaka University; 2009.

11. Van Vu D, Miyamoto M, Nishiyama N, Egashira Y, Ueyama K. Selective formation of para-xylene over H-ZSM-5 coated with polycrystalline silicalite crystals. Journal of Catalysis. 2006;243(2):389–394.

12. Chen N, Garwood W. Industrial application of shape-selective catalysis. Catalysis Reviews. 1986 Jun;28(2–3):185–264.

13. Müller U, Unger K. Sorption studies on large ZSM-5 crystals: the influence of aluminium content, the type of exchangeable cations and the temperature on nitrogen hysteresis effects. Studies ins Surface Science and Catalysis. 1988;39:101–108.

14. Von Ballmoos R, Meier W. Zoned aluminium distribution in synthetic zeolite ZSM-5. Nature. 1981;289:782–783.

15. Jung C, Young C. Aluminium distribution in large ZSM-5 crystals. Zeolites. 1988;8(1):82–85.

16. Shiralkar V, Joshi P, Eapen M, Rao B. Synthesis of ZSM-5 with variable crystallite size and its influence on physicochemical properties. Zeolites. 1991;11(5):511–516.

17. Shirazi L, Jamshidi E, Ghasemi M. The effect of Si/Al ratio of ZSM-5 zeolite on its morphology, acidity and crystal size. Crystal Research and Technology. 2008;43(12):1300–1306.

18. Meshram N, Hegde S, Kulkarni S. Active sites on Z S M - 5 zeolites for toluene disproportionation. Zeolites. 1986;6:434–438.

19. Derouane E, Védrine J, Pinto R, Borges P, Costa L, Lemos A, et al. The acidity of zeolites: Concepts, measurements and relation to catalysis: A review on experimental and theoretical methods for the study of zeolite acidity. Catalysis Reviews. 2013;55(4):454–515.

20. Chen N. Personal perspective of the development of para selective ZSM-5 catalysts. Industrial and Engineering Chemistry Research. 2001;40(20):4157–4161.

21. Al-Khattaf S, Ali M, Al-Amer A. Effect of reaction pressure and carrier gas on toluene disproportionation over molybdenum - ZSM-5 catalyst. Energy and Fuels. 2008;22(1):243–249.

22. Wan Z, Wang C, Yang H, Zhang D. Effect of crystal size of ZSM-5 on its catalytic activity for methanol to gasoline conversion. In Chemeca 2013 : challenging tomorrow. Vol. 1. Barton, ACT: Engineers Australia. 2013. p. 5.

23. Das J, Bhat Y, Halgeri A. Selective toluene disproportionation over pore size controlled MFI zeolite. Ind Eng Chem Res. 1994;33(2):246–250.

24. Velasco N, Machado M, Cardoso D. Ethylbenzene disproportionation on HZSM-5 zeolite : the effect of aluminum content and crystal size on the selectivity for p-diethylbenzene . Brazilian Journal of Chemical Engineering. 1998;15.

Chapter 6 Effect of Silylation by Chemical Liquid Deposition (CLD)

6.1 Introduction and Background

Silylation is a modification method performed over zeolites by depositing amorphous silica layers on the external surface; a schematic is shown in Figure 6-1. This can be achieved by either chemical vapour deposition (CVD) or chemical liquid deposition (CLD) [1]. Depositing an inert silica has been demonstrated to improve the p-xylene selectivity by inducing more diffusion constraints on the other isomers and suppressing the isomerization on the surface by deactivating the external acid sites and narrowing the pore mouth of ZSM-5 [2–4]. Niwa et al. successfully silylated ZSM-5 by CVD treatment shown in Figure 6-2 which led to a decrease in the pore size by 1-2 Å allowing an increase in p-xylene selectivity [5]. However, the CVD treatment was difficult to control, operate and reproduce, hindering its practical application. On the other hand, CLD was easier to transfer to an industrial scale [6].

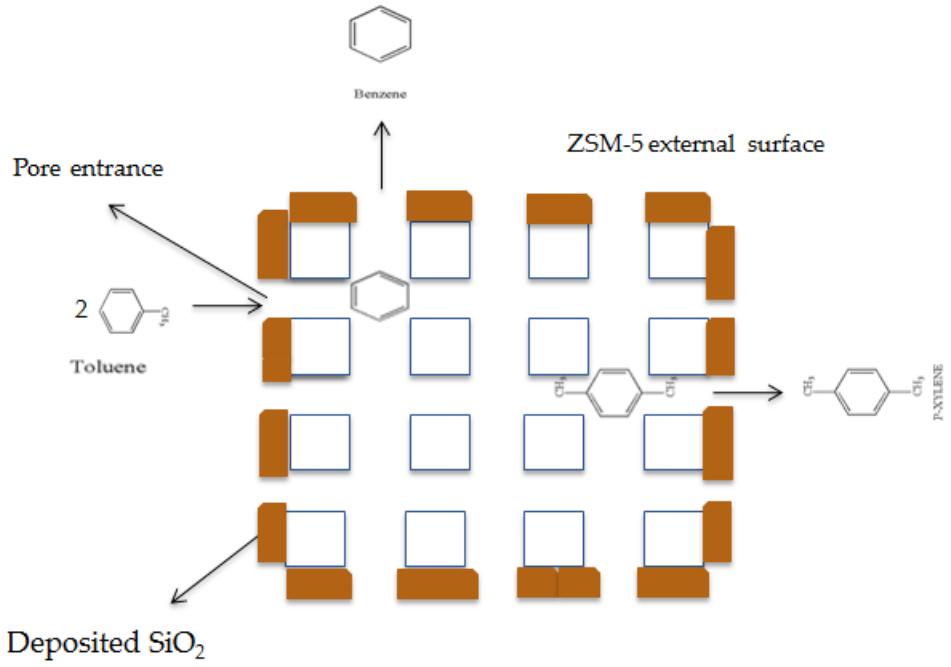

Figure 6-1: Silylation schematic diagram

Chang and Shihabi used different polysiloxane compounds as CLD agents to modify ZSM-5. They used PMS (phenylmethyl silicone), DMS (dimethyl silicone) and HMDS (hexamethyldisiloxane) and performed toluene disproportionation at 35 bar and 420 °C for 63 days on stream where they achieved high p-xylene selectivity (85 %) and a toluene conversion 30 % [7]. Zhu et al. used polysiloxane as well and attained 96 % p-xylene

selectivity after four cycles of modification [2]. However, deposition of large amounts of SiO_2 was required as it is difficult to create a uniform silica layer due to the high viscosity of polysiloxane. Other smaller molecules were used in the literature to deposit inert silica on the surface of zeolites such as TEOS (tetraethyl orthosilicate), but critically it has a molecular diameter (1.03 nm) larger than the pore mouth of ZSM-5 (0.56 nm) ensuring the deposition only occurs on the external surface and the pore mouth [6]. The reaction between the silylating agent and the hydroxyl groups, forming Si-O-Si or Si-O-Al bonds [8,9], leads to the passivation of the acid sites on the surface and narrowing the pores, reducing isomerization and making it more difficult for the m-xylene and o-xylene to diffuse out of the pores.

Silylation with TEOS was reported in the literature by Zheng and colleagues achieving 71% p-xylene selectivity. although, the conversion was very low (0.83%) and hence not industrially attractive [1]. This result showed that improving silylation could make an effective modification but maintaining high conversion with more active catalyst was required. Silylation can be controlled using different parameters. Manstien et al. suggested the use of multi-cycle CVD modification and low deposition temperatures (200-300) °C to attain uniform deposition of inert silica and have more effect on deactivation of the external acid sites [10]. Hui et al. studied different CLD conditions such as CLD agent, solvent, CLD time, deposition amount and number of cycles as shown in Table 6-1 [6].

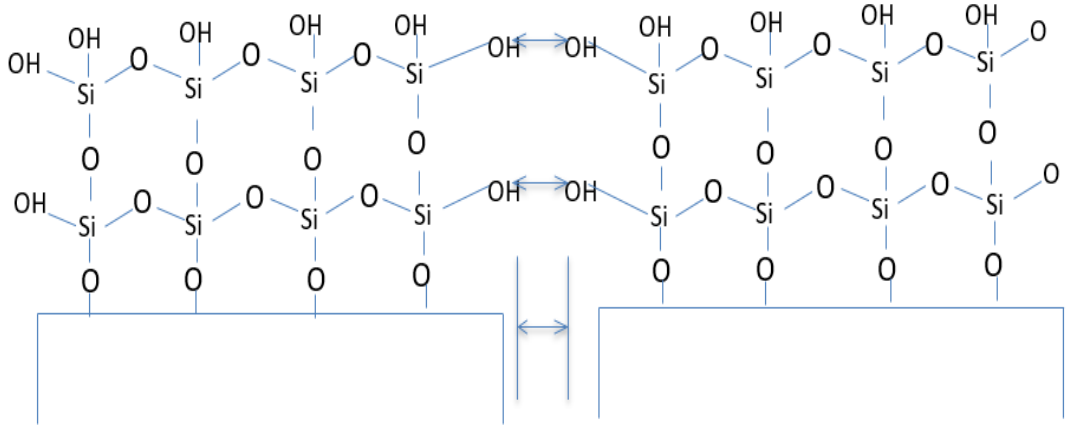

Figure 6-2: Pore narrowing by silylation [4]

Table 6-1: Literature CLD conditions and findings [6]

CLD conditions	Findings and conclusion	X%	Para-sel%
CLD agent DMS (dimethyl silicone), $(CH_3)_2SiHCl$ (DMCS), (3-chloropropyl) TMS, TEOS	TEOS showed the highest p-xylene selectivity and high conversion	30%	52%
CLD solvent Ethanol, 1,2,3 trimethylbenzene cyclohexane	Cyclohexane was more effective in the process and this was due to being non-polar. Polar solvents will compete with CLD agent in terms of adsorbing on the acid sites.	35%	45%
CLD agent amount	Increasing the amount of TEOS per gram of catalyst enhanced p-xylene selectivity. The best achieved selectivity and conversion was at 0.4 ml/g. increasing the amount over 0.4 does not affect the selectivity and results in decreasing the conversion.	25%	55%
CLD cycle	Increasing the number of cycles increased the selectivity whatever the amount of TEOS used. Three cycles with 0.1 ml TEOS showed the best p-xylene selectivity.	22.6%	79%
CLD time	CLD times from 0.5 h to 19 h were used with 7-10 h being the optimum.	26%	82%

Niwa et al. proposed that silylation of zeolites happened in two stages illustrated in Figure 6-3. Firstly, the reaction in liquid phase followed by calcination. During the liquid phase reaction, TEOS is hydrolysed producing hydroxy triethoxysilane which adsorbs on Lewis and Brønsted acid sites, forming Si-O-Al bond. The calcination step oxidizes the ethoxy groups into hydroxyl groups, followed by formation of Si-O-Si by condensation with adjacent silanol groups [4,11]. It was postulated that silylation initiates on the accessible bridging hydroxyl groups to the silylation agent. In theory, improving the selectivity towards p-xylene results from passivating the acid sites on the surface and narrowing the pores in parallel. Narrowing the pores can be achieved if the bridging hydroxyl groups are in the pore mouth [8]. Otherwise, only minor narrowing of the pores will occur from silylation of the external surface.

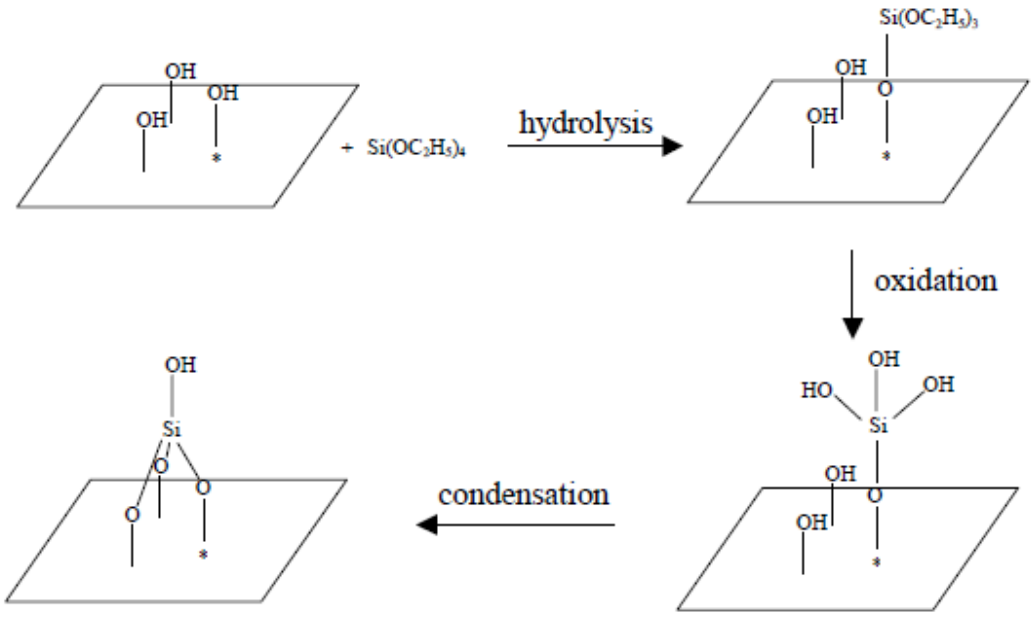

Figure 6-3: Schematic of silylation on HZSM-5 surface [9,12]

Zheng et al. used two different silylating agents with different molecular diameter, TEOS (1.03 nm) and tetramethoxysilane (TMOS) (0.89 nm). The results obtained suggested that more pore mouth narrowing occurred using TMOS because it can reach deeper into the pores and the results were in agreement with Aramaroli et al. [9,13]. Zheng suggested that the silanol groups formed by silylation are located in the pore mouth region of the zeolites [9]. Therefore, TEOS and 3-aminopropyltriethoxysilane (APTES) (0.8 nm) were studied in this thesis to investigate the effect of silylation on the surface and the pore size. Also, APTES contains an amino group which is strongly basic. This means that the APTES molecule will strongly adsorb on the acid sites on the surface of the zeolite. However, it should not penetrate the pores as APTES has a large diameter compared to the pore size of H-ZSM-5 [14].

6.2 Catalyst preparation

6.2.1 Materials

ZSM-5 zeolites with different crystal sizes SZ-0.5 (0.5 µm), LZ-5 (5 µm) and LZ-50 (100 µm) were silylated by CLD method with TEOS (sigma Aldrich, ≥ 99%) and 3-Aminopropyltriethoxysilane (APTES) (sigma Aldrich, 99%) mixed with cyclohexane.

6.2.2 Silylation

SZ-0.5 (Si/Al=25, 10g) was suspended in a solution of cyclohexane (Aldrich, 99.9%) (100 ml) and TEOS to obtain a modified catalyst with X wt. % SiO_2 as different amounts of loadings were utilized in this study (X = 10, 30 and 45 wt. %). The components were mixed together for 7 hours at 40 °C. Cyclohexane was evaporated at 80 °C while the mixture was stirring, and the catalyst was dried at 120 °C. The dried sample was calcined in a muffle furnace at 550 °C (6 hours) heating from ambient at a rate of 3 °C/min in a flowing air. The procedure was repeated to attain two cycles and so on. A sample (5g) of LZ-5 (Si/Al = 15.5) was mixed with 50 ml cyclohexane and 5.5 ml TEOS to load 30 wt. % SiO_2 on the zeolite using the above procedure.

SZ-0.5 (10 g) was silylated by mixing it with a solution of 100 ml of cyclohexane containing different amounts of APTES to achieve loadings (10, 50 wt. %). The mixture was stirred at 40 °C for 7 hours under reflux. Then, the cyclohexane was evaporated slowly at 120^{o}C. After that, the catalyst was calcined at 550^{o}C to form the silica modified H-ZSM-5 by decomposing the organosilicon compound.

Table 6-2 details the loading amounts, number of cycles and silylation agent used for the modification of the small and large ZSM-5 crystals.

Table 6-2: Silylation modification on different ZSM-5 zeolites

Zeolite	Silylation agent	Silica loading wt. %	No. cycles	Sample ID
SZ-0.5	TEOS	10 wt. %	1	SZ-0.5-T-1X10%
	TEOS	10 wt. %	2	SZ-0.5-T-2X10%
	TEOS	30 wt. %	1	SZ-0.5-T-1X30%
	TEOS	45 wt. %	1	SZ-0.5-T-1X45%
	APTES	10 wt. %	1	SZ-0.5-A-1X10%
	APTES	50 wt. %	1	SZ-0.5-A-1X50%
LZ-5	TEOS	30 wt. %	1	LZ-5-T-1X30%
	TEOS	30 wt. %	2	LZ-5-T-2X30%
LZ-50	TEOS	30 wt. %	2	LZ-50-T-2X30%
	TEOS	30 wt. %	4	LZ-5-T-4X30%

Where T=TEOS and A=APTES

6.3 Catalyst Characterization

6.3.1 X-ray Diffractometer (XRD)

XRD X'Pert Philips instrument was used to obtain patterns of the parent and the modified ZSM-5 zeolites following procedure described in section 4.4.1. XRD patterns for both large and small ZSM-5 unmodified and silylated were comparable with ZSM-5 reference pattern [15]. Patterns of SZ-0.5 silylated samples showed that the crystallinity of ZSM-5 was not severely affected by the modification and only a slight decrease in the intensities was noticed after loading 10 wt. % by one cycle of silylation. The slight reduction in intensities could be due to light dealumination during calcination process carried out after silylation – see Figure 6-4. However, after two modification cycles the crystallinity dropped by 15 %. Increasing the silica loading resulted in further decrease in crystallinity as illustrated in Table 6-3. Silylation modification is performed by loading amorphous layers of silica which will result in reducing the crystallinity of the zeolite. The XRD patterns of modified samples were compared with the parent to confirm that silica was loaded successfully on ZSM-5. It can be seen from the table below that as the loading amount increased the crystallinity dropped further as a result of diluting the sample.

Table 6-3: The effect of silica loading on crystallinity

Sample	SiO_2 agent	SiO_2 loading wt. %	Crystallinity %
SZ-0.5-T-1X10	TEOS	10	92 %
SZ-0.5-T-2X10	TEOS	10 (2 cycles)	85 %
SZ-0.5-T-1X30	TEOS	30	75 %
SZ-0.5-T-1X45	TEOS	45	66 %
SZ-0.5-A-1X10	APTES	10	90 %
SZ-0.5-A-1X50	APTES	50	60 %
LZ-5-T-1X30	TEOS	30	50 %
LZ-5-T-2X30	TEOS	30 (2 cycles)	42 %

It was observed that the peak intensities decreased drastically after modifying LZ-5 as the amount of SiO_2 used was high, 30 wt. %. The crystallinity was calculated based on the ASTM method discussed in section 4.4.1. The crystallinity decreased by 50 % and 60 % after one and two cycles, respectively as shown in Figure 6-5.

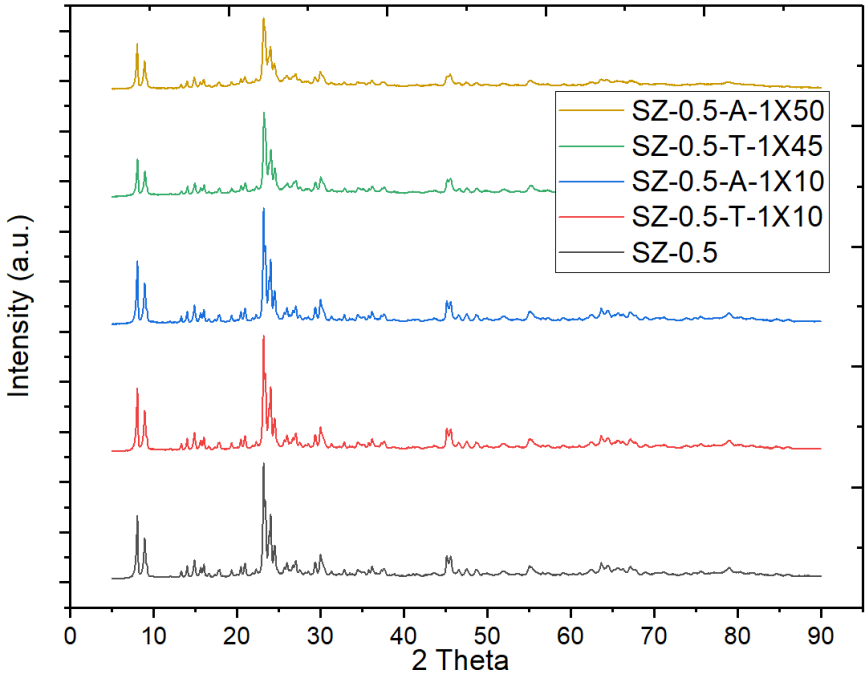

Figure 6-4: XRD patterns of SZ-0.5 parent and modified samples

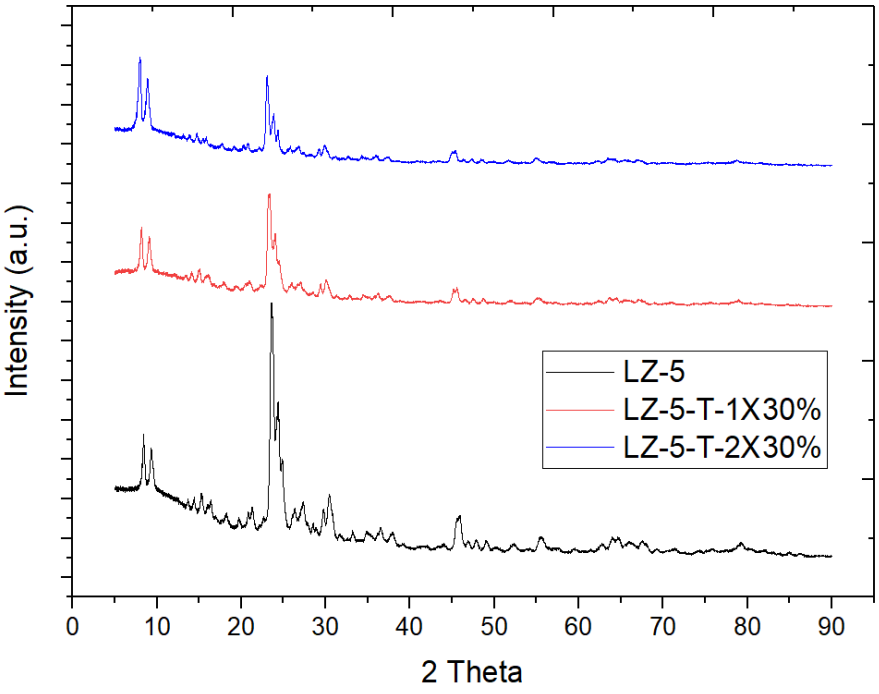

Figure 6-5: XRD patterns of LZ-5 parent and modified samples

Again, this could be a result of the dilution of the zeolite with the inert silica loaded on the surface. At the same time large ZSM-5 crystals are more sensitive to the pelleting and pressing procedures which can lead to further drop in the crystallinity.

6.3.2 Scanning Electron Microscopy (SEM)

SEM images for the parent and modified LZ-5 and SZ-0.5 ZSM-5 samples are shown in Figure 6-6. Considering the large crystals, the morphology of the crystals did not change after the modification, however, some amorphous silica layers and particles can be seen. Also, the uniformity of the modification should be improved as it is noticeable that some of the crystals are completely covered while other crystals are not sufficiently affected by the process. In the case of the small crystals changes were not easy to observe.

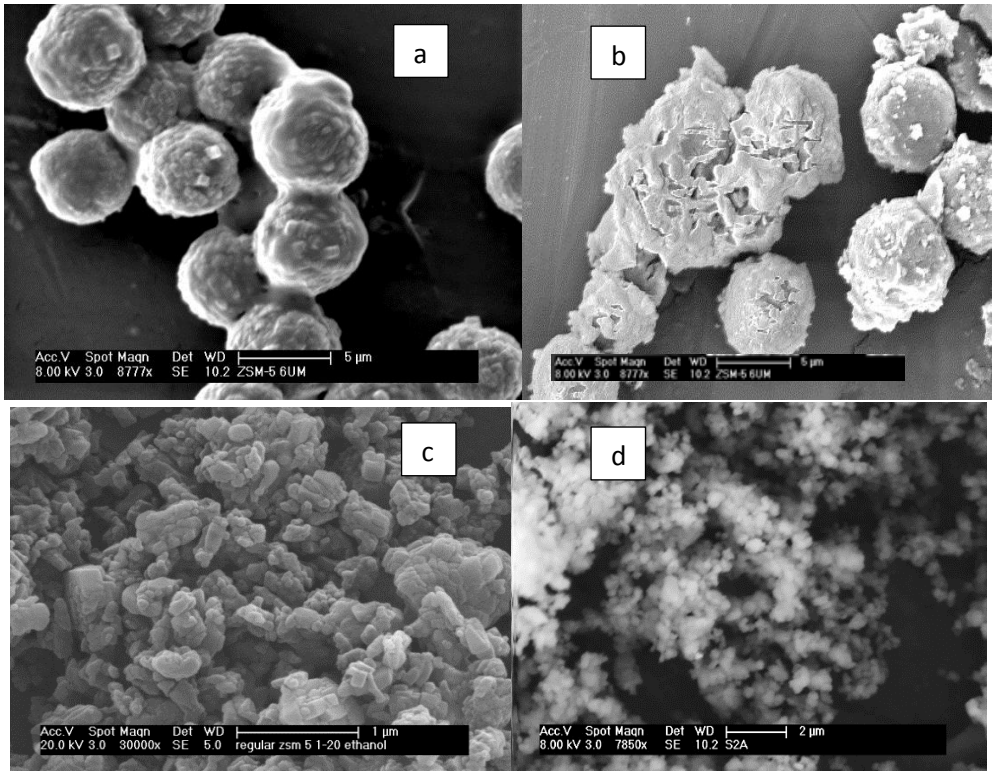

Figure 6-6:SEM Images of (a) parent LZ-5 (b) Silylated LZ-5 (c) SZ-0.5 (d) Silylated SZ-0.5

6.3.3 Acidity measurements

Acidity of ZSM-5 zeolites has major effects on the activity and selectivity. There is a direct relationship between framework acid sites and conversion of toluene on tested catalyst. Modification with silica deactivated the external acid sites to some extent which led to the reduction of Brønsted (BAS) and Lewis (LAS) acid sites. Furthermore, increasing

the loading amount of silica was accompanied by additional decrease in number of acid sites. The BAS and LAS of the parent and silylated ZSM-5 were investigated by pyridine adsorption. The region between 3500 – 3900 cm^{-1} shows the bridging hydroxyl group (3610 cm^{-1}) and the SiOH (3745 cm^{-1}).

All the bridging OH-groups of the parent and modified catalysts were accessible to pyridine as seen in Figure 6-7. The intensity of the bridging hydroxyl groups peak decreased with increasing the silica loading over the catalysts. A significant decrease in the Si(OH)Al groups was noticed after the modification with 3-aminopropyltriethoxysilane (APTES) as a silylation agent. Additional peak was detected at around 3650 cm^{-1} and it is assigned to the AlOH groups [13,16].

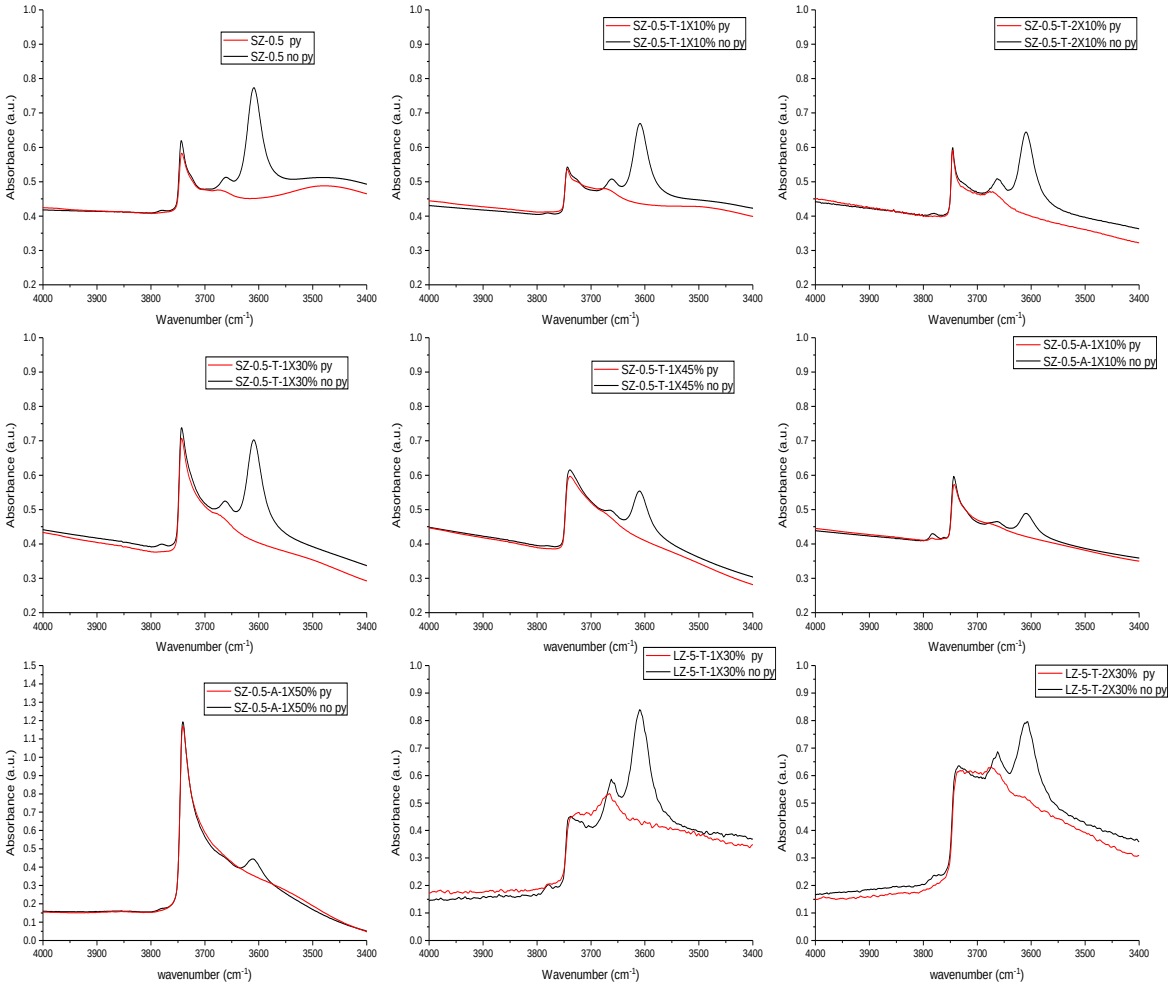

Figure 6-7: FTIR spectra in the hydroxyl region with and without pyridine

Furthermore, adsorption of pyridine was used for comparative characterisation of the acidic OH groups (Brønsted acid sites, BAS) and Lewis acid sites (LAS) was carried out by monitoring the intensity of the py-BAS and py-LAS peaks at 1546 and 1455 cm^{-1} were used to compare the number of active sites in the samples (Figure 6-8 and Figure 6-9). The quantitative data are compiled and presented in Table 6-4 and the Si/Al ratios were measured using EDAX and by chemical digestion followed by ICP-OES analysis.

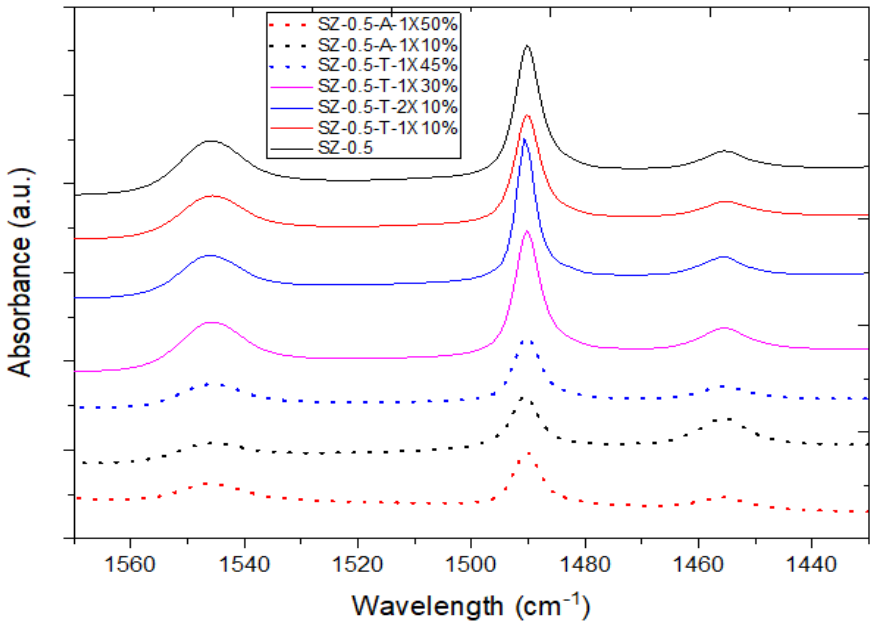

Figure 6-8: Py-FTIR adsorption profiles of parent SZ-0.5 and its modified samples

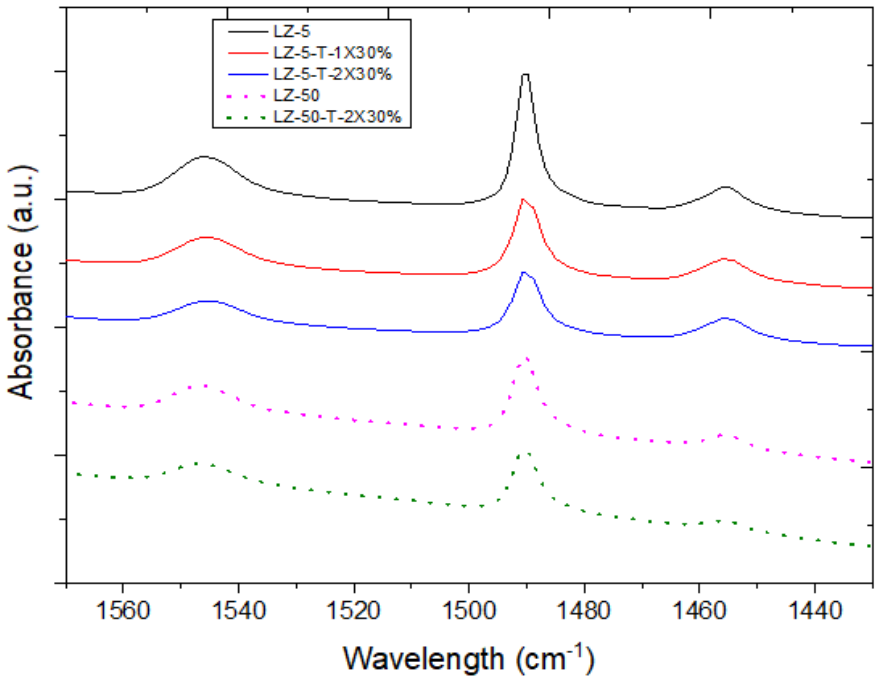

Figure 6-9: Py-FTIR adsorption profiles of LZ-5, LZ-50 and their modified samples

Table 6-4: Acidity characteristics of modified samples

Catalyst	Si/Al (EDX)	Si/Al (ICP)	BAS (mmol/g)	LAS (mmol/g)	B/L
SZ-0.5	29.6	26.3	0.31	0.08	3.90
SZ-0.5-T-1X10%	28.0	29.9	0.24	0.06	3.75
SZ-0.5-T-2X10%	-	31.7	0.20	0.07	2.83
SZ-0.5-T-1X30%	30.0	-	0.23	0.07	3.20
SZ-0.5-T-1X45%	39.4	-	0.19	0.07	2.50
SZ-0.5-A-1X10%	32.3	28.6	0.10	0.12	0.80
SZ-0.5-A-1X50%	44.8	-	0.12	0.05	2.20
LZ-5	16.4	15.9	0.37	0.17	2.15
LZ-5-T-1X30%	-	16.2	0.25	0.15	1.69
LZ-5-T-2X30%	-	20.1	0.20	0.13	1.52
LZ-50	30.2	58.2	0.19	0.06	3.08
LZ-50-T-2X30%	-	-	0.20	0.07	2.80

Although less accurate, the EDX technique gave reasonable agreement with bulk chemical analysis carried out by ICP-OES. The trend of increasing Si/Al with silylation and increasing silylation cycles and deposition amount is also shown. These findings are similar to those published by Weber et al [17]. As might be expected, addition of SiO_2 reduced the number of acid sites with BAS showing clear reduction. LAS remained unchanged around 0.07 mmol/g ± 0.01 mmol/g.

6.3.3.1 Effect of silylation on BAS using TEOS and APTES

As can be seen in Figure 6-10, TEOS decreased the number of BAS by approximately a third; however, the APTES targeted acid sites, significantly reduced BAS by around two thirds at only a 10 wt. % level and there was a significant change in B/L ratio. Silylating SZ-0.5 with APTES decreased the BAS drastically compared to TEOS at the same loading amount. This can be attributed to that APTES contains strong basic amino groups leading to strong adsorption on the acid sites[14]. LAS increased after 10 wt. % APTES modification where similar findings were observed by Huang et al. They silylated ZSM-5 with HMDS (hexamethyldisiloxane) and they noticed a decrease in BAS and increase in LAS. It was concluded that the destruction of some BASs upon silylation generated LASs [18].

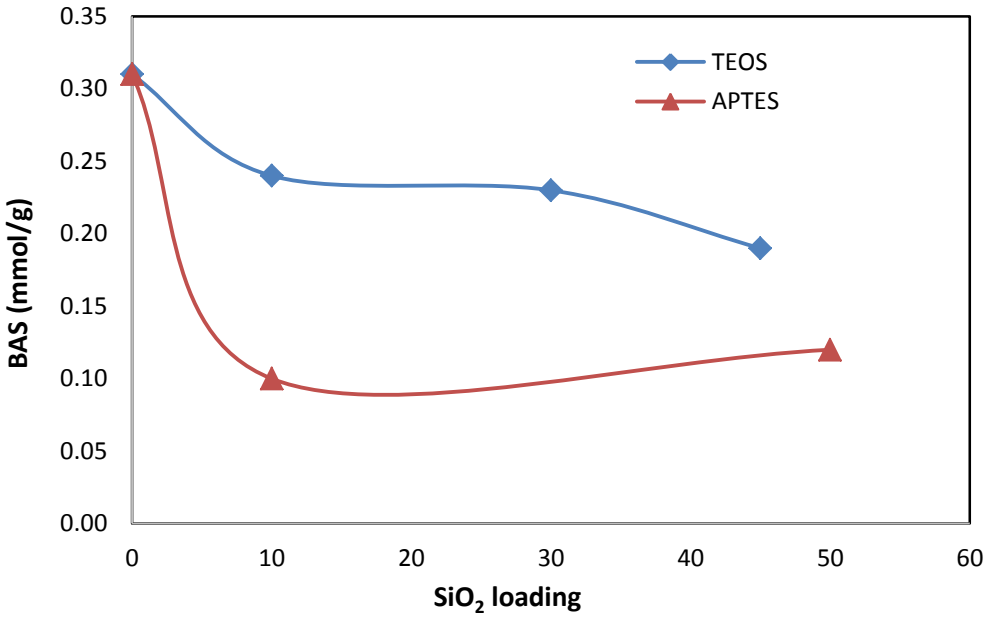

Figure 6-10: Effect of sylilation with TEOS and APTES on Bronsted acid sites

6.3.3.2 Effect of silylation using TEOS and multiple TEOS loadings

TEOS loading is less specific than APTES however multiple additions showed decrease in B/L (Figure 6-11) and as the amount of TEOS was increased there was almost a linear decrease in the B/L ratio with wt. % SiO_2 loading, Figure 6-12.

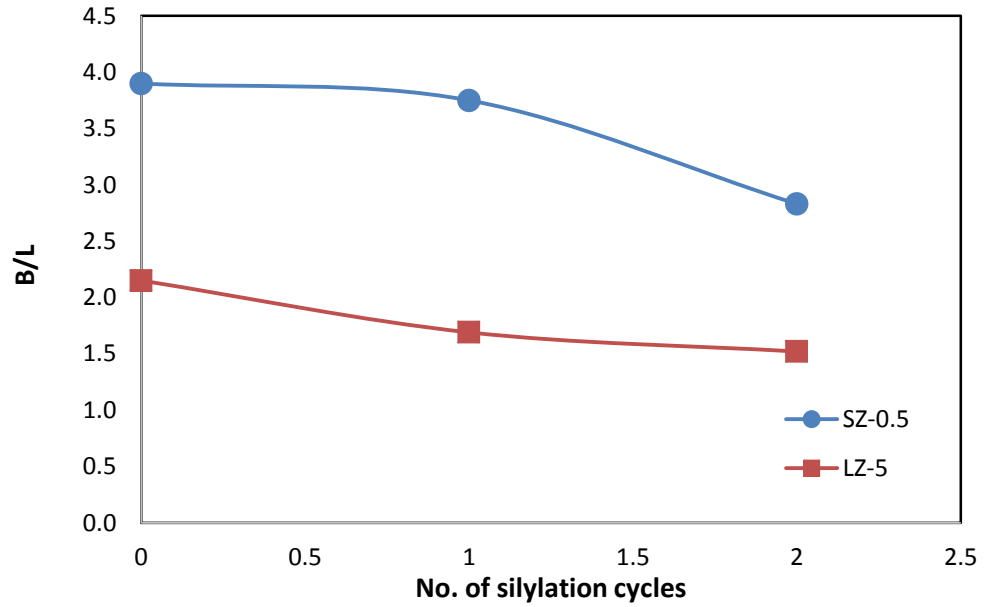

Figure 6-11: Effect of number of cycles on B/L ratio

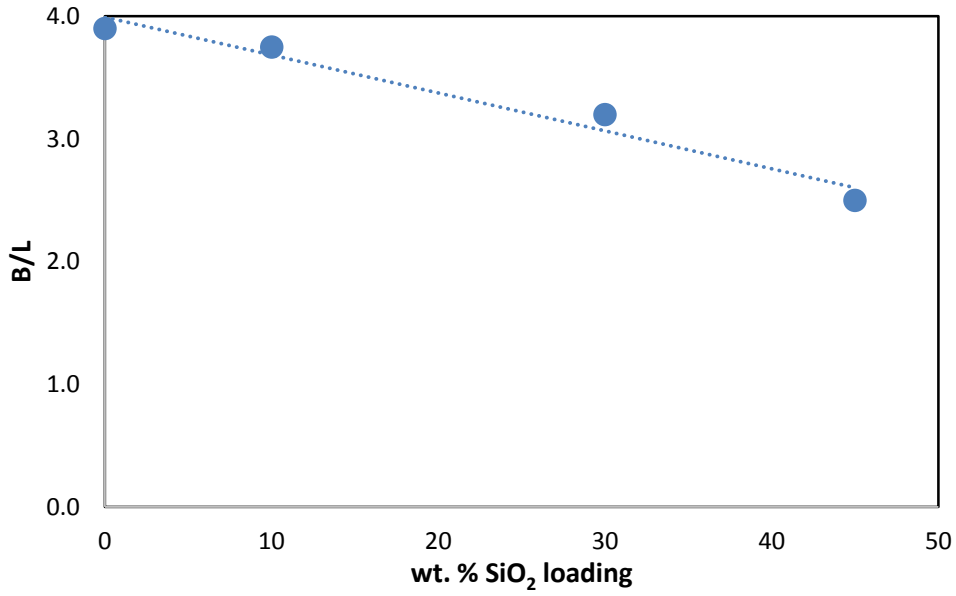

Figure 6-12: Effect of silica loading on B/L ratio

It can be observed from Table 6-4 that Loading 30 wt. % SiO_2 on ZSM-5 with 5 µm crystals (LZ-5) through two successive cycles resulted in 46 % and 23 % decrease in BAS and LAS, respectively. The higher loading amount of silica applied the more reduction in acid sites observed. The modification of LZ-50 twice with 30 wt. % SiO_2 did not affect the acidity by much and only reduced BAS by about 6.5 %. This can be ascribed to the less available acid sites on the surface to be targeted by the silylation agent.

6.3.4 Magic angle spinning- nuclear magnetic resonance (MAS-NMR)

Parent and modified samples were characterized by 29 Si NMR to study the effect of silylation on the silicon nature (Q4, Q3, Q2 and Q1) in the catalysts. It is well known in the literature that there are three major peaks resulting at around - 112 ppm (Q4), -116 ppm (Q4) and - 106 ppm (Q3) represent (SiO_3)SiOH and Si(1Al), respectively [19,20]. Figure 6-13 shows NMR signals for both the parent (SZ-0.5) and silylated samples.

After the two cycles of silylation with 10 wt. % SiO_2, the intensity of Q4 (- 112 ppm) signal increased noticeably suggesting that the silica was deposited through the hydrolysis of TEOS where hydroxyl triethoxysilane adsorbed on Brønsted acid sites and formed Si-O-Si bonds following calcination and condensation. This resulted in increasing (SiO_3) SiOH amount on the surface of the catalyst. On the other hand, the peak at -106 ppm

representing Si(1Al) is difficult to compare without deconvolution, as the peak overlaps with a major peak at -112 ppm.

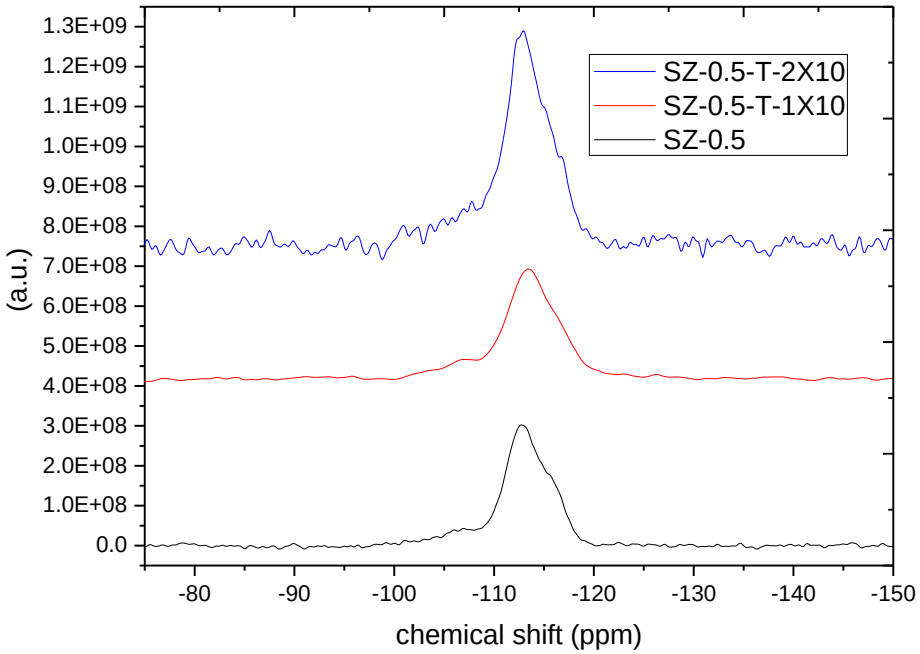

Figure 6-13: [29] Si MAS NMR spectra for parent and silylated samples

To identify the individual contribution of each peak it was necessary to use Gaussian peak fitting formula by originlab software as seen in Figure 6-14 below. It is more obvious from the deconvoluted peaks at -116, -112 representing Si(0Al) and -106 ppm representing Si(1Al) were increased after two cycles of silylation with TEOS.

The signal intensity of the terminal silanol groups (-106 ppm) increased noticeably by about 50 % after the modification. Bauer et al [21] had a similar observation where the same peak increased after silylation. It was proposed that the increase in peak intensity was due to newly formed silanol groups located near the pore openings as a result of silylation [21]. In the case of modification with large amount of APTES two extra peaks can be observed at around -103 and -92 (Figure 6-14). Boxhoorn et al. [22] observed similar peaks in ZSM-5 zeolite and they were attributed to silanol groups based on that silicic acid yields peaks at -92 and -103 which are assigned to silicon atoms with two, one and zero hydroxyl groups.

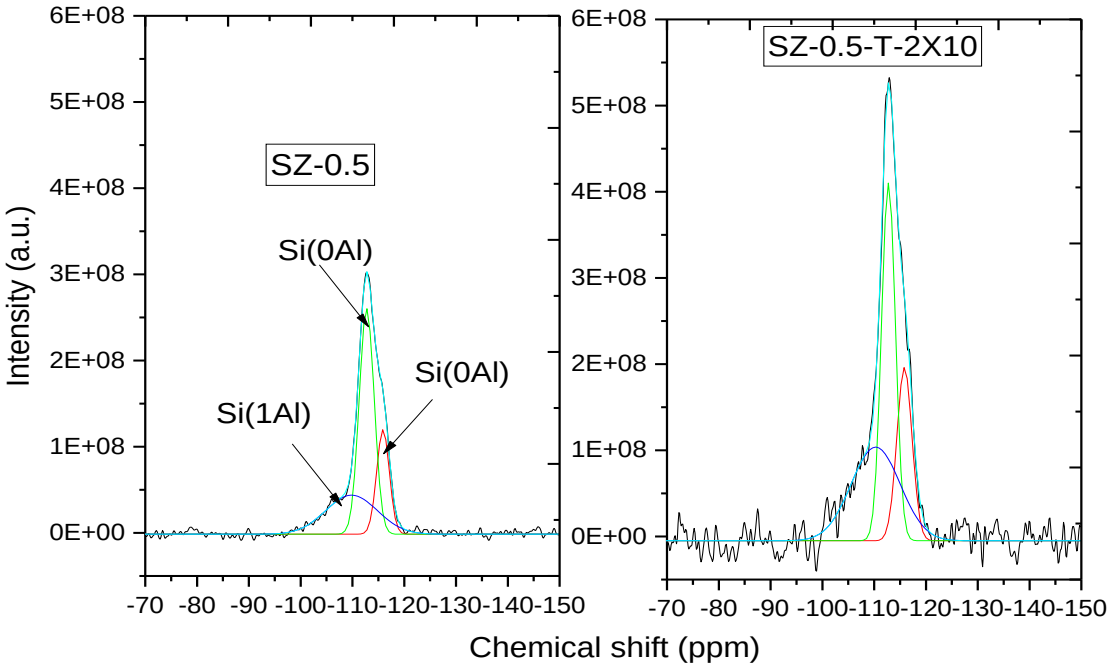

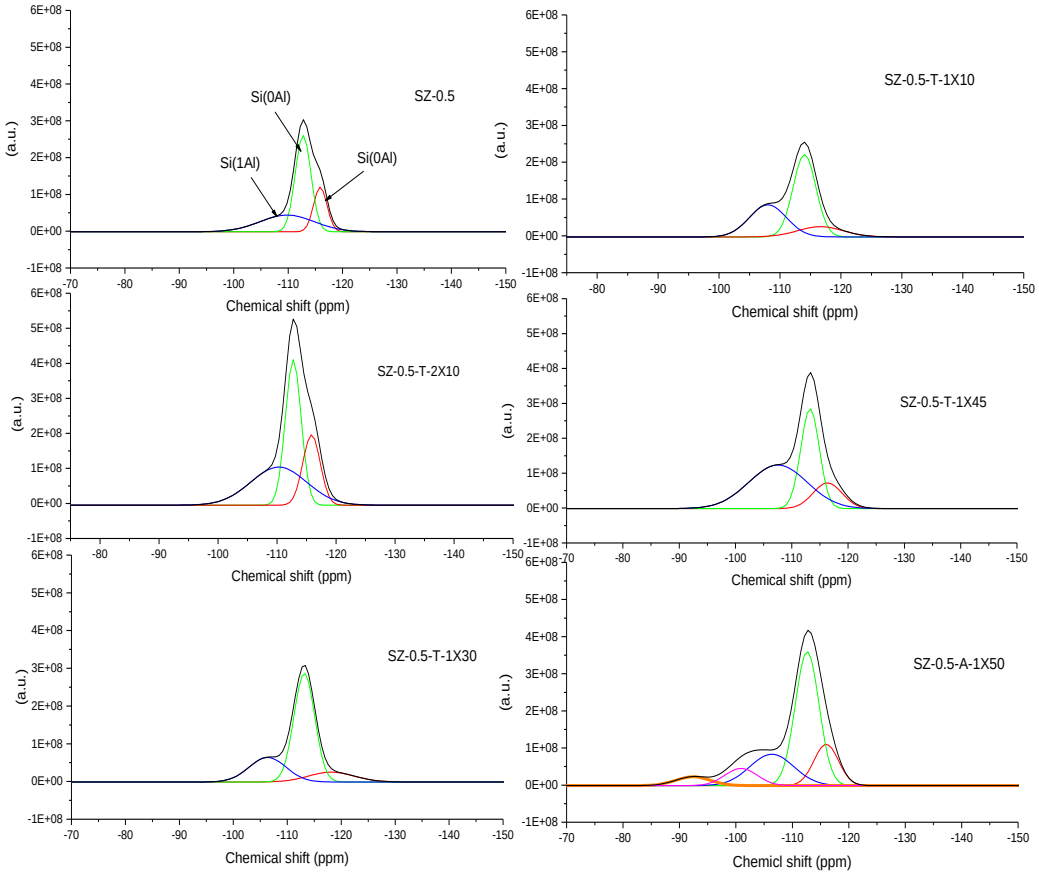

Figure 6-14: Deconvolution of ^{29} Si MAS NMR spectra for parent and modified samples

Solid state 27 Al MAS NMR was utilized to study the variations of Al coordination in the framework of the parent and modified catalysts. The peaks at chemical shift 56 and 0

ppm are assigned to framework Al (FAL) and extraframework Al (EFAL), respectively [16]. After silylation, EFAL slightly increased but did not vary significantly from the parent as the sample was calcined sensibly with a very slow ramping rate (3 °C/min) after the addition of TEOS in this case – see Figure 6-15. Similar findings were observed by Zheng where the FAL and EFAL ratios did not change after the modification and were similar to the parent [9].

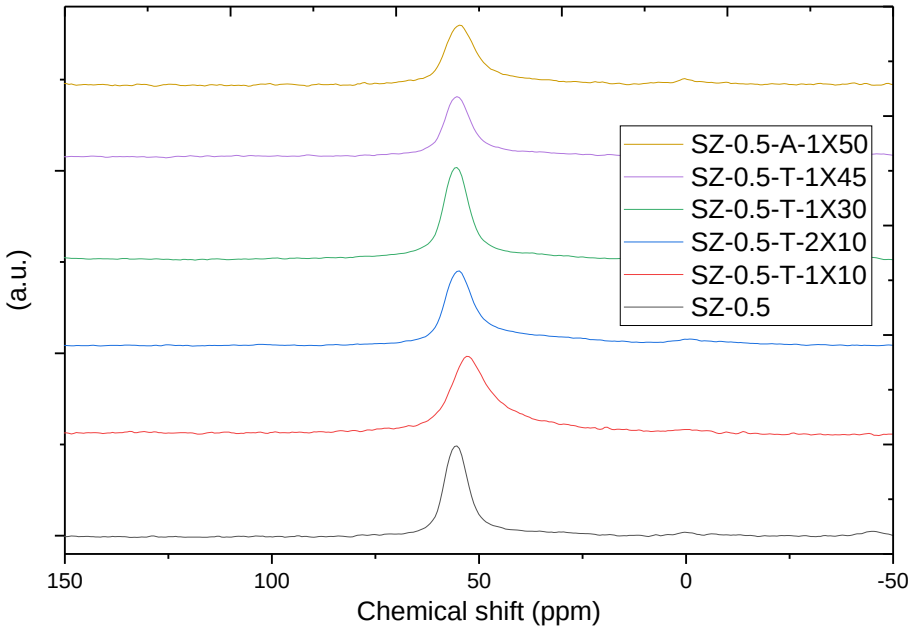

Figure 6-15: 27 Al MAS NMR Spectra

6.3.5 Surface area and pore volume

Catalyst samples BET surface area was determined following the procedure discussed in section 4.4.4. Surface area measurements were performed to investigate the effects of CLD of silica on pore volume, external surface area and total surface area.

It can be observed from Table 6-5 that loading inert silica layer on ZSM-5 decreased the BET surface area, pore volume, and micropore area indicating that this modification procedure does not only affect the external surface but also narrow the pores and channels by adsorbing on the acid sites around the pores reducing accessibility of bulky molecules favouring diffusion of p-xylene. Furthermore, during the calcination process after adding TEOS, the formation of $Si(OH)_x(OC_2H_5)_{4\_x}$ due to hydrolysis reactions is to be hypothesized leading to maybe trace amount of small silicon species to go into the intracrystaline voids [21]. Treating the catalyst with a second cycle of silylation resulted in

a further decrease in the textural properties. This could be attributed to that during the first cycle TEOS would interact with the easily accessible acid site and as TEOS is a bulky molecule it may hinder other TEOS molecules to access adjacent acid sites if the concentration of acid sites is high. However, they become accessible during the second cycle of silylation as calcination after the first cycle will remove the bulky ethoxyl groups on TEOS. This leads to having homogeneous silica layers (without bulky ethoxyl groups), meaning larger amounts of acid sites will be deactivated as discussed above besides to narrowing the pores. This suggests that modifying the catalyst with multiple cycles is more effective than loading a large amount of silica in one cycle. A Larger decrease in surface area was observed by TEOS than APTES. Inversely, pore volume and micropore area were more affected by APTES. BET results showed decreasing trend with Increasing the loading of SiO_2 (Figure 6-16). Similarly, multiple loadings of TEOS at 10 wt. % on SZ-0.5 and 30 wt. % for LZ-5, showed reduction in surface area as seen in Figure 6-17.

It is noticeable that LZ-50 was the least affected by silylation and this is can be related to having less amount of Brønsted and Lewis acid sites (see Table 6-4) amongst the other catalysts, meaning less accessible acid sites to the silylating agent.

Table 6-5: Textural properties of parents and modified ZSM-5

Catalyst	BET surface area (m^2/g)	pore volume (cm^3/g)	Micropore area (m^2/g)	External surface area (m^2/g)
SZ-0.5	339	0.113	188	151
SZ-0.5-T-1X10%	299	0.103	171	128
SZ-0.5-T-2X10%	276	0.095	157	119
SZ-0.5-T-1X30%	314	0.106	176	138
SZ-0.5-T-1X45%	288	0.103	175	113
SZ-0.5-A-1X10%	308	0.095	157	151
SZ-0.5-A-1X50%	301	0.090	154	147
LZ-5	280	0.110	187	93.0
LZ-5-T-1X30%	261	0.097	166	94.8
LZ-5-T-2X30%	237	0.096	165	72.4
LZ-50	321	0.090	139	181
LZ-50-T-2X30%	310	0.088	137	173

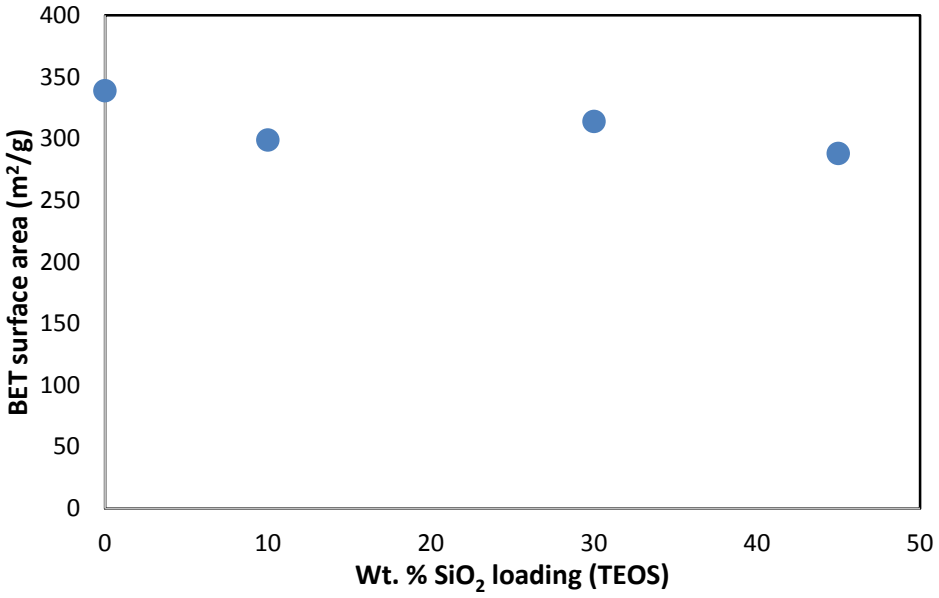

Figure 6-16: Effect of SiO_2 loading on BET surface area

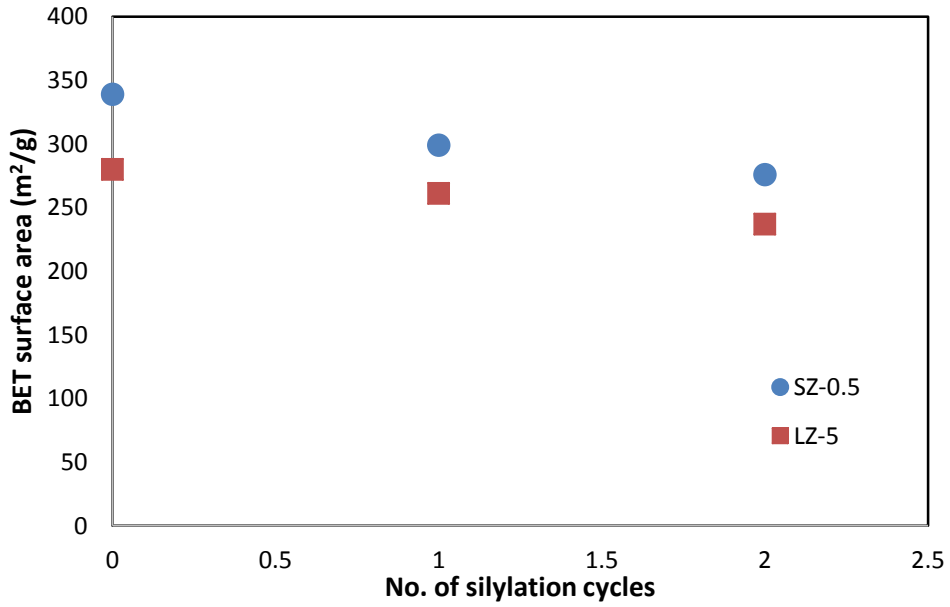

Figure 6-17: Effect of silylation multiple cycles on surface area

6.4 Catalytic evaluation

ZSM-5 zeolites having different crystal sizes (0.5, 5 and 50 µm) were silylated using different silica agents, loading amounts and number of modification cycles with the aim of suppressing the isomerization on the non-selective acid sites on the external surface leading to enhanced p-xylene selectivity.

6.4.1 Effect of silylation agent

The effects of two different silylation agents on p-xylene selectivity and toluene conversion were studied. APTES and TEOS were used to deactivate the external acid sites on the surface of the catalyst. Both agents have larger molecular diameters (TEOS-1.03 nm and APTES- 0.8 nm) than the pore diameter of ZSM-5. In addition, APTES has a strong basic amino group which should target zeolite acid sites. The catalytic testing was carried out at a temperature of 475 °C and at atmospheric pressure. At the same time, the WHSV was varied between 3 and 83 h^{-1} to significantly reduce the contact time of feed with catalyst and hence reduce isomerization. As shown in the previous chapter, the p-xylene selectivity was around the thermodynamic equilibrium value when parent ZSM-5 with small crystal size (0.5 μm) was tested. Increasing the toluene flowrate did not show a noticeable change in the selectivity. Both silylation agents improved p-xylene selectivity (Figure 6-18) with TEOS being better than APTES for p-selectivity. Increasing WHSV led to a noticeable increase in p-xylene selectivity with both silylation agents, with the TEOS modification showing very high selectivity, around 70 % at the highest WHSV 83 h^{-1}, compared with only around 37 % at the highest WHSV when APTES was used.

As expected conversion over the modified catalysts with both agents was reduced, ATPES modified catalyst delivered the lowest conversion at all WHSVs. Silylation with TEOS dropped the conversion by 45 % from the achieved value by the parent. This is attributed to the decrease in the Brønsted acidity confirmed by pyridine FTIR results. The results from FTIR showed that the acid sites of the catalyst were decreased even more by APTES which explains the very low conversion delivered by this catalyst.

Table 6-6: Characteristics of APTES and TEOS modified samples

	BET (m^2/g)	Pore volume (cm^3/g)	BAS (mmol/g)	LAS (mmol/g)
Parent	339	0.113	0.31	0.08
SZ-0.5-T-1X10%	299	0.103	0.24	0.12
SZ-0.5-A-1X10%	308	0.095	0.10	0.06

BET surface area was decreased by both silylation agents by around 10 %. Also, pore volume was reduced in both modifications but a little more in the case of APTES which could be an indication of a little pore blockage. It can be seen in Table 6-6 that the main difference is the BAS amount which was clearly more affected by APTES resulting in the low attained conversion.

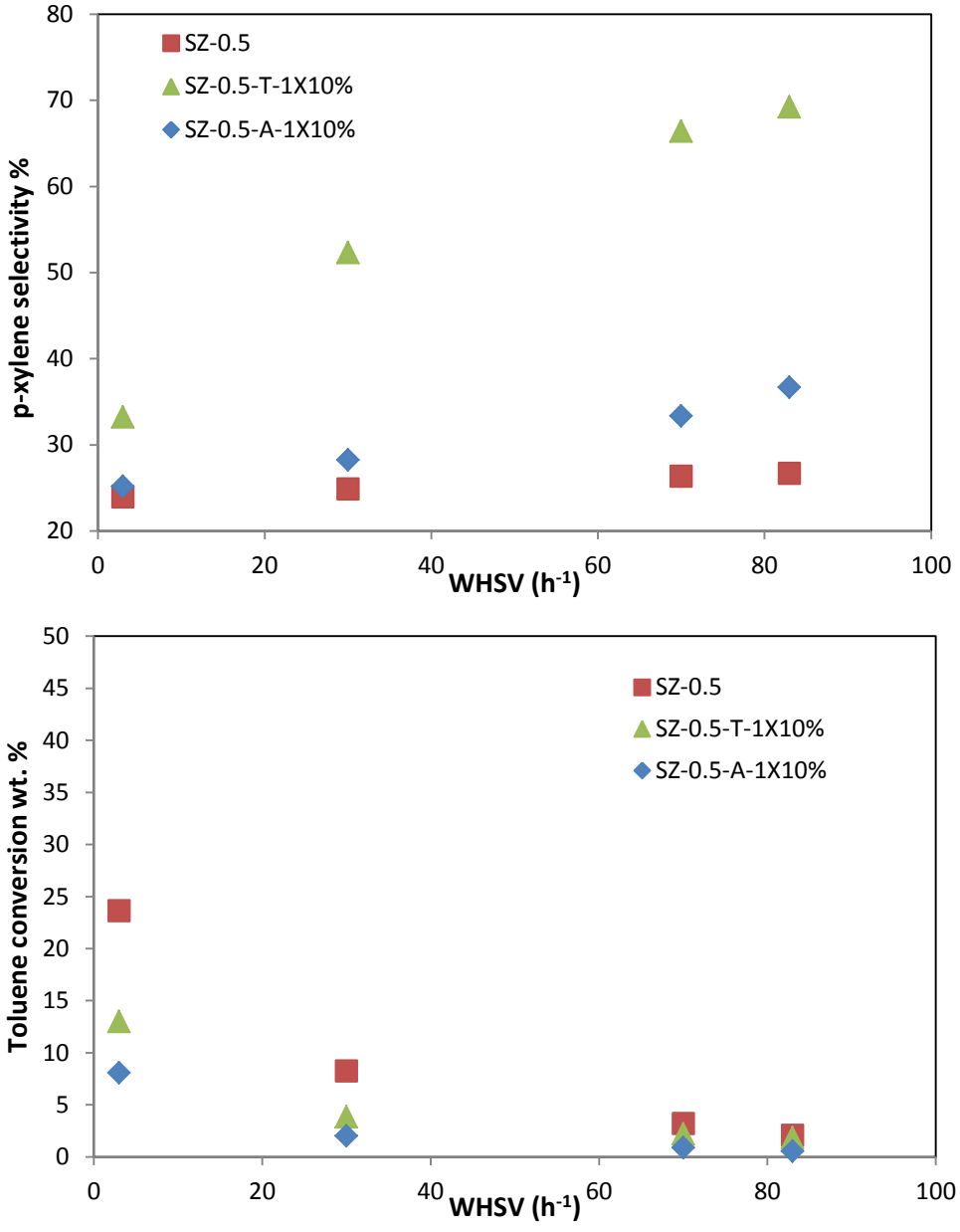

Figure 6-18: The effects of Silyation agent on p-xylene selectivity and toluene conversion

Based on the results in Figure 6-18, it can be observed that using TEOS as a silylation agent was better than APTES in terms of achieving high p-xylene selectivity. APTES might have blocked some pores as indicated by the pore volume results shown in Table 6-5 which affected the conversion.

6.4.2 Effect of SiO_2 loading amount

ZSM-5 with small crystal size (0.5 µm) was modified with different loading amounts of SiO_2 (10, 30 and 45 wt. %) using TEOS as a silylation agent to study the effect of loading amount on p-xylene selectivity and toluene conversion.

Table 6-7: Acidity measurements of silylated samples by py-FTIR

Sample	BAS (mmole/g)	LAS (mmole/g)	B/L
SZ-0.5	0.31	0.08	3.90
SZ-0.5-T-1X10%	0.24	0.06	3.75
SZ-0.5-T-1X30%	0.23	0.07	3.20
SZ-0.5-T-1X45%	0.19	0.07	2.50

It was anticipated that increasing the loading amount of silica will lead to higher p-xylene selectivity however the results obtained suggested otherwise (Figure 6-19). All modified catalysts showed higher selectivity than the parent and this was more obvious with increasing WHSV and 10 % and 45 % silica loaded catalysts showed about the same p-xylene selectivity at all WHSVs. However, loading the catalyst with 30 wt. % silica interestingly delivered lower para-selectivity and similar results were observed by Hui et al [6]. They noticed that the use of excess silica loading can lead to a decrease in the p-xylene selectivity. This was attributed to an excess TEOS causing the formation of uneven silica layer resulting in low p-xylene selectivity. However, this was not the case with 45 wt. % loading which could be due to that the large amount of silica resulted in pore blockage. This can be seen from BET results were the pore volume was decreased more by the 45 wt. % compared to 30 wt. %. The BET surface area results in Table 6-5 shows that 10 % of silica decreased the surface area more than when 30 % of silica was used. This could suggest that the 30 % silica was not uniformly distributed on the surface and uneven silica layer might had been formed.

All modified catalysts showed lower toluene conversion than the parent suggesting some acid sites have been deactivated by the deposited inert silica. This was confirmed by the FTIR characterization in Table 6-7. As it was expected, the catalyst loaded with 10% silica showed slightly higher conversion amongst the modified ones as it had the highest

number of acid sites. Increasing the amount of Silica loading resulted in further decrease in the number of Brønsted acid sites, especially in the case of 45 wt. % loading whereas the 30 wt.% surprisingly did not decrease the acidity further from the 10 wt. %. On the other hand, Lewis acid sites were not much affected by the modification (Table 6-7).

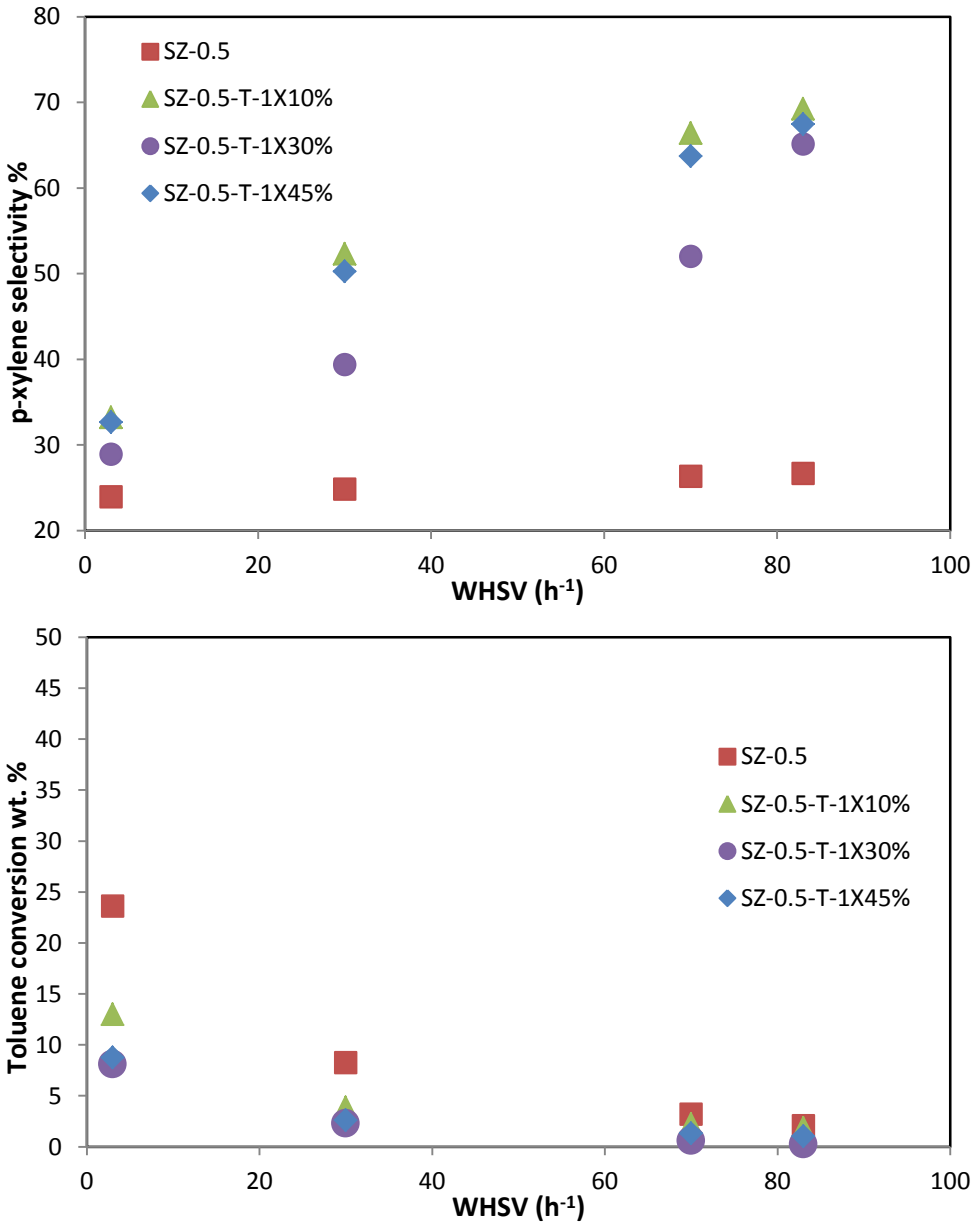

Figure 6-19: The effects of SiO_2 amount on p-xylene selectivity and toluene conversion on SZ-0.5

To investigate the effect of silica loading amount on ZSM-5 with 5 µm crystal size (LZ-5), it was silylated with 10 and 30 wt. % SiO_2. It was concluded that the 30 wt. % silica loading had better effects on the p-xylene selectivity-see Figure 6-20. It can be observed that 10 wt. % SiO_2 loading did not improve the p-xylene selectivity which gave around the same results as the parent. Whereas, higher p-xylene selectivity was achieved when 30 wt. %

SiO_2 loading was applied. The reason behind this could be that 10 wt. % SiO_2 was not sufficient to deactivate unselective surface acid sites, the large crystal (LZ-5) has a lower Si/Al ratio (Si/Al = 15.9) than the parent with smaller crystals. This additional acidity would result in more acid sites on the surface requiring the use of higher silica loading amount. Also, the large crystal size is likely to require higher amount of silica and more than one cycle of modification.

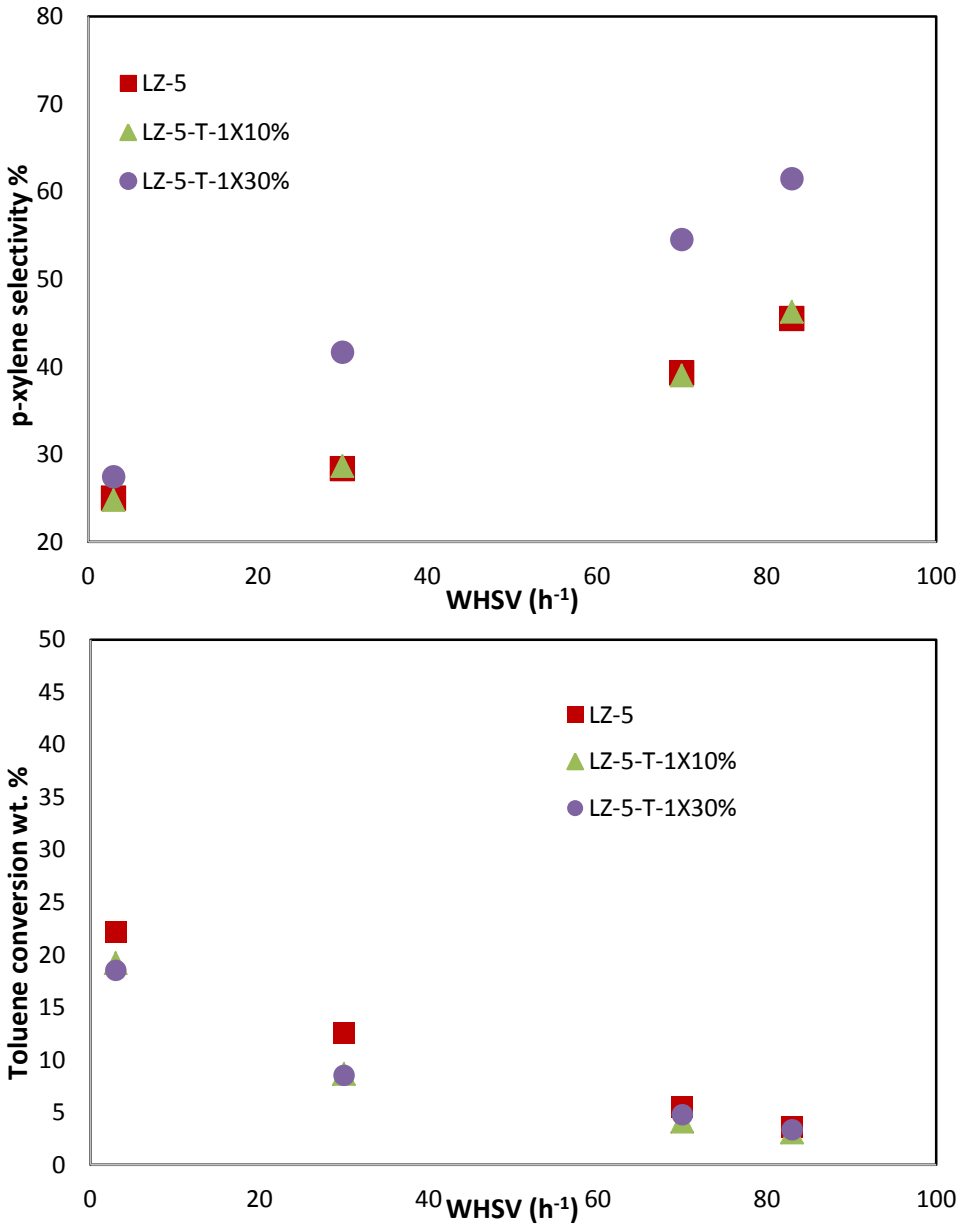

Figure 6-20: The effects of silica loading amount on p-xylene selectivity and toluene disproportionation on LZ-5

To conclude, the effect of different loadings of silica on ZSM-5 showed that 10 % loading on SZ-0.5 achieved the best combination of p-xylene selectivity and toluene conversion,

whereas, 30 wt. % silica loading was required to achieve the best results over the ZSM-5 with large crystals, LZ-5.

6.4.3 Effect of number of cycles

In the previous sections, all the silylation modifications by chemical liquid deposition (CLD) were based on one treatment only. However, there is evidence in the literature that multi cycle silylation would improve the p-xylene selectivity significantly by increasing the amount of silica on the external surface and improving the uniformity of the silica layer [6]. The performance of all catalysts modified with different number of cycles by CLD is shown in Table 6-8.

Table 6-8: Effect of the silylation number of cycles on the catalysts performance at 1 bar

Sample	No. of cycles	SiO_2 wt. %	BAS (mmole/g)	LAS (mmole/g)	X_T (wt. %)	S_P (%)
SZ-0.5	-	-	0.31	0.08	23.6	24.0
SZ-0.5-T-1X10%	1	10	0.24	0.06	13.0	33.2
SZ-0.5-T-2X10%	2	10	0.20	0.07	12.8	36.6
LZ-5	-	-	0.37	0.17	22.2	25.0
LZ-5-T-1X30%	1	30	0.25	0.15	18.5	27.5
LZ-5-T-2X30%	2	30	0.20	0.13	13.3	39.3

WHSV = 3 h^{-1}, Pressure = 1 bar, X_T = toluene conversion, S_P = p-xylene selectivity

It can be seen from the table above, the activity decreased with the number of accessible sites, mainly the number of Brønsted acid sites whereas the number of Lewis acid sites was predominantly unchanged.

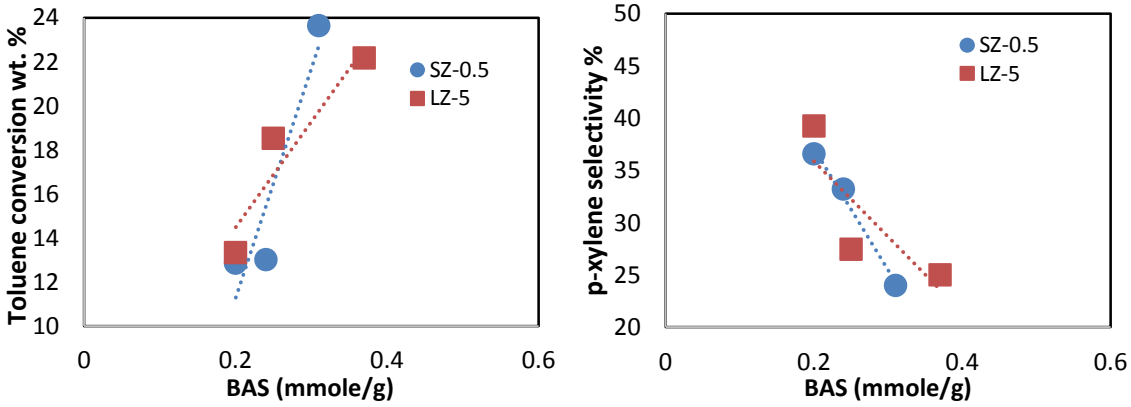

Figure 6-21: Correlation study between BAS and toluene conversion and p-xylene selectivity

SZ-0.5 and LZ-5 showed almost similar trends where the decrease in the number of Brønsted acid sites was accompanied by an increase in p-xylene selectivity. The effect of WHSV was investigated over the one cycle and two cycles silylated samples with different crystal sizes as seen in Figure 6-22.

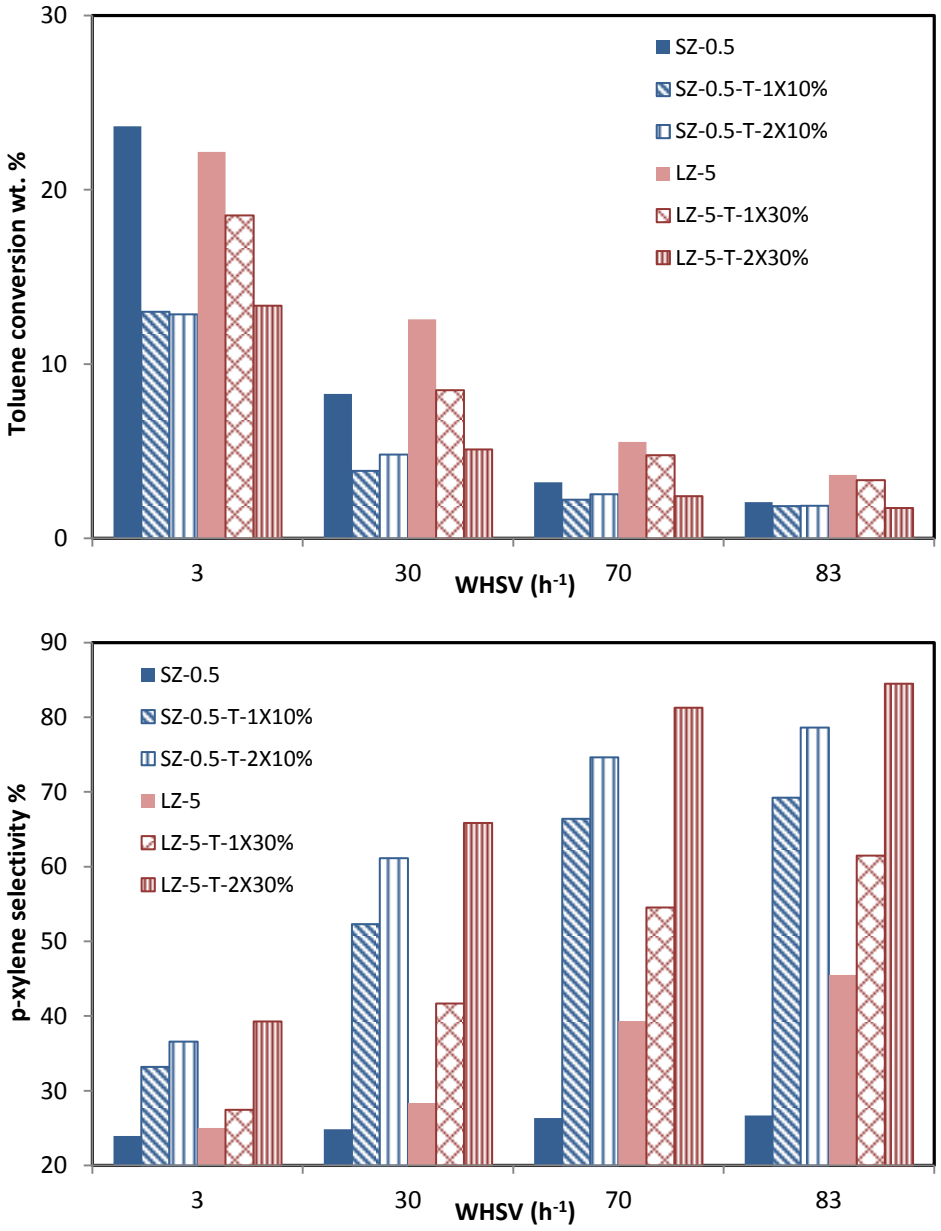

Figure 6-22: CLD cycle number effect on p-xylene selectivity and toluene conversion at 1 bar

All the modified catalysts gave lower toluene conversion as the addition of inert silica on the catalyst had reduced the number of external acid sites. One cycle silylation suppressed the isomerization of p-xylene to other isomers to some extent. The p-xylene selectivity had increased above the thermodynamic equilibrium value in both cases of large and small ZSM-5 crystals (Figure 6-22). The second cycle of silylation enhanced the

selectivity further. Increasing the flow rate of toluene was accompanied by an increase in p-xylene selectivity to 84 % at a WHSV of 83 h^{-1} for the two-cycle modified ZSM-5 with 5 µm crystal size (LZ-5-T-2X30%). however, this lead to a drastic drop in toluene conversion (2 %) as a result of the less contact time between the catalyst and the feed.

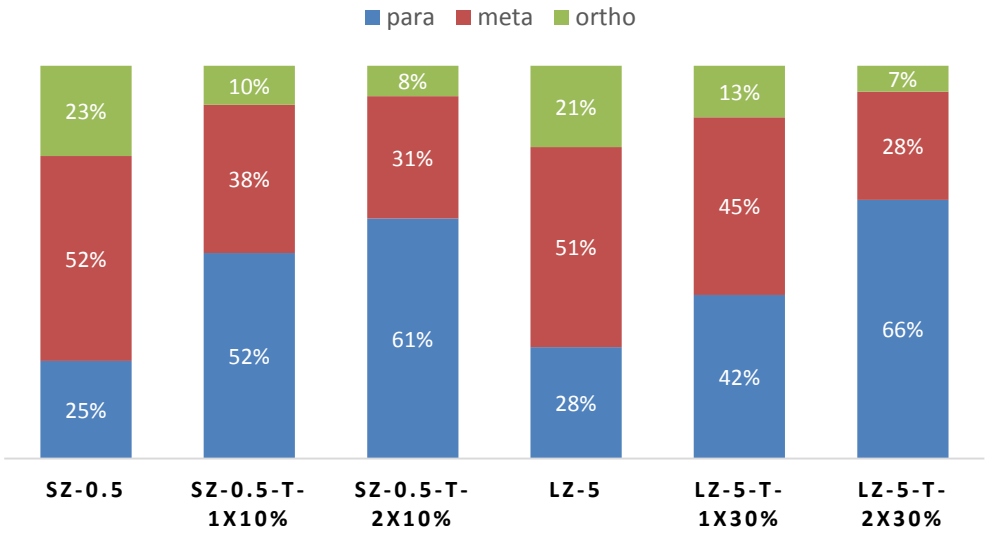

Figure 6-23: Xylene isomers distribution at WHSV=30 h^{-1} and atmospheric pressure

6.4.3.1 *Effect of elevated pressure (10 bar) on toluene conversion and p-xylene selectivity*

Increasing the pressure to 10 bar almost doubled the conversion for all samples and dropped the selectivity back to the thermodynamic equilibrium value (24 %). Conversely, Increasing WHSV of toluene increased the selectivity for all samples. The best selectivity was achieved by the large ZSM-5 crystal silylated twice (LZ-5-T-2X30%) at all WHSVs reaching the highest value of about 65 % at the highest WHSV=83 h^{-1}. However, the toluene conversion decreased as the selectivity increased which is attributed to the less contact between the catalyst and the feed at high flowrates (Figure 6-24). In terms of yield, the higher the conversion of toluene the higher the p-xylene yield. However, the overall selectivity to p-xylene will be lower. For example, testing (LZ-5-T-2X30%) at 10 bar and a WHSV of 70 h^{-1} gave a toluene conversion of 8 % and 60 % p-xylene selectivity with a yield of around 2.5 % in the total products (Table 6-9). This result compares favourably with literature where Ali et al. tested ZSM-5 catalyst silylated three times with TEOS and reported that at a toluene conversion around 10 % and p-xylene selectivity of 50 % with the yield of about 2 % [3]. Also, ethylbenzene, C_9 and C_{10} were reduced by silylation.

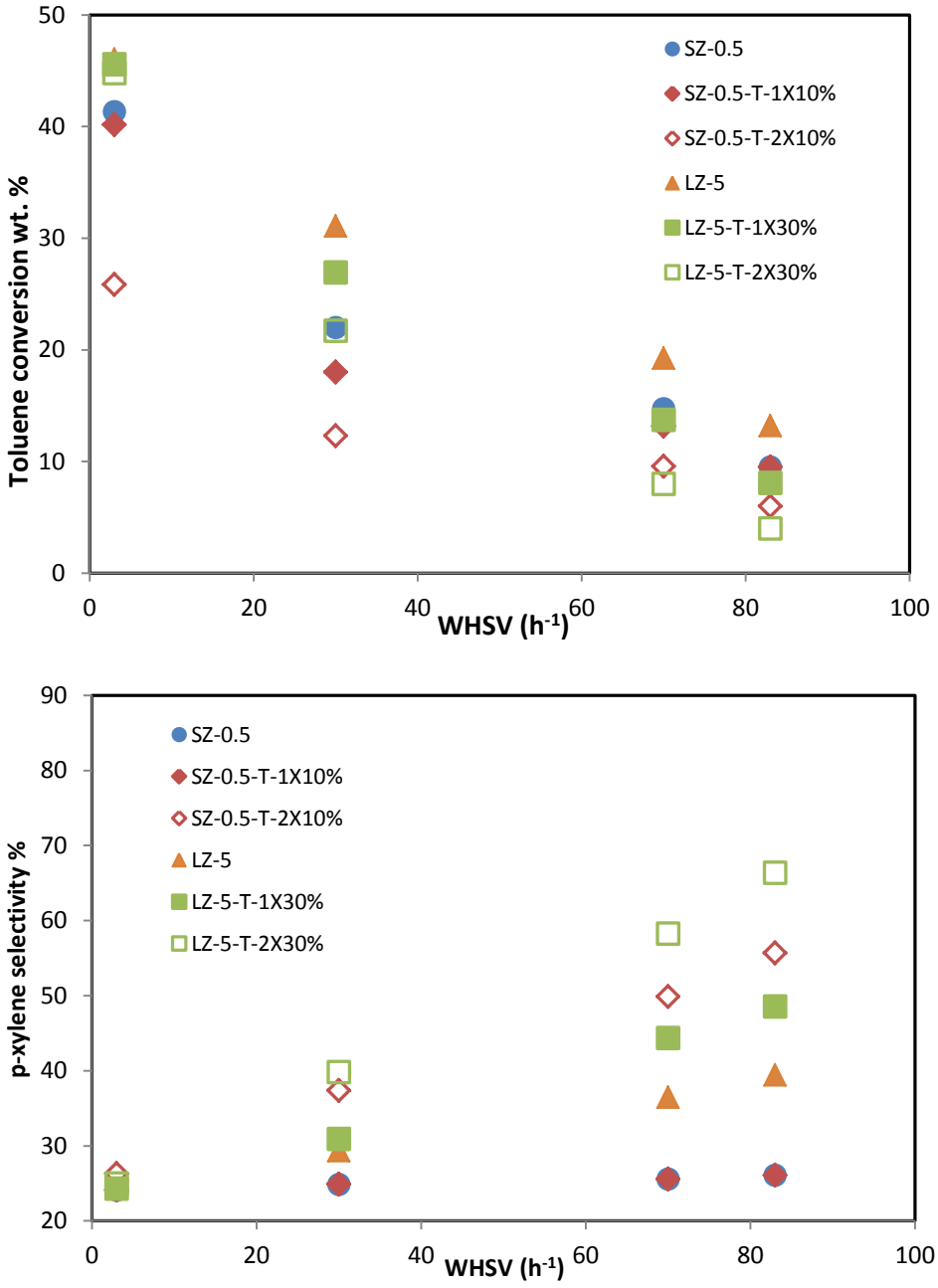

Figure 6-24: The effect of CLD cycle number on p-xylene selectivity and conversion at 10 bar

Table 6-9: product distribution over parent ZSM-5 (5 µm) and silica modified at 10 bar

	LZ-5			LZ-5-T-1X30%			LZ-5-T-2X30%		
WHSV (h^{-1})	3	30	70	3	30	70	3	30	70
Products wt. %									
Benzene	23.27	14.81	8.82	19.99	12.43	6.55	23.92	10.55	3.87
Toluene	53.86	68.94	80.75	57.83	73.04	86.39	55.22	78.32	91.93
ethylbenzene	0.65	0.29	0.12	0.40	0.20	0.00	0.35	0.10	0.00
p-xylene	4.84	4.33	3.65	5.07	4.04	3.15	4.67	4.00	2.45
m-xylene	10.37	7.61	4.77	10.45	6.53	3.05	9.89	4.72	1.43
o-xylene	4.63	2.83	1.58	4.51	2.47	0.87	4.09	1.32	0.32
C_9	2.24	0.76	0.26	1.80	1.29	0.00	1.86	0.99	0.00
C_{10}	0.14	0.43	0.05	0.00	0.00	0.00	0.00	0.00	0.00
B/X	1.17	1.00	0.88	1.00	0.95	0.93	1.28	1.05	0.58
X_T (wt. %)	46.14	31.06	19.25	42.17	26.96	13.62	44.78	21.68	8.07
S_P (%)	24.40	29.35	36.49	25.30	30.96	44.61	25.02	39.87	58.28

X_T=Toluene conversion, S_P=p-xylene selectivity

Figure 6-25 shows that decreasing the number of Brønsted acid sites decrease toluene conversion. Inversely, p-xylene selectivity increased suggesting that some of the external acid sites were deactivated by the modification, especially after two cycles of SiO_2 loading.

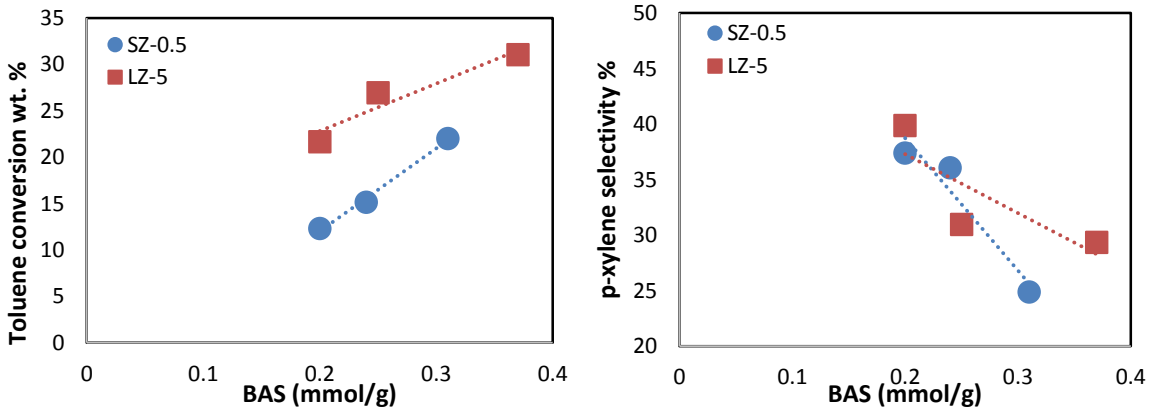

Figure 6-25: Effect of BAS on conversion and p-xylene selectivity at WHSV 30 h^{-1} and 10 bar

Furthermore, Silylation modification had been performed on the large ZSM-5 with 50 µm crystal size (LZ-50). The silica was loaded through two cycles of silylation using 30 wt. %

SiO_2 in each cycle. As seen in the py-FTIR results (Table 6-4), the number of Brønsted acid sites is already low compared to the other ZSM-5 samples and hence the silylation might not affect the performance of the catalyst as it did to the other parents. This could be attributed to that less acidic OH groups were available on the surface to react with TEOS. The parent and modified catalysts were tested at atmospheric pressure and 10 bar - see Figure 6-26.

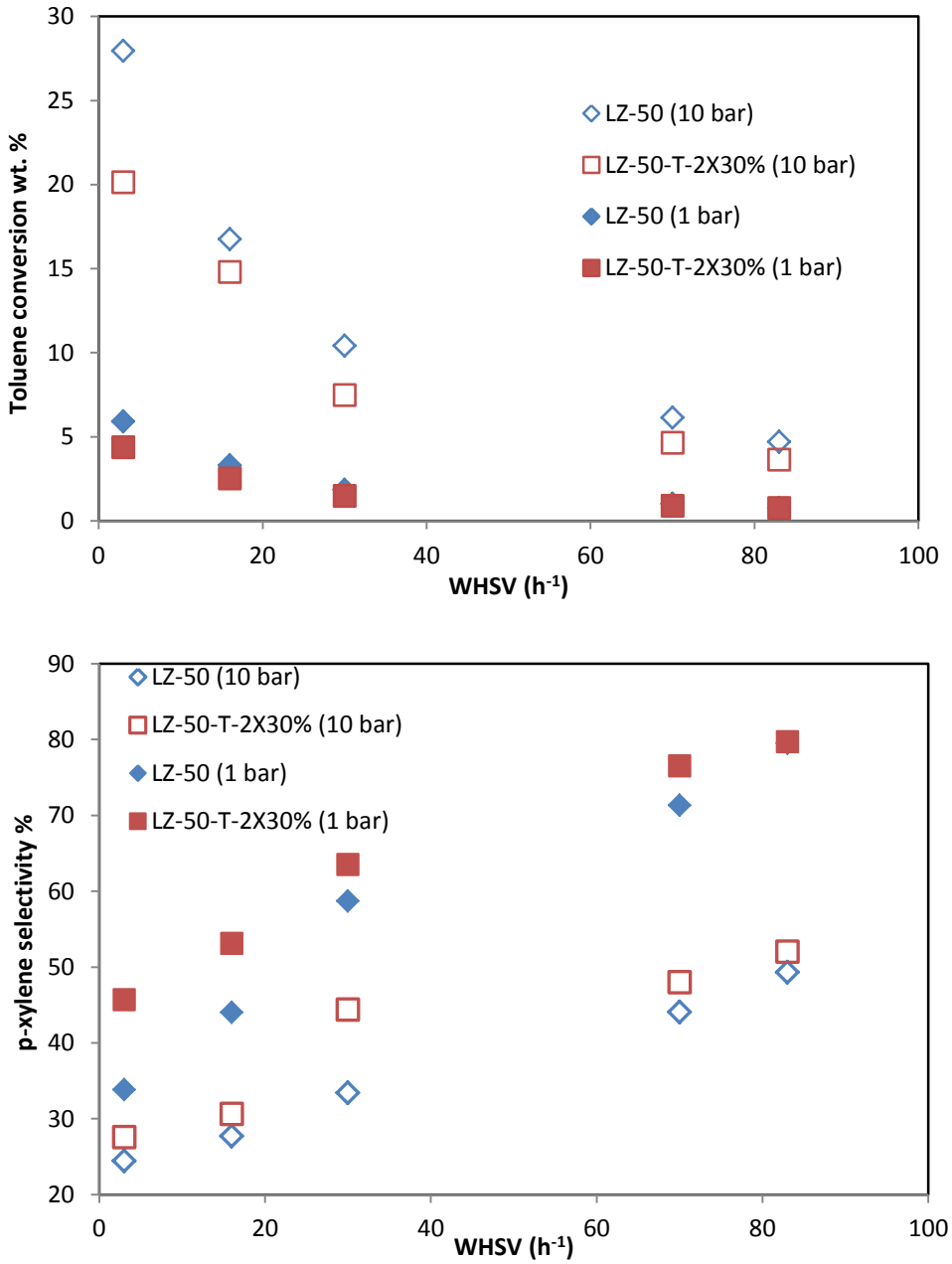

Figure 6-26: The effect of silylation on large crystals (50 µm) at varied pressure and WHSV

As the FTIR results suggested that small amount of Brønsted acid sites were deactivated after the modification, the parent and modified catalysts did not show a noticeable

difference in terms of toluene conversion when the reaction was performed at 1 bar. The p-xylene selectivity was improved to some extent by the modified sample at WHSV 30 h^{-1}. Increasing the pressure to 10 bar, increased both the parent and modified catalysts conversion while the selectivity was decreased. It was observed that the selectivity of the silylated sample at 10 bar was not far from the parent. It was not improved as much as by the ZSM-5 zeolites with smaller crystal sizes (SZ-0.5 and LZ-5). This proposes that only small amount of acid sites were deactivated on the surface. The reason behind this could be the non-uniform distribution of the acid sites in the large crystals (> 30 µm) as discussed in section 5.1 [23].

6.4.4 Effect of silylation on observed reaction rate constant (Kobs)

The observed reaction rate constant was calculated for parent and silylated ZSM-5 catalysts by plotting a first order kinetic model. It was found as the slope of ln (1/1-X) vs W/F, where X is toluene conversion, W is the weight of the catalyst and F is the feed flowrate. The effect of acidity and surface area on the reaction rate constant was studied. It can be seen from Table 6-10 that reaction rate on ZSM-5 zeolite with small crystals decreased with decreasing the surface area and Brønsted acid sites as a result of silica modification on the surface. In contrast, the reaction rate constant observed on parent and modified 5 µm (LZ-5) did not show any correlation with surface area or acidity.

Table 6-10: The effect of surface area and acidity on the kinetic reaction rate (K_{obs})

Sample	k (rate constant) at 10 bar	k (mol h^{-1} m^{-2})x 10^3	K (mol h^{-1} $mmol^{-1}$)	SA (m^2/g)	BAS (mmol/g)	X (wt. %)	Sp (%)	WHSV (h^{-1})
SZ-0.5	0.07	0.21	0.22	339	0.31	14.7	25.6	70
SZ-0.5-1X10%	0.05	0.17	0.21	299	0.24	13.4	25.6	70
SZ-0.5-2X10%	0.03	0.11	0.15	276	0.2	12.0	37.4	30
LZ-5	0.12	0.43	0.32	280	0.37	13.2	39.5	83
LZ-5-1X30%	0.12	0.46	0.48	261	0.25	13.7	44.4	70
LZ-5-2X30%	0.11	0.46	0.55	237	0.2	13.5	39.3	3

X = Toluene conversion, Sp = p-xylene selectivity

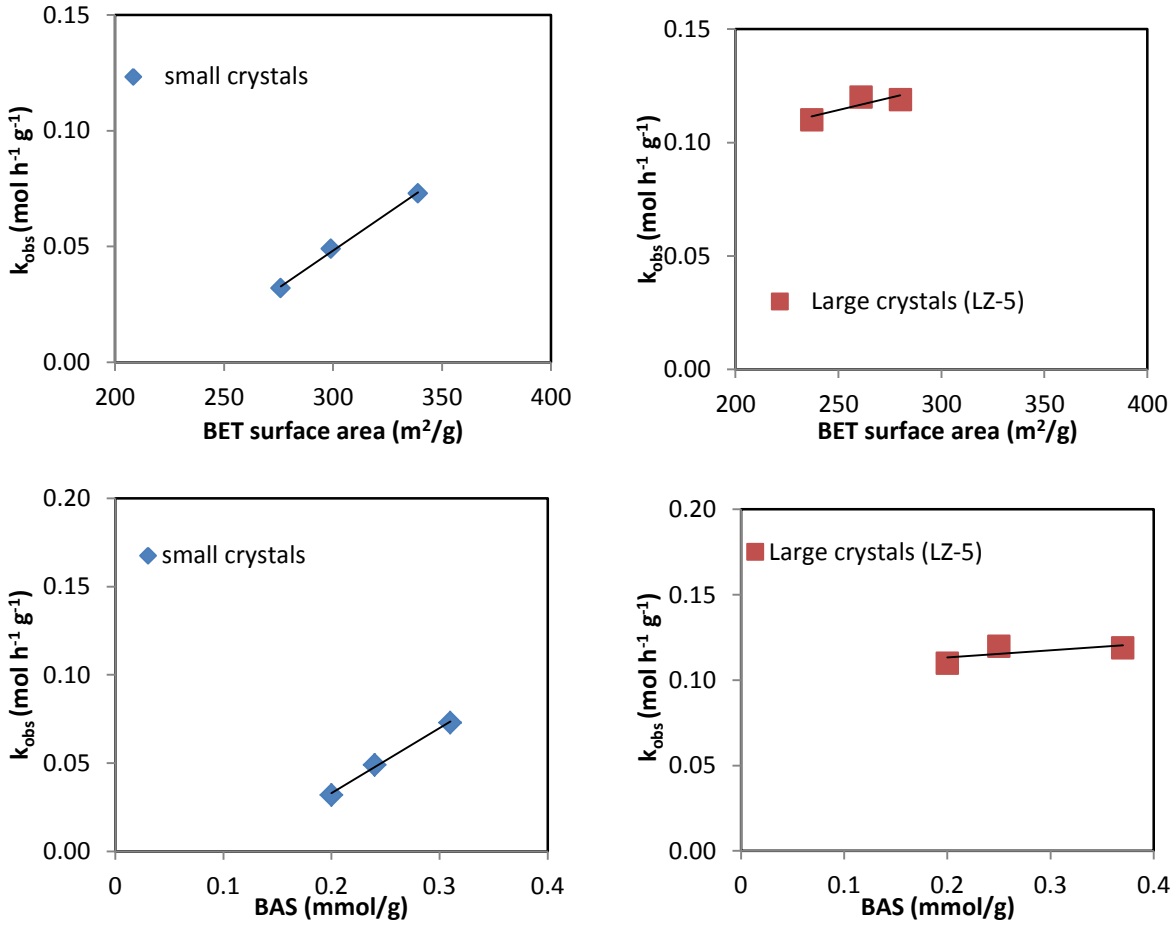

Figure 6-27: The effect of acidity and surface area on the reaction rate for small and large crystals

6.5 Conclusions

ZSM-5 zeolites with different crystal sizes (0.5, 5 and 50) µm were subjected to silica modification by chemical liquid deposition (CLD) to study the effects on p-xylene selectivity and toluene conversion. The effects of silylation agent, silica loading amount and number of cycles were investigated. The obtained results suggested that TEOS was better than APTES as a modification agent, providing high p-xylene selectivity (80%) and a reasonable conversion. Silica coating amount was the key factor in the modification process. It is important to use the right amount as loading larger amount of silica on the surface can lead to non-uniform layers, meaning some acid sites will not be deactivated as the bulky ethoxyl groups of TEOS might hinder the accessibility of TEOS to the remaining acid sites. However, using multiple cycles silylation proved to improve the p-xylene selectivity as calcination of the first cycle will remove the ethoxyl groups allowing TEOS molecules to access the remaining acid sites during the second cycle of

modification. Two cycle modification helped achieving higher selectivity than one cycle in this work. Samples (LZ-5) subjected to two cycles silylation showed a significant increase in p-xylene selectivity to 85 % at atmospheric pressure. Increasing the pressure decreased the selectivity to 65% whereas the total conversion improved reaching 8 %. It can be concluded that silylation led to the deactivation of unselective acid sites on the surface to some extent alongside narrowing the pore openings suggested by the decrease in pore volume (Table 6-5). Furthermore, silylation proved to be an effective method to enhance the p-xylene selectivity.

Results obtained from py-FTIR showed that silylation decreased the acid sites, especially Brønsted acid sites. It was found that the more severe the modification the higher the decrease in catalyst acidity. Decreasing the acid sites was accompanied by an improvement in p-xylene selectivity, suggesting that acid sites on the surface were deactivated. Overall, the results suggest that the appropriate loading for large crystals can be optimised to improve p-xylene selectivity as shown by the 5 µm (LZ-5) results (Figure 6-28). This suggests that the large 50 µm will, when optimised, give the best p-xylene selectivity.

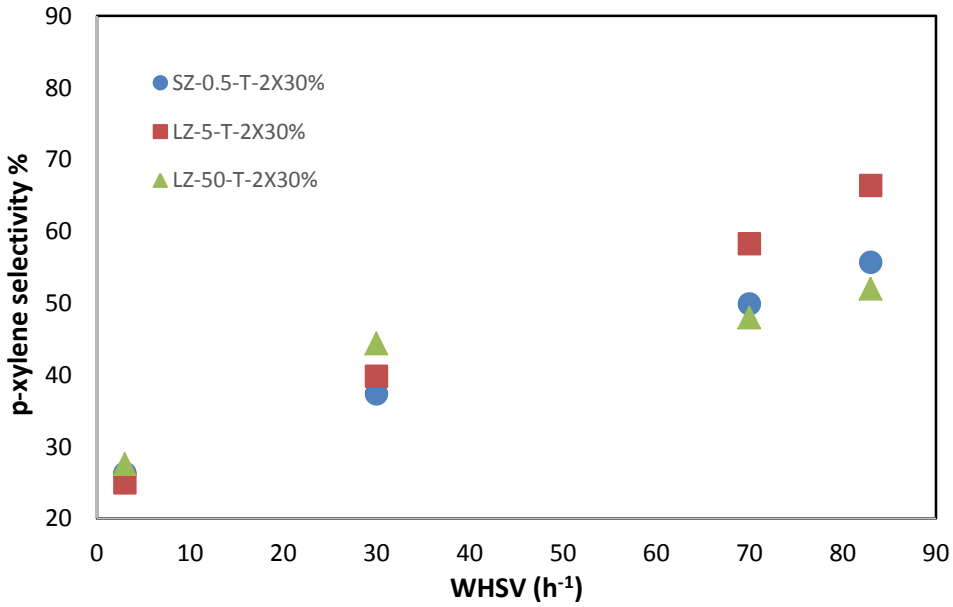

Figure 6-28: comparing para-selectivity on silica modified ZSM-5 with varied crystal size at 10 bar

6.6 References

1. Zheng S, Heydenrych H, Röger H, Jentys A, Lercher J. On the enhanced selectivity of HZSM-5 modified by chemical liquid deposition. Topics in Catalysis. 2003;22(1–

2):101–106.

2. Zhu Z, Xie Z, Chen Q, Kong D, Li W, Yang W, et al. Chemical liquid deposition with polysiloxane of ZSM-5 and its effect on acidity and catalytic properties. Microporous and Mesoporous Materials. 2007;101:169–175.

3. Ali M, Ali S, Al-Nawad K. Disproportionation of toluene: enhanced para-xylene selectivity over modified HZSM-5. Current Catalysis. 2013;2(2):96–110.

4. Shaikh R, Hegde S, Behlekar A, Rao B. Enhancement of acidity and paraselectivity by the silynation in pentasil zeolites. Catalysis Today. 1999;49(1):201–209.

5. Niwa M, Kawashima Y, Hibino T, Murakami Y. Mechanism of chemical vapour deposition of silicon alkoxide on mordenites. Journal of the Chemical Society, Faraday Transactions. 1988;84(12):4327–4336.

6. Hui T, Wang J, Ren X, Chen D. Disproportionation of toluene by modified zsm-5 zeolite catalysts with high shape-selectivity prepared using chemical liquid deposition with tetraethyl orthosilicate. Chinese Journal of Chemical Engineering. 2011;19(2):292–298.

7. Clarence C, David S. catalyst and process for the selective production of para-dialkyl substituted benzenes. US 5243117 A, 1993.

8. Niwa M. Generation of acid sites by SiO_2 deposition on groups IVB metal oxides. Journal of Catalysis. 1992;134(1):340–348.

9. Zheng S. Surface modification of HZSM-5 zeolite. PhD Thesis. Institute for Technical Chemistry II of the Technical University of Munich; 2002.

10. Manstein H, Möller K, Böhringer W, O'Connor C. Effect of the deposition temperature on the chemical vapour deposition of tetraethoxysilane on ZSM-5. Microporous and Mesoporous Materials. 2002;51(1):35–42.

11. Hibino T, Niwa M, Murakami Y. Inactivation of external surface of mordenite and ZSM-5 by chemical vapor deposition of silicon alkoxide. Zeolites. 1993;13(7):518–523.

12. Zheng S, Heydenrych H, Jentys A, Lercher J. Influence of surface modification on the acid site distribution of HZSM-5. Journal of Physical Chemistry B. 2002;106(37):9552–9558.

13. Armaroli T, Trombetta M, Gutièrrez Alejandre A, Ramirez Solis J, Busca G. FTIR study of the interaction of some branched aliphatic molecules with the external and internal sites of H-ZSM5 zeolite. Physical Chemistry Chemical Physics. 2000;2(14):3341–3348.

14. Ding W, Meitzner G, Iglesia E. The effects of silanation of external acid sites on the structure and catalytic behavior of Mo/H–ZSM5. Journal of Catalysis. 2002;206(1):14–22.

15. Treacy MMJ, Higgins JB, editors. Collection of simulated XRD powder patterns for zeolites. 4th ed. Elsevier. 2001.

16. Chen W, Tsai T, Jong S, Zhao Q, Tsai C, Wang I, et al. Effects of surface modification on coking, deactivation and para-selectivity of H-ZSM-5 zeolites during ethylbenzene disproportionation. Journal of Molecular Catalysis A: Chemical. 2002;181(1–2):41–55.

17. Weber R, Möller K, Unger M, O'Connor C. The chemical vapour and liquid deposition of tetraethoxysilane on the external surface of ZSM-5. Microporous and Mesoporous Materials. 1998;23:179–187.

18. Huang M, Adnot A, Kaliaguine S. Silylation of H-ZSM-5: an X-ray photoelectron and infrared spectroscopy study. Journal of the Chemical Society, Faraday Transactions. 1993;89(23):4231.

19. Engelhardt G, Michel D. High resolution solid state NMR of silicates and zeolites. John Wiley & Sons, Australia, 1987.

20. Wu T, Chen S, Yuan G, Cao Y, Su K. Enhanced catalytic performance in butylene cracking by hierarchical surface silicon-rich ZSM-5. Fuel Processing Technology. 2017;167:162–170.

21. Bauer F, Chen W, Ernst H, Huang S, Freyer A, Liu S. Selectivity improvement in

xylene isomerization. Microporous and Mesoporous Materials. 2004;72(1–3):81–89.

22. Boxhoorn G, Kortbeek A, Hays G, Alma N. A high-resolution solid-state ^{29}Si n.m.r. study of ZSM-5 type zeolites. Zeolites. 1984;4:15–21.

23. Müller U, Unger K. Sorption studies on large ZSM-5 crystals:the influence of aluminium content, the type of exchangeable cations and the temperature on nitrogen hysteresis effects. Studies in Surface Science and Catalysis. 1988;39:101–108.

Chapter 7 Effects of additives and metal loadings on p-xylene selectivity

7.1 Introduction and Background

Shape selective catalysis has been investigated heavily in the chemical industry as it forms less bulky isomers as a result of steric constraints caused by pore narrowing and attempts to deactivate the external acid sites. It was proposed in the literature by many researchers that the para-isomer is selectively produced inside the pores of H-ZSM-5 zeolite. However, the faster isomerization reaction occurring on the external surface results in the thermodynamic equilibrium of the isomers (namely para- 24%, meta- 50% and ortho- 26%). This led many workers to study the deactivation of the external acid sites and narrowing the pores by the addition of different elements and metals such as phosphorus, lanthanum, magnesium and nickel [1–6]. Modifying ZSM-5 by either impregnation or ion exchange can lead to an increase in the selectivity towards p-xylene. If deposited on the surface, these additives can deactivate some acid sites or narrow the pores by entering the channels or pore mouths thus increasing diffusion limitations preventing production of undesired isomers.

Kaeding et al. studied the effects of adding phosphorus, boron and magnesium and reported that modifying H-ZSM-5 with phosphorus increased the p-xylene selectivity to 65 % in toluene disproportionation, although at a low conversion between 0.3 to 4.4% [7]. These results were obtained at elevated temperatures (550-700^{o}C), and therefore led to increased demethylation of toluene and as a result more benzene was produced leading to an increase in the benzene/xylene ratio [7]. It was suggested that these additives reduce the pore openings of H-ZSM-5 helping p-xylene to diffuse at faster rate than the other isomers. Rahman et al. found that at a low loading, most of the phosphorous goes inside the pores and the remaining amount segregate on the surface of the zeolite. It was reported using IR that Brønsted acid site were poisoned progressively which explained the very low conversion [2]. Nemdo et al. modified H-ZSM-5 with a combination of phosphorus and magnesium impregnation [8]. A high selectivity (75%) towards p-xylene was achieved with a conversion of 7%. Increasing WHSV from 4 to 10 h^{-1} helped to improve the selectivity up to 90% while the conversion decreased to 2%. This could be explained by the fact that increasing the flow rate reduced the contact time with the zeolite and hence isomerisation. Therefore, the p-xylene yield was increased. Several authors (Kaeding and Vedrine) proposed a model for the phosphorus modification of H-

ZSM-5, and suggested that the OH^- was replaced with $H_2PO_4^-$ and as a result the strong Brønsted acid sites were reduced and the number of weak acid sites increased (Figure 7-1) [7,9].

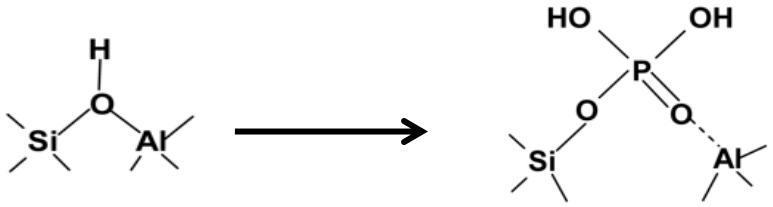

Figure 7-1: proposed mechanism for phosphorus modification of H-ZSM-5 acid sites [9]

It was proposed that the pore opening of ZSM-5 was reduced by the phosphorus modification which further limited the ortho and meta isomers and increased the selectivity towards para-xylene isomer. Moreover, the phosphorus atoms will also block acid sites on the surface preventing the unwanted and more rapid secondary isomerization reaction from taking place on the non-selective external acid sites [10].

Kareem et al. ion exchanged ZSM-5 with 4 wt. % of a range of elements Ni, Cr, Mg, Bi and Zn to attempt to increase the selectivity towards p-xylene. Performing toluene disproportionation at 550 ^oC on the modified catalysts they achieved p-xylene selectivity in the order Ni (53%) > Bi (42%) > Mg (35%) > Zn (32%) > Cr (30%) [11]. Uguina et al. modified large crystals ZSM-5 (7.4 µm, Si/Al = 29) with 0.4 to 0.9 wt. % magnesium by impregnation and improved the selectivity towards p-xylene up to 80 % at a toluene conversion around 8 % [12]. Mg molecules can enter the pores and deposit on the surface modifying the acid sites inside the pores and on the external surface of the catalyst which can be linked to the decrease in activity.

Lanthanum oxide is a potential modifying agent to the external surface of ZSM-5 as it's cation is too large to enter the pores. Sugi et al. reported that the cracking of 1,3,5-TIPB decreased after loading lanthanum on ZSM-5 suggesting the deactivation of the external surface acid sites to some extent [13]. Hartford et al. proposed that the smallest form of lanthanum ionic species after zeolite modification is $La(H_20)_6^{3+}$ with a diameter of 6.6 Å, while ZSM-5 zeolite has a pore diameter of 5.6 Å [14]. This supported the argument that Lanthanum ions will be loaded on the external surface as it is difficult to enter the pores.

However, upon calcination at 550 °C, the lanthanum molecules are stripped of the water molecules which could result in some of the La^{+3} ions to go inside the pore during the process.

The enhancement of p-xylene selectivity in toluene disproportionation reaction by the addition of rare earth metals such as lanthanum and cerium was also studied by Sugi et al and concluded that lanthanum had more effect on p-xylene than cerium [13]. They performed toluene disproportionation at 600 °C and atmospheric pressure over ZSM-5 (SiO_2/Al_2O_3 = 190) impregnated with lanthanum (10 – 30 wt. %). The enhancement of p-xylene selectivity up to 60 % with a toluene conversion of less than 10 % was reported. It was concluded that 10 wt.% loading level of lanthanum was sufficient to deactivate the external acid sites and narrow the pores (Figure 7-2).

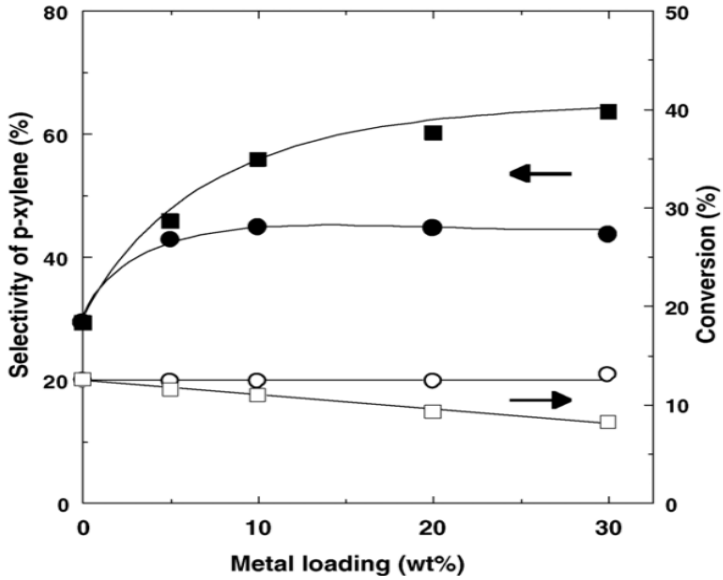

Figure 7-2: Effect of loading amount of lanthanum and cerium on p-xylene selectivity (■ La/H-ZSM-5, ● Ce/H-ZSM-5) and toluene conversion (□ La/H-ZSM-5, ○ Ce/H-ZSM-5) [13].

In this chapter, the effect of phosphorus modified ZSM-5 catalyst on p-xylene selectivity and toluene conversion was studied. SZ-0.5 was loaded with three different phosphorus loadings (0.75, 1.5 and 3 wt. %) using phosphoric acid (H_3PO_4) solution (Sigma Aldrich, 85 wt. %). Furthermore, SZ-0.5 and LZ-5 were modified with different loadings of lanthanum (5 and 10 wt. %) using lanthanum nitrate hexahydrate solution (Sigma Aldrich > 99.9%). All modified catalysts were characterized using different techniques such as py-FTIR, BET surface area and ICP-OES to investigate the effects imposed on acidity, surface area and

pore volume (as described in chapter 4). Finally, the modified ZSM-5 zeolites were evaluated for toluene disproportionation (as described in chapter 4).

7.2 Catalyst preparation:

7.2.1 Phosphorus modification

NH_4 ZSM-5 zeolite (SZ-0.5) with 0.5 µm crystal size purchased from Alfa Aesar was calcined at 550 °C for 6 hours in a muffle furnace. The phosphorus addition was performed via wet impregnation using H_3PO_4 (85 wt. % in H_2O). Firstly, the catalyst was mixed with water at 60 °C for 1 hour. Then, H_3PO_4 was added according to the desired amount of P loading and kept stirring for further 1 hour (an example of calculation is shown in appendix A). After that, the samples were dried at 120 °C. Finally, they were calcined at 550 °C for 6 hours, pelletised and sieved (250 – 425 µm). The effect of pH was varied by adding ammonium hydroxide (NH_4OH) (Sigma Aldrich, 90 wt. %) dropwise alongside H_3PO_4 to keep the pH value around 5. Furthermore, a washing step was performed on few samples after calcination treatment by mixing the modified catalyst with water at 80 °C for 12 hours followed by drying overnight. Lischke et al. reported that washing with hot water results in the recovery of some strong acid sites by the elution of some phosphorus on the surface [15]. Table 7-1 lists the samples modified with different P loading levels.

7.2.2 Lanthanum modification

ZSM-5 zeolites with different crystal sizes (0.5 and 5 µm) were impregnated with lanthanum. A mixture of the desired catalyst (5 g) and an aqueous solution of lanthanum nitrated hexahydrate ($La(NO_3)_3$. $6\ H_2O$) was stirred for 1 hour (an example of calculation is given in appendix A). Then, the temperature was raised to slowly evaporate the water while the mixture was stirred. After that, the catalyst was dried overnight in the oven at 120 ˚C and finally, the modified ZSM-5 was calcined by ramping the temperature from ambient to 550 ˚C at a rate of 2 ˚C /min and held for 6 hours. The intention was to load SZ-0.5 with 5 wt. % La and LZ-5 with 5 and 10 wt. % La to compare the effects of loading alongside studying the effect of the modification on different ZSM-5 zeolites with different crystal sizes (Table 7-1 lists samples prepared).

Table 7-1: Phosphorus and lanthanum loading on ZSM-5 zeolites with different crystal sizes

Zeolite	modification agent	Loading wt. %	Sample ID
SZ-0.5	H_3PO_4	0.75 wt. %	SZ-0.5-0.75P
	H_3PO_4	1.5 wt. %	SZ-0.5-1.5P
	H_3PO_4	3.0 wt. %	SZ-0.5-3P
	La $(NO_3)_3$. 6 H_2O	5.0 wt. %	SZ-0.5-5La
LZ-5	La $(NO_3)_3$. 6 H_2O	5.0 wt. %	LZ-5-5La
	La $(NO_3)_3$. 6 H_2O	10.0 wt. %	LZ-5-10La

7.3 Catalyst Characterization:

7.3.1 X-Ray Diffraction (XRD)

Parent and modified samples were characterized using XRD to study the effects of modifications on crystallinity. XRD X'Pert Philips instrument was used following the procedure explained in section 4.4.1. All phosphorus modified ZSM-5 (SZ-0.5) samples showed a good crystallinity as seen in Figure 7-3 with slight change with loading up to 1.5 % P. However, the intensities of the peaks decreased more markedly at 3 wt. % phosphorus loading indicating around a 10 % decrease in crystallinity compared to the parent as calculated using peak area summation following the ASTM method described in section 4.4.1. The decrease in crystallinity could be explained by the dealumination during the impregnation process of phosphorus using phosphoric acid.

Figure 7-4 shows typical XRD patterns of lanthanum impregnated samples on ZSM-5 large crystals (LZ-5) post calcination. The peak intensities of the modified samples clearly decreased with lanthanum loading, dropping by 60 % at 10 % La loading and this was found to be in agreement with the literature where Sugi et al. observed a decrease in the crystallinity with 10 % lanthanum loading on H-ZSM-5 zeolite and decreased further with higher loadings [13]. The decrease in peak intensities was expected with high loading level of lanthanum (5 and 10 wt. %) as Zhang et al. demonstrated that the crystallinity of lanthanum modified ZSM-5 decreased even at low levels (La = 0.13-0.87 wt. %) [16]. It was reported in the literature that the average diameter of La^{+3} is 0.12 nm, which is smaller than the pore mouth of ZSM-5 zeolite, after stripping the water molecules off by

calcination. This suggests that part of the La^{+3} cations might enter the channels of the zeolite during the modification process resulting in the decrease in the peak intensities below 10˚ 2θ as they are sensitive to anything inside the channels [16]. Furthermore, the lanthanum peak was not detected implying that the metal was well dispersed on the zeolite [16].

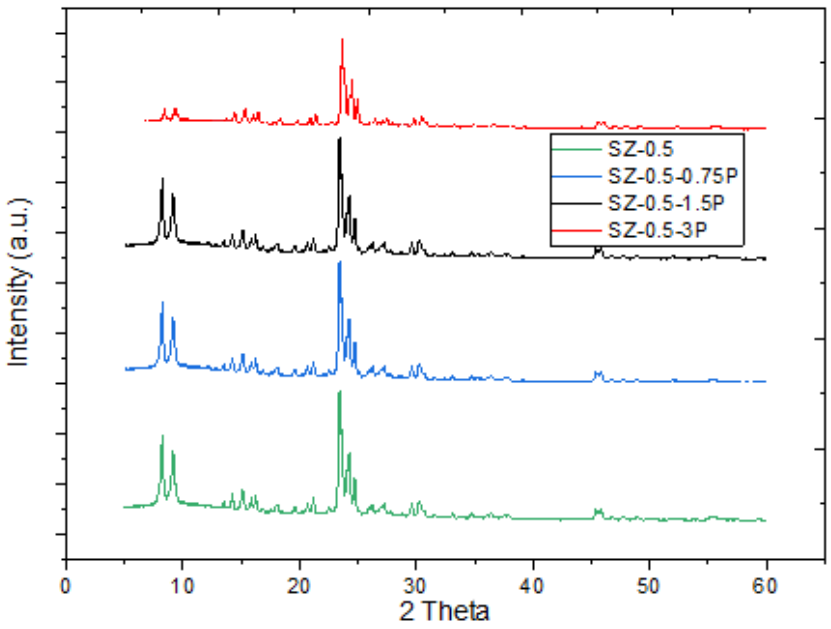

Figure 7-3: XRD patterns of parent and phosphorus modified SZ-0.5

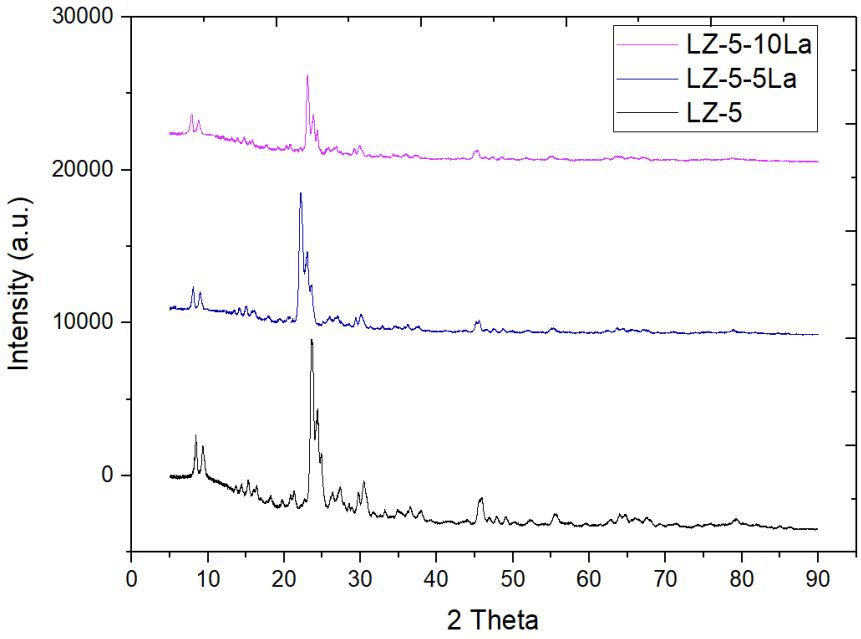

Figure 7-4: XRD patterns of parent and lanthanum modified LZ-5 post calcination

7.3.2 Acidity measurements

Pyridine FTIR was utilized to measure the Brønsted and Lewis acidity of the parent and modified catalysts. The region 3500 – 3900 cm^{-1} shows the bridging hydroxyl group (3610 cm^{-1}) and terminal SiOH (3745 cm^{-1}). It was observed from Figure 7-5 that all the bridging OH-groups of the parent and modified catalysts were accessible to pyridine. The intensity of the bridging hydroxyls decreased with increasing both lanthanum and phosphorus loading. BAS and LAS were measured by introducing pyridine to the catalyst. After the adsorption of pyridine, BAS and LAS were measured in the region 1400 - 1700 cm^{-1}. The intensity of the py-BAS and py-LAS peaks at ~ 1546 and 1455 cm^{-1} were used to compare the number of active sites in the parent and modified samples (Table 7-2).

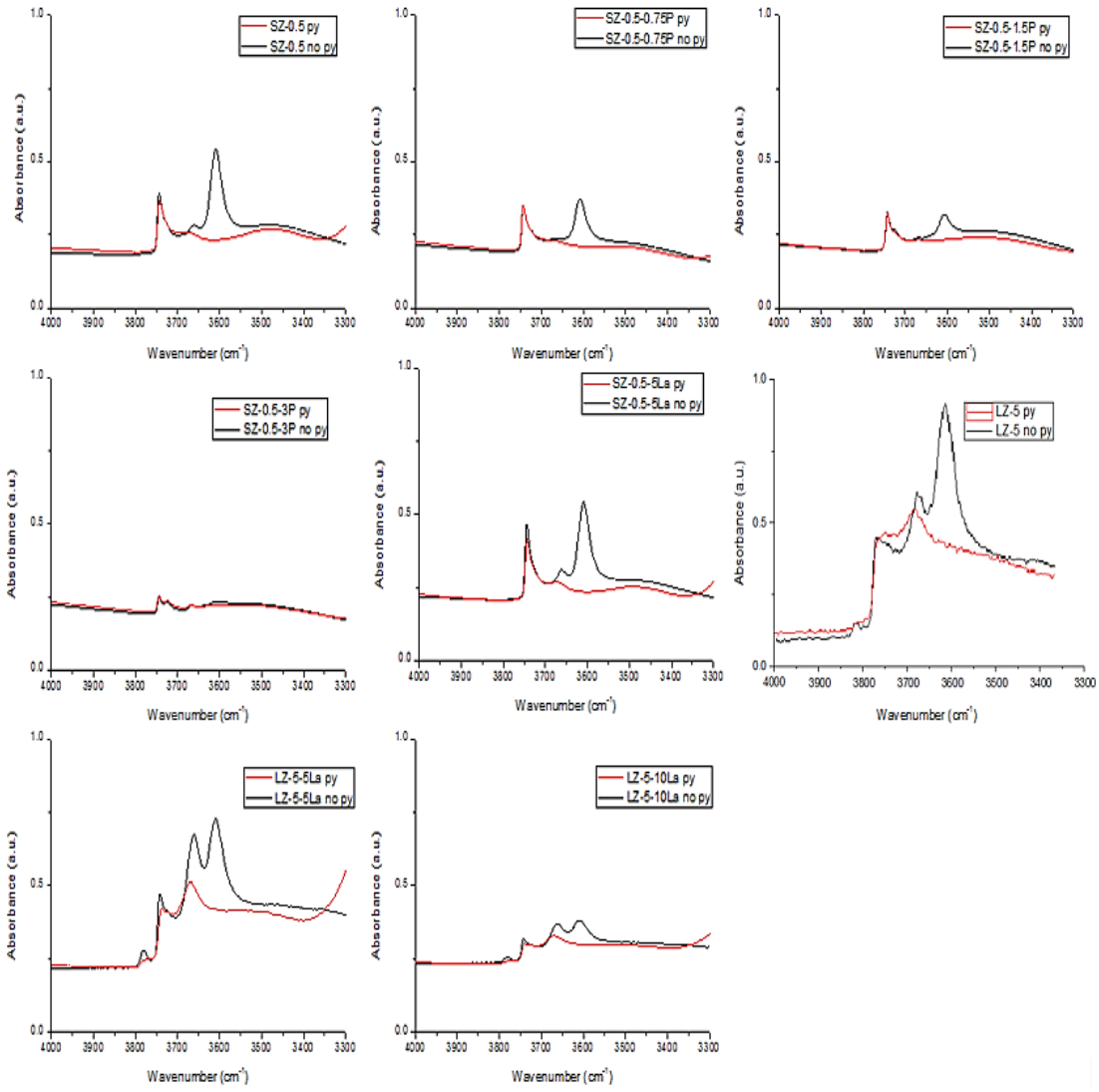

Figure 7-5: FTIR spectra in the hydroxyl region with and without pyridine

From the results (Figure 7-5), it was noted that increasing the phosphorus loading level was accompanied by a sharp decrease in the intensity of the bridging hydroxyl groups (3610 cm^{-1}) and the peak disappeared at a loading of 3 wt. % suggesting that almost all Brønsted acid sites were blocked by phosphorus. In terms of BAS and LAS, all samples showed the characteristic peaks at 1540 and 1450 cm^{-1} (Figure 7-6) and the loading of phosphorus decreased both acid sites drastically as seen in Table 7-2. The acidity was decreased further as the severity of the modification increased. Similar findings were published by Lischke et al. where impregnation of ZSM-5 (Si/Al = 19) with 2.5 wt. % phosphorus by an aqueous solution of phosphoric acid decreased the number of Brønsted acid sites after thermal treatment by around 70% [15].

Increasing lanthanum loading level on the large crystal ZSM-5 (LZ-5) led to a decrease in the bridging hydroxyl peaks. On the other hand, the peak at (3650 cm^{-1}) allocated to AlOH groups increased after lanthanum impregnation on the catalyst. Table 7-2 and Figure 7-7 show that modifying ZSM-5 with lanthanum increased the Lewis acidity while the Brønsted acidity was decreased.

Table 7-2: Brønsted and Lewis acidity of parents and modified samples

Catalyst	BAS (mmol/g)	LAS (mmol/g)	BAS/LAS
SZ-0.5	0.31	0.08	3.90
SZ-0.5-0.75P	0.17	0.05	3.40
SZ-0.5-1.5P	0.08	0.02	4.00
SZ-0.5-3P	0.05	0.01	5.00
SZ-0.5-5La	0.27	0.11	2.45
LZ-5	0.37	0.17	2.15
LZ-5-5La	0.22	0.19	1.16
LZ-5-10La	0.19	0.20	1.27

The increase in LAS could be due to the acidic properties of lanthanum oxides. Zhang et al. suggested that La^{+3} cations are considered to be weak acid sites and they might interfere in the measurements of the acid densities [16]. Inversely, the lanthanum can

interact with the bridging hydroxyl groups resulting in a decrease in the number of BAS.

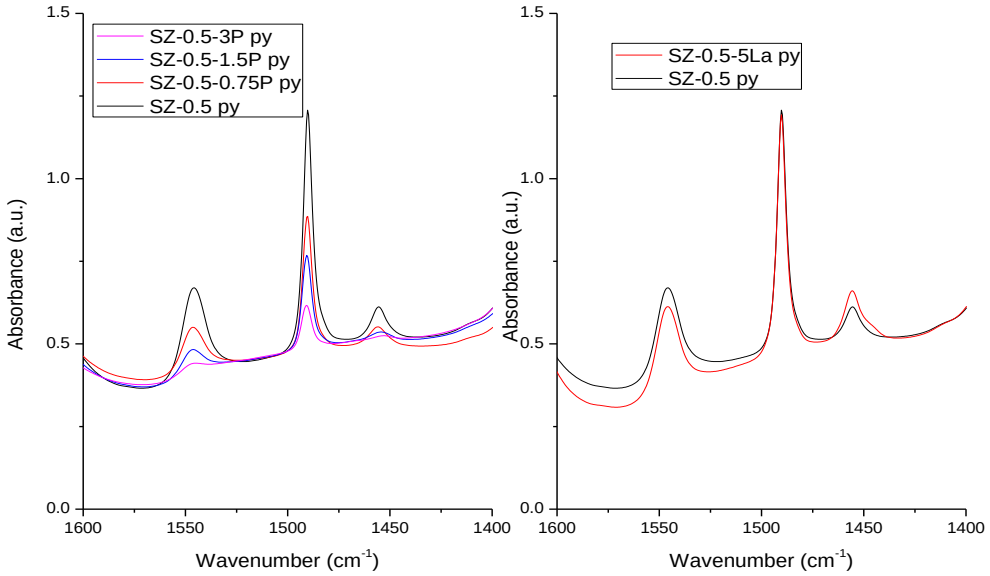

Figure 7-6: Pyridine FTIR in the BAS and LAS region for parent SZ-0.5 and P + La modified samples

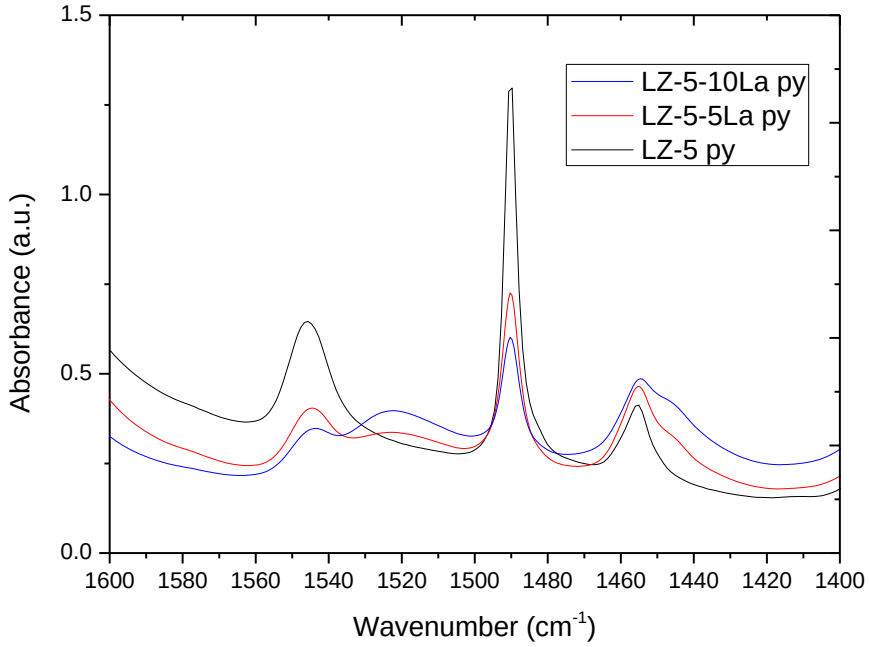

Figure 7-7: Pyridine FTIR in the BAS and LAS region for parent LZ-5 and La impregnated samples

In summary, the modification with phosphorus reduced the number of acid sites more drastically than lanthanum even though the phosphorus loading level was significantly less than that of lanthanum (Figure 7-8).

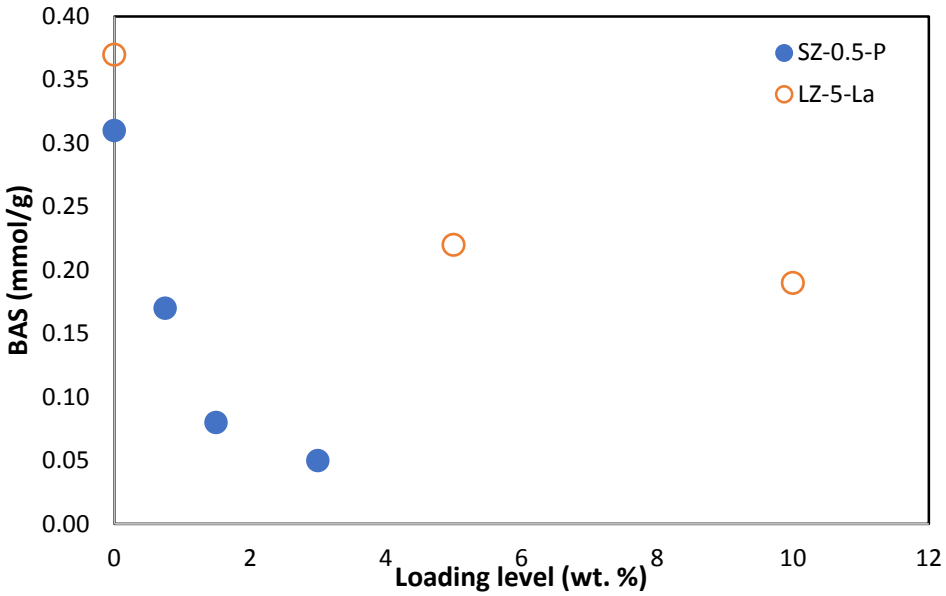

Figure 7-8: Effect of P and La loading on Brønsted acid sites

7.3.3 Energy Dispersive X-ray (EDX) and Inductively Coupled Plasma (ICP-OES)

ICP analysis was performed outside the university by MEDAC LTD and EDX analysis were carried using Philips XL-30 instrument internally by taking the average of 10 measurement points for each sample. The results of both techniques presented in Table 7-3 confirmed that elements had been loaded and that the values were close to the target wt. %.

Table 7-3: Elemental analysis by EDX and ICP

Catalyst	EDX	ICP
SZ-0.5-0.75P	0.74	0.65
SZ-0.5-1.5P	1.4	1.5
SZ-0.5-3P	2.23	2.32
SZ-0.5-5La	4.5	4.8
LZ-5-5La	4.6	-
LZ-5-10La	9.4	-

7.3.4 BET surface area and pore volume measurements by N_2 adsorption

The measurements were carried out following the procedure explained in section 4.4.4. The addition of phosphorus to the parent ZSM-5 reduced the surface area, the pore volume, and the external surface area as shown in Table 7-4 and indicated that some phosphorus atoms may have entered the pores of ZSM-5 as well as covering the surface post calcination. It can be observed from Table 7-4 that as the lanthanum content increased in the catalyst, the BET surface area and the microporous volumes of the modified catalyst decreased. The decrease in pore volume most likely attributed to some lanthanum cations entering the channels of ZSM-5 while the rest is located on the external surface, as reported by Zhang et al [16].

Table 7-4: Textural properties of parents and modified catalysts

Catalyst	BET surface area (m^2/g)	pore volume (cm^3/g)	External surface area (m^2/g)
SZ-0.5	338	0.113	151
SZ-0.5-0.75P	315	0.101	149
SZ-0.5-1.5P	271	0.093	116
SZ-0.5-3P	228	0.091	72
SZ-0.5-5La	293	0.100	126
LZ-5	280	0.110	93
LZ-5-5La	238	0.095	75
LZ-5-10La	227	0.089	73

Figure 7-9 shows that as phosphorus loading level increased the total surface area decreased almost linearly with the 3 wt. % loading showing about 35 % reduction. In the case of pore volume, it can be observed that the increase in loading level was accompanied by drop in pore volume up to 1.5 wt.%. Increasing the loading level of lanthanum had similar effects resulting in a decrease in the surface area and the pore volume (Figure 7-10).

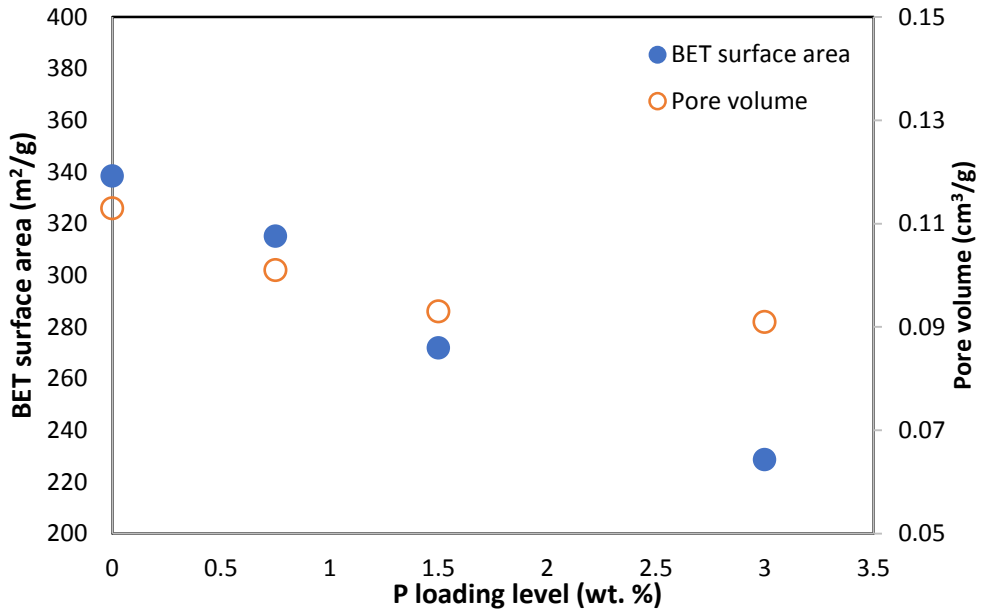

Figure 7-9: Effect of P loading on BET surface area and pore volume

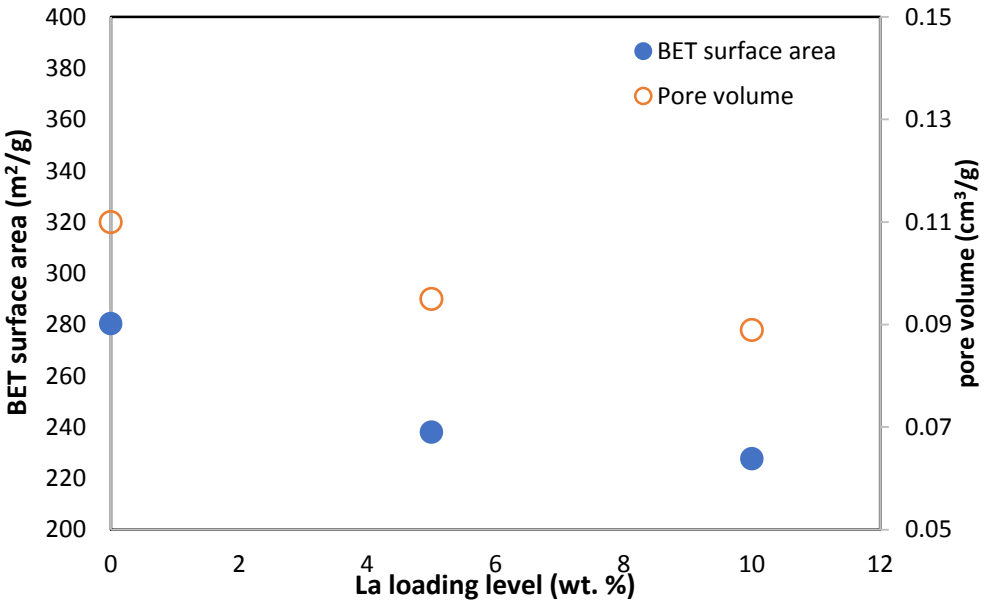

Figure 7-10: Effect of La loading on BET surface area and pore volume of LZ-5

7.4 Catalytic evaluation

All parent and modified catalyst were pelleted, sieved (250-420 µm) and loaded (1g) into the reactor. The catalysts were tested for toluene disproportionation at 475 °C and the WHSV was varied (3 - 83 h^{-1}). The phosphorus modified catalysts were tested at 1 atmospheric pressure whilst the lanthanum impregnated zeolites were tested at 1 and 10 bar pressure.

7.4.1 Effect of phosphorus on toluene conversion and p-xylene selectivity

7.4.1.1 Effect of phosphorus loading

As expected at the lowest WHSV (h^{-1}) increasing the loading level of phosphorus consequently decreased the toluene conversion, where the lowest conversion (0.8 wt. %) was observed using the 3 wt. % phosphorus loaded catalyst (SZ-0.5-3P) (Figure 7-11).

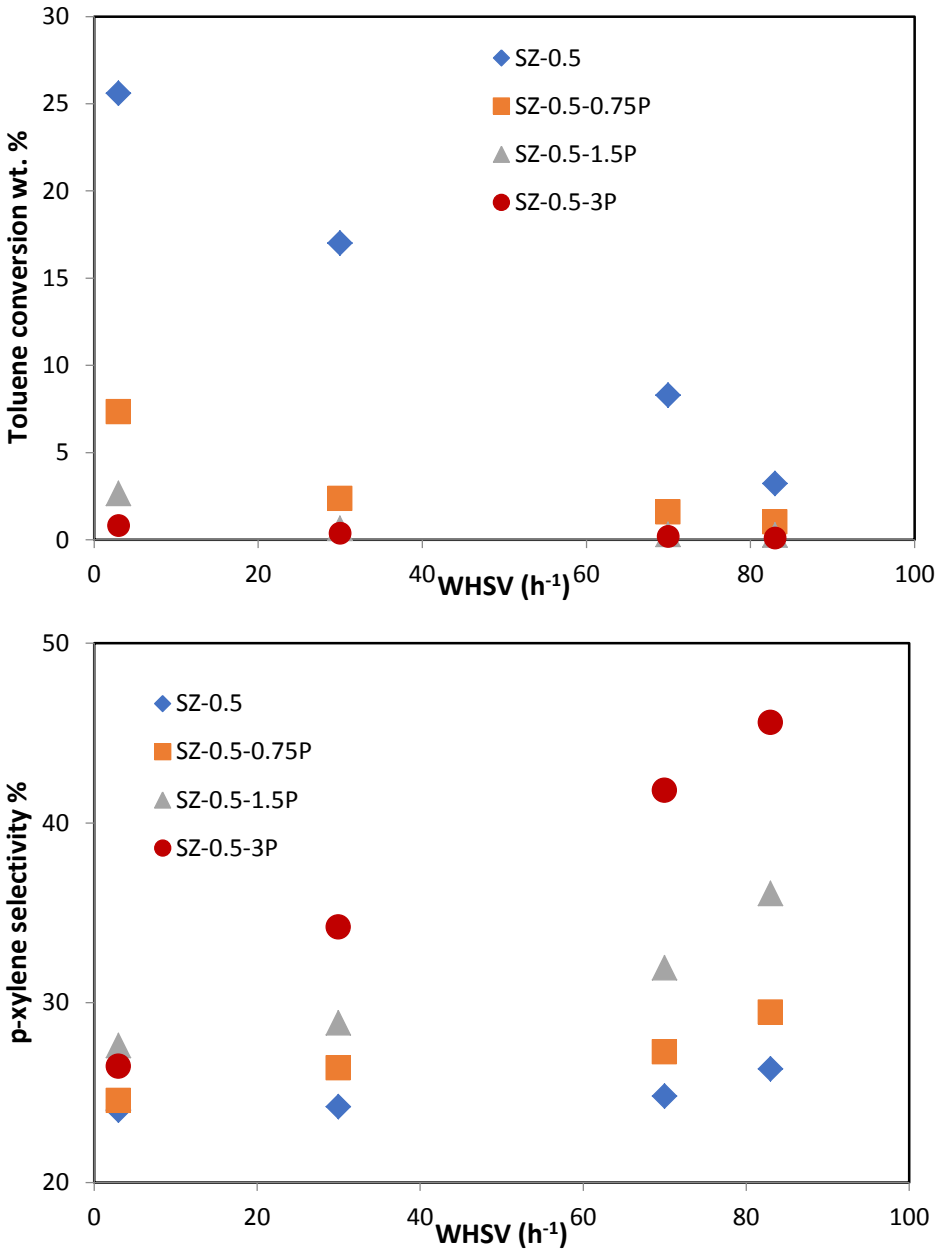

Figure 7-11: Effect of phosphorus loading on toluene conversion and p-xylene selectivity

Increasing the flowrate was accompanied by a decrease in the conversion of toluene by all modified and parent catalysts. Inversely, p-xylene selectivity increased with increased loading of phosphorus which was more marked at higher WHSVs, reaching about 45 % at

a WHSV 83 h^{-1} by SZ-0.5-3P. Increasing the flowrate allowed less contact between the catalyst and the feed, resulting in reduced isomerization on the external surface of the catalyst and hence led to higher p-xylene selectivity. However, the phosphorus modification improved the p-xylene selectivity at increased WHSVs whereas no noticeable change was observed by the unmodified parent.

7.4.1.2 Effect of washing and pH control

It was discussed in section 7.2.1 that washing can lead to regaining some acid sites, so the effect of washing the catalyst after the modification on p-xylene selectivity and toluene conversion was studied and the results are illustrated in Figure 7-12.

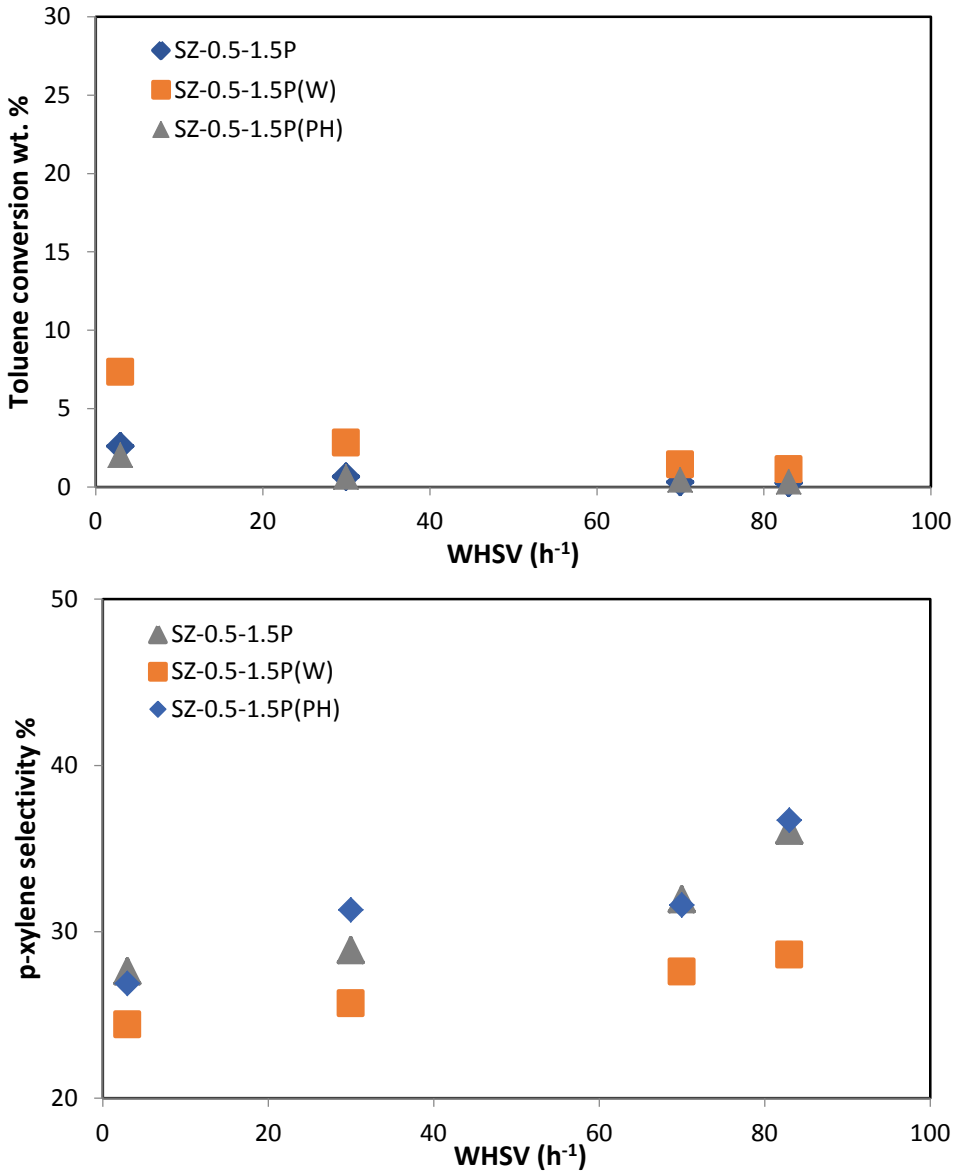

Figure 7-12: Effect of washing and pH control steps on conversion and para selectivity over phosphorus modified ZSM-5

Both washed (SZ-0.5-1.5P(W)) and unwashed (SZ-0.5-1.5P) samples were tested to investigate the effect of washing on the activity. As seen in Figure 7-12, the washing step resulted in an increase in the conversion of toluene. However, it was accompanied by a decrease in the p-xylene selectivity. On the other hand, the sample prepared with pH control (SZ-0.5-1.5P(PH)) did not result in a noticeable change in the toluene conversion or the p-xylene selectivity.

7.4.2 Effect of lanthanum modified ZSM-5 on toluene disproportionation

7.4.2.1 Effect of lanthanum loading

The effect of impregnating SZ-0.5 and LZ-5 with lanthanum on toluene conversion and p-xylene selectivity was studied. Figure 7-13 shows that conversion was decreased as result of lanthanum loading on SZ-0.5. The same observation was made when LZ-5 was modified. The conversion was further decreased as the loading level increased from 5 to 10 wt. %. The decrease in conversion can be attributed to the decrease in surface area, pore volume and acidity as shown by py-FTIR and N_2 adsorption results compiled in Table 7-2 and Table 7-4.

In contrast, the p-xylene selectivity increased with increasing the level of lanthanum loading on LZ-5 whereas there was a slight increase over the modified ZSM-5 with small crystals (SZ-0.5). The increase in p-xylene selectivity was more evident with increasing the toluene flow rate. The highest p-xylene selectivity (62 %) was achieved by LZ-5-10La, unfortunately the toluene conversion dropped to around 2.5 wt. % - see Figure 7-13. To increase the conversion reaction pressure had to be increased.

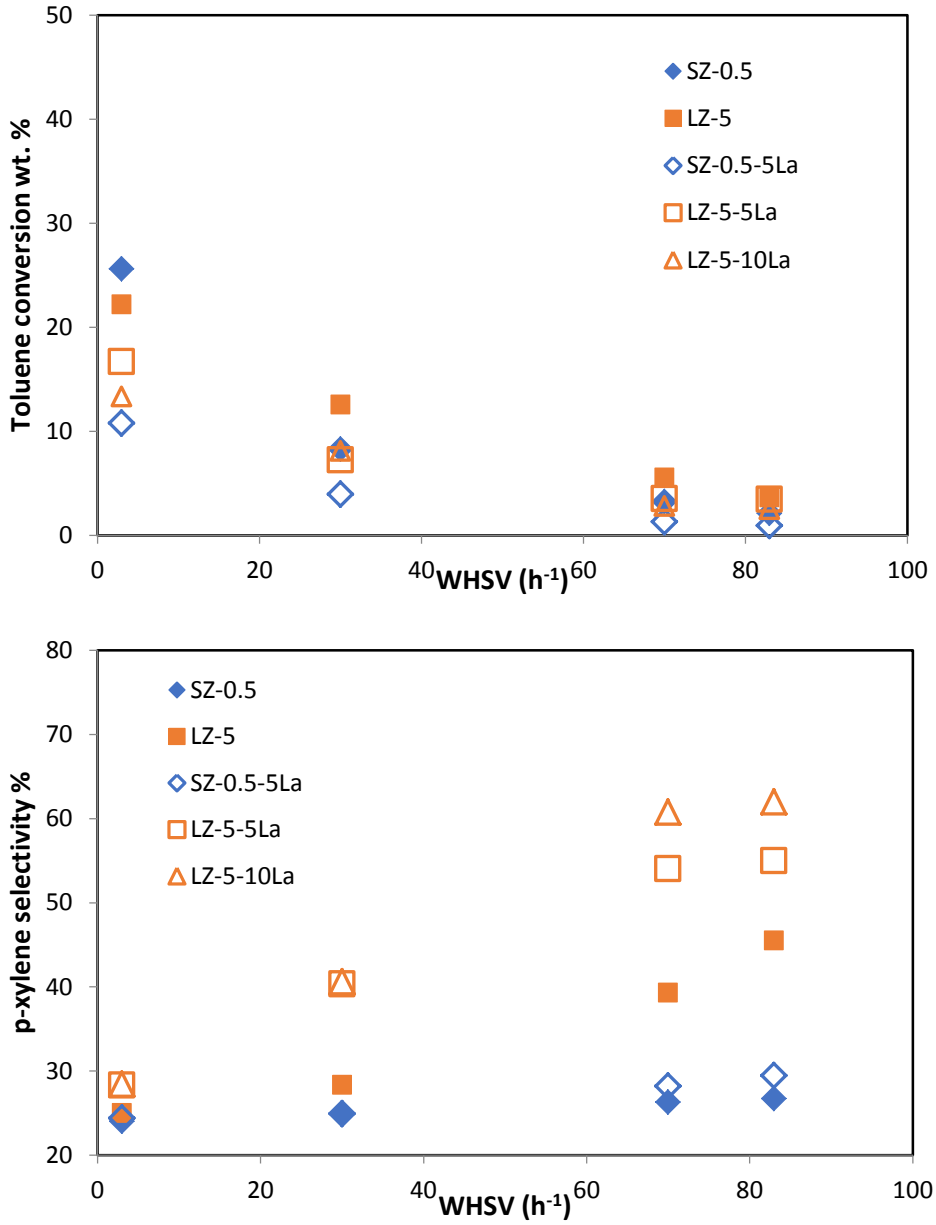

Figure 7-13: Effect of lanthanum loading

7.4.2.2 Effect of pressure

The pressure was increased to 10 bar in attempt to improve the toluene conversion. The conversion almost doubled for both parent catalysts. Interestingly, 5 wt. % lanthanum loaded catalysts showed a conversion that is three times higher than those achieved at atmospheric pressure. Moreover, conversions achieved at 10 bar and WHSV (3 h^{-1}) for 5 wt. % lanthanum loaded catalysts were higher than what was achieved by the parent as seen in Figure 7-14. Most noticeably with SZ-0.5-5La producing a conversion of 48 % compared to its parent (41 %). The high conversion achieved by the modified

catalysts can be attributed to newly formed Lewis acid sites by the lanthanum cations addition on the catalyst (Table 7-2). Similar effects were observed by Zhang et al. through different type of reaction where lanthanum addition increased the conversion of propane and improved the catalyst stability with time on stream [17]. However, the opposite effect was observed as the lanthanum loading was increased to 10 wt. % (LZ-5-10La) dropping the conversion slightly lower than the parent (LZ-5).

Table 7-5: Product distribution of parent and modified samples at 10 bar

	catalyst	Benzene	Toluene	Et benzene	p-Xylene	m-Xylene	o-Xylene	C_9	C_{10}
WHSV (3 h^{-1})	SZ-0.5	17.0	61.0	0.0	4.7	10.5	4.4	0.7	0.1
	SZ-0.5-5La	15.1	52.9	0.4	6.6	14.4	7.0	3.1	0.3
	LZ-5	23.3	53.9	0.6	4.8	10.4	4.6	1.2	0.1
	LZ-5-5La	17.7	51.8	0.7	6.4	14.0	6.8	1.8	0.7
	LZ-5-10La	15.9	56.0	0.5	6.2	13.3	6.2	1.4	0.5
WHSV (30 h^{-1})	SZ-0.5	9.9	78.0	0.0	3.0	6.2	2.7	0.2	0.0
	SZ-0.5-5La	11.1	69.0	0.2	4.3	9.4	4.5	1.4	0.1
	LZ-5	14.7	68.9	0.3	4.3	7.6	2.8	0.5	0.5
	LZ-5-5La	13.1	65.3	0.3	5.5	10.3	4.4	0.7	0.3
	LZ-5-10La	11.8	70.0	0.1	5.6	8.1	3.7	0.3	0.1

Table 7-5 shows the product distribution for the parent and lanthanum modified ZSM-5 zeolites. It can be clearly seen in the table that 5 wt. % La loading on SZ-0.5 and LZ-5 resulted in higher conversions than the parent. The increase in toluene conversion led to higher p-xylene yield (Figure 7-15). The decrease in conversion after 10 wt. % La loading can be attributed to further pore mouth blockage and the decrease in Brønsted acid sites (Table 7-2 and Table 7-4).

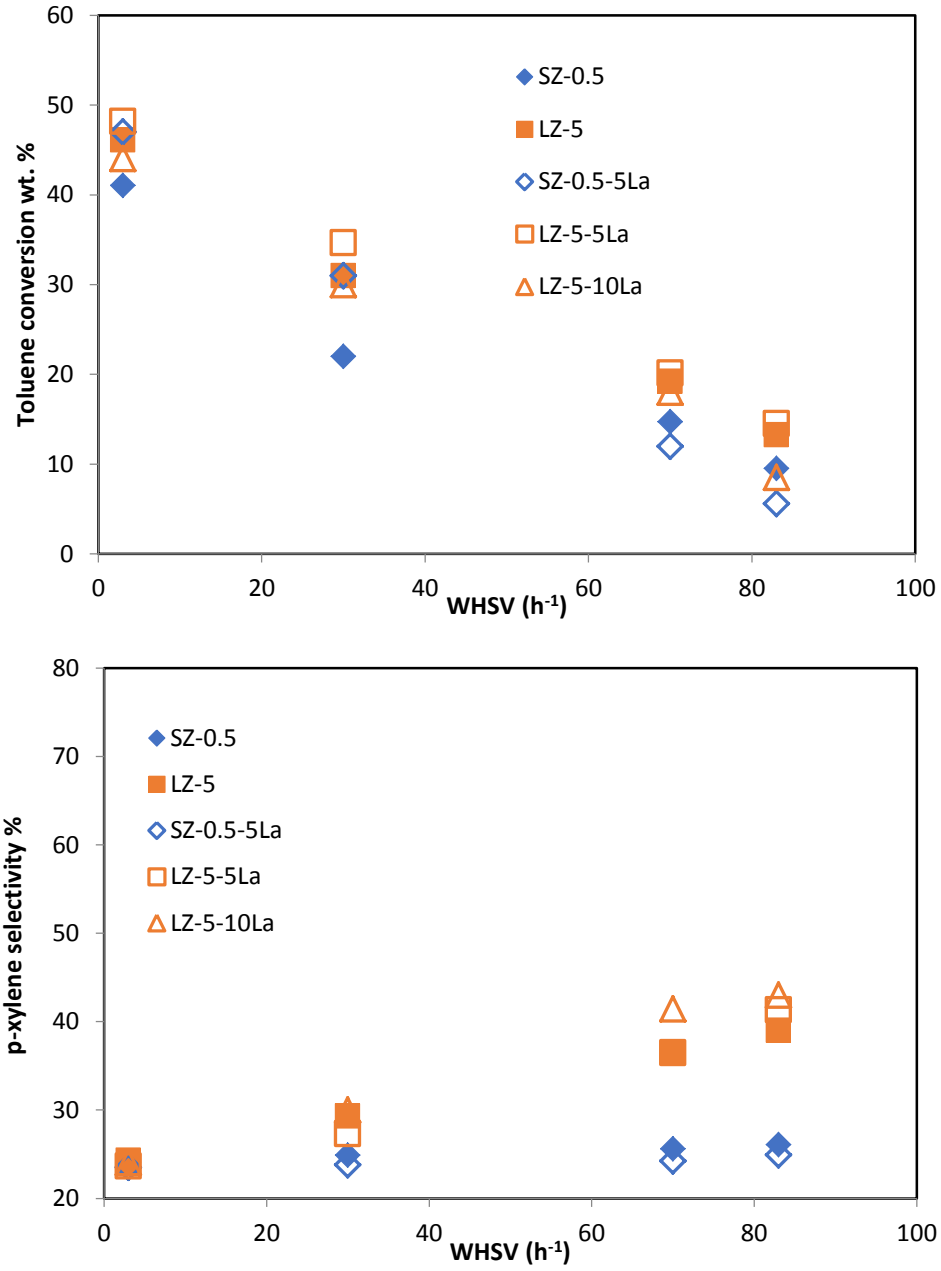

Figure 7-14: Effect of pressure on toluene conversion and p-xylene selectivity

Increasing the pressure reduced p-xylene selectivity as the conversion increased indicating a trade-off between conversion and selectivity, meaning a balance need to be struck to obtain good para-xylene yield. Both 5 wt. % and 10 wt. % modified large crystals showed higher p-xylene selectivity (41 % and 43 %, respectively) than the thermodynamic equilibrium value (24 %) at the highest WHSV (83 h^{-1}). It can be concluded that LZ-5-5La showed the best combination of toluene conversion (14.5 wt. %) and p-xylene selectivity (41 %).

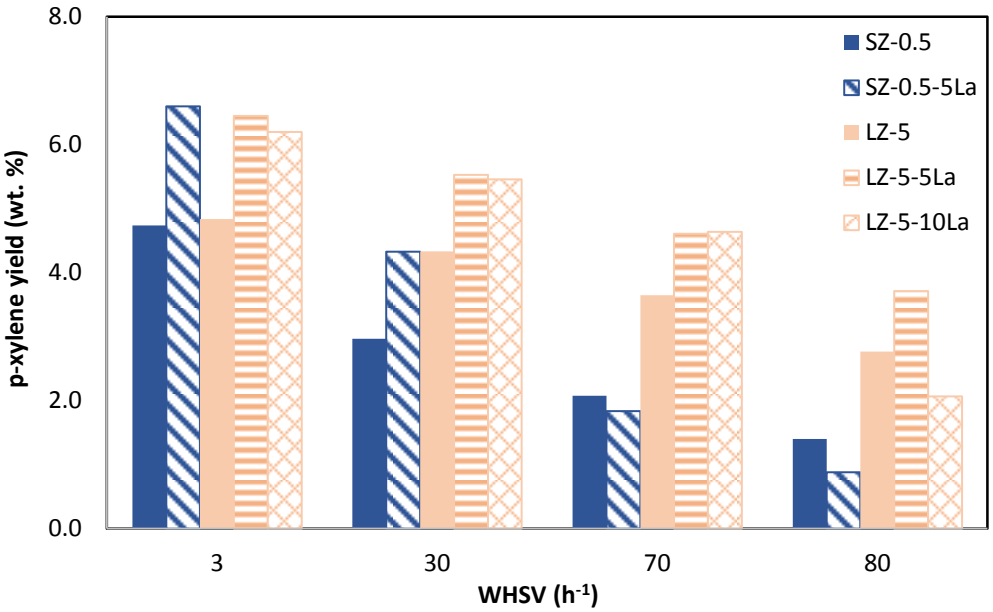

Figure 7-15: p-xylene yield for parents and La modified catalysts at 10 bar

7.5 Conclusions

In this chapter, the modification of ZSM-5 zeolite with phosphorus and lanthanum was carried out to investigate the effects it could have on p-xylene selectivity. SZ-0.5 was modified with three levels of phosphorus loading (0.75, 1.5 and 3 wt. %) and both Brønsted and Lewis acid sites drastically decreased because of the modification. This led to large drop in the activity of the catalysts. However, the p-xylene selectivity increased reaching 45 % by the 3 wt. % modified ZSM-5 (SZ-0.5-3P).

Lanthanum was impregnated on ZSM-5 with small crystal size (SZ-0.5) and large crystal size (LZ-5) to study the deactivation of the external acid sites and modify the size of the pore mouth. The modification successfully deactivated some of the external acid sites as indicated by the pyridine FTIR results. The overall acidity decreased with the increase in lanthanum loading, with Brønsted acid sites reduced preferentially. Also, BET surface area and pore volume decreased. This suggests that lanthanum was deposited on the surface and near the pore mouth increasing the selectivity towards p-xylene. However, this was accompanied by a loss in activity. The improvement in p-xylene selectivity was due to the suppression of the isomerization reaction on the surface. Moreover, the narrowing of pores openings restricted the bulkier isomers (o-xylene). The best combination of p-xylene selectivity (41%) and toluene conversion (14.5 wt. %) was achieved on the large

crystals modified with 5 wt. % lanthanum (LZ-5-5La) at the highest WHSV (83 h^{-1}) and a pressure of 10 bar.

7.6 References

1. Suganuma S, Nakamura K, Okuda A, Katada N. Enhancement of activity and selectivity for toluene disproportionation by ZSM-5 zeolite modified with Nickel. 8th Internation Symposium on Acid-Base Catalysis. 2017 May 7-10. Rio de janeiro, Brazil.

2. Rahman A, Burelle S, Adnot A, Lemay G, Kaliaguine S. Characterization of catalysts prepared by adsorption of phosphorus and rhodium complexes on H-ZSM-5 zeolites. Catalysis Today. 1989;6:123–132.

3. Al-Khattaf S, Ali M, Al-Amer A. Effect of reaction pressure and carrier gas on toluene disproportionation over molybdenum - ZSM-5 catalyst. Energy and Fuels. 2008;22(1):243–249.

4. Chaudhari P, Saini P, Chand S. Comparative performance of ion-exchanged ZSM -5 and Y-zeolite catalysts for toluene disproportionation reaction. Journal of Scientific and Industrial Research (India). 2002;61:810–816.

5. Cabral de Menezes S, Lam Y, Damodaran K, Pruski M. Modification of H-ZSM-5 zeolites with phosphorus. 1. Identification of aluminum species by 27Al solid-state NMR and characterization of their catalytic properties. Microporous and Mesoporous Materials. 2006;95:286–295.

6. van der Bij H, Weckhuysen B. Phosphorus promotion and poisoning in zeolite-based materials: synthesis, characterisation and catalysis. Chemical Society Reviews. 2015;44(20):7406–7428.

7. Kaeding W, Chu C, Young L, Weinstein B, Butter S. Selective alkylation of toluene with methanol to produce para-xylene. Journal of Catalysis. 1981;67(1):159–174.

8. Meshram N. Selective toluene disproportionation over ZSM-5 zeolites. Journal of Chemical Technology and Biotechnology. 1987;37(2):111–122.

9. Védrine J, Auroux A, Dejaifve P, Ducarme V, Hoser H, Zhou S. Catalytic and physical properties of phosphorus-modified ZSM-5 zeolite. Journal of Catalysis. 1982;73(1):147–160.

10. Vinek H, Rumplmayr G, Lercher J. Catalytic properties of postsynthesis phosphorus-modified H-ZSM5 zeolites. Journal of Catalysis. 1989;115(2):291–300.

11. Kareem A, Chand S, Mishra I. Disproportionation of toluene to produce benzene and p- xylene - A review. Journal of Scientific and Industrial Research (India). 2001;60(4):319–327.

12. Uguina M, Sotelo J, Serrano D, Grieken R. Magnesium and silicon as ZSM-5 modifier agents for selective toluene disproportionation. Industrial and Engineering Chemistry Research. 1992;31(8):1875–1880.

13. Sugi Y, Kubota Y, Komura K, Sugiyama N, Hayashi M, Kim J, et al. Shape-selective alkylation and related reactions of mononuclear aromatic hydrocarbons over H-ZSM-5 zeolites modified with lanthanum and cerium oxides. Applied Catalysis A General. 2006;299:157–166.

14. Hartford R, Kojima M, O'Connor C. Lanthanum ion exchange on HZSM-5. Industrial and Engineering Chemistry Research. 1989;28(12):1748–1752.

15. Lischke G, Eckelt R, Jerschkewitz H, Parlitz B, Schreier E, Storek W, et al. Spectroscopic and physicochemical characterization of P-modified H-ZSM-5. Jouranl of Catalysis. 1991;132(1):229–243.

16. Zhang L, Gao J, Hu J, Li W, Wang J. Lanthanum oxides-improved catalytic performance of ZSM-5 in toluene alkylation with methanol. Catalysis Letters. 2009;130:355–361.

17. Zhang Y, Zhou Y, Liu H, Wang Y, Xu Y, Wu P. Effect of La addition on catalytic performance of PtSnNa / ZSM-5 catalyst for propane dehydrogenation. Applied Catalysis A General. 2007;333:202–210.

Chapter 8 Conclusions and future work

8.1 Conclusions

Para-xylene is a key raw material for the synthesis of several petrochemical intermediates such as terephthalic acid [1–3]. China is the largest consumer of p-xylene where its consumption has increased by 7 % since 2011. The high demand on p-xylene is mainly driven by the high consumption of polyester, speculated to reach 70 million tonnes by 2020 [4]. The level of consumption is creating a big supply and demand gap that needs to be filled over the next 15 years.

As stated earlier xylenes are produced typically close to the thermodynamic equilibrium value (24% p-: 50% m-: 26% o-) and ZSM-5 zeolite is preferred over large pore zeolites because of its unique shape selectivity imposed by the straight and interconnecting channels very close to the kinetic diameter of xylene isomers [7]. Para-xylene has the smallest kinetic diameter (0.58 nm) allowing it to diffuse up to a 1000 times faster through ZSM-5, leading to a higher p-xylene product stream [8,9]. The available acid sites on the external surface of the catalyst rapidly isomerize p-xylene towards the thermodynamic equilibrium [6]. To enhance the p-xylene selectivity, different modifications to ZSM-5 are required such as increasing the crystal size, narrowing the pores and deactivating the external acid sites. Increasing the diffusion path through the synthesis of large crystals was used in this work and elsewhere to impose more diffusion constraints on the bulkier isomers (o- and m-) requiring them to isomerize and form more p-xylene [10–13]. Deactivation of the acid sites on the external surface through silica deposition by chemical liquid deposition (studied also in this thesis) or chemical vapour deposition are common strategies to improve p-xylene selectivity better than 80% [14–16].

In this study, improving p-xylene selectivity was attempted through the investigation of the effect of crystal size and different modification methods. The physicochemical properties of all prepared catalysts were thoroughly studied using different characterisation techniques. They include XRD, py-FTIR, SEM, ICP and N_2 adsorption. The catalytic behaviour of each catalysts was evaluated over a range of WHSV (3-83 h^{-1}), a temperature of 475 ˚C and two different pressures (1 and 10 bar).

8.1.1 Crystal size

To explore the effect of crystal size, various syntheses of ZSM-5 produced differing crystals sizes (5, 50 + 100 µm) were carried out in this thesis. SEM showed that the crystals had varied sizes as well as different morphologies. Overall, this study showed that increasing the crystal size enhanced p-xylene selectivity due to the diffusion constraints imposed by the increased length of the diffusion path. However, toluene conversion decreased as a result of the combination of larger crystal length and lower acidity. ZSM-5 zeolite with 100 µm crystals (LZ-100) showed the best para-selectivity (58 %) at the highest WHSV (83 h^{-1}). Toluene conversion was very low (2%) as a result of the high Si/Al ratio (Table 5-2). On the other hand, ZSM-5 with 5 µm crystals (LZ-5) delivered the best results in terms of combined toluene conversion (12%) and p-xylene selectivity (38 %). Figure 8-1 shows the effect of crystal size on p-xylene selectivity at different WHSVs. Further studies to optimize the synthesis of large crystals should be pursued to find the right balance between crystal size and Si/Al ratio.

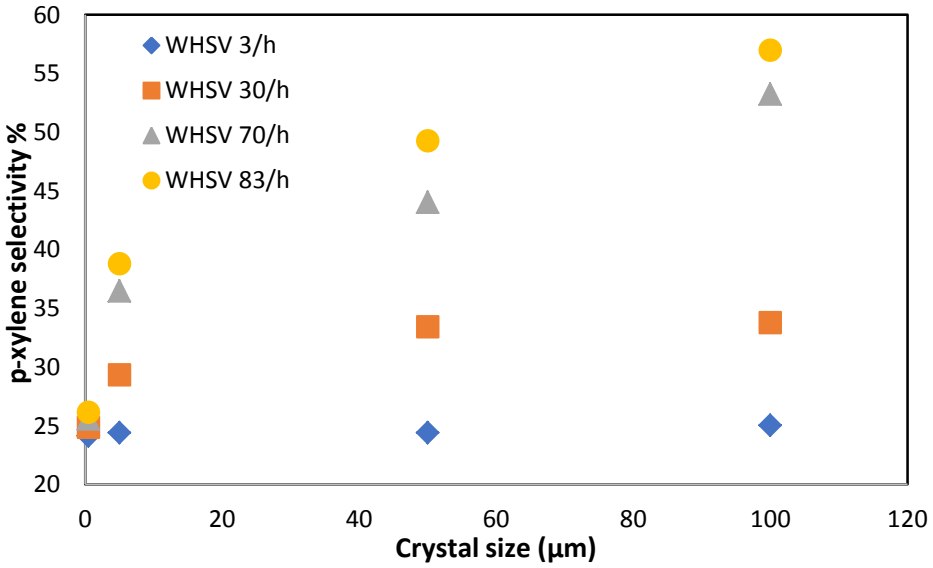

Figure 8-1: Effect of crystal size on p-xylene selectivity at varied WHSV and at 10 bar

8.1.2 Silylation

ZSM-5 with different crystal sizes were modified further by silylation through chemical liquid deposition (CLD) in an attempt to further enhance p-xylene selectivity by deactivating the undesired external acid sites responsible for the isomerization reaction. Different silylation agents, silica loading amounts and number of silylation cycles effects

were investigated (Table 6-2). The results obtained suggest that TEOS was better that APTES. In terms of silica loading amount, it was found that the loading amount should be optimized based on the catalyst crystal size and aluminium content. The use of multiple cycles of silylation was shown to be an important factor in achieving the deposition of uniform silica layers to deactivate the highest amount of external acid sites. Silica deposition on the external surface decreased the number of Brønsted and Lewis acid sites supported by the py-FTIR results (section 6.4). The decrease in acidity led to the improvement of p-xylene selectivity, suggesting that some acid sites on the external surface were deactivated. The loss in acidity unsurprisingly negatively impacted toluene conversion. The results also showed that modifying the catalyst with multiple cycles was essential to further improve the p-xylene selectivity. The highest p-xylene selectivity was achieved over two time silylated ZSM-5 with 5 µm crystals (LZ-5-T-2X30%) reaching 85% at the highest WHSV (83 h^{-1}) and this was at the cost of toluene conversion (2%). Increasing the pressure to 10 bar doubled the toluene conversion and dropped p-xylene selectivity to (65 %) as a result of the trade-off between selectivity and conversion. High selectivities were typically achieved at high feed flow rates, short residence time, providing less contact between the catalyst surface and feed and hence reduced isomerization of p-xylene. As expected the unmodified small ZSM-5 crystals did not achieve p-xylene selectivity higher than the thermodynamic value which confirmed that modifications studied in this work namely increasing the crystals size and deactivation of the external surface by silica deposition are important for enhanced p-xylene selectivity. Further studies are required to improve the p-xylene selectivity at an industrial WHSV typically 2-6 h^{-1}.

8.1.3 P and La modification

Modifying the acidity and narrowing the pores of ZSM-5 was studied by the addition of phosphorus and lanthanum to the catalyst. The addition of phosphorus (0.75, 1.5 and 3 wt. %) drastically decreased the number of acid sites measured by py-FTIR (section 7.3.2). The massive reduction in the acid sites led to a very low toluene conversion even at the slowest WHSV (3 h^{-1}). On the other hand, p-xylene selectivity was increased to 45% at the highest loading (3 wt. %). Impregnation of lanthanum (5 and 10 wt. %) on ZSM-5 was achieved successfully as suggested by ICP-OES analysis. Pyridine-

FTIR and N_2 adsorption revealed that the number of Brønsted acid sites, BET surface area and pore volume were decreased after the addition of lanthanum. However, the number of Lewis acid sites increased after impregnation of lanthanum and was attributed to its weak acidic properties which can interfere in the measurements (sections 7.3.2 and 7.3.4). The large crystals loaded with 5 wt. % lanthanum (LZ-5-5La) delivered the best results in terms of combination of p-xylene selectivity (41 %) and toluene conversion (14.5 wt. %) at WHSV 83 h^{-1} and a pressure of 10 bar.

8.2 Future work and recommendations

In this study, it was difficult to control the synthesis where the very large crystals were produced with low aluminium content (high Si/Al ratio) (Table 8-1). The synthesis can be improved further by studying several factors affecting it such as temperature, aging time, crystallization time, and silica and alumina sources.

Table 8-1: Synthesized large crystals

Crystal size (µm)	5	50	100
Si/Al (ICP)	16	58	64

Aluminium distribution was found previously to be non-uniform in large crystals which can affect the catalytic results and reduces the effects of post modification methods targeting the acid sites. For example, if the aluminium is concentrated at the edges of ZSM-5 crystals it will be difficult to control the modification (eg. Silylation) in a way to target these acid sites [17]. Aluminium distribution across a large crystal can be studied using electron micro probe analysis (EMPA) which is far more accurate than SEM-EDX and can detect very low amount of aluminium [17]. A thorough study should be conducted to find the optimised combination of crystal size alongside Si/Al ratio to be able to achieve the right balance between toluene conversion and p-xylene selectivity.

Pre-coking had been investigated extensively in the literature and already applied in industry providing high p-xylene selectivity (> 80 %) [18]. During the initial stages of this thesis, pre-coking experiments was carried out over commercial ZSM-5 (0.5 µm, Si/Al = 26) using 1,3,5 trimethylbenzene (TMB) as described in Figure 8-2 at 550 °C for 3 to 9 hours to investigate the effect on p-xylene selectivity, where toluene disproportionation

was performed over the pre-coked samples at 475 °C and atmospheric pressure using nitrogen as carrier gas (150 ml/min). The results suggested that pre-coking can improve para-selectivity and as the coke amount increased, p-xylene selectivity increased. However, further work must be done in terms of investigating pre-coking time and coking agent to find the optimum amount of coke to be deposited on the catalyst to obtain high p-xylene selectivity. Furthermore, the type of coke (soft or hard) should be studied by TGA analysis as it can have a significant impact. To properly assess para-selectivity and conversion, the reaction should be performed at elevated pressure to increase the toluene conversion. This work has indicated that pre-coking should be carried over ZSM-5 with large crystals as it was shown that large crystals increased para-selectivity compared to small crystals.

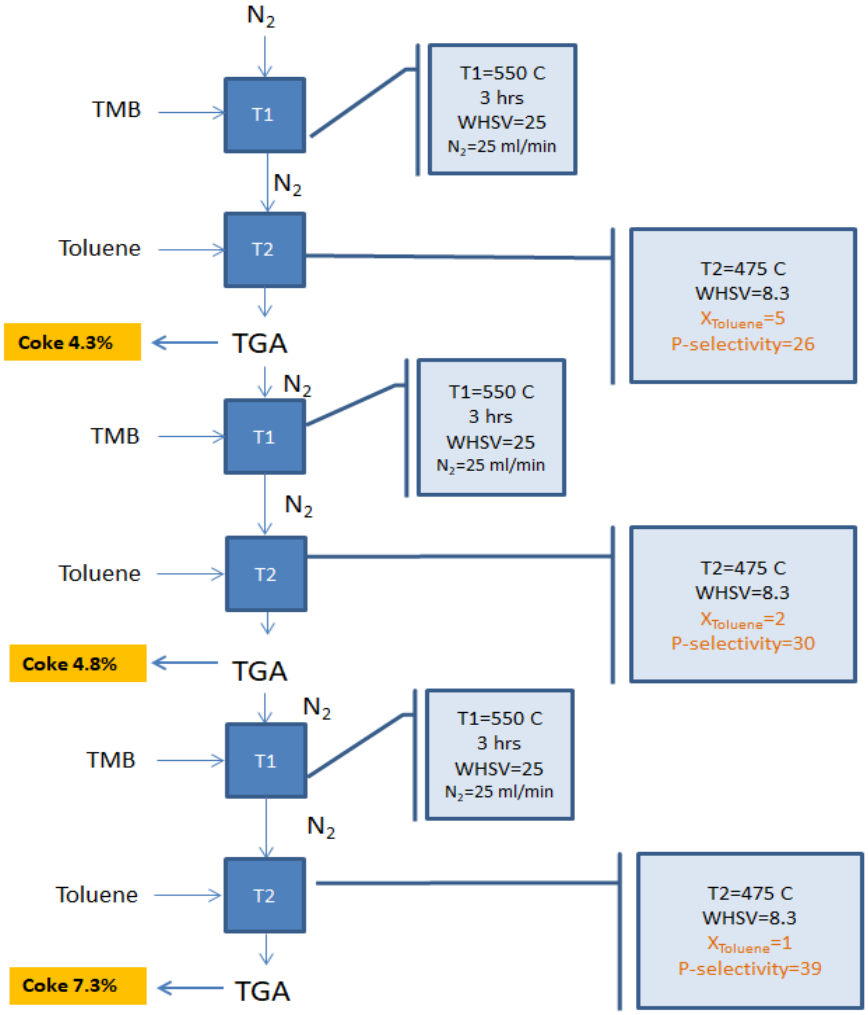

Figure 8-2: A schematic of pre-coking methodology and toluene disproportionation

To improve p-xylene selectivity, suppression of isomerization on the surface of ZSM-5 is required by deactivating the acid sites. Dung et al. [19] developed an interesting novel composite catalyst aiming to increase p-xylene selectivity in the alkylation of toluene with methanol. The catalyst consisted of H-ZSM-5 covered with a thin layer of inactive silicalite-1. This was obtained by dipping H-ZSM-5 crystals in a silicalite synthesis gel allowing the inactive silicalite crystals to form a thin layer covering H-ZSM-5 crystals. Implementing this catalyst, they achieved excellent p-xylene (99.9 %) compared to the uncoated H-ZSM-5 (40 %). However, it has been shown that the alkylation of toluene with methanol produces higher para-selectivity than the thermodynamic value even on the unmodified ZSM-5 catalysts, for example Dung et al. delivered 40 % para-selectivity on the used parent with Si/Al = 30 and a crystal size of 7 µm. This composite catalyst can be synthesized and optimized for use in toluene disproportionation. Different factors can be examined to improve toluene conversion and p-xylene selectivity over silicalite/H-ZSM-5 catalyst such as the thickness of the silicalite layer as having a very thick layer can lead to high p-xylene selectivity. However, conversion will drop drastically as the reaction rate will be very low and the thicker the layer the more difficult it is for the products to diffuse. There are other factors that can be investigated such as the number of silicalite synthesis cycles and the Si/Al ratio which was proved to play a key role in the produced thickness of inactive layer. Performing this modification on optimised large crystals H-ZSM-5 can lead to excellent p-xylene selectivity.

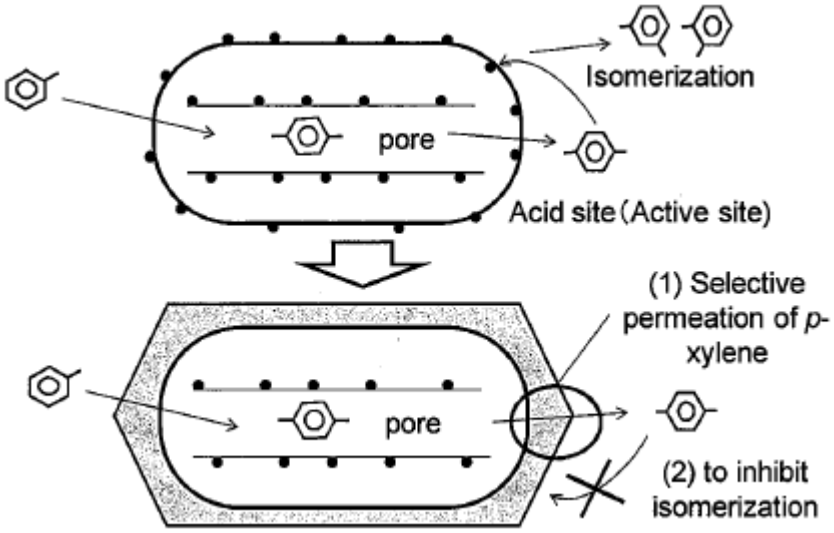

Figure 8-3: Concept of composite catalyst (Silicalite-1/H-ZSM-5) [20]

In this thesis, it was shown that different modifications of the external surface such as silylation can increase p-xylene selectivity. Nevertheless, the modified catalyst did not deliver the anticipated results. The reason could be that crushing and pelleting the catalyst after the modification led to opening up the structure again and made acid sites available which subsequently isomerised p-xylene. A very recent study by Mitsuyoshi et al. [21] showed that this was the case as p-xylene selectivity dropped from 99% to 47% after pelletization of a CVD modified catalyst. Thus, it is advised to pelletise the catalysts into shaped extrudates made of binder and zeolites mixture followed by the modification (eg. Silylation).

In industry, for zeolites to be used in catalysis they should be shaped into mechanically stable geometries, known as extrudates. This is achieved through mixing the zeolite powders with binders where the addition of binder increases the mechanical strength. Different type of binders can be applied such as alumina or natural clays (montmorillonite) [22]. An alumina based binder can affect the acidity of zeolite through the insertion of aluminium into the zeolite framework. In contrast, Uguina et al. [10,22] claimed that sodium montmorillonite neutralized a large number of acid sites which led to significant reduction in toluene conversion and increase in p-xylene selectivity. Since acid treatment of the catalyst restored the activity this suggested that some acid sites were poisoned by Na^+ and hence the selectivity was increased due to some pore blockage or narrowing.

To summarise, there are several strategies that would be logical to pursue in future work:

1) Tailored and characterised study of large crystals ZSM-5.
2) Optimising pre-coking conditions and test pre-coked ZSM-5 at high pressure.
3) Silylation of extruded catalyst with large crystals ZSM-5.

8.3 References

1. Kareem A, Chand S, Mishra IM. Disproportionation of toluene to produce benzene and p- Xylene - A Review. Journal of Scientific and Industrial Research (India). 2001;60(4):319–27.

2. Ali MA, Ali SA, Al-Nawad K. Disproportionation of toluene: enhanced para-xylene

selectivity over modified HZSM-5. Current Catalysis. 2013;2(2):96–110.

3. Ashraf MT, Chebbi R, Darwish NA. Process of p-xylene production by highly selective methylation of toluene. Industrial and Engineering Chemistry Research. 2013;52:13730–13737.

4. Jenkins S. Paraxylene - is the tail wagging the dog ?. [Presentation] IOC Petrochemical conclave. New Delhi, India; 2013. Available from: http://www.petrochemconclave.com/presentation/2013/Mr.SJenkins.pdf

5. Tsai T. Disproportionation and transalkylation of alkylbenzenes over zeolite catalysts. Applied Catalysis A General. 1999;181(2):355–398.

6. Al-Khattaf S, Ali SA, Aitani AM, Žilková N, Kubička D, Čejka J. Recent advances in reactions of alkylbenzenes over novel zeolites: the effects of zeolite structure and morphology. Catalysis Reviews. 2014;56:333–402.

7. Waziri SM, Aitani AM, Al-Khattaf S. Transformation of toluene and 1,2,4-trimethylbenzene over ZSM-5 and mordenite catalysts: A comprehensive kinetic model with reversibility. Industrial and Engineering Chemistry Research. 2010;49(14):6376–6387.

8. Zheng S, Jentys A, Lercher JA. Xylene isomerization with surface-modified HZSM-5 zeolite catalysts: an in situ IR study. Journal of Catalysis. 2006;241(2):304–311.

9. Xie J, Chen L, Wang W-H, Wang P, Au C-T, Yin S-F. Direct dual-template synthesis of HZSM-5 zeolite for enhanced p-xylene selectivity in toluene methylation with CH_3Br. Catalysis Science and Technology. 2017;7(5):1211–1216.

10. Uguina MA, Sotelo JL, Serrano DP. Toluene disproportionation over ZSM-5 zeolite. Effects of crystal size, silicon-to-aluminum ratio, activation method and pelletization. Applied Catalysis. 1991;76(2):183–198.

11. Ratnasamy P, Babu GP, Chandwadkar AJ, Kulkarni SB. Influence of crystal size of HZSM-5 on activity and shape selectivity in xylene isomerization. Zeolites. 1986;6(2):98–100.

12. Shiralkar VP, Joshi PN, Eapen MJ, Rao BS. Synthesis of ZSM-5 with variable crystallite size and its influence on physicochemical properties. Zeolites. 1991;11(5):511–516.

13. Chen NY. Reactions of mixtures of toluene and methanol over ZSM-5. Journal of Catalysis. 1988;114(1):17–22.

14. Zhu Z, Xie Z, Chen Q, Kong D, Li W, Yang W, et al. Chemical liquid deposition with polysiloxane of ZSM-5 and its effect on acidity and catalytic properties. Microporous and Mesoporous Mater. 2007;101(1–2):169–175.

15. Zheng S, Heydenrych HR, Röger HP, Jentys A, Lercher JA. On the enhanced selectivity of HZSM-5 modified by chemical liquid deposition. Topics in Catalysis. 2003;22:101–106.

16. Hui T, Wang J, Ren X, Chen D. Disproportionation of toluene by modified zsm-5 zeolite catalysts with high shape-selectivity prepared using chemical liquid deposition with tetraethyl orthosilicate. Chinese Journal of Chemical Engineering. 2011;19(2):292–298.

17. Von Ballmoos R, Meier WM. Zoned aluminium distribution in synthetic zeolite ZSM-5. Nature. 1981;289:782–783.

18. Tsai T. Disproportionation and transalkylation of alkylbenzenes over zeolite catalysts. Applied Catalysis A General. 1999;181(2):355–398.

19. Van Vu D, Miyamoto M, Nishiyama N, Egashira Y, Ueyama K. Selective formation of para-xylene over H-ZSM-5 coated with polycrystalline silicalite crystals. Journal of Catalysis. 2006;243(2):389–394.

20. Van Vu D. MFI Zeolite Catalysts for Selective Production of para-Xylene and Light Olefins. PhD. Thesis. Osaka University; 2009.

21. Mitsuyoshi D, Kuroiwa K, Kataoka Y, Nakagawa T, Kosaka M, Nakamura K, et al. Shape selectivity in toluene disproportionation into para-xylene generated by chemical vapor deposition of tetramethoxysilane on MFI zeolite catalyst.

Microporous and Mesoporous Materials. 2017;242:118–126.

22. Mitchell S, Michels NL, Pérez-Ramírez J. From powder to technical body: the undervalued science of catalyst scale up. Chemical Society Reviews. 2013;42(14):6094-6112.

23. Uguina MA, Sotelo JL, Serrano DP. Roles of ZSM-5 modifier agents in selective toluene disproportionation. Canadian Journal of Chemical Engineering. 1993;71(4):558–563.

APPENDIX A

Examples of calculations used for different post modifications

1. Silylation

For example, to load 30 wt. % SiO_2 on 5 grams of ZSM-5 zeolite

Therefore for 30 wt. % SiO_2:

$$0.3 \times \text{Catalyst weight} = 0.3 \times 5 = 1.5 \text{ g of } SiO_2$$

MWT of TEOS = 208.3 g mol^{-1}

MWT of SiO_2 = 60.08 g mol^{-1}

So,

$$208.3 \text{ g TEOS} \longrightarrow 60.08 \text{ g } SiO_2$$

$$X \longrightarrow 1.5 \text{ g } SiO_2$$

Therefore, to get the required amount of TEOS (X):

$$X = \frac{1.5 \times 208.3}{60.08} = 5.2 \text{ g of TEOS}$$

The volume of TEOS solution needed is 5.2 ÷ 0.933 = 5.57 mL, where the density, $\rho = 0.933$ g mL^{-1}

2. Impregnation of phosphorus (P)

For example, If the desired amount of phosphorus is 1.5 wt.%, so:

The mass of phosphorus needed for 10 grams of zeolite is:

$$0.015 \text{ P} \times \text{Catalyst weight} = 0.015 \times 10 = 0.15 \text{ g of P}$$

The mass of phosphoric acid that contains the desired mass of phosphorus is:

$$31 \text{ g P} \longrightarrow 98 \text{ g } H_3PO_4$$

$$0.15 \text{ P} \longrightarrow X \text{ g } H_3PO_4$$

Therefore, to get the required amount of H_3PO_4 (X):

$$X = \frac{0.15 \times 98}{31} = 0.48 \text{ g of } H_3PO_4$$

If the solution of phosphoric acid is 85 wt. % in water, the mass of solution needed is:

$$85 \text{ g } H_3PO_4 \longrightarrow 100 \text{ g solution}$$

$$0.48 \text{ g } H_3PO_4 \longrightarrow X \text{ g solution}$$

$$X = 0.56 \text{ g solution}$$

Then, the volume of the solution needed is calculated as:

The volume of solution needed is 0.56 ÷ 1.685 = 0.3361 mL, where the density, $\rho = 1.685 \text{ g mL}^{-1}$

3. Lanthanum Impregnation

For example, to load 5 wt. % La on 5 grams of ZSM-5 zeolite

Therefore for 5 wt. % La:

$$0.05 \times \text{Catalyst weight} = 0.05 \times 5 = 0.25 \text{ g of } SiO_2$$

MWT of lanthanum nitrate hexahydrate= 433.01 g mol^{-1}

MWT of La = 138.9 g mol^{-1}

So,

$$433.01 \text{ g } La(NO_3)_3 \cdot 6\ H_2O \longrightarrow 138.9 \text{ g La}$$

$$X \longrightarrow 0.25 \text{ g La}$$

Therefore, to get the required amount of $La(NO_3)_3 \cdot 6\ H_2O$ (X):

$$X = \frac{0.25 \times 433.01}{138.9} = 0.78 \text{ g of La}$$

APPENDIX B

Instrumentation used for catalytic testing and WHSV calculations

1. Catalytic rig

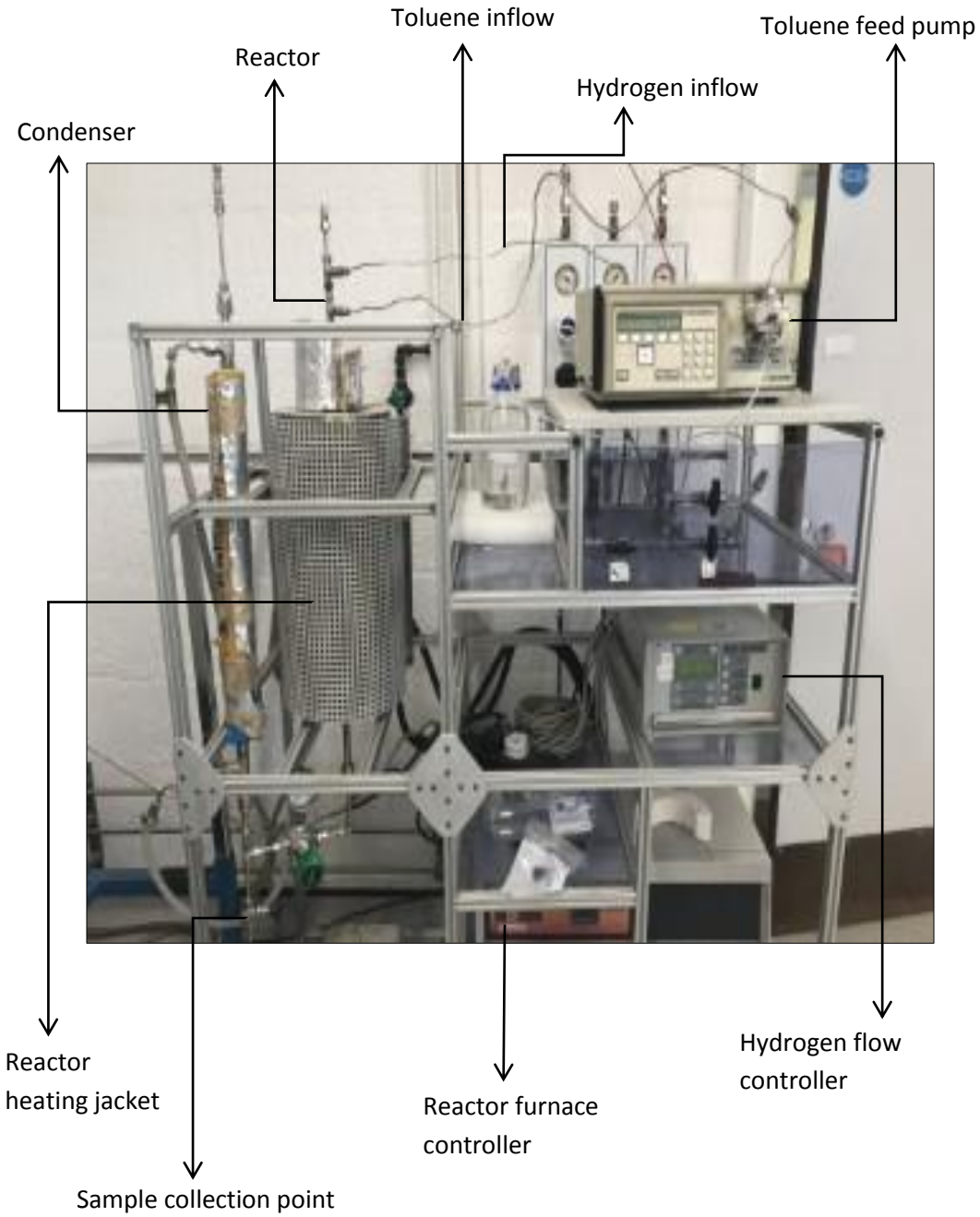

2. WHSV (weight hourly space velocity) and W/F Calculations

WHSV can be defined as follows

$$WHSV\ (h^{-1}) = \frac{feed\ mas\ flow\ rate\ (g\ h^{-1})}{catalyst\ weight\ (g)}$$

W/F can be defined as follows

$$W/F\ (\mathrm{g\ h}\ mol^{-1}) = \frac{catalyst\ weight\ (g)}{feed\ molar\ flow\ rate\ (mol\ h^{-1})}$$

Toluene molecular weight = 92.14 mol/g, Toluene density = 0.87 g/mol

The following table shows the WHSVs and toluene flowrates used in this study

Feed flow rate (ml h^{-1})	Catalyst weight (g)	WHSV (h^{-1})	W/F (g h mol^{-1})
3.6	1	3.1	29.4
36		31	2.94
81		70.5	1.3
96		83.5	1.1

APPENDIX C

Standard peaks retention time identified by GC

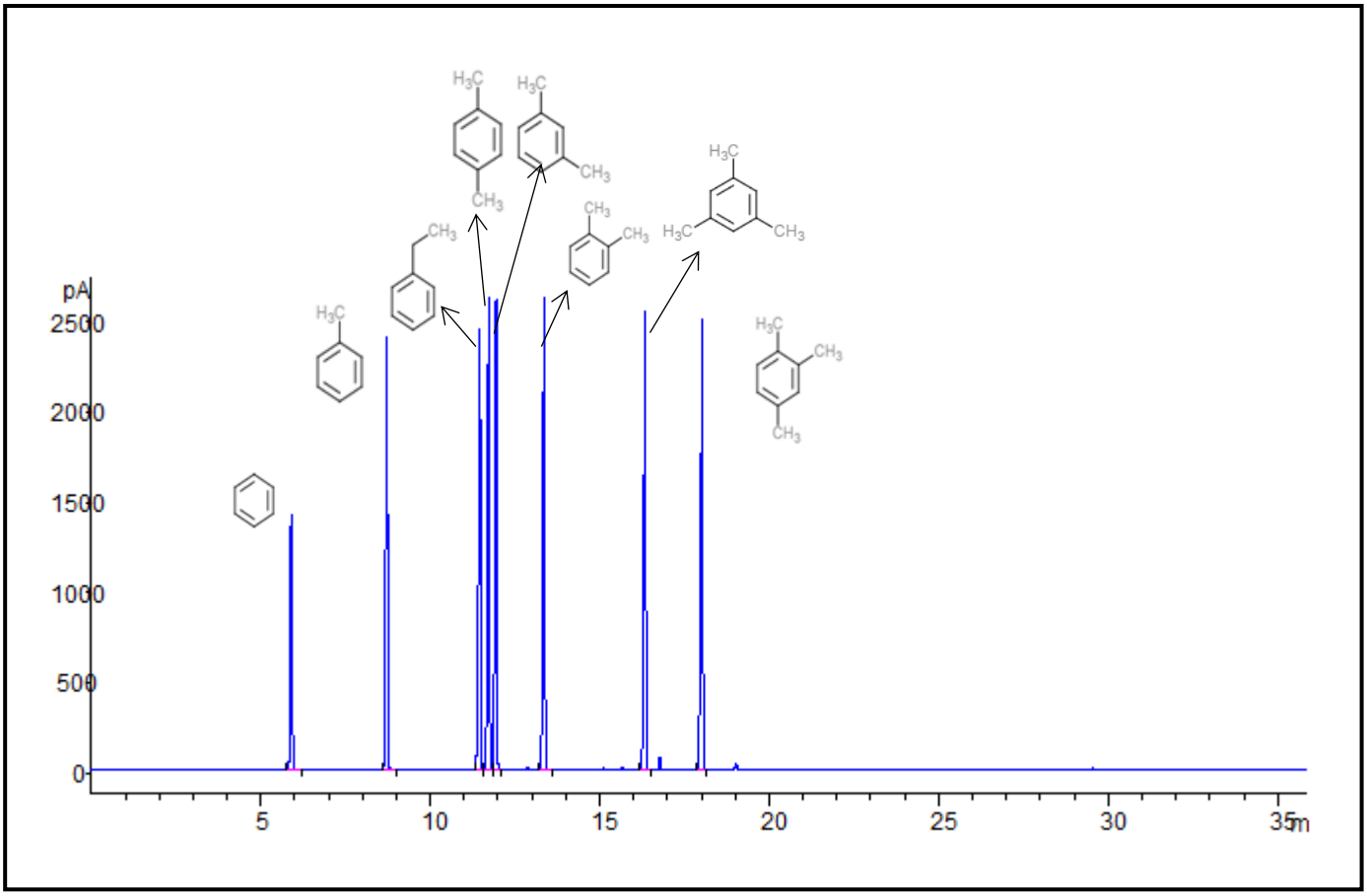

APPENDIX D

Publications and presentations

Publications

Albahar M, Li C, Zholobenko VL, Garforth A. Selective Toluene Disproportionation to produce para-Xylene over Modified ZSM-5. Chemical Engineering Transactions. 2017 Mar 26;57:907-912.

Presentations

Albahar M, Li C, Zholobenko VL, Garforth A. Selective Toluene Disproportionation to produce para-Xylene over Modified ZSM-5, In the 13th International Conference on Chemical and Process Engineering (ICheaP13), 28-31 May, 2017 - Milano, Italy.

Albahar M, Garforth A. Selective toluene disproportionation over ZSM-5, In the annual postgraduate research conference, 20 May, 2016 – Manchester, UK.

Poster presentations

Albahar, M., Garforth A. Selective toluene disproportionation over ZSM-5, in the British Zeolite Conference (BZA), 2014: Chester, UK.